THE MECHANICAL AND OTHER PROPERTIES OF IONOMER CEMENTS

A thesis submitted for the degree of Doctor of Philosophy

by Michael John Read

Department of Non-Metallic Materials, Brunel University,

September 1981

D E D I C A T I O N

To RUTH and CAROLINE

ACKNOWLEDGEMENTS

The author is indebted to Blue Circle Technical Limited for financial support during the course of this study through the award of an Industrial Studentship.

The author wishes to express his gratitude to Dr. K.A. Hodd (B.U.), Dr. W.G. Davies (B.C.T.) and Dr. G. Bye (B.C.T.) for their advice, assistance and helpful discussion during this investigation.

ABSTRACT

Ionomer cements, a novel composite material, are formed at ambient temperatures by mixing an aqueous polyacid with an ion-leachable powder. The glass ionomer cement known as ASPA, a dental restorative material, produces strong and hydrolytically stable cements. Applications of this material outside of dentistry have been restricted by its rapid set, its poor mechanical performance in dry environments and its high cost. The objective of this research have been to modify the ASPA system and develop other ionomer cements for applications outside of dentistry and to provide a further understanding of the mechanical properties of ionomer cements.

The rapid set of ASPA cements was reduced by acid treatment of the ion-leachable glass. Cements prepared from this acid treated glass (ATG) were mechanically superior to the ASPA cements and retained their mechanical properties in environments of low humidity due to a greater extent of aluminium polyacrylate formation than in the ASPA cement.

The rapid set of the ASPA system was also reduced by replacing the ion-leachable glass with various fillers. The mechanical properties of these filled ASPA cements were dependent upon the physical characteristics of the filler and were poor in low humidity environments.

Other zinc-glass ionomer cements and certain treated mineral ionomer cements showed promise as low cost alternatives to the ASPA glass.

The mechanical properties of ionomer cements were dependent upon the size and packing properties of the glass particles, the volume fraction of glass in the cement and the interfacial wetting properties between the glass and the polyacid matrix.

Ionomer cements were mechanically superior and more resistant to hydrothermal ageing than epoxy and polyester composites. It was proposed that this was due to a more water tolerant matrix and due to stable primary interfacial bonds being formed at the glass-polyacid interface.

CONTENTS

CONTENTS PAGE NO

CONTENTS PAGE NO

CONTENTS

1. INTRODUCTION

IONOMER CEMENTS - CLASSIFICATION AND DEFINITION

1.1 Ionomer Cements are a novel type of filled polymeric material which are formed at room temperature by mixing an aqueous solution of a polyacid with an ion-leachable inorganic powder, such as some specially formulated glasses (1,43,44), certain natural or synthetic minerals (1,7,8), or certain metal oxides (4,49). Upon mixing an acid-base reaction occurs and metallic ions are liberated from the powder surface and react with the polyacid to form insoluble salts. This type of reaction, where metallic salt crosslinks are formed, is shown schematically in figure 1.1 and is considered in more detail later. Such reactions result in the formation of rigid materials with a composite microstructure comprising of a continuous phase of crosslinked metal polyacrylate gel with a dispersed phase of the inorganic powder. Ionomer cements may thus be classified as both a polymeric composite material and as an ionomer, that is a polymer system which contains both covalent and ionic bonds within its network structure normally with the covalent bonds forming a polymeric backbone and the ionic bonds pendant to this main chain. (5,6).

Terminology

The term ionomer, which is not well established, was originally used by Du Pont de Nemours (5,6)) to describe an ionically crosslinked thermoplastic known as Suryln A (5,19) but the term is currently finding more general use to describe other polymer systems which contain ionic bonds. The literature provides a number of synonyms for this class of material, for example ionomers are also known as ionic polymers (3,53,54), organic

Figure 1.1 Schematic Representation of The Curing Mechanism of Ionomer Cements

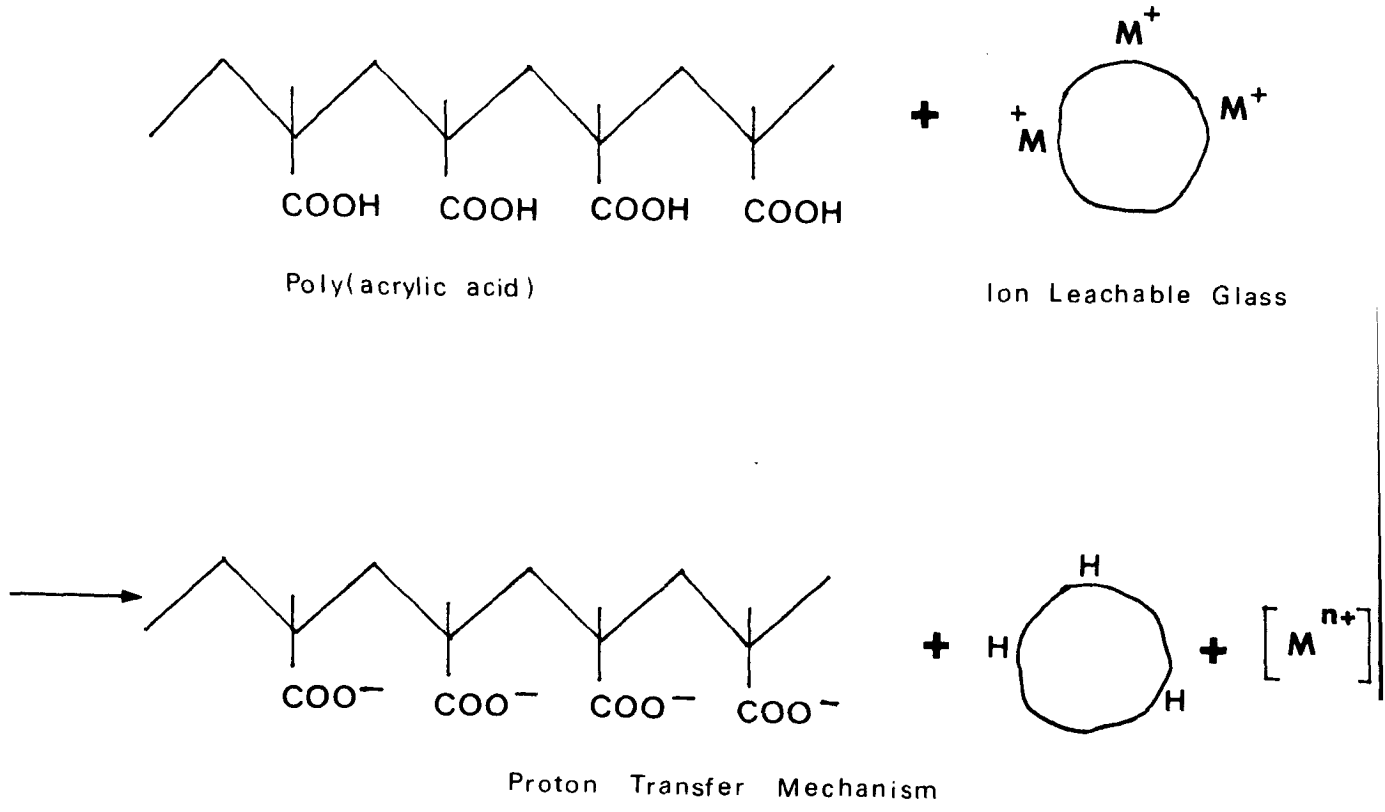

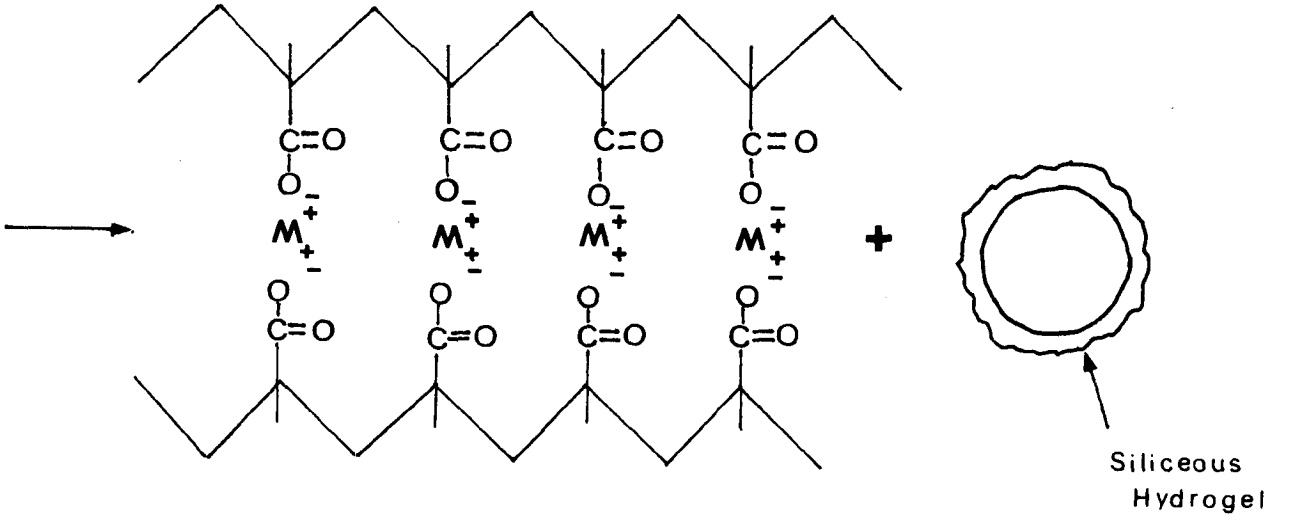

ionic polymers (9), organolithic macromolecular materials (1) ion-containing polymers (11), ionic acrylates and polyelectrolyte salts (16-18). The term ionomer will be used here to describe this type of material but a distinction between ionomers and ionomer cements is necessary. Ionomer cements are ionomers which have a composite microstructure, where the matrix is hydrated and where the reaction products remain in a hydrated state (or solvated state if a non-aqueous solvent is used). Again, the literature provides many synonyms for this type of material such as ionic polymer cements (49), poly(carboxylate) cements (22,28,29), water hardenable powder materials (24), surgical cements (24) and mineral polyacid cements (7,8). For the purposes of this thesis the term ionomer cement will be used to describe this type of material but the prefixes of glass, mineral or metal oxide will be used to identify the nature of the ion leachable source.

Glass-ionomer cements are currently used as a dental restorative material (1,20,21,22,28,29) and commercially the most important ionomer cement is the ASPA system. This material has been examined in detail and these studies have provided the basis of the present understanding of ionomer cements in general. The modification and development of this material has been fundamental to this research and consequently this system is described in detail in the next section.

1.2 The ASPA System

ASPA is an acronym for aluminosilicate poly(acrylic acid) (1,26) This material was patented in 1969 by Wilson and

Kent (21) for use in dentistry. The physical properties of this material, its components and the cement forming reaction are described in the subsequent sections where particular attention is given to factors affecting the mechanical properties.

1.2.1. The Use of ASPA in Dentistry

The ASPA ionomer cement was developed as a filler for erosion cavities, for restoration of anterior teeth, for cavity lining and for other general dental cementation purposes (26,27). This material was evolved from the zinc poly(carboxylate) ionomer cements of Smith (28,29) having improved translucency, superior strength properties and a lower initial pH thus causing less pulpal irritation. Both these ionomer cements heralded a significant advance in dentistry by providing specific adhesion towards tooth material, which is predominently hydroxyapatite (30-32). Most other dental cements, such as dental amalgam, are non-adhesive towards hydroxyapatite and are retained in the tooth by mechanical keying which requires extensive under-cutting of the cavity walls with the removal of sound tooth material. A marginal gap exists at the interface between the filler and the tooth material with such systems through which marginal seepage can occur. Marginal seepage promotes both plaque forming streptococcal growth and percolation of sugar and polysaccharide solutions around the interface, these solutions are degraded by micro-organisms into lactic acid which erodes the restoration necessitating refilling every few years with further removal of sound tissue. The use of adhesive dental materials eliminates the problems associated with marginal

seepage and gives a greater degree of permanency to the restoration with less removal of sound tissue during preparation (1,31).

However, the ASPA system has received a number of criticisms, not all dentists agree on its permanency and its translucency may have lower cosmetic value than other filling materials (33-40). Further, others have suggested that the hydrolytic stability could be improved and that the adhesion to dentine is poor (34), although this latter observation is most probably due to incorrect cavity preparation (52).

The mechanical and thermal properties of the ASPA system and other dental filling are different from that of tooth material as shown in Table 1.1. These differences in properties can lead to differential strains occurring at the tooth-filler interface under conditions of stress or extremes of temperature. This leads to the development of interfacial stresses which cause premature failure (40). However, it is the cosmetic value of ASPA which has caused most concern and it has recently been commercially superseded by another ionomer cement with greater translucency and known as Chemfil (60).

1.2.2. The ASPA polyacid solution

Various types of polyacid solutions have been evaluated for use in ionomer cements and some of these are shown in Table 1.2 (4,35). The ASPA system initially used a 50% aqueous solution of poly(acrylic acid) (PAA) with a molecular weight of cira 23,000 but this polymer gelled within a few weeks of storage due to hydrogen bond formation (35,36,39). To overcome this problem copolymers of acrylic acid and itaconic acid

Table 1.1 Physical Properties of Dental and Tooth Materials

Property	Silver Amalgam (40)	Zinc Polycarboxylate (28)	ASPA (1)	Chemfil (60)	Dentine (1,40)	Enamel (1,40)
Compressive Strength (MPa)	400	125	214	220	207-345	97-386
Compressive Modulus (GPa)	14-19	-	19	-	19	80
Thermal Expansion (ppm/^{o}c)	25	-	26	-	7-8	12
Opacity $C_{0.7}$	Opaque	0.69	0.72	0.55	0.51-0.93	0.21-0.67
Adhesion to Enamel (MPa)	0	10.4	4.0	4.0	-	-
Adhesion to Dentine (MPa)	0	3.5	2.9	-	-	-

Table 1.2 Polyacids with Ionomer Cement Forming Ability (4)

Weak Synthetic Polyacids

Poly(acrylic acid) (PAA)

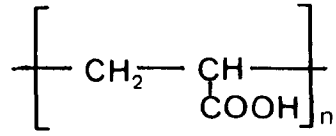

Acrylic acid/Itaconic acid Copolymer (PAA/IA)

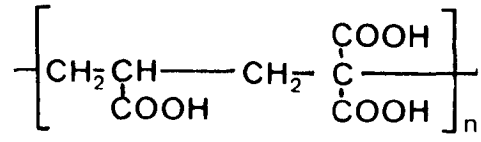

Poly(methacrylic acid) (PMAA)

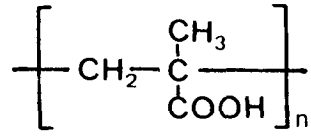

Ethylene-Maleic acid alternate Copolymer (EMA)

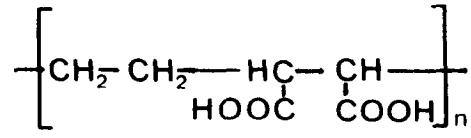

Vinyl Alkyl Ethylene - Maleic acid alternate Copolymer (VAEMA)

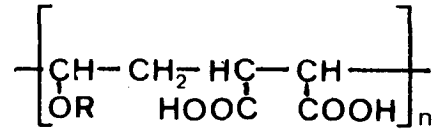

R = CH_3, C_2H_5.

Styrene-Maleic acid alternate Copolymer (SMA)

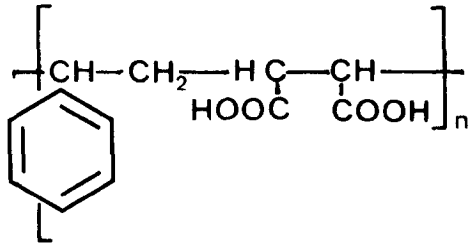

Other Synthetic Polyacids

Poly(ethylene sulphonic acid) (PESA)

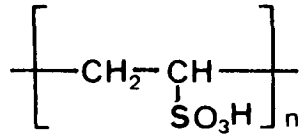

Poly(vinyl phosphoric acid) (PVPA)

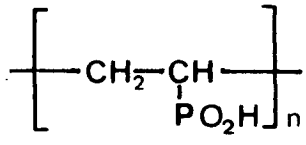

Polyphosphoric acid (PPA)

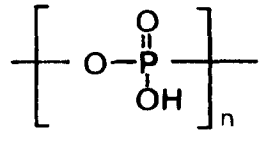

Partially sulphonated poly(vinyl alcohol) (PSPVA)

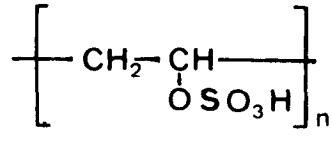

(PAA/IA) are used with a molecular weight of circa 10,000. This polyacid has a lower viscosity than the PAA solution which improves the mixing properties of the cement and the increased occurrence of carboxylic acid groups increases the rapidity of set. Other additives, such as monomeric chelating agents like tartaric acid, are commercially added to the polyacid to enhance the setting properties of the cement.

1.2.3 The ASPA Glass

The glass used in ASPA cements is known as G200 glass and has the formulation and properties shown in Table 1.3. This glass is produced by fusing mixtures of quartz and aluminia in a flux of aluminium phosphate and calcium and aluminium fluorides at temperatures of 1050°C to 1350°C for 40 to 50 minutes. The melt is then shock cooled and ground to pass a 45 micron sieve (1,42). The microstructure of this material has been established by electron microscopy to be a multiphase glass with a continuous aluminosilicate phase interdispersed with fluorite (CaF_2) droplets (1,37,42). The properties of these droplets are dependent upon thermal history and the dental glass is fused at 1150°C which gives crystaline droplets of 1.67 microns mean diameter with a volume fraction of circa 20% at the glass surface. At higher fusion temperatures both the size of the droplets and their crystalinity are reduced producing glasses with poor cementing properties.

1.2.4 The Setting Mechanism of ASPA Cements

The proposed setting mechanism for ASPA and other ionomer cements is an acid-base reaction producing cements which set by salt formation as described in Section 1.1. This reaction has been

Table 1.3

The Formulation and General Properties of ASPA Glass G200 (I)

	Fusion Mixture	% Composition (by weight)
Quartz	SiO_2	29.0
Alumina	Al_2O_3	16.6
Fluorite	CaF_2	34.3
Cryolite	Na_3AlF_6	5.0
Aluminium trifluoride	AlF_3	5.3
Aluminium phosphate	$AlPO_4$	9.9
	Fusion Temperature	1150°C
	Density of glass	2.77 Mg/m^3
	Refractive Index (20°C)	1.486
	Mean Particle size (μm)	10

studied by infra-red spectroscopy (38,181) which has demonstrated that on mixing of the ASPA glass and the polyacid the carboxylic acid groups (-COOH) of the polymer are ionised to carboxylate groups ($-COO^-$). The freed hydrogen protons are capable of reacting at the glass surface and, by a protonic transfer mechanism, metallic cations are liberated from the surface and eventually form salts with the carboxylate groups. These liberated cations have been identified as being predominantly divalent calcium ions and trivalent aluminium ions which exist as either individual ions or as fluoride complexes (AlF^{2+}, AlF_2^+, CaF^+). The rate of salt formation was studied individually as calcium and aluminium polyacrylate have separate absorption bands at 1540 cm^{-1} and 1600 cm^{-1} respectively. This demonstrated that calcium polyacrylate is formed within the first few minutes of mixing whilst aluminium polyacrylate is only formed in appreciable amounts about one hour after mixing. This behaviour was attributed to the higher entropy required to orient three carboxylate groups round the aluminium ion than two carboxylate groups round the calcium ion and because the aluminium ions were bound in the silicate network of the glass whereas the calcium ions were readily liberated from the dispersed phase of the glass. These observations have led to the proposal that the formation of calcium polyacrylate is responsible for the rapid setting properties of the cement whilst the formation of aluminium polyacrylate is responsible for the high strength of the cements (1,39,41). It has also been proposed that this cement forming mechanism leaves the glass particles completely sheathed in a siliceous hydrogel containing isolated fluorite crystallites (1, 42). Silica gel has been identified by infra-red spectroscopy (38) and its geometric location has been indicated by depletion of functional cations at

the glass particle surface by electron microprobe analysis of the set cement (1,37).

With multivalent metallic ions the nature of the salt formation is of interest as this is believed to influence the mechanical properties of the cement. The exact structure of the salt forms in ASPA cements remains speculative but a number of possible configurations have been proposed (1,39) as shown in Figure 1.2. Stress relaxation studies (39,41) have shown that bond interchange mechanisms and molecular mobility occurs in young ASPA cements indicating calcium polyacrylate to have an in-chain disalt or pendant half-salt form. The development of rigidity with time suggests that aluminium polyacrylate forms cross-chain disalts (41).

1.2.5. The Function of Water in ASPA Cements

Water is an integral part of the ASPA system providing about 20% of the total weight in a freshly prepared cement mixed at a powder to liquid ratio of 2:1 (g/ml). It has been established that this water performs two functions (1,39,45,49).

1. It acts as a solvent for the polyacid
2. It hydrates the reaction products.

These two functions enable the ion-leaching reaction and subsequent salt formations to occur. Thermogravimetric studies (45,49) and weight loss studies (1,40,45,49) have shown that there are two types of bound water in the set cement, tightly and loosely bound water.

The tightly bound water is believed to exist in two ways.

1. Water co-ordinated to metallic ions,
2. Water hydrating the carboxyl groups on the polyacid chain.

Figure 1.2 Hypothetical Structures of Molecular Species in Ionomers and Ionomer Cements (1,17,40)

1.

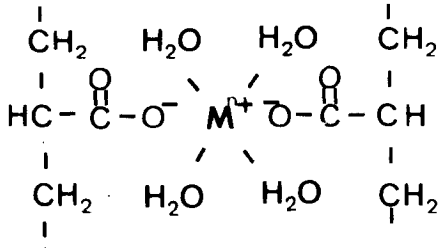

2.

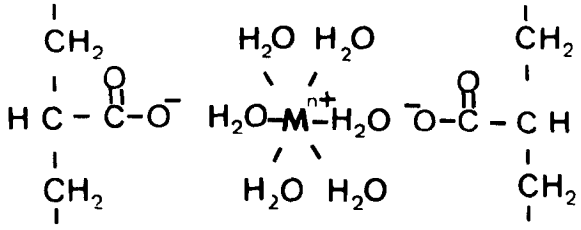

3.

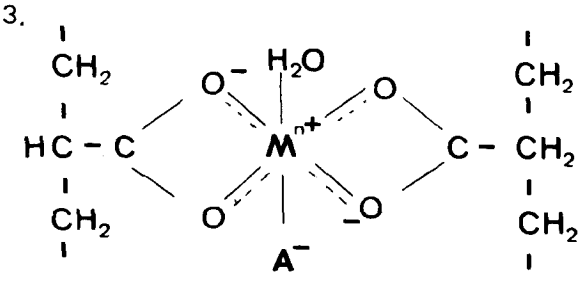

CROSS CHAIN DISALTS

4.

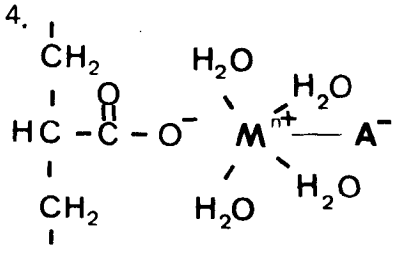

5.

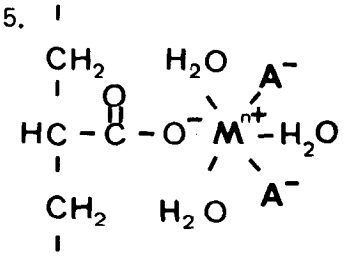

PENDANT HALF SALTS

6.

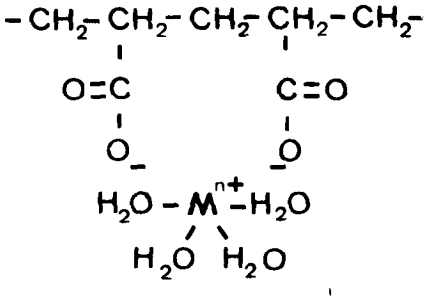

IN CHAIN DISALT

For ASPA M^{n+} = Ca^{2+} or Al^{3+} & A^- = F^- or H_2O

The proposed mechanisms of the nature of water bound to the metallic ions is shown in Figure 1.2. Both aluminium and magnesium are known to each have six water ligands attached to give $Al(H_2O)_6^{3+}$ and $Mg(H_2O)_6^{2+}$ respectively. The cases for other ions such as calcium and zinc is less certain but they are thought to behave in a similar manner (1,39,186). Magnesium and zinc are the functional ions in the dental zinc(polycarboxylate) ionomer cements of Smith (28,29).

The water tightly bound to carboxyl groups on the polyacid chain is believed to behave according to the model proposed by Ikegami (48) as shown in Figure 1.3. Each anion (COO^-) is hydrated by oriented or intrinsic water which in turn is sheathed by a cylinder of secondary or less tightly bound water. Wilson and Crisp (1,40) have proposed that each anion retains 4-6 molecules of water depending upon the powder to liquid ratio of the cement and the ratio of carboxyl groups to carbon atoms in the unit structure of the polyacid.

The loosely bound water is defined as the water which can be removed by desiccation at low humidities (1,40,49). However, some discrepancies arise in the amount of loose water in the cement. Wilson and Crisp have proposed that only 1-3% of the total cement weight is due to loose water (1,40), whilst others (45,49) suggest that up to 12% of the total cement weight can be lost by desiccation at 0% humidity.

1.2.6. The Mechanical Properties of ASPA Cements

The mechanical properties of ASPA cements are influenced by a large number of variables and have been found to be dependent on the glass

Figure 1.3 The Ikegami Model for Intrinsic and Secondary Water in Polyacrylate Chains (48)

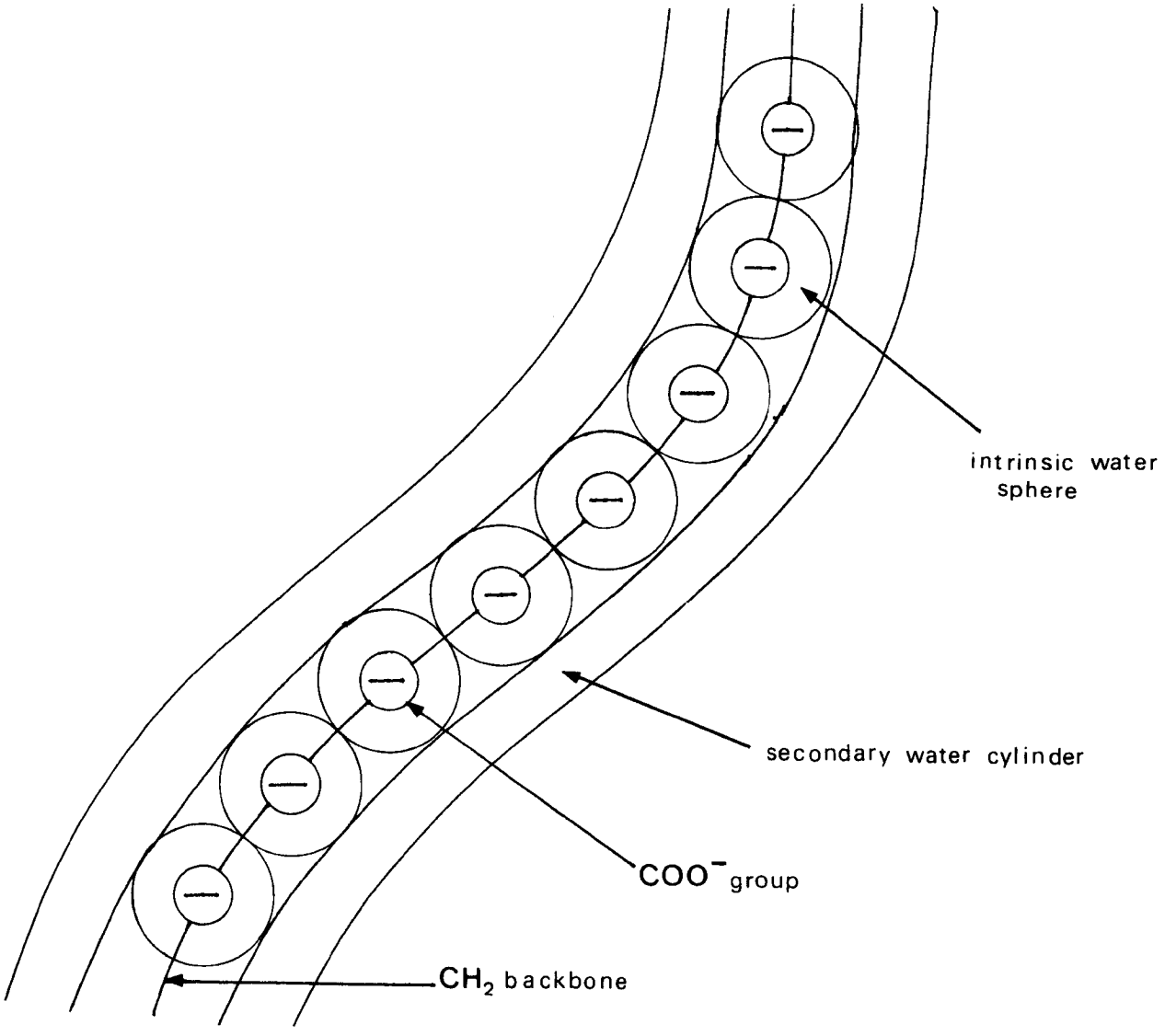

composition, the nature of the polyacid, the volume fraction of glass in the cement mix, the age of the cement and its water content and shrinkage properties.

The Effects of Glass Composition

Wilson and co-workers have studied the effects of glass composition on the mechanical properties of a range of fluoroaluminosilicate glass ionomer cements and of non-fluoride containing glass ionomer cements (43,44). These studies demonstrated that slight variations in the composition and fusion temperature of the glass led to variations in mechanical properties of the cement due to the complex microstructure of these multi-phase glasses. However, it is evident that glasses of high aluminosilicate ratios (Si:Al) have extended manipulative and setting properties whilst mechanical performance is impeded at ratios of less than 1:3. Increases in the aluminium phosphate content of the glass are also known to extend setting times and improve mechanical properties of the cement and a fluorite content of 30-40% by weight is required to confer mechanical strength. Generally, high fluoride content glasses are preferred in dentistry as these produce cements of the required workability and with cariostatic properties. The glass G200 was selected by Wilson for its balance of dental properties.

The Effects of Polyacid Variations

The type of polyacid has been found to effect the properties of ASPA cements with copolymers of PAA (PAA/IA and PAA/MA) producing cements with enhanced workability, sharper set but with similar mechanical properties to cements prepared from the homopolymer (35). Variations in the molecular weight of PAA solutions from 14,000 - 23,000 also had little effect on the mechanical properties of the cement (35). However, decreases in the concentration of the

the polymer in the aqueous polyacid solution is known to reduce mechanical performance of the cement with, for example, a decrease in polymer content from 50-25% in the polyacid solution giving a corresponding decrease in compressive strength of 130-50 MPa, with the weaker cement showing more ductile behaviour (46).

The Effects of the Volume Fraction of the Glass in the Ionomer Cement

The volume fraction of the ASPA glass in the cement has significant effects upon its mechanical properties. In dental technology the volume faction of the glass is expressed as the powder to liquid ratio (P:L g ml^{-1}) and the effects of varying this ratio are shown in Table 1.4. The greater the proportion of the glass used, the more reactive and stronger the cement up to a limiting P:L ratio of circa 3:1; at higher ratios the cements are difficult to mix and strength declines (1,49).

The Effects of Cement Age

The age of ASPA cements is known to influence their mechanical properties as they show a progressive increase in strength with time as shown in Figure 1.4. This increase in strength has been attributed to continuing salt formation of metallic ions with the PAA matrix and to more water becoming tightly bound within the set cement (40,45,49).

The Effects of Water Loss and Shrinkage

The humidity of the storage environment has considerable effects on both the mechanical and dimentional properties of freshly prepared ASPA cements as shown in Figure 1.5. Loosely bound water is lost and shrinkage occurs as the cement obtains an equilibrium with its environment. On desiccation from 100% to 70%

Table 1.4 The Physical Properties of ASPA Cements (1,35,49)

Property	Powder to Liquid (P:L) Ratio (g:mls)					
	3.5:1	3.0:1	2.5:1	2.0:1	1.5:1	1.0:1
Work time (mins)	-	3.5 *	4.25 *	-	-	-
Setting time (mins)	3.5 *	4.75*	7.25 *	-	-	-
Compressive Strength 7 Days (M Pa)	214 *	222 *	144	174	148	114
Compressive Modulus 7 Days (M Pa)	3580	3620	3030	2670	3045	2380
Diametrial Tensile Strength 24 hours (M Pa)	13	15	-	-	-	-

All cements formed with 47.5 w/w PAA and stored at 80% RH

* 50.0 w/w PAA and stored in water.

Figure 1.4 The Ageing Properties of ASPA Cements (45,49)

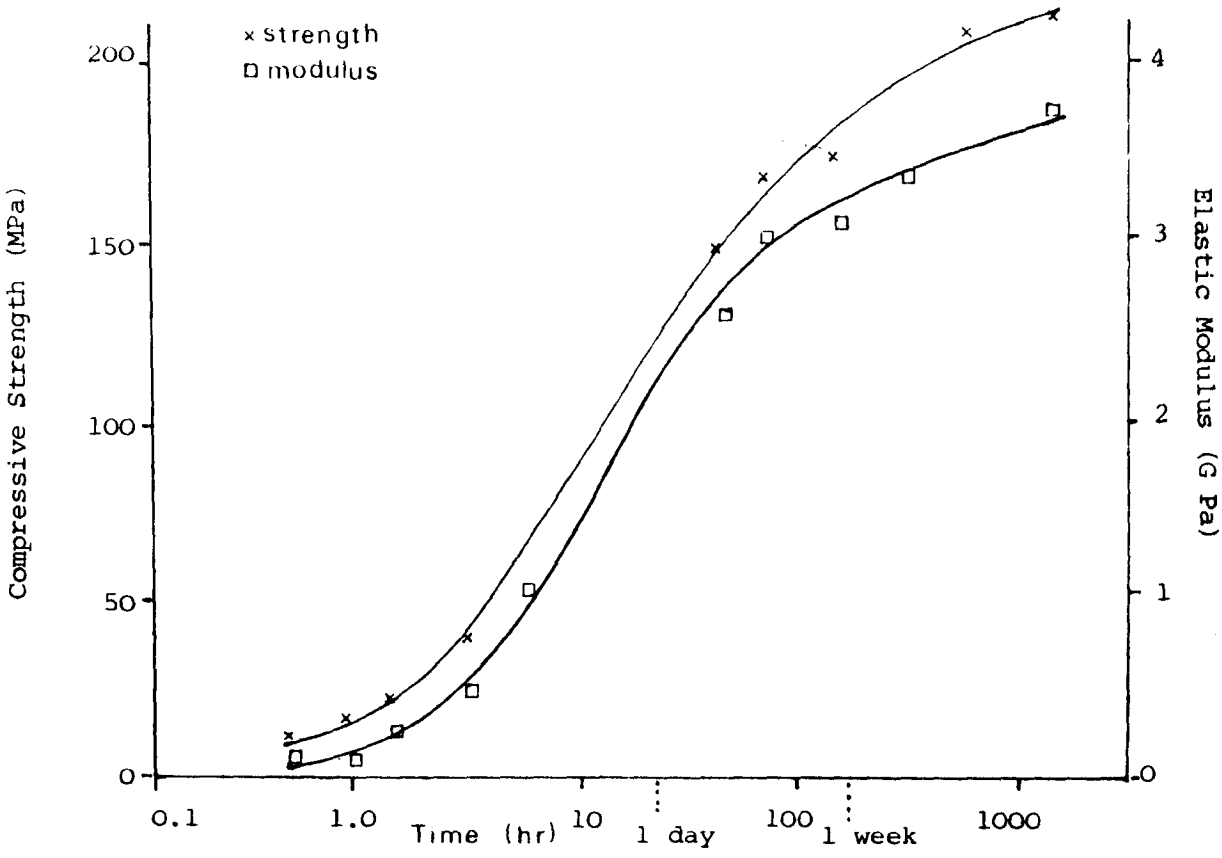

Figure 1.5 The Effects of Relative Humidity on the Mechanical Properties of ASPA Cements (45,49)

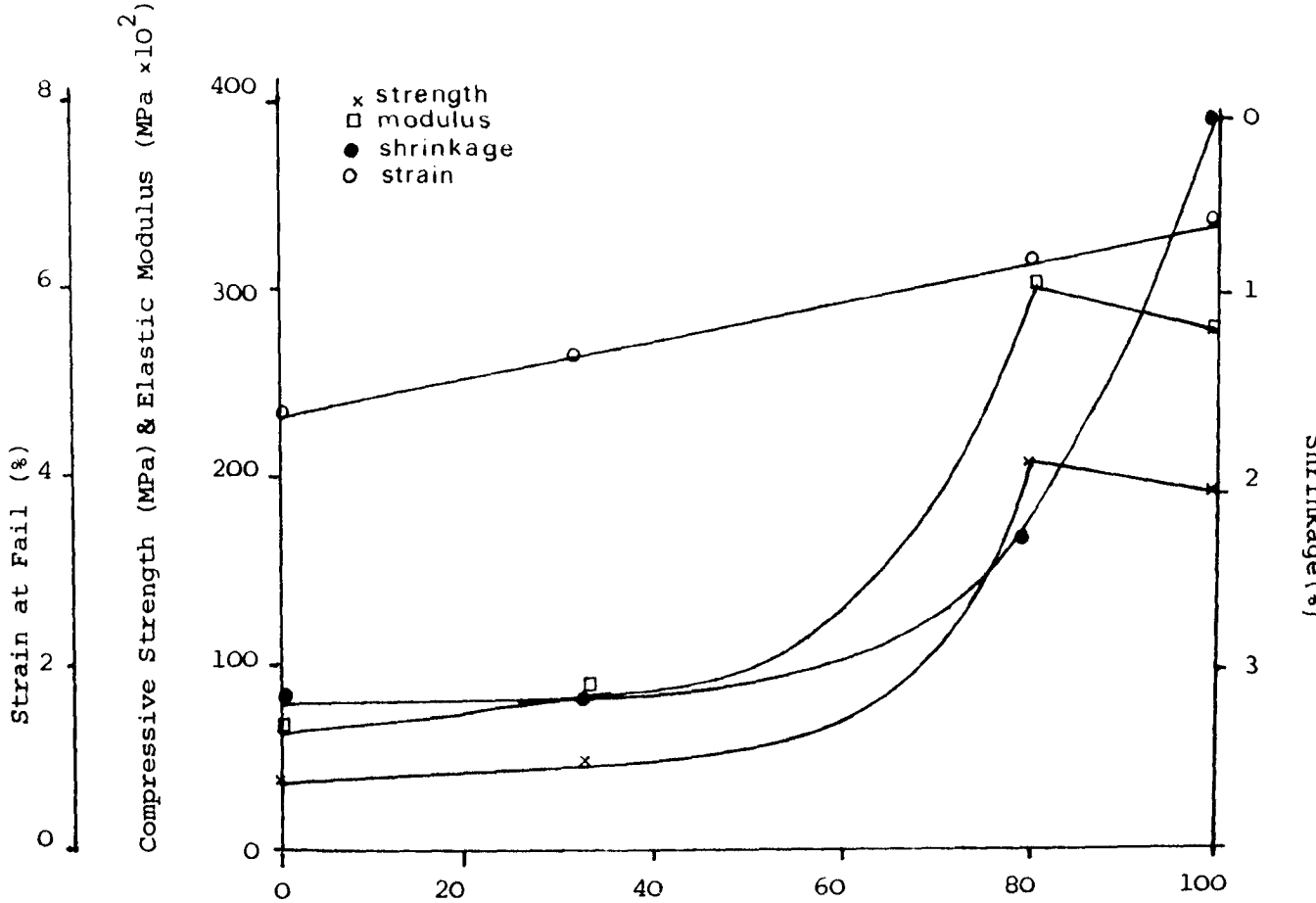

humidity slight shrinkage occurs which generally tightens the cement structure and improves mechanical properties,but further water loss and shrinkage at lower storage humidities causes a rapid deterioration of cement properties. This has been attributed to the shrinkage of the cement causing contact between the glass particles and to microcracks occurring at the glass-matrix interface (40,45,49). Samples aged at 100% humidity prior to exposure at low humidities displayed lower weight loss and shrinkage and had improved mechanical properties, this was attributed to more water becoming tightly bound with time in the set cement. From these studies it has been proposed that a matrix shrinkage in excess of 7% causes the marked loss in mechanical properties (187).

1.3 Other Ionomer Cements

1.3.1 Glass-Ionomer Cements

Little work has been published on the use of glass-ionomer cement for applications outside dentistry but Wilson and co-workers evaluated a range of aluminosilicate glasses designed to be less complex than ASPA glass (43,44) and they investigated the potential of non-fluoride containing glasses (49). Glasses with a high fluoride content, such as ASPA glass are corrosive towards crucibles and furnace linings at fusion temperatures and the use of alternative fluxes, such as calcium oxide, is advantageous. This work demonstrated that strong and hydrolytically stable ionomer cements could be produced with calcium oxide containing glasses and such cements had longer work times and setting times but were generally weaker than glasses prepared with calcium fluoride at similar Al:Si ratios. Further cements from

these glasses showed similar dependencies on factors such as the Al:Si ratio and the additions of aluminium phosphate as did cements from calcium fluoride containing glasses.

1.3.2 Mineral - Ionomer Cements

A range of naturally occurring minerals and some synthetic minerals have been found to react with aqueous solutions of PAA (7,8,49) and with other polyacids (49). Ionomer cements are formed from minerals which are able to decompose under acid attack and liberate metallic cations for subsequent salt formation with the polyanions. The susceptibility of these minerals to acid attack is related to their structural type and composition with island silicates being more readily attacked than the more complex structures of the chain and sheet silicates which in turn are more reactive than the three-dimensional silicates. This order also reflects the order of basicity of the minerals with the less reactive minerals having higher contents of the acidic SiO_2 group. However, there were exceptions to this order, notably minerals having high Al:Si ratios were susceptible to acid attack irrespective of structure. The hydrolytic stability of mineral-ionomer cements has been found to be dependent on the nature of the functional cations present. Minerals containing only calcium cations formed hydrolytically unstable cements whilst mineral cements containing zinc or aluminium ions formed hydrolytically stable cements. The mechanical properties of mineral-ionomer cements are generally inferior to ASPA cements but this has been attributed to the lower powder to liquid ratios used in these studies and to the higher void content of the mineral cements. A selection of mineral-ionomer cements which display strength and hydrolytic stability are shown in Table 1.5.

Table 1.5 Mineral-Ionomer Cements displaying good strength and hydrolytic stability (7,8,49)

Mineral	Structure	Comp. Strength (1) (MPa)
Island Silicates		
Willemite	$Zn_2(SiO_7)$	34.0
Hemimorphite	$Zn_4(Si_2O_7)(OH)_2H_2O$	20.6
Hardystonite	$Ca_2Zn(Si_2O_7)$	12.0
Chain Silicates		
Wollastonite (2)	β - $Ca(SiO_3)$	0.2
Sheet Silicates		
Aphrosiderite (3)	$(FeMgAl)_{12}(Si,Al)_8O_{20}(OH)_{16}$	50.0
Thuringite (3)	$(FeMgAl)_{12}(Si,Al)_8O_{20}(OH,F)_7$	23.0
Muscovite	$K_2Al_4(Si_6Al_2O_{20})(OH,F)_4$	24.0
3-Dimensional Silicates		
Scolecite	$Ca(Al_2Si_3O_{10})3H_2O$	17.6
Hackmanite (4)	$Na_8(Al_6Si_6O_{24})(Cl_2S)$	40.0

N.B. All cements prepared with 50% aqueous PAA solution and with P:L ratios of between 2 - 3:1

(1) Compressive strength variable depending on age, storage conditions, etc. generally cements were stored for 7 days in a humid environment or in water.

(2) Softened in water

(3) Simplified structure

(4) Stored in paraffin.

1.3.3 Metal Oxide - Ionomer Cements

The reactions of metal oxide powders with aqueous polyacid solutions has been investigated by a number of researchers (4,38,45,49,50). Infra-red spectroscopic studies (38,49) have revealed that certain metal oxides (ZnO, MgO, CuO, HgO, Y_2O_3), react completely with aqueous PAA as characterised by the absence of absorption bands associated with the unreacted polyacid. Other metal oxides, such as trivalent metal ions (Al_2O_3, Bi_2O_3) and alkaline earth metals (CaO, SrO, BaO) display partial reaction with the polyacid whilst other less basic oxides (V_2O_5, $Cr\ O_3$ and $Mo\ O_3$) are slower in reacting or are inert. Such behaviour has been attributed to the basicity of the metal oxide and to the poor reactivity of highly stabilised crystal structures of some basic metal oxides (TiO_2, Fe_2O_3) (49).

The hydrolytic stability of metal oxide cements followed these trends with the more basic metal oxides producing cements of greater stability. These trends of stability are also reflected by the metallic ion - carboxylate stability constants (4,50) which had the following sequence with polyacrylates below zinc in the series being hydrolytically unstable.

$$Cu^{2+} > Zn^{2+} > Ni^{2+} > Co^{2+} > Ca^{2+} > Mg^{2+}$$

Spectroscopic studies (38) have further suggested that Cu, Al, Li, Bi and possibly Zn metal-polyacrylate bonds have some degree of covalency whereas the less stable Mg and Ca metal polycarboxylate bonds are purely ionic.

The mechanical properties of metal oxide-ionomer cements are inferior to ASPA cements as shown in Table 1.6. Direct comparison of these cements is difficult due to variations in the P:L ratios, variations

Table 1.6

The Mechanical Properties of Metal Oxide-Ionomer Cements (45,49)

Cement	P:L ratio	Comp. Strength MPa	Comp Mod MPa	Strain at fail (%)	Porosity (%)
ZnO/PAA	1:1	76	1400	5.4	18
CuO/PAA	2:1	83	1020	8.1	24
PbO/PAA	2:1	26	610	4.3	26
HgO/PAA	1:1	29	660	4.4	25
Bi_2O_3/PAA	2:1	32	970	3.3	12
MgO/PAA	1:1	58	450	12.9	-
B_2O_3/PAA	1:2	38	480	5.6	-
ASPA/PAA	2:1	174	2670	6.4	5

PAA = 46.7 w/w aqueous solution

in the porosity and because some metal oxides reacted rapidly with the polyacid prohibiting thorough mixing; in particular ZnO required deactivation by thermal treatments before coherent cements could be produced. Zinc oxide cements were noticeably stronger and stiffer than other metal oxide-ionomer cements and have been used in dentistry where advantage is take of the rapid setting properties (28,29).

1.3.4. Modified ASPA Cements

As the preceding sections have demonstrated, the ASPA system is mechanically superior to other forms of ionomer cements. However, the ASPA system has a number of limitations which has restricted its use in applications outside dentistry. Notably these are its high cost, its loss of strength and rigidity in environments of low humidity and its rapidity of set which prevents the fabrication of mouldings larger than dental fillings. To overcome these limitations attempts have been made to modify the ASPA system and broadly two approaches have been adopted.

1. Methods for controlling the setting rate.
2. Methods of preventing water loss from the cement at low humidities.

Methods of controlling Setting Rate of ASPA Cements

The setting rates of ASPA cements have been retarded by partial replacement of the ASPA glass with fillers to give materials referred to as filled-ionomer cements. Various studies of these materials (45,49,55-58) have revealed similar tendences with progressive replacement of the ASPA glass producing cements of extended moulding and setting times but with decreased mechanical performance. The mechanical properties of filled-ionomer cements has been shown to

be dependent upon the characteristics of the filler. Carrillo (58) has demonstrated that the strength of filled ionomer cements are improved by decreasing the particle size of the filler, as shown in Figure 1.6., but the smallest filler used had a particle size of 90 microns, which is considerably larger than the mean particle size of ASPA glass, and only low levels of ASPA replacement were employed. Asbestos fibres have also been used as fillers (58) but produced weaker composites than particulate filled ionomer cements due to poor wetting of the fibre by the polyacid and to a high incidence of voids in fibre filled cements. Others have observed that the mechanical properties of filled ionomer cements can be improved by using fillers coated with a silane coupling agent (49,57), by using fillers of high surface area (57), by using fillers with slow reactivity towards the polyacid and by using carbon fibres (55). However, these observations were not systematically examined.

Methods of Preventing Water Loss from ASPA cements at low humidities

The shrinkage of ionomer cements, which occurs as water is lost at lower humidities, is known to decrease as the powder to liquid ratio is increased (45,49). However, problems in mixing ASPA cements occur at P:L ratios higher than 3.0, but with filled-ionomer cements P:L ratio of 4.0 can be employed and shrinkage is retarded, but this study was inconclusive as the filled cements were not mechanically tested a low humidities.

The water in aqueous PAA solutions can be replaced by 10-50% aqueous solutions or organic solvents such as dioxane, dimethyl formamide, acetone and isopropylalcohol. Cements prepared from

Figure 1.6 The Effect of Filler Particle Size on the Tensile Strength of Filled-ASPA Cements (58)

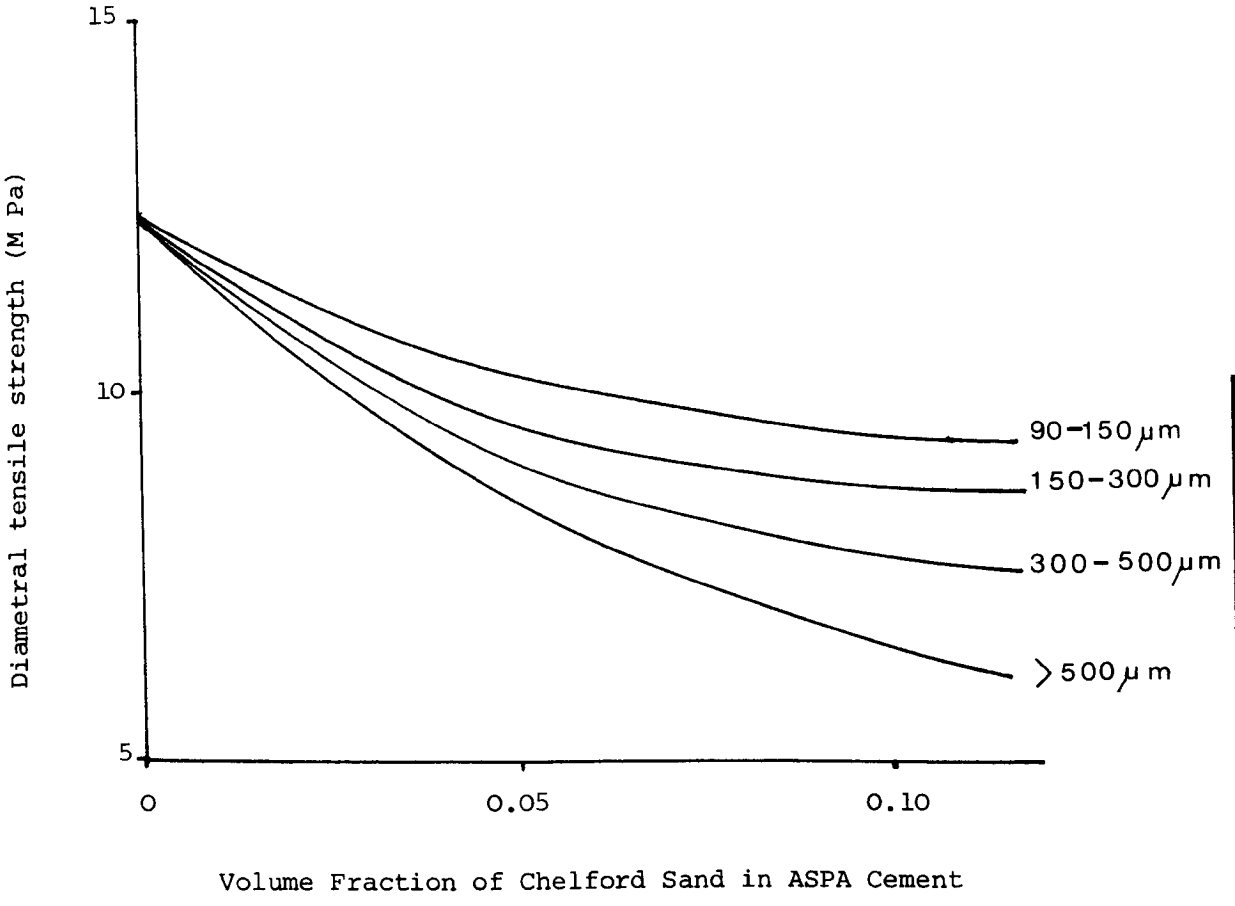

these solutions display less weight loss and superior mechanical performance to the water based ASPA cements at low humidities but are weaker than the water based cements when stored in environments of high humidity. This effect was not fully explained by the vapour pressure of the solvent mixture as some were more volatile than water (49).

1.4 Other Ionomer Systems

The physical and mechanical properties of anhydrous ionomer systems have been studied by Eisenberg and co-workers (9-15,53,54) and by Neilsen and co-workers (16-18). These systems are of interest as they demonstrate the effects of metallic ion addition on the properties of various polymers and the dependence of these properties on the nature and concentration of the metallic ions. These studies provide information on properties such as transition temperatures and flexural mechanical properties which, for various reasons, have not been fully studied with ionomer cements. These studies also demonstrate the effects on mechanical properties of cements prepared with low water contents and the effects of moulding conditions as, for example, ionomers are generally fabricated by compression moulding under pressure (70Pa) and at elevated temperatures (300^{o}C) whereas ionomer cements are moulded at ambient temperatures and under low pressure conditions.

1.4.1. Mechanical Properties of Ionomers

The strength and stiffness of ionomers has been investigated by Neilsen (18) and a selection of his results are given in Table 1.7. But, the polyacrylic acid copolymer used contained residual water which vapourised during moulding necessitating mould venting and produced defective samples which weakened the materials and made comparison difficult. However, the results demonstrate that the addition of metallic ions improves the mechanical properties of the polymer and shows that zinc polyacrylate ionomers are substantially stiffer and stronger than similar calcium or lead polyacrylate ionomers. It is also evident that further additions of fillers reinforced the zinc ionomer and produced high performance composites with moduli several times that of the unfilled zinc polyacrylate and of other unfilled conventional polymers such as polystyrene. Neilsen (17,18) has also shown that zinc ionomers retain their stiffness at temperatures in excess of 300^{o}C. This has been attributed to the high glass transition temperatures (Tg) of these materials brought about by the addition of metallic ions. Eisenberg's studies have revealed that increases in the metallic ion content of an ionomer progressively increases its Tg but the rate of increase is dependent on the ionic charge of the cation and the inter-nuclear distance between the cation and the anion and is thus dependent upon the host polymer and metallic ions used.

1.4.2 The Behaviour of Metallic Ions in Ionomers

Neilsen and Fields (17) suggest that three zinc polyacrylate molecular forms are possible, the in-chain disalt, cross-chain disalt and pendant half-salt as shown in Figure 1.2 but without the associated water. It is believed that the two disalt forms

Table 1.7 The Mechanical Properties of Polyacrylate Ionomers (18)

Polymer	Filler	Volume Fraction	Shear Modulus (G Pa)	Flex. Modulus (G Pa)	Flex. Strength (M Pa)	Comp. Strength (M Pa)
Polystyrene	-	-	1.20	-	-	102.7
Poly(acrylic acid)	-	-	2.78	7.17	-	174.4
Ca-PAA	-	-	5.56	-	-	106.2
Pb-PAA	-	-	5.16	-	-	128.3
Zn-PAA	-	-	6.20	18.34	67.78	373.0
"	'E' Glass fibres (a)	0.40	8.83	20.75	85.98	139.1
"	Stainless steel fibres (b)	0.46	-	61.92	558.3	-
"	Treated Mica	0.40	18.7	37.0	140.7	156.5
"	Boron Fibre	0.42	16.9	127.7	777.6	-

a = unoriented fibures

b = oriented fibres

provide the stiffening effect in ionomers giving rise to their high mechanical performance and high Tg. The half-salt formation, which is expected to predominate in ionomers where the reaction is incomplete or where the Zn^{2+} content is stoichiometrically higher than the carboxylate content of the polyacid, would result in lower modulus ionomers with reduced Tg's and with enhanced damping properties. This has been attributed to the transient behaviour of the half-salt form which is capable of bond interchange at temperatures lower than the Tg of the ionomer.

1.5. The Mechanical Properties of Particulate Filled composites

Fillers are used to modify the properties of polymers, the effects of their addition to polymers can be summarised as follows (64,68, 69,86).

1. Fillers generally improve the stiffness and dimensional stability of polymers. However, other mechanical properties such as strength, damping and impact resistance may be improved by the addition of fillers but incorrect selection of the filler may impair these properties.
2. Fillers improve and control the physical properties of polymers such as their heat distortion temperature, thermal conductivity, permeability to gases and liquids and can be used to modify electrical and density properties.
3. Fillers can be used to reduce the costs of polymeric materials.

Filled polymers have a composite structure, as described in Section 1.1; the properties of composites are dependent upon a number of variables such as the moduli of the various phases, the volumes occupied by the filler in the matrix and the

characteristics of the filler. Polymer composites are normally classified according to the nature of the dispersed phase as follows (64).

1. Particulate filled composites. These are normally isotropic materials filled with either rigid particles, such as the ASPA system, or with rubbery particle such as in impact resistant polystyrenes.

2. Fibre filled composites. These are usually thermosetting polymers filled with glass or carbon fibres. The use of oriented fibres confers greater composite stiffness than with particulate fillers but this introduces anisotropic behaviour to the system.

3. Skeletal or inter-penetrating network structures.

This review is concerned with the mechanical properties of particulate filled composites and in particular composites filled with rigid particles as such materials have similar characteristics to ionomer cements.

Theoretical approaches towards the understanding of the mechanical properties of particulate composites has been reviewed by a number of authors (58,62-75), the majority of these approaches consider the enhancement of modulus with the progressive addition of a filler. The strength and strain behaviour of particulate composites has been described in a less quantitative manner because these properties are more sensitive to the physical characteristics of the filler and the interfacial adhesion between the filler and the matrix than stiffness. Further, modulus is normally measured at lower strains than strength and is thus prone to less variation. Consequently the stiffness and strength properties of particulate composites are reviewed separately.

1.5.1. The Modulus Properties of Particulate Filled Composites

Many of the theories that have been developed to explain the reinforcing effect of a particulate filler in a composite are derived from Einstein's hydrodynamic equation (1.1) for the rheological behaviour of a suspension of spheres in a Newtonian liquid.

$$\eta_c = \eta_1 (1 + K_E \ \phi_2) \qquad 1.1$$

where the symbols used are defined in Table 1.8.

By applying the relationship between relative viscosity and relative shear modulus (equation 1.2), the Einstein relationship has been modified to describe the modulus behaviour of composites.

$$\frac{\eta_c}{\eta_1} = \frac{G_c}{G_1} = (1 + K_E \ \phi_2) \qquad 1.2$$

The Einstein coefficient (K_E) can be varied to account for non-spherical shapes but this equation is only valid for dilute suspensions and the relationship between relative viscosity and relative shear modulus only holds for composites where the Poisson's ratio is 0.5, that is where no volume change occurs on extension (64,65,76).

Despite these limitations, these equations demonstrate that the most dominant factor influencing modulus properties is the volume fraction of the filler (ϕ_2) but excludes other factors such as interparticle contact, matrix-particle interfacial adhesion and the effects of voids. Consequently, equation 1.2 has been modified by a number of workers and other approaches have been developed to more fully describe the stiffness properties of composite materials; a number of these theories are given in Appendix 1. These theories take the generalised form proposed by the Neilsen equation (64,65,77) as follows:

Table 1.8 Nomenclature used to Describe the Mechanical Properties of Composites

Symbols

$\emptyset$ = Volume fraction

M = Generalised modulus term

Mr = Relative modulus = $\frac{M_c}{M_1}$

G = Shear modulus

E = Elastic modulus

K = Bulk modulus

ν = Poisson's ratio

η = Viscosity

σ = Tensile strength

σ_y = Tensile yield strength

ϵ = Strain

ϵ_f = Strain at fail

$\emptyset$ max = Volumetric packing fraction = $\frac{\text{true volume}}{\text{apparent volume}}$

a = Aspect ratio = l/d

d = Particle diameter

l = Particle length

Other symbols are defined in the text.

Suffixes

c = Property of the composite

1 = Property of the matrix

2 = Property of the filler

v = Property of a void phase

$$\frac{M_c}{M_1} = \frac{1 + AB\,\phi_2}{1 - BC\,\phi_2} \qquad 1.3$$

where the symbols are defined in Table 1.8 and where:

A = a factor dependent on the geometry of the filler and the Poisson's ratio of the matrix.

B = a factor dependent on the relative moduli (M_c/M_1) of the composite.

C = a factor to account for the packing behaviour and state of agglomeration of the filler

$$C = 1 + \phi_2 \frac{(1 - \phi\ max)}{\phi^2\ max}$$

A selection of these theories are shown graphically in Figure 1.7 along with practical data for glass spheres in epoxy and polyester matricies (67). None of these theories fully explains the relationship between modulus and volume fraction of the filler in a composite and assumptions are made which are practically invalid, such as the existence of perfect interfacial adhesion between the filler and the matrix, that uniform dispersion of the particles occurs and that there is an absence of voids in the composite. In practice particle agglomeration and voids are known to exist and interfacial adhesion can be variable; these effects have been examined in isolation. For example, the Mooney relationship and the Neilsen equation (1.3) are the only approaches which consider the effects particle agglomeration by considering the volumetric packing fraction (Ø max). As the value of Ø max increases and particle packing becomes more efficient, then the extent of inter-particle contact is increased which can seriously weaken a composite. However, the Mooney relationship is only valid for a Poisson's ratio of 0.5 and gives unrealistically high

Figure 1.7 Theoretical Relationships Between the Volume Fraction of Filler and the Relative Modulus of Particulate Composites

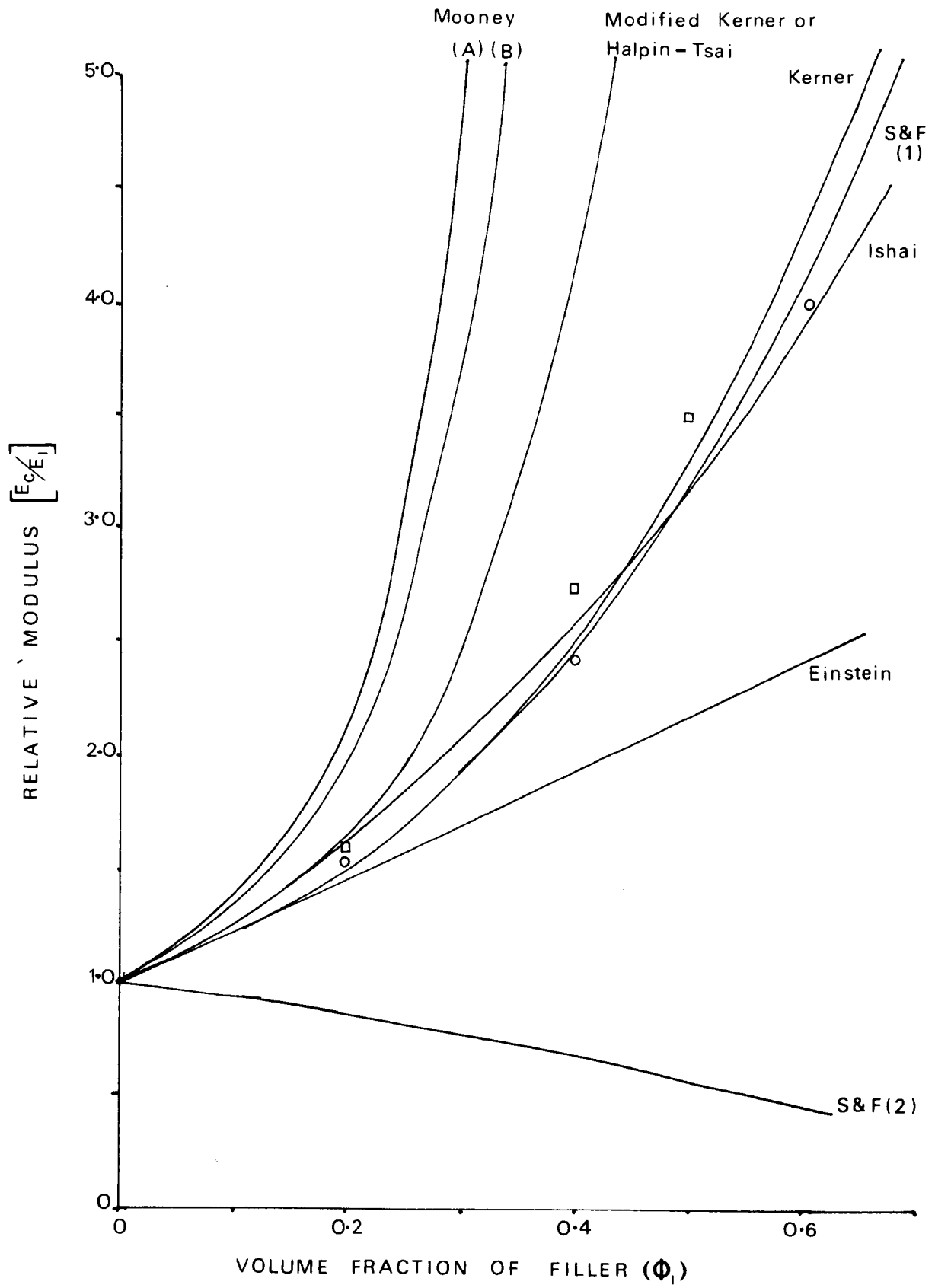

N.B. S & F = Sato - Furukawa; 1 = Perfect Adhesion ; 2 = Poor Adhesion
Mooney; A = Φ max 0·55 ; B = Φ max 0·71
□ = Glass - Epoxy & ○ = Glass - Polyester Composites (67)

values of relative modulus.

The Kerner equation, which incidentally agrees well with practical data for spherical inclusions in a rigid polymer matrix, takes no account of particle size, shape or interfacial adhesion. The approach by Sato and Furakawa (78), which is based on the concept of internal deformation of a material displaying rubber elasticity, is the only approach which considers interfacial adhesion. It was postulated that where adhesion is poor the deformation of the matrix leads to dewetting at the glass particle interface with the subsequent formation of ellipsoidal cavities around the particles which reduces the composite stiffness. The adhesion cavitation factor is difficult to measure experimentally and this approach is only valid for spherical inclusions in rubbery matrices. The approaches by Cohen and Isahi (79,80) and by Price and Nelson (81) are the only approaches which consider voids as a third phase in a composite. However, these theories do not account for variations in void size neither do they consider the variables of the rigid filler phase.

All of the above theories predict that the moduli of particulate composites are independent of particle size but in practice size can have marked influence on the moduli of composites (82) and of filled ionomer cements (58) with stiffness increasing with decreasing particle size.

1.5.2. The Strength and Other Mechanical Properties of Particulate Filled Composites

A number of approaches have been adopted to characterise the stress-strain behaviour of particulate filled composites. At a first approximation, it would be reasonable to assume that an enhancement of modulus would be accompanied by increases in strength of the composite. However, in practice there is a tendency for filler to decrease strength with increasing volume fraction (64,65,83-87) but

there are also cases where no decrease in strength occurs (64,65,71 82,88-90) and where good interfacial adhesion exists composite strength can be increased (64,82,90). There is a tendency for fillers to reduce the strain at fail of composites (64,65) but again situations exist where this property is increased with filler addition (85,86). Also, the fracture energy of particulate composites has been found to vary and is influenced by the degree of interfacial adhesion.

Stress-strain Property Relationships

Nicolais and co-workers (84-88) have studied the yielding behaviour of composites filled with glass spheres and have developed generalised relationships for the yield stress of composites where perfect and poor interfacial adhesion occurs.

For perfect interfacial adhesion:

$$\sigma_{yc} = \sigma_{y1} \qquad 1.4$$

For poor interfacial adhesion:

$$\sigma_{yc} = \sigma_{y1} \quad (1 - 1.21 \, \phi_2^{2/3}) \qquad 1.5$$

Where the symbols are defined in Table 1.8 and these relationships are shown graphically in Figure 1.8.

Although these equations apply well to glass particles in rigid polymer matricies such as polystyrene copolymers, ABS and epoxy resins, they fail to account for the effects of particle size, particle packing properties, deviations from the spherical shape and the effects of voids which all have considerable influence on the strength of composites as discussed in the following sections.

The strain behaviour of composites has been studied by Neilsen (67, 65) who derived a generalised equation (1.6) for the reduction in strain at failure which occurs with the addition of fillers.

Figure 1.8 Theoretical Relationship between the Volume Fraction of Filler and the Relative Strength of Particulate composites(86)

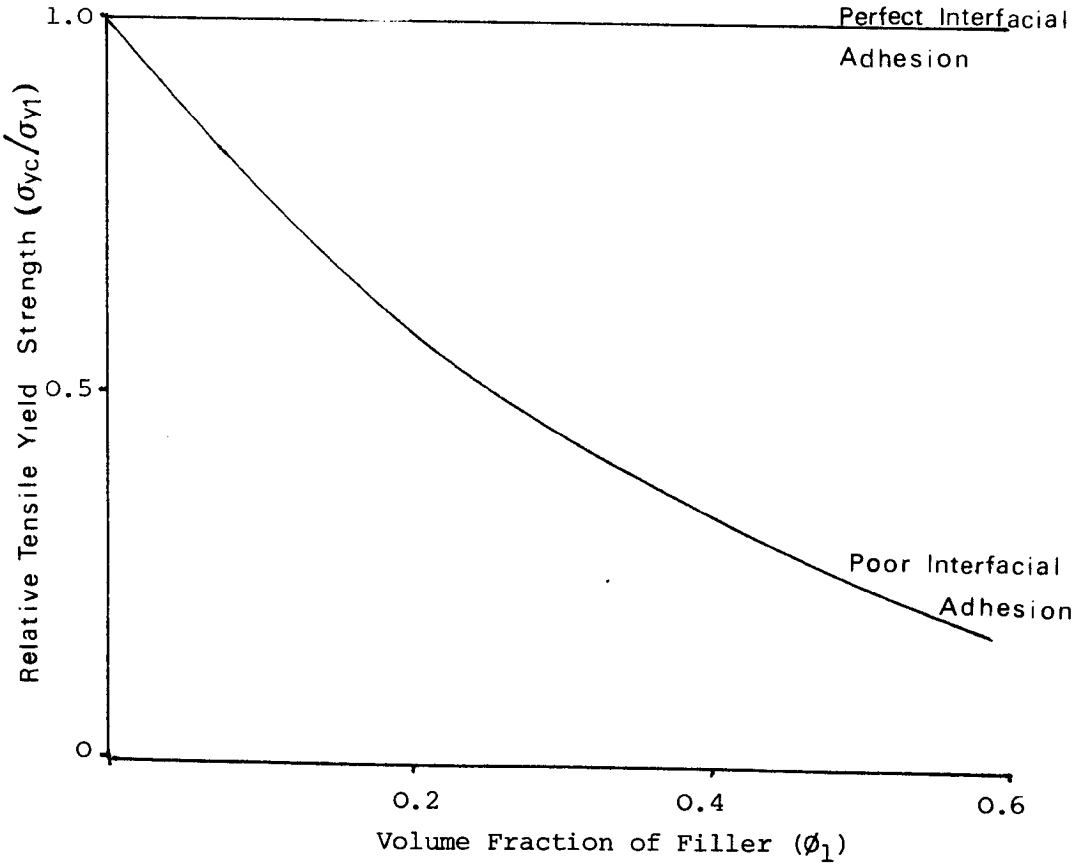

Figure 1.9 Relationship Between the Volume Fraction of Filler and (1) the Energy to Break and (2) the Ultimate Strain of Particulate Composites (85,86).

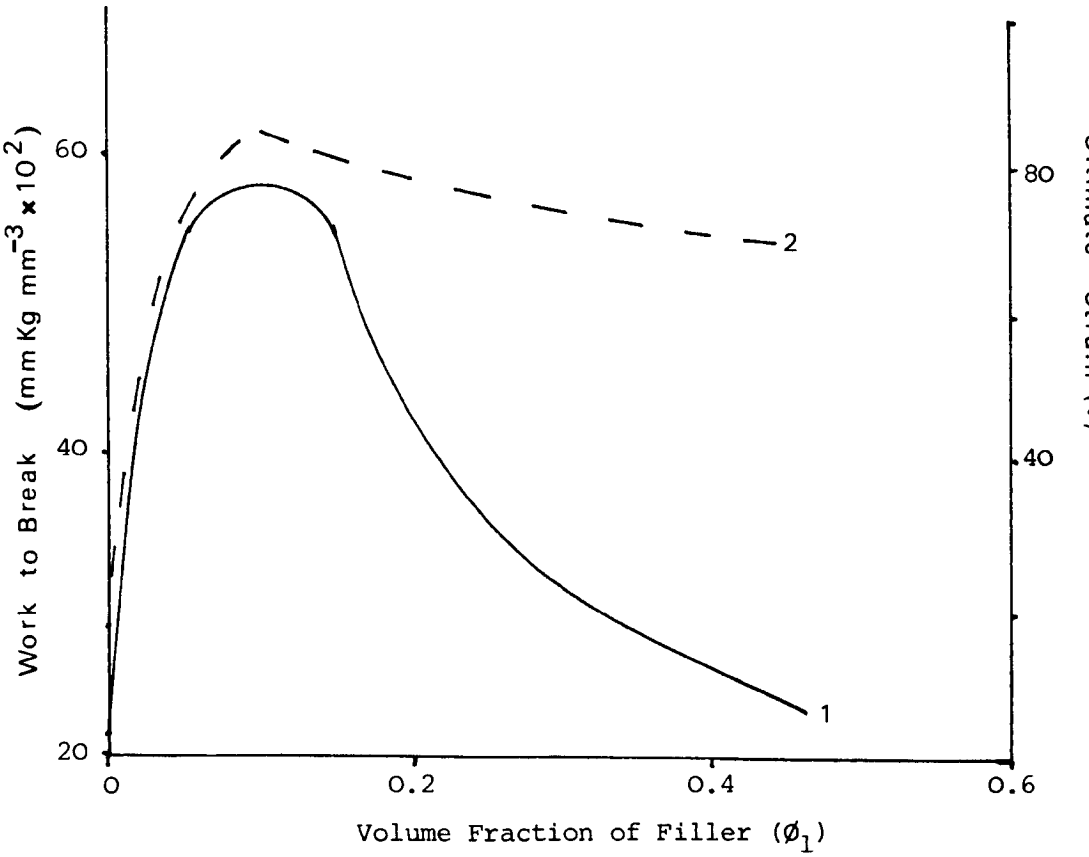

For perfect interfacial adhesion

$$\frac{\epsilon_{fc}}{\epsilon_{f1}} \doteq 1 - \phi_2^{1/3} \qquad 1.6$$

Neilsen further proposed that the true strain behaviour of the polymer is unaffected by the filler and that the decrease in strain was due to the reduction in the polymers cross sectional area brought about by the addition of the filler. However, the strain behaviour of polymers can be enhanced by the addition of fillers where poor interfacial adhesion exists (85-87). In this case the filler acts as a stress concentrator and delocalises primary crack growth by initiating cracks and crazes in other directions giving an increase in both strain at fail and in fracture toughness as shown in Figure 1.9. Nocolais and Narkis (84) derived an expression to account for this stress concentration effect on the tensile strength of composites as follows:

$$\frac{\sigma_c}{\sigma_1} = (1 - \phi^{2/3})S \qquad 1.7$$

where S = a stress concentration factor which, for spherical inclusions poorly adhered to the polymer matrix, has a value of circa 0.5.

1.5.3 The Effects of Particle Size

It is well established that for any given volume fraction the strength and modulus properties of particulate composites are enhanced by using smaller particles (64,82,83,94-96) as shown in Figure 1.10 but this effect is only directly accounted for by the empirical relationship of Landon, Lewis and Boden (83) as follows:

$$\sigma_c = \sigma_1 (1- \phi_2) - K\phi_2 d \qquad 1.8$$

where symbols used are those defined in Table 1.8 and where

K = slope of a plot of particle size against composite strength.

This enhancement of composite properties with decreasing particle size has been attributed to several factors.

1. For any given volume fraction of filler, a decrease in particle size is accompanied by an increase in surface area which increases the extent of interfacial adhesion in particular where good interfacial bonding exists (64,65).
2. The dependence of strength properties with particle size is most pronounced at volume fractions of about 0.2 (83), the fracture energy of composites also shows a maximum at this volume fraction (85-87, 91-93) and are thought to arise from the same effect. This has been attributed to the pinning of an advancing crack front at the particle and the subsequent deformation of the crack front between the particles. As the interparticle distance is decreased beyond a certain point, as is consistent with using smaller particles or increasing the volume fraction of the filler, then the radius of curvature through which the advancing crack front is bent is decreased and more energy is required to deform the crack and the fracture toughness is increased. However, at smaller interparticle distances the crack front is unable to deform in this manner and other modes of fracture are energetically preferred causing a loss of strength and fracture toughness as is evident with volume fractions greater than 0.2 in Figure 1.9. These alternative fracture modes were not clearly specified but are believed to be due to the crack propagating through the particle without bowing (155), to dewetting at the interface and to crazing of the polymer (86).

1.5.4. The Effects of Particle Shape

The effects of variations in the particle shape are not altogether clear although Chow (74) predicts that enhanced stiffening occurs

Figure 1.10 The Effects of Filler Particle Size on the Strength of Polyurethane-Glass Sphere Composites (88)

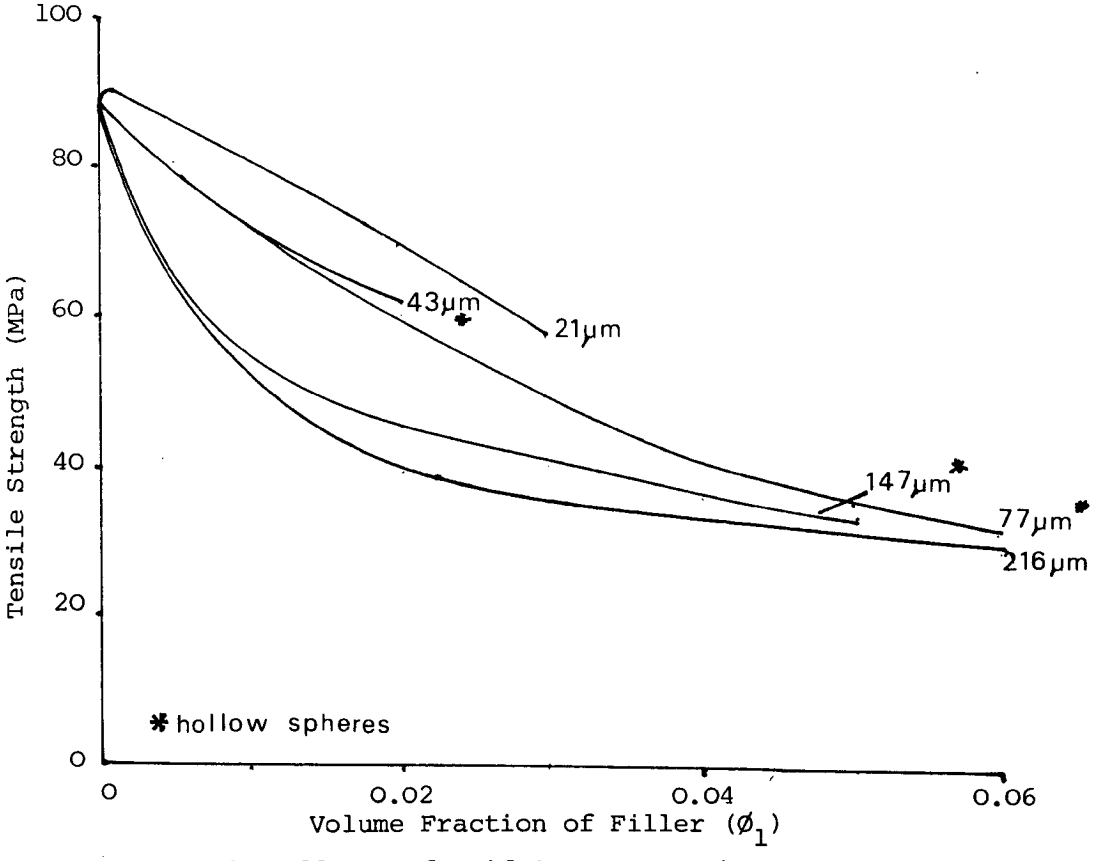

Figure 1.11 The Effects of Void Content on the Compressive Strength of Hydrated Portland Cement

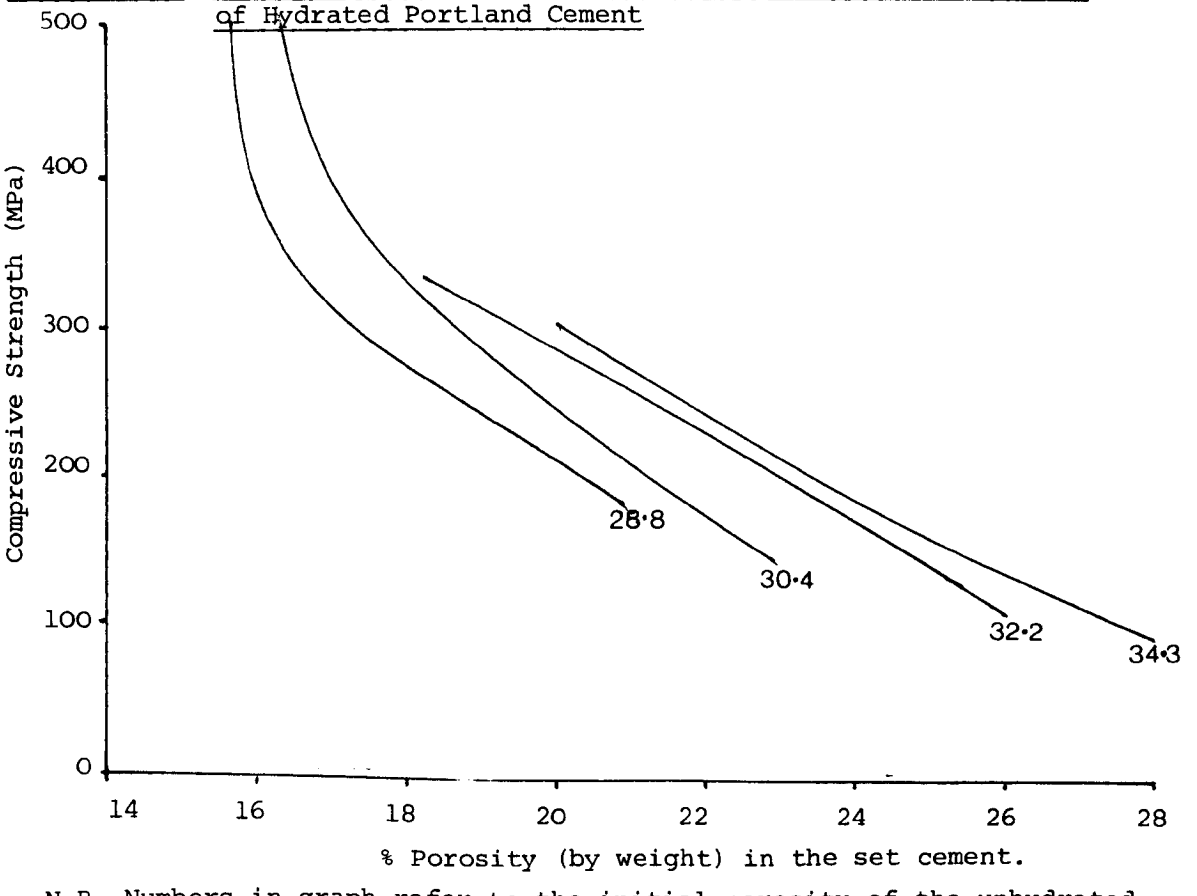

N.B. Numbers in graph refer to the initial porosity of the unhydrated cement compact

with fillers of high aspect ratio, in particular where fibres are used. The use of platelet shaped particles, such as mica, has produced composites of enhanced strength and stiffness in comparison with similar glass sphere filled composites. This enhancement was found to increase with aspect ratio and where the platelets were aligned (97). Piggott and Leidner (93) have postulated that particle shape may have greater effect on composite strength than particle size because non-spherical shapes increase the number of stress concentrations in a system, particularly if the particle has sharp corners and angular edges, causing a loss of strength even at low concentrations.

1.5.5 The Effects of Particle Packing

Efficient particle packing at high values of the volumetric packing fraction generally leads to composites of inferior mechanical performance due to greater inter-particle contact and aggregation (64,65). Aggregates occur in practice even at low filler concentrations but can be reduced by physical processes such as milling (94,98). However, by using bi-modal or multi-modal particle size distributions, good packing can be obtained which improves mechanical properties providing aggregation is limited. In such cases small particles position themselves at the interstices of the larger particles but remain wetted by the matrix, thus allowing higher volume fractions of fillers to be used and greater stiffnesses and strengths to be achieved. This effect only occurs where monodispersed particle sizes are used and where large differences in the ratios of the particle diameters exist. For example optimum packing of spheres occurs with diameter ratios of 7-10:1 (99,105) and

ratios of 10-1 for minerals such as feldspar and quartz (103). The use of bi-modal particle size distributions has been found to increase the mechanical performance of specialised cements (98) and the use of small glass particles to fill resin rich areas in fibre composites has been found to improve their strength (105)

1.5.6. The Effects of Porosity

As already demonstrated in Figure 1.7, the inclusion of voids as a third phase in a composite impairs its modulus (79,81).

Empirically, the effects of voids on strength has been described by the following relationships:

For failure stress (64,65,107)

$$\sigma_c = \sigma_1 e^{-b\phi v} \qquad 1.9$$

where symbols used are given in Table 1.8 and where

b = a constant

σ_1 = failure stress of unvoided matrix

For compressive or tensile yield stresses (80):

$$\sigma_{yc} = \sigma_{y1} \left[\frac{1}{1 - 1.2\ \phi_v^{2/3}} \right] \qquad 1.10$$

Both of these relationships are derived from the reduction of cross sectional area due to the void and assume spherical voids. Neither equation accounts for the effects of the particulate phase of the composite nor for the size distribution of the voids.

Voids in composites are generated in a number of ways such as poor penetration of the matrix around the filler, particularly if the filler is agglomerated or closely packed, from imperfections at the filler-matrix interface, from air entrained during the mixing process and they may also be generated from volatiles of the resin curing process (107,108).

The effects of voids on the mechanical properties of composites is dramatic, low levels of voiding (ϕ_v = 0.12) have been found to reduce the burst strengths of carbon fibre composites by 50% (107). In composites of cements and concretes reduction in porosity can lead to improvements in strength of over 100% (98,109) as shown in Figure 1.11.

1.5.7. The Effects of Interfacial Adhesion

The mechanical properties of composites are strongly influenced by the degree of interfacial adhesion between the filler and the matrix. Good adhesion aids the transfer of stress from matrix to the filler and leads to composites of high mechanical strength (89,92,110,147) although impact properties may be impeded (89). For example Sahu and Broutman (67) showed that composites of glass spheres treated with a mould release agent produced markedly weaker composites than with untreated glass spheres as shown in Figure 1.12.

Good adhesion is obtained where good interfacial wetting occurs or where silane coupling agents are used, these factors are considered separately.

Interfacial Wetting

The extent of intimate contact between any solid and wetting liquid is dependent upon the surface free energies of the solid and the liquid, the angle of contact between them and other factors such as the roughness of the surface and the viscosity of the wetting liquid. These factors have been extensively reviewed in classical wetting theories (111-117) and in relation to composites (112,117, 118). Fundamental to the wetting theory are the Young equation

Figure 1.12 The Effects of Interfacial Adhesion on the Mechanical Properties of Particulate Composites (67).

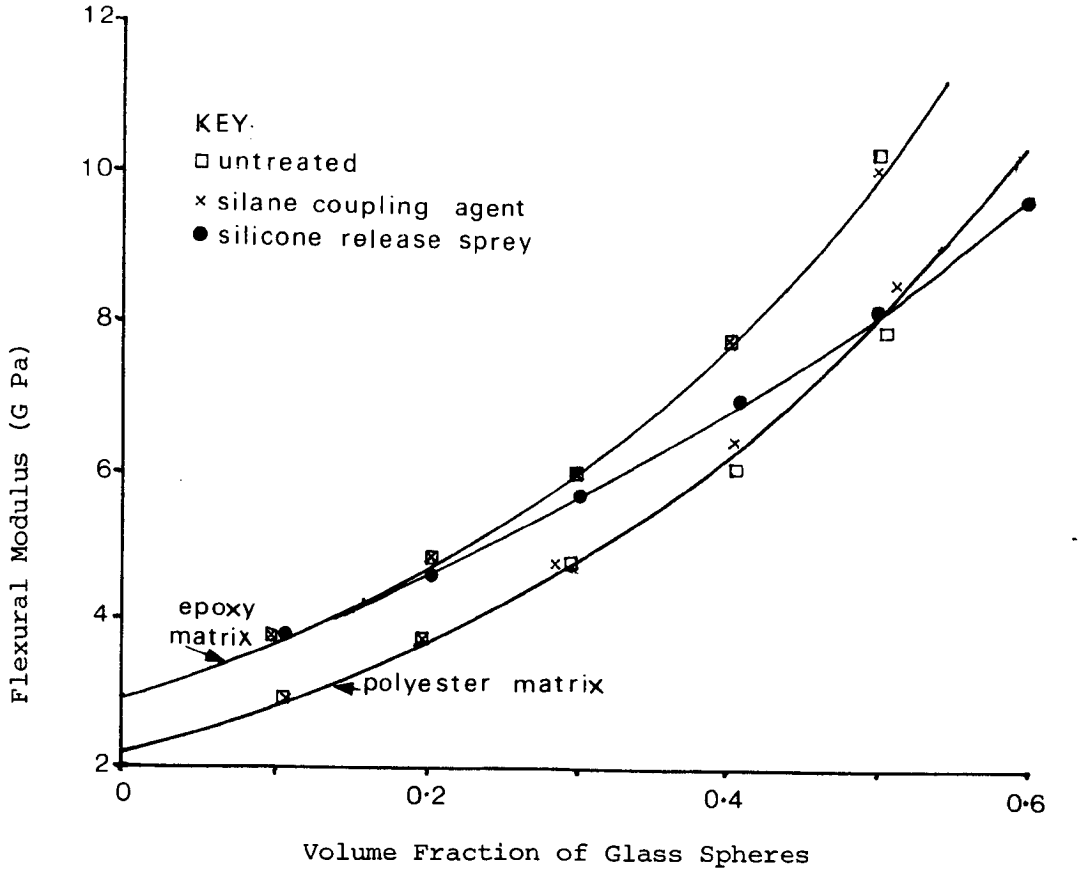

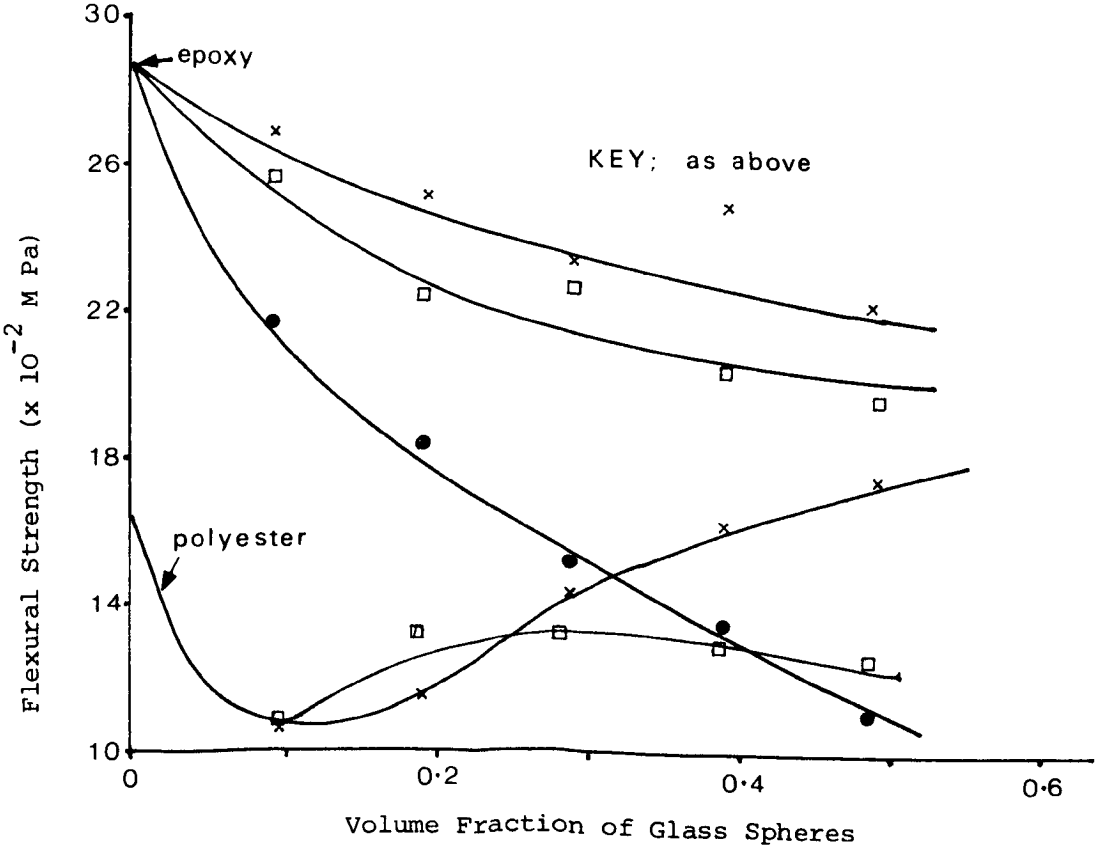

(1.11) and the Young-Dupre equation which are considered below (1.12).

The Young Equation

Young resolved the forces acting upon a drop of liquid resting on a smooth solid surface, as shown in Figure 1.13, to give:

$$\gamma_{sv} = \gamma_{sl} + \gamma_{lv} \cos \theta \qquad 1.11$$

where:

γ_{sv} = the surface free energy of a solid in equilibrium with its surrounding vapour

γ_{lv} = the surface free energy of a liquid in equilibrium with its surrounding vapour

γ_{sl} = the interfacial energy between the solid and the liquid

θ = the contact angle between the solid surface and the liquid

This equation defines the relationships between the surface free energies of a solid and a liquid and the contact angle between them. In practice, this equation is normally combined with the Dupré equation due to difficulties in measuring γ_{sv} and γ_{lv}.

The Young Dupré Equation

$$Wa = \gamma_l (1 + \text{Cos } \theta) + \pi \qquad 1.12$$

where:

Wa = the thermodynamic work of adhesion

γ_l = γ_{lv} (the vapour suffix is normally dropped in the Young-Dupré equation).

π = $\gamma_{so} - \gamma_s$ = the spreading pressure

γ_{so} = surface free energy of fresh solid surface

γ_s = surface free energy of solid oxide surface with absorbed moisture

Figure 1.13 Young's Model of a Liquid Wetting a Solid Surface

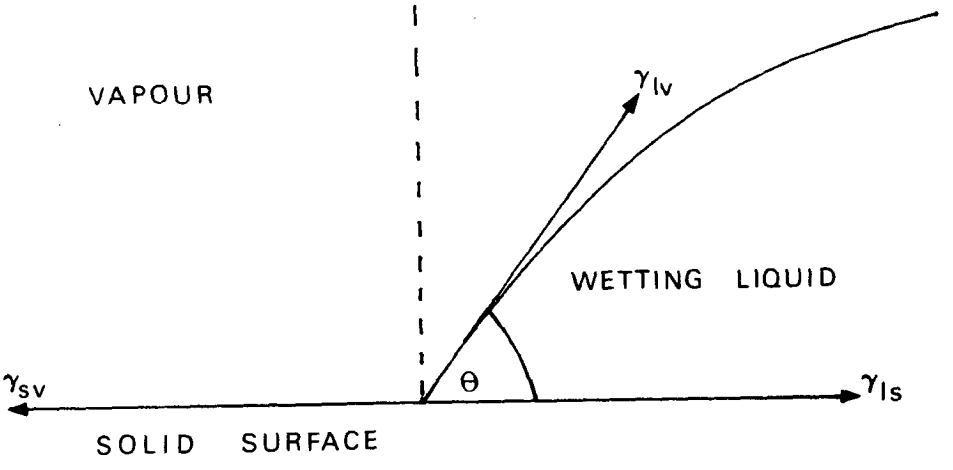

This equation is particularly useful in composites as it relates the strength of the interfacial bond, the work of adhesion, to the extent of wetting by the liquid and considers the effect of contamination of the solid surface. The equation demonstrates that the interfacial adhesion approaches a maximum value as the contact angle approaches zero to give conditions of spontaneous or ideal wetting. For this situation to occur it is essential that γ_s is considerably greater than γ_l. Many surfaces such as metals and glasses are classified as high energy surfaces and should be readily wetted by low energy liquids such as organic resins. However, these surfaces have high values of the spreading pressure (111) which can create surfaces which become hydrophobic and are not readily wetted by organic resins thus reducing the extent of interfacial adhesion. For example both water (γ_l = 72.7 mNm^{-1} (181)) and epoxy resins (γ_l = 35 - 45 mNm^{-1} (118)) form appreciable contact angles on 'E' glass surfaces as shown in Table 1.10.

Silane Coupling Agents

Silane coupling agents are complex molecules containing hydrolysible silane groups attached to an organic polymer or monomeric backbone. The silane group is capable of bond formation with the mineral surface and the organic backbone is capable of reacting with the resin either to copolymerise or to form inter-penetrating network systems (118-123). Silane coupling agents do not necessarily improve interfacial wetting properties and may even retard the rate of wetting . However, they promote adhesion by providing an intermediate layer bonded to both the mineral surface and to the resin (118).

Table 1.10 Contact Angles between E Glass Surfaces and Wetting Liquids (118,147)

Wetting Liquid	Glass Treatment	Contact Angle (deg)
Glass Slides:-		
1. Water	None	40-60
2. Water	Heat cleaned	16
3. Water	Acid cleaned	0-8
4. Water	Acid cleaned aged overnight	16
Glass Fibres:-		
1. Water	Silane treated and dried at 125°C for 15 mins	70
2. Epoxy	As above	55

Silane coupling agents can be used on a wide range of mineral and metal oxide surfaces (123) but careful selection is required to ensure compatibility with the resin. Typical improvements in composite properties as a result of using coupling agents are also shown in Figure 1.12.

1.5.8. The Limitations of Composite Materials

The technological and economic advantages of using both particulate and fibre filled composites in the manufacturing, marine, aerospace and construction industries is well established (64,68,69,124-130). In particular fibre reinforced polymers find widespread use due to their ease of fabrication, high strength to weight ratios and stiffness properties. However, conventional composites of glass fillers in either polyester or epoxy resins have a number of limitations, the most serious of which are their poor hydrolytic stabilities and their high level of residual stress formation as is described below.

Hydrolytic Stability

The mechanical properties of conventional composites are degraded by exposure to water or to environments of high humidity (134-154). For example glass fibre-epoxy composites lose up to 10% of their tensile strengths within 12 weeks when aged at ambient temperatures in a 95% humidity environment (134) and can lose even greater percentages of their initial strengths on immersion in boiling water (118) as shown in Figure 1.14.

However, the extent of degradation of the composite depends upon the nature of the property measured and the storage conditions. Strength properties are more sensitive to hydrolytic attack than modulus properties and shear strength is more sensitive than flexural

Figure 1·14 Loss of Mechanical Properties in Fibre Composites on Accelerated Ageing (118)

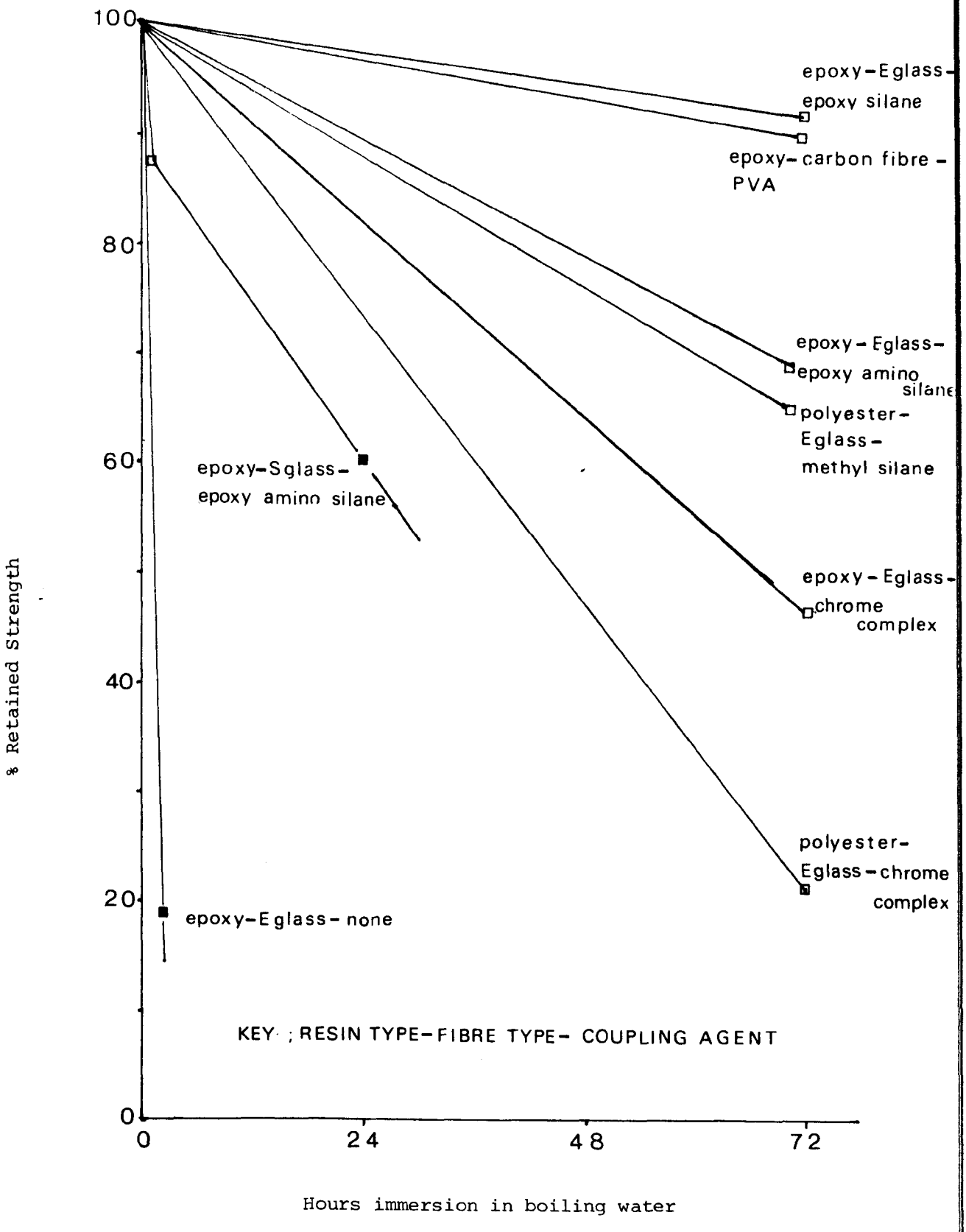

or tensile and compressive strengths (140,142,145).

The rate of mechanical degradation is accelerated at higher temperatures (137,151-153), where high alkali content glasses are used and under conditions of stress (133,136,140,142-146) which can also cause extensive crazing in both epoxy and polyester composites (135,143).

Water is known to enter a composite by diffusion through the resin and is absorbed at the matrix-filler interface displacing the resin and destroying the interfacial bond (112,138,140,147). Water is also know to plasticise and degrade epoxy and polyester resins and in particular attack ester and ether groups (112,118, 139,140,149,154).

Generally, this hydrolytic instability is improved,but not prevented, by the use of surface treatments such as silane coupling agents (118,133-137,140,147,150), by the removal of free alkali from the glass surface (149) and by the use of external protective coatings (131,136).

The development of residual stresses in composites is largely due to the differences in coefficients of thermal expansion between the glass and the resin as shown in Table 1.11. Thermosetting resins are exothermic in cure and are frequently reacted at elevated temperatures. Thus, during cooling the resins shrink more rapidly than the filler and residual (or shrinkage) stresses are developed at the filler-matrix interface and this is known to reduce the strength of the composite (112,120,121,131).

1.6 Research Objectives

The objectives of this research were defined as follows:

1. To investigate factors which influence the setting rate and

the mechanical properties of ASPA and other ionomer cements. In particular, to examine the influence of the nature of the dispersed phase on the mechanical properties of the composite.

2. To develop ionomer cements which retain their mechanical properties in environments of low humidity.

3. To develop ionomer cement systems of slower setting rates than the ASPA system to provide materials of potential value in non-dental applications.

4. To examine the potential of low cost glasses, minerals and metal oxides as alternatives to ASPA glass in ionomer cements.

Table 1.11 Coefficients of Thermal Expansion of Materials used to prepare Composites (121) and of Ionomers (18)

Material	Coefficient of thermal expansion $\times 10^{-6}\ ^{o}C^{-1}$
Fillers and Fibres	
Silica Glass	0.6
Alkali (soft) Glass	9.0
Alumina	8.7
Steel	10-14
Carbon fibre	7-8
Thermosetting Resins	
Epoxy	45-65
Polyester	55-100
Poly mide	38-54
Phenolic	60-80
Silicone	160-180
Thermoplastic Resins	
Polystyrene	60-80
Polypropylene	100-200
Polyacrylic acid (anhydrous)	55
Ionomers	
Zinc Polyacrylate	14.4

2. EXPERIMENTAL

2.1 Materials

ASPA Cements

ASPA glass (G200) was supplied by Amalgamated Dental International Limited.

Poly(acrylic acid) was supplied in an anhydrous form by Allied Colloids Ltd., the molecular weight of the polyacid had been determined by dilute solution viscometry to be 23,000 (156,157).

50% w/w aqueous solutions of PAA were prepared by slowly adding the anhydrous material to warm water with stirring and then allowing the suspension to stand for 48 hours for complete solution to occur. The exact water content was determined by weight change of the solution after drying at 60°C under vacuum and any necessary adjustments were made.

Fillers

Silica fillers were supplied from Joseph Crossfields & Sons Ltd. (159-163).

Ballotini glass spheres and the silicas Garosil and Garogel were obtained from Plastichem Ltd. (164-165)

Pozzolan (a pulverised fly ash) was obtained from the C.E.G.B.(166)

Samples of pseudo-Wollastonite and ß-Wollastonite were supplied by Blue Circle Technical Ltd. (167).

Other fillers were obtained from Brunel University stocks; the aggregate filler had the following composition (49):

Parts by weight	Mean Particle size (microns μm)
50% Quartz sand	210
25% Cristolbalite	50
25% Zirconium Silicate	50

Alternative Glasses to ASPA Glass

A number of novel ion-leachable glass formulations were prepared as shown in Table 2.1. The calcium aluminosilicate glasses were fused by Blue Circle Technical (167)and the zinc based glasses were fused in a high temperature furnace at Brunel. Original samples of the zinc based glass Znl and samples of zinc borate were supplied by R.T.Z. Borax Holdings Ltd. (171).

All these glasses were ground on a Glen Creston Reverse Oscillating Ball Mill and then passed through a 45 μm Endecott sieve.

Alternative Matrix Materials to Polyacids

Two alternative matrix materials to the polyacids were used to prepare composites, these were:

1. Ciba-Geigy Araldite epoxy resin (Bisphenol A resin) cured by mixing with an equal volume of a polyaminoamide paste hardener (172).
2. Strand Glass Polyester Resin A in Styrene cured with a 50% aqueous solution of methyl ethyl ketone peroxide mixed at a ratio of 1 ml of catalyst to 100g of resin (173)

Wetting Agents

Three wetting agents (surfactants) were used, these were:

1. Ethylan BCP, a non-ionic surfactant of Lankro Chemicals Ltd. (168)
2. Monflor 31, an anionic surfactant from I.C.I. Ltd. (169).
3. Monflor 51, a non-ionic surfactant from I.C.I. Ltd. (170)

2.2 Ionomer Cement Preparation and Storage

Two techniques of cement preparation were employed, the majority of the cements were prepared by the aqueous method but studies of the wetting properties of ASPA cements used the anhydrous method.

Table 2.1 Fusion Mixtures and Fusion Temperatures of Glass Formulations

1. CALCIUM CONTAINING GLASSES

Fusion Mixture	% Composition (by weight) BCI 1	BCI 2	BCI 3
SiO_2	43.3	31.8	39.7
Al_2O_3	24.1	26.2	33.6
CaF_2	14.5	-	-
$AlPO_4$	18.1	-	-
CaO	-	42.0	26.7
Fusion Temperature	1500°C	1500°C	1500°C

2. ZINC CONTAINING GLASSES

Fusion Mixture	% Composition (by weight) Zn1	Zn2	Zn3	Zn4
B_2O_5	18.5	18.5	-	18.5
P_2O_5	15.5	15.5	15.5	15.5
ZnO	66	-	-	-
Zn_2BO_3	-	66	84.5	-
Fusion Temperature	1,000°C	1,000°C	1,000°C	1,000°C

The Aqueous Method

By this method weighed amounts of ASPA glass were spatulated at ambient temperatures with measured volumes of a 50% aqueous PAA solution dispersed from a syringe, the weight of glass and volume of polyacid depended on the powder to liquid ratio (P:L g/ml) used. The mixing was conducted on a glass slab with half of the powder being spatulated with the polyacid in the first 15 seconds of mixing, a further quarter in the following 15 seconds and the remaining quarter in the next 15 seconds. The whole mix was then spatulated for another 15-20 seconds to give thorough mixing and then pressed into moulds and left to harden under pressure from hand tightened G-clamps. With less reactive systems and where larger mouldings were prepared longer mixing times were employed. Initial studies demonstrated that both mechanical and manipulative properties were optimised at a P:L ratio of 2:1 and this was used for most cements unless otherwise stated.

The Anhydrous Method

This technique used a dry powder mixture of ASPA glass and anhydrous PAA to which water was added and a procedure similar to the aqueous method then adopted. Initial studies demonstrated that a mix ratio by weight of 4 parts ASPA glass, 1 part PAA and 1 part water conferred good mechanical and good manipulative properties and was used for all the cements prepared by this technique.

Cement Storage

The ionomer cements were stored at room temperature in desiccators of controlled humidity. A humidity of 66% was used to be representative of conditions for a general cementation product.

In general cements were stored for seven days before testing unless otherwise stated.

In some cases the humidity of the storage environment was an experimental variable and different humidities were obtained from saturated salt solutions as shown in Table 2.2. Where humidity variations were used, weight change (to 3 decimal places) and dimensional change (micrometer) studies were also conducted.

Table 2.2 Humidities of Storage Environments at 23°C (174)

Humidity	Saturated Salt Solution
0%	P_2O_5
33%	$Ca\ Cl_2\ 6\ H_2O$
66%	$Na\ NO_2$
79%	$NH_4\ Cl$
100%	Distilled Water

2.3 Manipulative Properties

Cement Workability

The workability of all the cements was subjectively measured as the time from the commencement of mixing to the time where the cement became too viscous to mould. The workabilities of cements which displayed either typical or unusual behaviour were measured on a Wallace-Shawbury Curometer (175).

Setting Times

The setting times of selected cements were measured by dropping a Gilmore needle (diameter 1 mm) through a height of 10 mm under a load of 455 g onto the cement. The setting time was taken as the point where the needle left no visible impression on the cement surface (176).

2.4 Mechanical Testing

The mechanical testing was conducted in compression on Instron Model T.M. Four samples were tested for each experimental variable and values of strength, modulus and strain at fail obtained. The results are expressed as the mean and the standard deviation of these values unless otherwise stated. Cement samples with visible defects and samples which revealed obvious defects upon fractures were rejected.

Compression Testing

The samples for compression testing were prepared in split cylindrical moulds of diameter 6 mm and height 12 mm in accordance with dental method B.S. 3365 (176). Prior to testing the ends of the samples were flattened to ensure even loading and their dimensions measured. During testing moist filter paper was placed at the cylindrical ends of the sample as this is known to marginally reduce the variability of the results (177).

Initial studies, as shown in Figure 2.1, and previous workers (160) had shown that at slow speeds the rate of testing had little effect on the mechanical properties and consequently a crosshead speed of 5.08 mm min^{-1} was employed in conjunction with a chart speed of 254 mm min^{-1}.

Diametrial Tensile Testing

The samples for diametrial tensile testing were prepared in cylindrical moulds of 20 mm diameter and 9 mm thickness. The samples were tested in compression with moist filter paper between the specimen and the anvils of the instrument to aid even loading. A cross-head speed of 0.5 mm min^{-1} was used in conjunction with a chart speed of 25.4 mm min^{-1}.

Figure 2.1 The Effects of Compression Rate on the strength of ASPA Cements

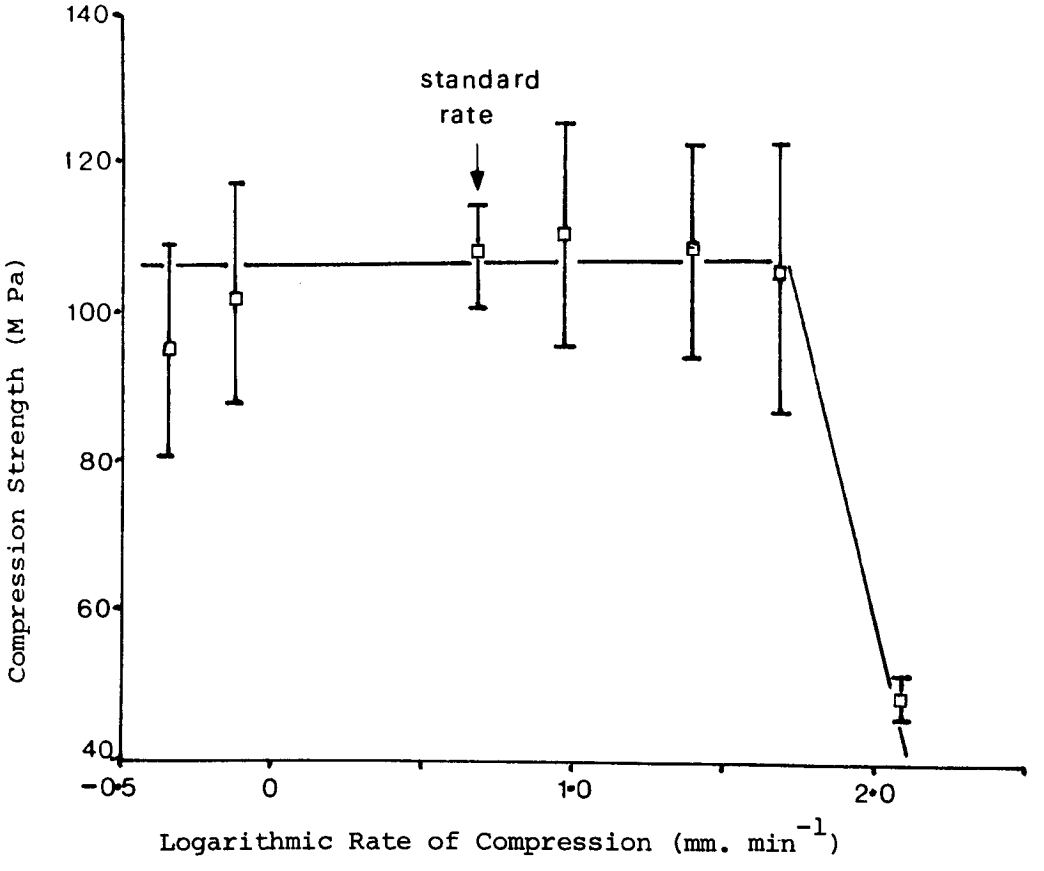

Stress Relaxation Behaviour

The stress relaxation properties of certain ionomer cements were measured in compression by the method described by Paddon and Wilson (41) using cylindrical samples of the same dimensions as for compressive testing. The samples were loaded to circa 450 N and the relaxation recorded as a function of time.

2.5 Hydrolytic Stability

The hydrolytic stabilities of various inonomer cements were determined by two techniques.

1. Weight gain after water immersion at ambient temperatures.
2. Change in mechanical performance after boiling in water for periods of 24 and 48 hours.

Samples for weight gain studies were prepared from moulds of 20 mm diameter and 2 mm thickness (176) and samples for boiling water immersion were prepared in the compression testing moulds.

2.6 Modification of the ASPA System

2.6.1. Acid Treatment

The ASPA glass was immersed in hydrochloric acid for 24 hours at a ratio of 25g of glass to 100 mls of acid. Various strengths of the acid were used ranging from its concentrated form to a pH of 2.8. The pH of these solutions and the pH change during treatment was measured on a Pye Unicam 290 Mk 2 pH meter. After treatment the glass was filtered, dried under vacuum at 110^{o}C and passed through a 45 micron Endecott sieve to eliminate aggregates.

Physical Change at the Glass Particle surface

The physical changes at the glass particle surface were examined on a Cambridge S4 Steroscan electron microscope (S.E.M.). The samples

were initially sputter coated with a gold-palladium mixture.

Chemical Change at the Glass Particle Surface

Chemical changes at the glass particle surface were examined by the technique of electron spectroscopy for chemical analysis (E.S.C.A.) on a Kratos E.S.300 instrument using both Al Kα and Mg Kα monoenergetic X-ray sources. A vacuum of circa 1.3 n Bars was used and initially a kineric energy range of 300-1550 e.v. was employed but on latter scans more selective energy ranges were used to give more accurately resolved peaks (180).

2.6.2. Filled Ionomer Cements

Various fillers were used to volumetrically replace proportions of the ASPA glass in the cement mix but so as to maintain a constant volume of powder (filler + ion-leachable glass) as the dispersed phase. Three values of volume fraction replacement (ϕ_R) were used, 0.25, 0.50 and 0.75. The weight of filler required for each volume fraction replacement was calculated from its bulk density which was determined from the weight of filler in a vessel of known volume and filled under vibratory conditions (64).

Particle Size Analysis

Particle size distributions of the various fillers and of ASPA glasses were determined on a Model D Industrial Coulter Counter (178) with samples suspended in a 2% w/w aqueous sodium chloride electrolyte with either glycerol or Nonidet P40 as the dispersing agent. However, some fillers were not suitable for analysis by this technique and in such cases the Optomax Automatic Particle Sizer was used in conjunction with a Zeiss Universal optical microscope (179).

Particle Shape Analysis

The shape of the filler particles was determined by electron microscopy (S.E.M.). Calculations of the aspect ratios of the fillers were made from measurements taken from the electron micrographs.

Filler Reactivity

The reactivity of the various fillers was determined by mixing with aqueous PAA. Fillers which displayed hardening properties after 24 hours were classified as reactive. The reactive surface ions of certain fillers were examined by the ESCA technique (180).

Particle Density and Filler Packing Fractions

The density of various fillers and of ASPA and other ion-leachable glasses were determined by pyknometry using a 25 ml specific gravity bottle (182).

The packing efficiency of the various fillers and glasses was expressed as the volumetric packing fraction (Ø max) (103,105,177) where:

$$\text{Ø max} = \frac{\text{True volume}}{\text{Apparent volume}} = \frac{\text{Bulk Density}}{\text{True Density}}$$

2.6.3 Particle Size Fractionation

Samples of ASPA glass were classified to give discrete particle size ranges by Alpine Process Technology Ltd., size ranges of the following order were obtained:

Sample No.	Size range (microns μm)
1	<10
2	10-20
3	20-30
4	30-40
5	40-45

The surface areas of these glass fractions were determined on a Ströhlein Area Meter by Blue Circle Technical (167).

Larger particle size fractions were obtained by grinding and sieving unrefined ASPA glass through a series of Endecott sieves with mesh sizes of 45,63,75,90 and 106 microns.

Bi-modal Particle Size Distributions

Fractionated glass samples were used to prepare optimum packing glass particles with bi-modal particle size distributions as follows:

1. 73% 63-75 μm + 27% 0-10 μm (acid treated)
2. 73% 30-40 μm + 27% 0-10 μm (acid treated)

2.7 Interfacial Effects in Ionomer Cements

The effects of wetting agents (surfactants) on the properties of ASPA cements were investigated for cements prepared by the anhydrous method where the water was replaced by surfactant solutions. The effects of the surfactants on the surface free energy of distilled water was measured by the Du Nouy ring method at 21°C which is known to be accurate to $\pm$ 2.0% (114).

2.8 Alternative Ion-leachable Sources for Ionomer Cements

A number of novel glasses and minerals were evaluated as replacements for ASPA glass. Cements were prepared from these materials at P:L ratios of 2:1 and at glass volume fractions of 0.42 to give cements with the same volume of the dispersed phase as with the ASPA system. Certain minerals were treated with IM HCl until any signs of chemical activity had subsided. These minerals were then filtered, dried and sieved in a similar manner to the acid treated ASPA glasses.

2.9 Fracture surface Examination

The fracture surfaces of ionomer cements were examined by electron

microscopy (S.E.M.) and by light microscopy on a Beck Zoomax Stereo Microscope.

2.10 Thermogravimetric Studies

Thermogravimetric analysis (T.G.A.) of ion-leachable glasses was conducted on a Stanton Automatic Thermo-recording Balance (Model TR-02) in conjunction with a Stanton Redcroft Variable Rate Temperature Programmer (LPU /CA10) at a heating rate of $2^{\circ}K$ per minute.

3. RESULTS AND DISCUSSION

3.1 Variations in the Mechanical Properties of Ionomer Cements

A variable mechanical performance can be expected from composite materials due to their heterogeneous nature but ionomer cements displayed greater variations in mechanical properties than similar polyester or epoxy composites as indicated by the magnitude of their standard deviations as shown in Figures 3.41 and 3.42. This behaviour was found to be dependent on the properties of the matrix and on the properties of the dispersed phase as discussed below. The ASPA cements also displayed considerable batch variation as is evident in Table 3.1.

Batch Variations

The variable performance between batches of ASPA glass was due to two effects:

1. Differences in the glass particle size.
2. Differences in the microstructure of the glass.

The two batches of ASPA glass used in this investigation had different particle size distributions as shown in Figure 3.1, with the mechanically superior and more reactive second batch containing smaller particles than the first batch. It is known that smaller particles produce stronger composites than larger particles at any given volume fraction (64,82,83,94,95,96) and with ionomer cements the increased surface area of the smaller glass would liberate more functional cations for subsequent salt formation to further increase the cements mechanical properties and increase its rapidity of set. The effects of glass particle size in ionomer cements is more fully discussed in section 3.5.1.

The differences in the glass particle microstructure between the two batches can be seen by comparing the acid etched glasses in Figure 3.7. This shows that the dispersed phase of fluorite existed as smaller and more numerous droplets in the second batch and were more resistant to acid attack than in the first batch. Such differences in microstructure are known to be dependent upon the thermal history of the glass with glasses fused at higher temperatures (circa 1300^{o}C) having a smaller and less crystalline dispersed phase than glasses fused at 1150^{o}C. These glasses fused at higher temperatures are known to produce more reactive cements as was consistent with the second batch.

These findings demonstrate the sensitivity of these multi-phase glasses to thermal history and the difficulties involved in their preparation. Such variable behaviour could well be the cause of the criticisms of the ASPA system as described in Section 1.2.1.

Intra-Batch Variations

The variation in the mechanical properties of ASPA cements was found to be dependent upon a number of factors, as follows:

1. The humidity of the storage environment.
2. The volume fraction of the glass in the composite.
3. The particle size of the glass.

To demonstrate these effects the standard deviations of the cements were expressed as a percentage of the mean to give the factor called here the percentage scatter. This was plotted against humidity, particle size and volume fraction as shown in Figures 3.2 to 3.4. respectively.

Figure 3.1 Particle Size Distributions of ASPA Glass Batches

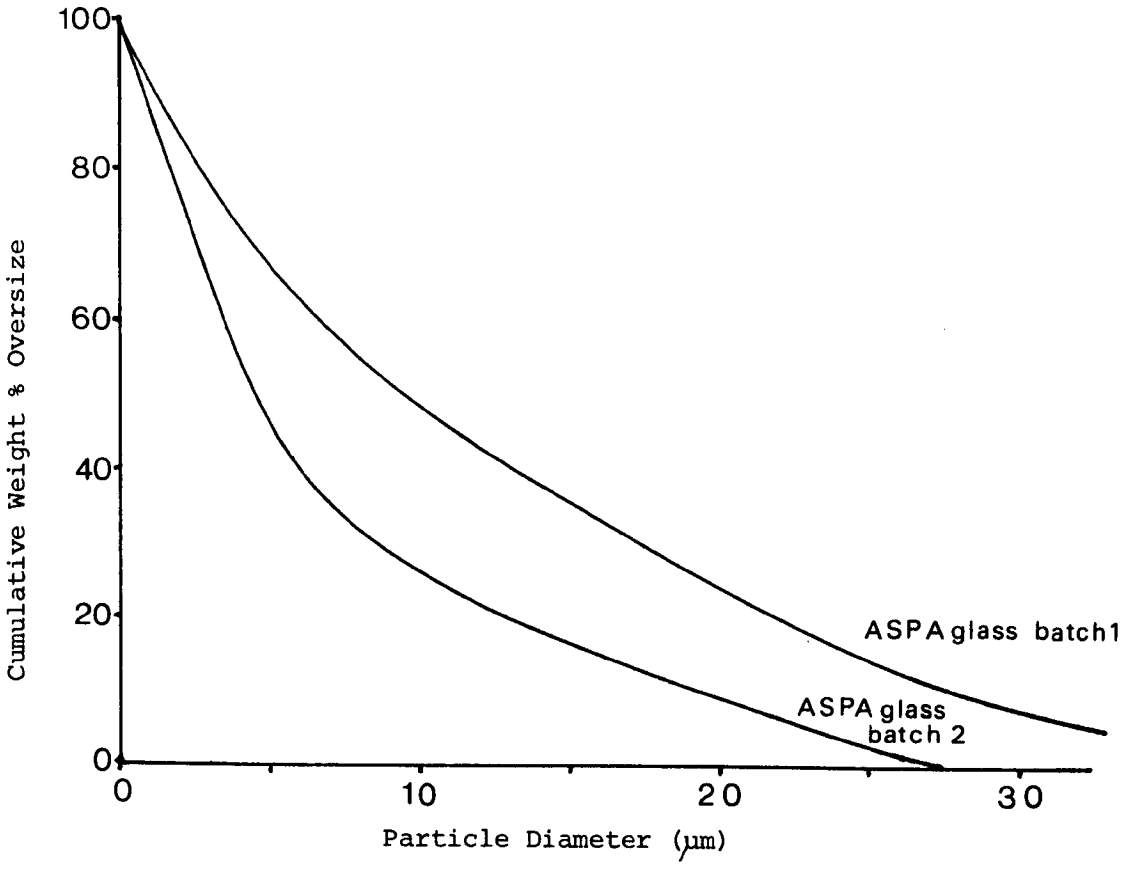

Figure 3.2 Variations in Strength of Ionomer Cements with Storage Humidity

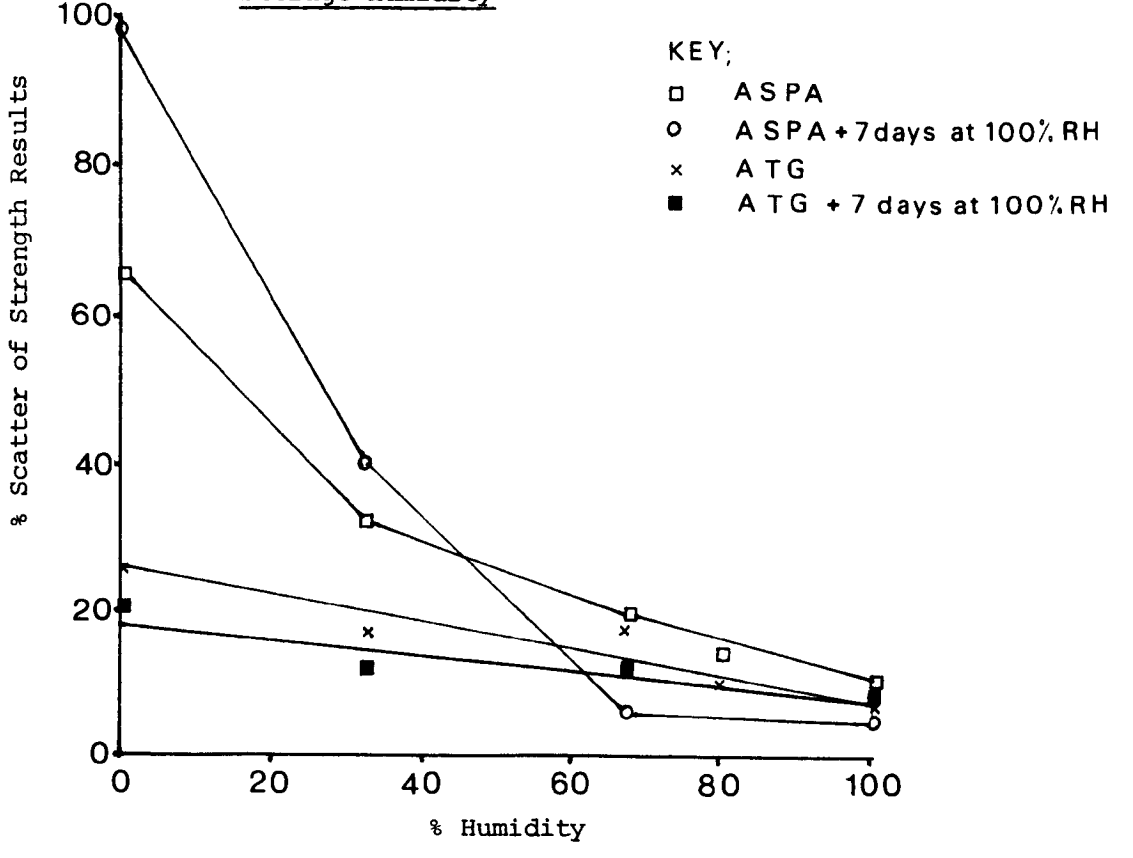

Note: ATG = Acid Treated Glass Cement

The increase in variability of the results with decreasing humidity of the storage environment can be attributed to weight loss and shrinkage of the matrix increasing the internal stress and void formation of the systems as is discussed in Section 3.4. Cements which displayed better weight (water) retention, such as the ATG cements and ASPA cements cured for seven days at 100% humidity prior to exposure at low humidities, displayed less scatter of results.

The use of smaller particles and increases in the volume fraction of the glass both increased the scatter of results. This was attributed to the increased surface area of the glass phase not being adequately wetted by the polyacid within the constraints of the work time of the cement. The less reactive acid treated ASPA glass (ATG) system had generally less scatter than the ASPA system. The increased scatter of results of glasses with particle sizes greater than 60 μm was attributed to increases in the packing fraction (Table 3.13) producing a greater degree of inter-particle contact and aggregation. The effects of particle size and volume fraction are more fully discussed in Sections 3.5.1 and 3.5.2 respectively.

Comparison with Previous Work

At a first approximation the strengths of the ASPA cements presented here are inferior to previous investigations of the mechanical properties of ASPA cements (1,45,49,58) where compressive strengths of the order of 130-200 MPa were generally obtained. Strengths comparable to the dental system were frequently recorded in this study but the mean stength values were reduced by including low results as these occurred consistently and were thus a true reflection of the material's behaviour. In dental practice low

strength results are ignored, an initial mean is calculated and results 15% below this mean are omitted and the mean recalculated (173). For example, typical values of compressive strength recorded here were 108.0 MPa (mean of 18 results) but by applying dental procedures the mean is increased to 126.1 MPa (mean of 7 results). The modulus values recorded here were frequently higher than those of previous studies because the modulus was calculated here from the tangent of the Hookean portion of the stress-strain curve. Others have assumed a linear stress-strain response and have expressed the modulus as the stress at fail divided by the strain at fail. This latter approach is inaccurate as ASPA cements displayed a slight departure from Hookean behaviour at higher strains and some filled ionomer cements and some mineral-ionomer cements were found to display plastic behaviour.

The cement storage conditions employed here (66% humidity at ambient temperatures) were generally different from conditions used in previous studies. In dentistry it is common practice for ASPA cements to be stored in water at 37^{o}C to simulate the oral environment (1,27,28,39,42,43,177). This high humidity would reduce the percentage scatter of the results, as just discussed, and the higher temperatures would accelerate the cement forming reaction and possibly promote greater strengths. Hornsby (49) and co-workers (45) demonstrated that the mechanical properties of ASPA cements were seriously degraded by storage at 66% humidity as described in Section 1.2.6. However, the cements used here, in particular cements from the second batch of glass, were superior to Hornsby's results and displayed maximum mechanical performance at this humidity. Such differences in mechanical behaviour can only be attributed to variations in the batches of ASPA glass.

Figure 3.3 Variations in Strength of Ionomer Cements with Glass Particle Size

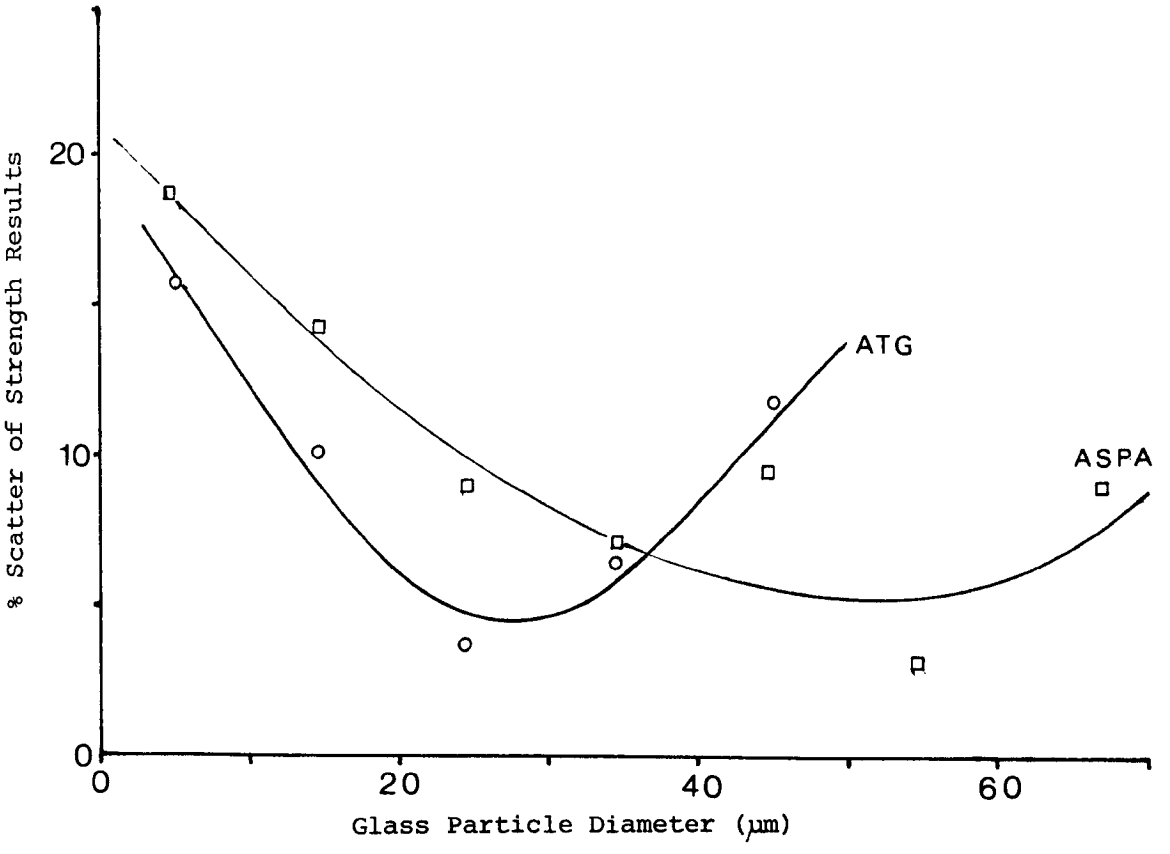

Figure 3.4 Variation in Strength of Ionomer Cements with Volume Fractions of Glass

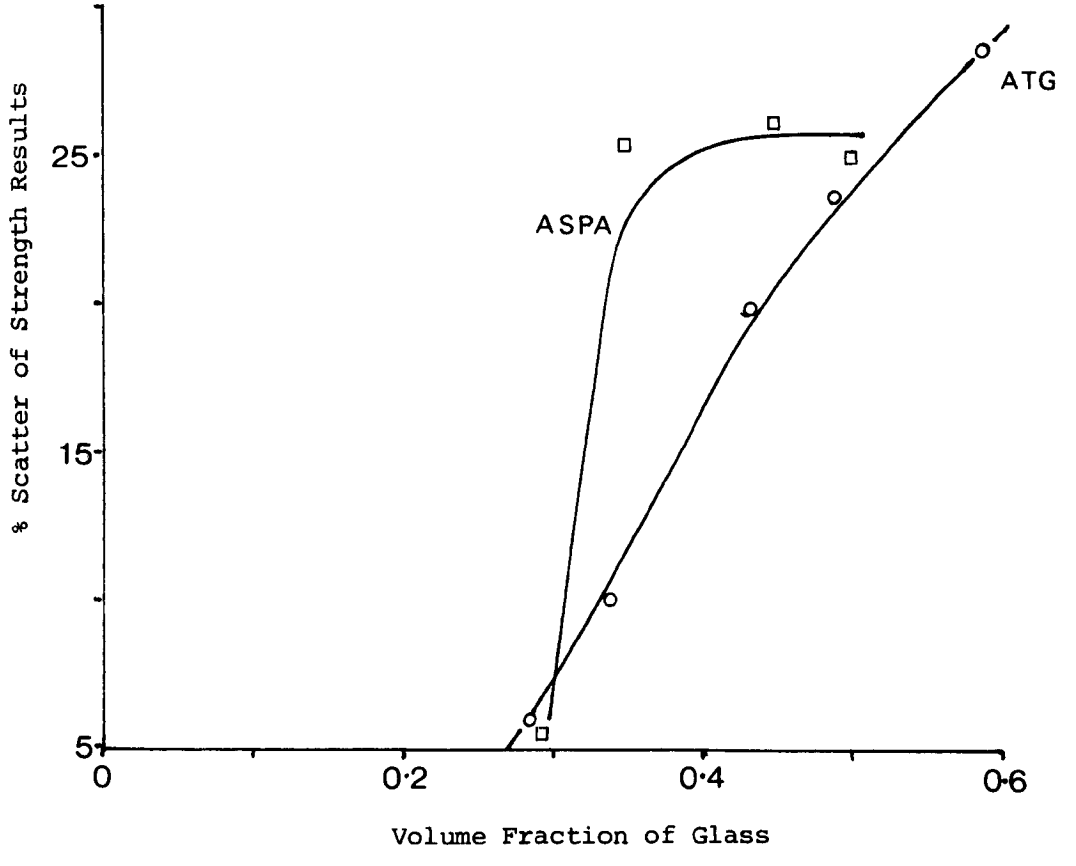

Other differences between dental practice and the approach adopted here were evident. In dentistry higher volume fractions of the glass are employed than in this study, but this factor may not have such a great influence on strength as discussed in Section 3.5.2. Also, in dentistry the work time of the cement mix is subjectively taken as the time in which the cement remained carvable and deformable for the purposes of restorative filling whereas the more rapid time taken to reach an unmouldable state was considered here.

Table 3.1 Batch Variations of ASPA Cements

Batch No.	P:L	Work Time (Min)	Setting Time (Min)	Comp. Strength (MPa)	Comp. Modulus (MPa)	Strain at fail (%)
1	2:1	3.0	80	47.6 ± 10.4	2601 ± 831	2.41 ± 0.94
2	2:1	1.0	30	91.7 ± 7.3	3739 ± 507	2.79 ± 0.29

3.2 Acid Treatment of ASPA Glass

The functional cations at the surface of the ASPA glass particle are known to be readily leached by acid attack as described in Section 1.2.4. Consequently, these cations were removed from the glass surface prior to cement formation by acid treatment. This treatment process was found to produce glasses which were less reactive towards PAA than the ASPA glass and allowed further study of the setting mechanisms of ionomer cements.

The acid treatment process was found to produce both chemical and physical changes at the glass particle surface and cements prepared from acid treated glass (ATG) were found to have a superior mechanical performance to the ASPA system irrespective of the acid strength used. Treatment by an acid with an initial pH of 1.0 also produced ATG cements with extended workability and retarded setting properties as shown in Table 3.2 and in the rheometer (curometer) trace of Figure 3.6.

3.2.1 The Acid Treatment Process

ASPA glass was treated with various strengths of hydrochloric acid and the rate of reaction of this process was followed by measuring the pH change of the glass suspension with time, typical results are shown in Figure 3.5. where an initial pH of 1.2 was used. This demonstrates that the glass particle is readily attacked by the acid giving an initial rapid change in pH within the first few minutes of treatment but little change occurred after 60 minutes indicating the treatment process to be complete.

Figure 3.5 Acid Treatment of ASPA Glass; The Change in pH with Treatment Time

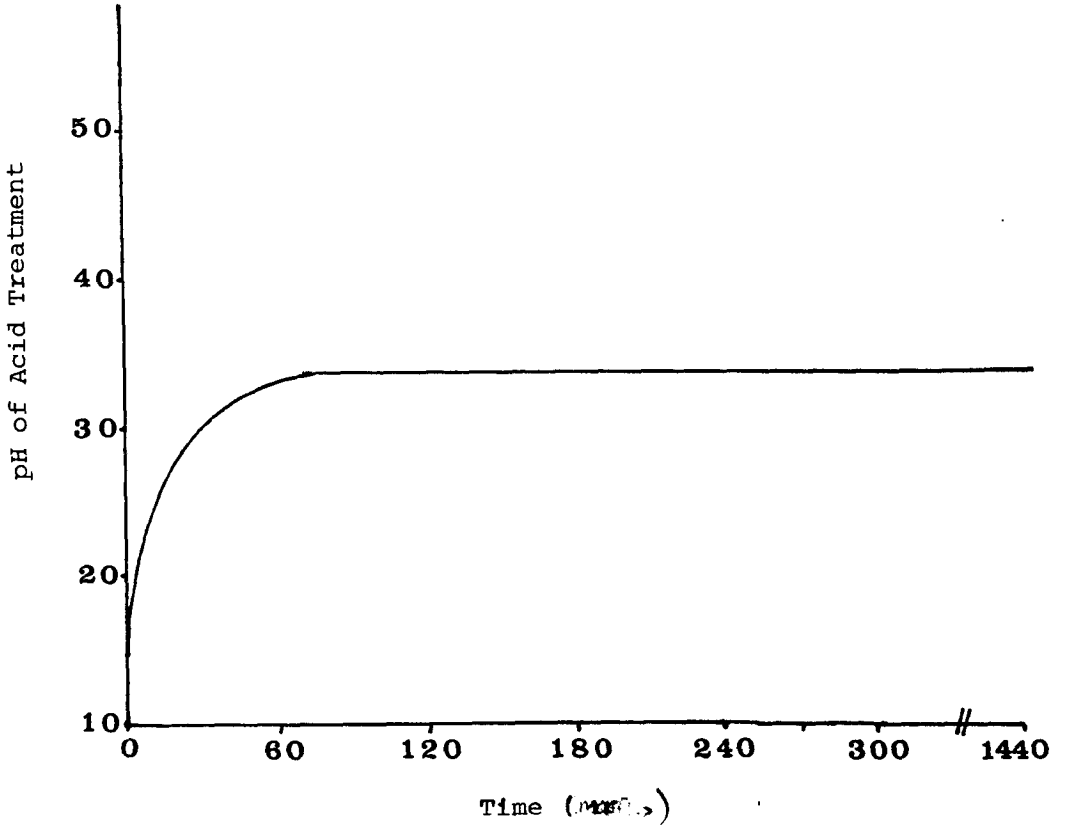

Figure 3.6 Manipulative Properties of ATG Cements

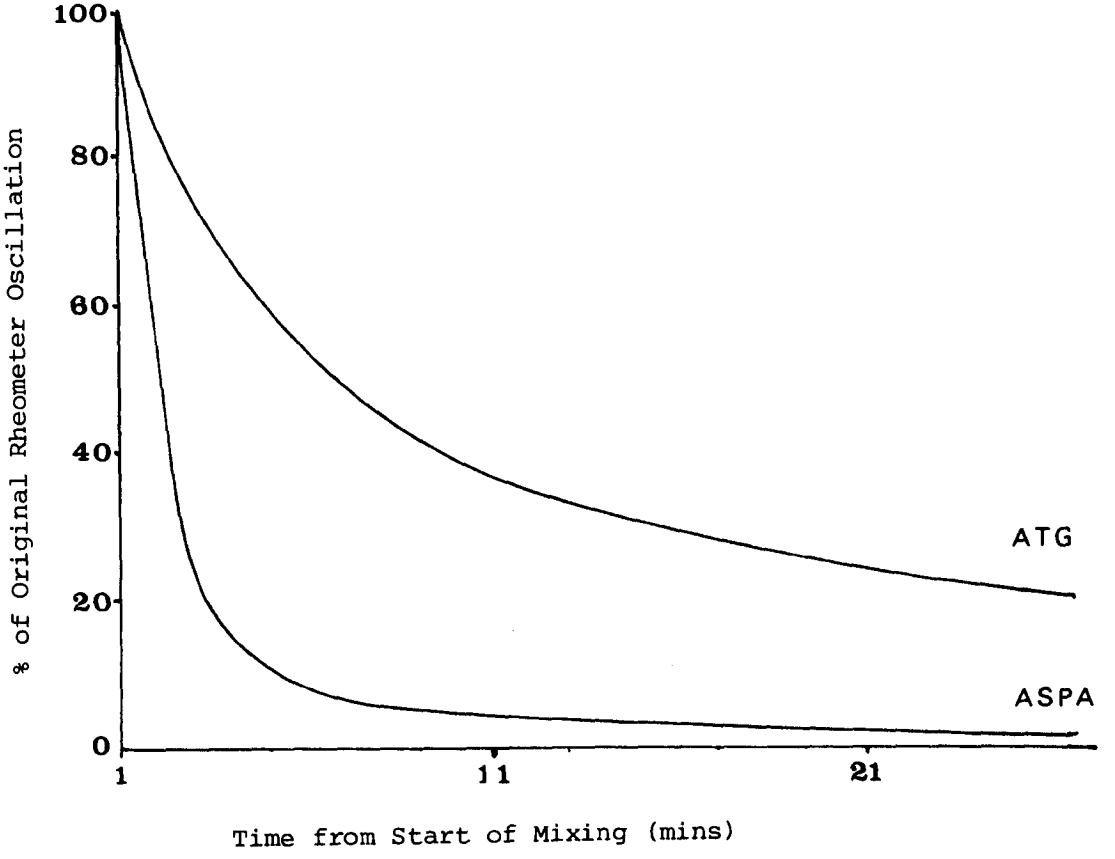

3.2.2 The Chemical and Physical Effects of Acid Treatment

The surface structure of the ASPA glass particle was physically changed by acid treatment as shown in the electron micrographs of figure 3.7. These micrographs show the ASPA glass to have a complex surface structure with both a dispersed phase evident and with other irregular shaped particles adhering to the surface. Treatments with weak acids (pH 3.0) produced no noticeable changes to the ASPA glass but glasses treated with stronger acids (pH 1.0) showed that the dispersed phase had been removed leaving a surface with numerous pits and holes of varying diameter. The amount of loosely adhered particles at the surface was also reduced and those particles which remained were unaffected by the acid. Treatment with strong acids, such as concentrated HCl, also showed removal of the dispersed phase with attack of the main glass core revealing a plate-like or layered structure.

The effects of acid treatment on the surface chemical characteristics of ASPA glass was studied by Electron Probe Micro Analysis (EPMA) and by ESCA.

The EPMA results were found not to be reproducible and were sensitive to factors such as the orientation of the glass particle in the electron beam, the technique only examined small areas of the glass and the X-Ray dispersive technique used was not capable of detecting lighter elements such as fluorine. Consequently, the ESCA technique was preferred as it produced replicable results, analysed larger areas of the glass powder and resolved the lighter elements. Quantitative comparisons of the effects of acid treatment was conducted by measuring the ratio of the peak heights between the treated and untreated glasses

Figure 3.7 The Physical Structures of Acid Treated ASPA Glass

1. UNTREATED ASPA GLASS

1.1 Magnification 6.5 K (batch 1)

1.2 Magnification 1 K (batch 2)

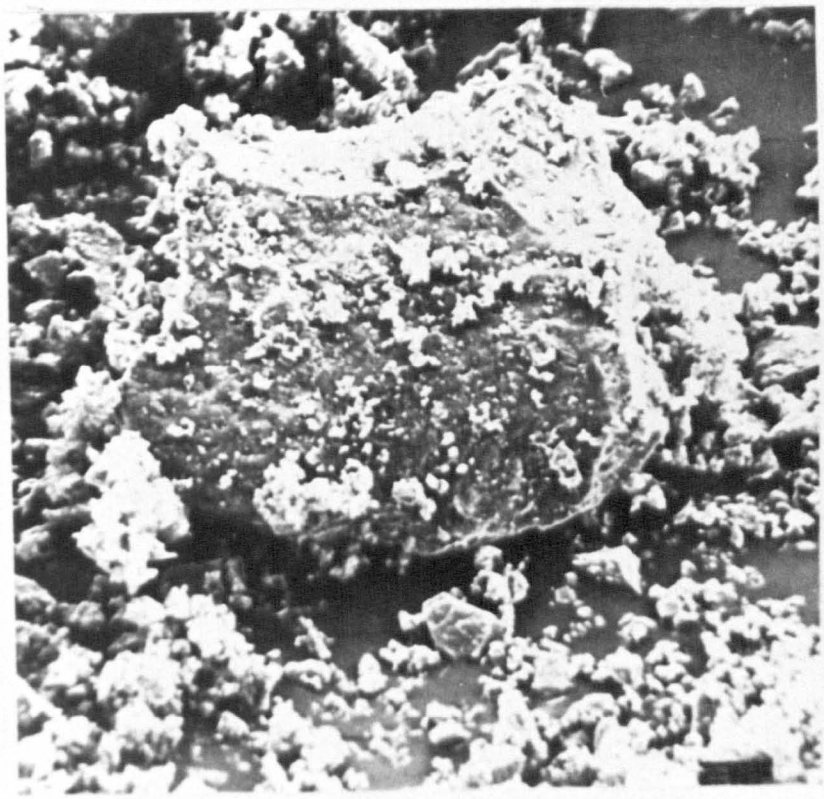

Figure 3.7 Continued

1.3 Magnification 5 K (batch 2)

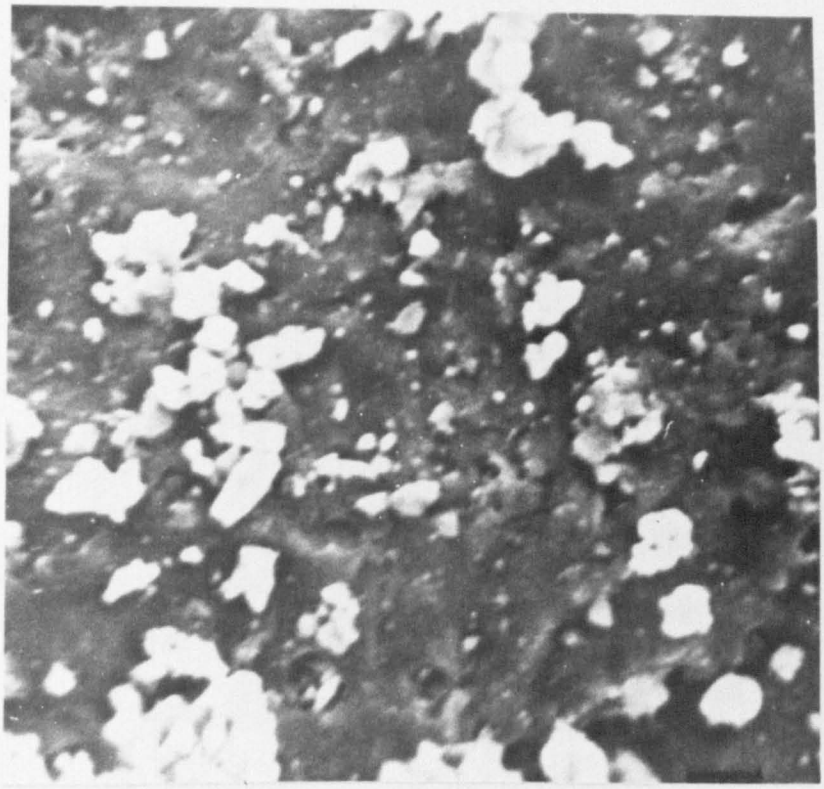

2. ACID TREATED GLASS; pH 3.0

2.1 Magnification 6.5 K (batch 1)

Figure 3.7 Continued

3. ACID TREATED GLASS; pH 1.0

3.1 Magnification 6.5 K (batch 1)

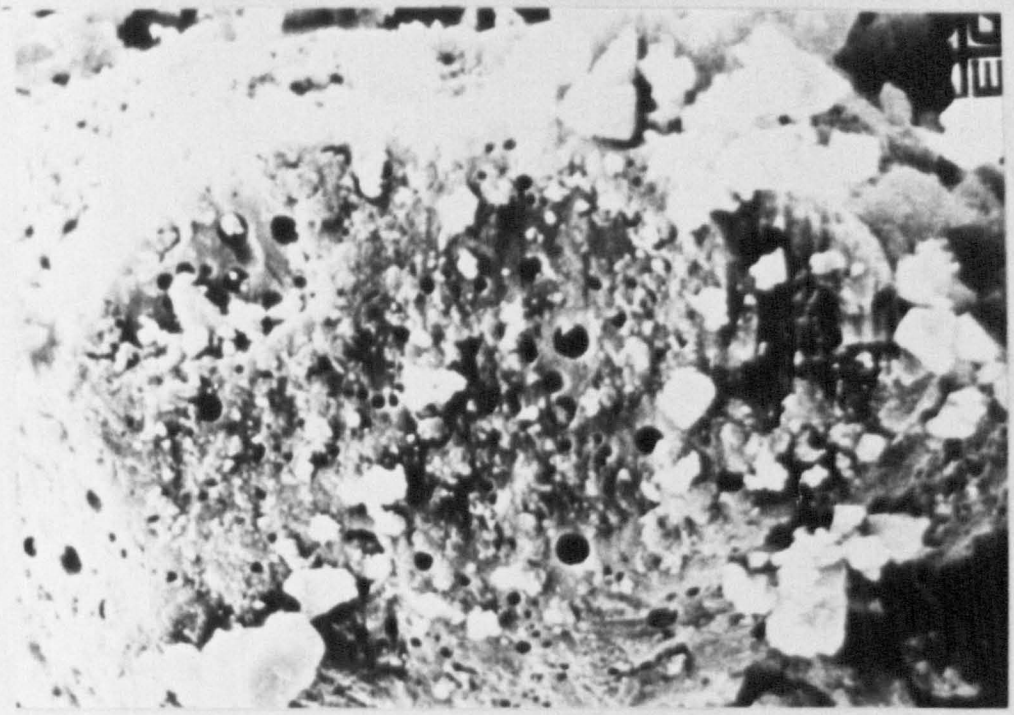

3.2 Magnification 13 K (batch 1)

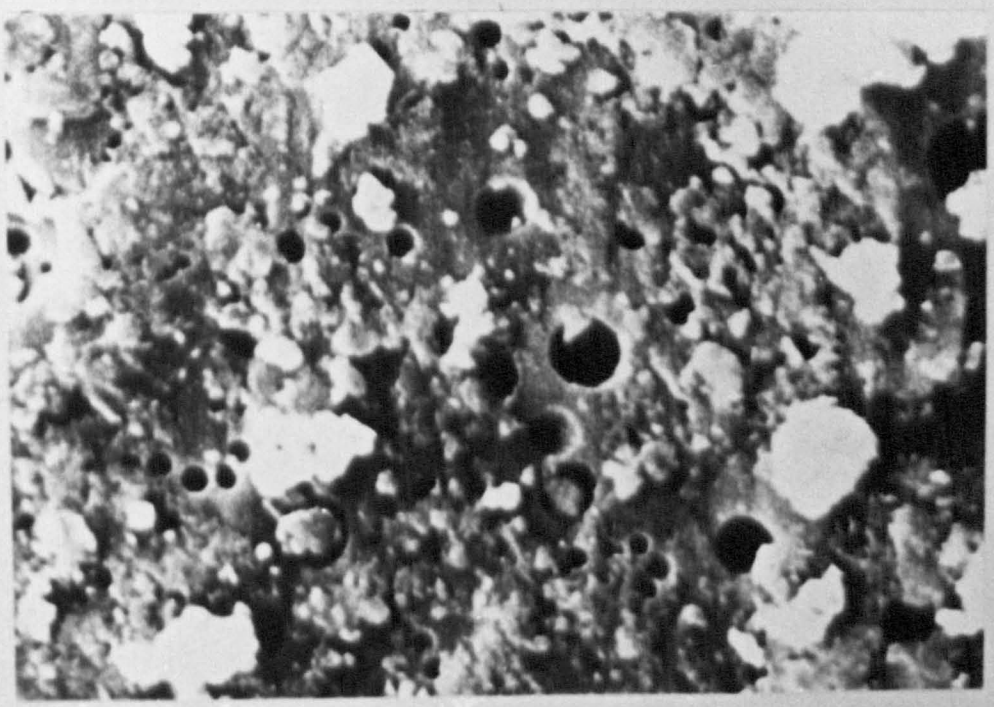

Figure 3.7 Continued

3.3 Magnification 5 K (batch 2)

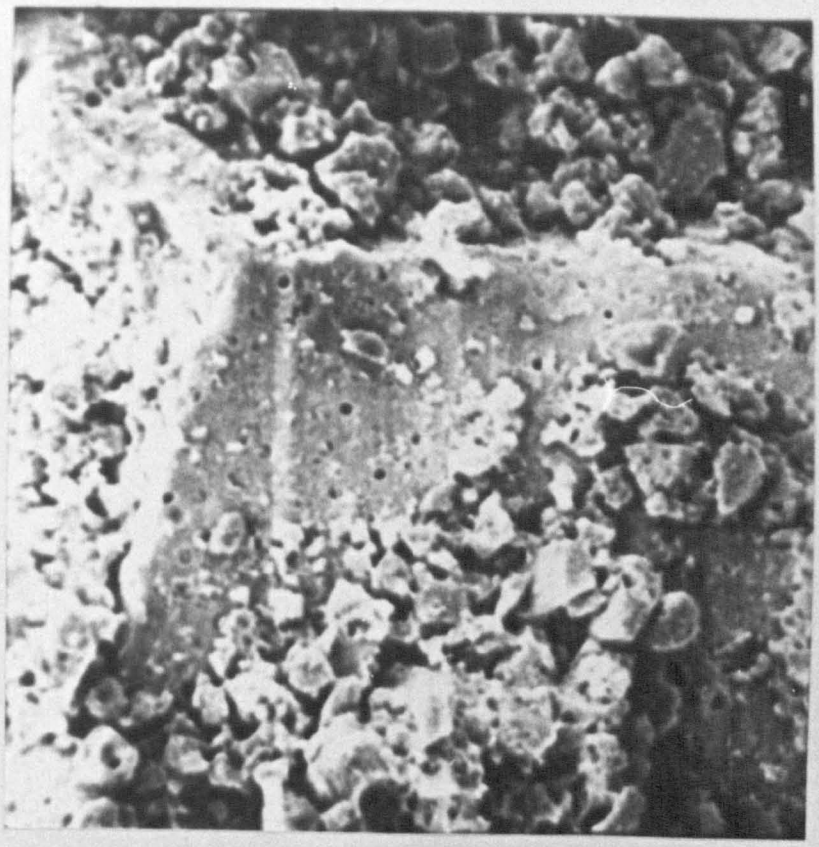

3.4 Magnification 10 K (batch 2)

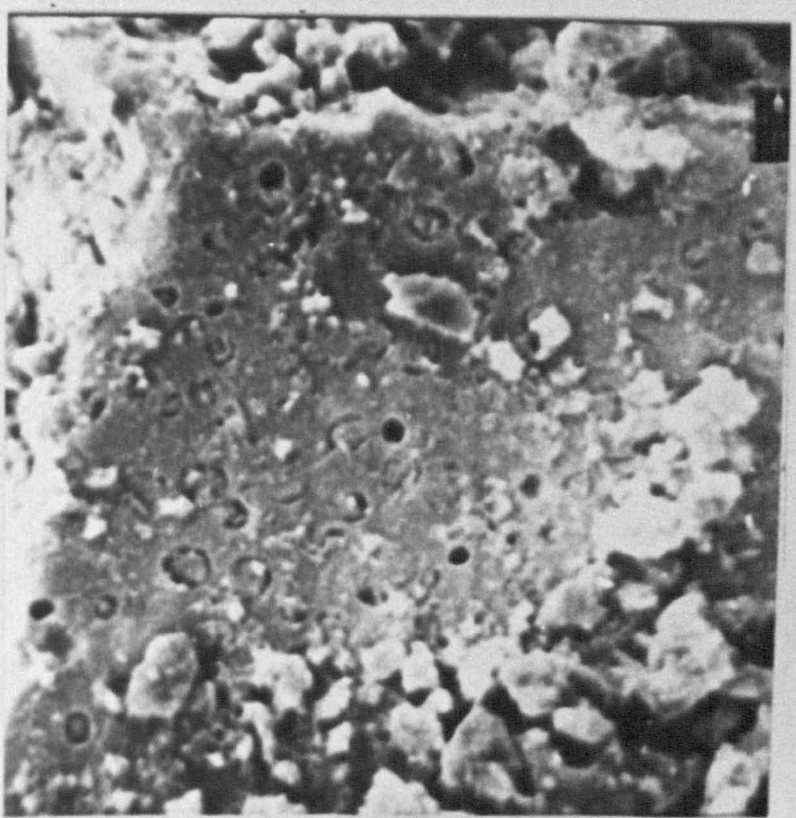

Figure 3.7 Continued

4. ACID TREATED GLASS; conc H Cl

4.1 Magnification 6.5 K (batch 1)

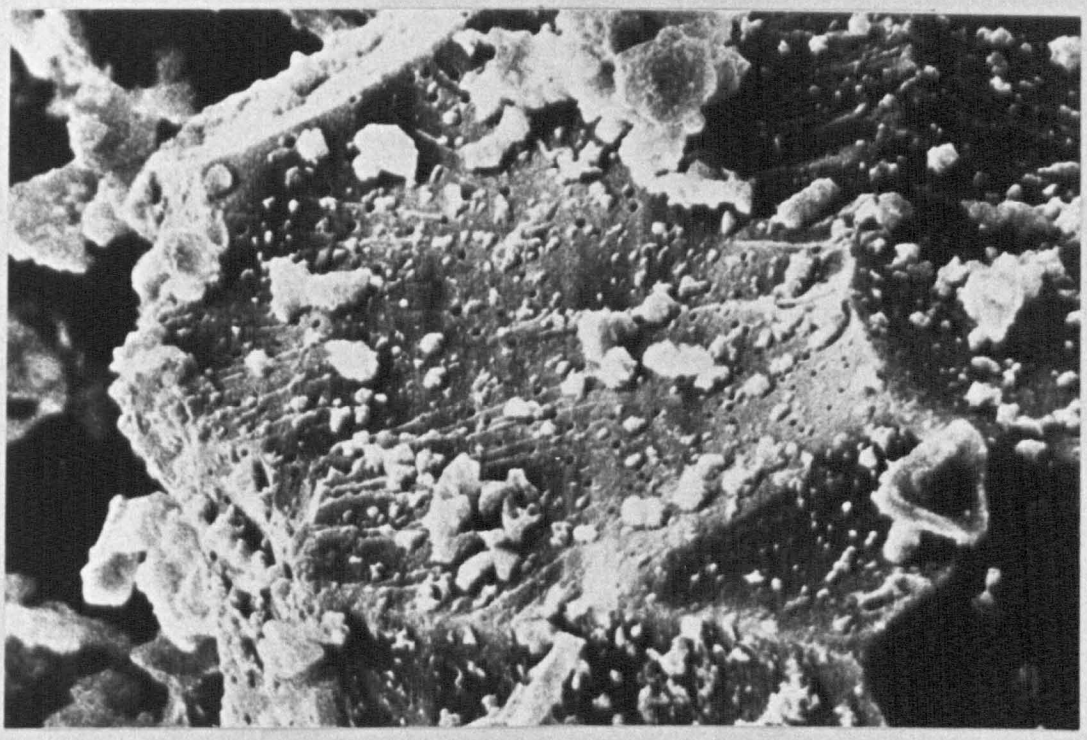

4.2 Magnification 13 K (batch 1)

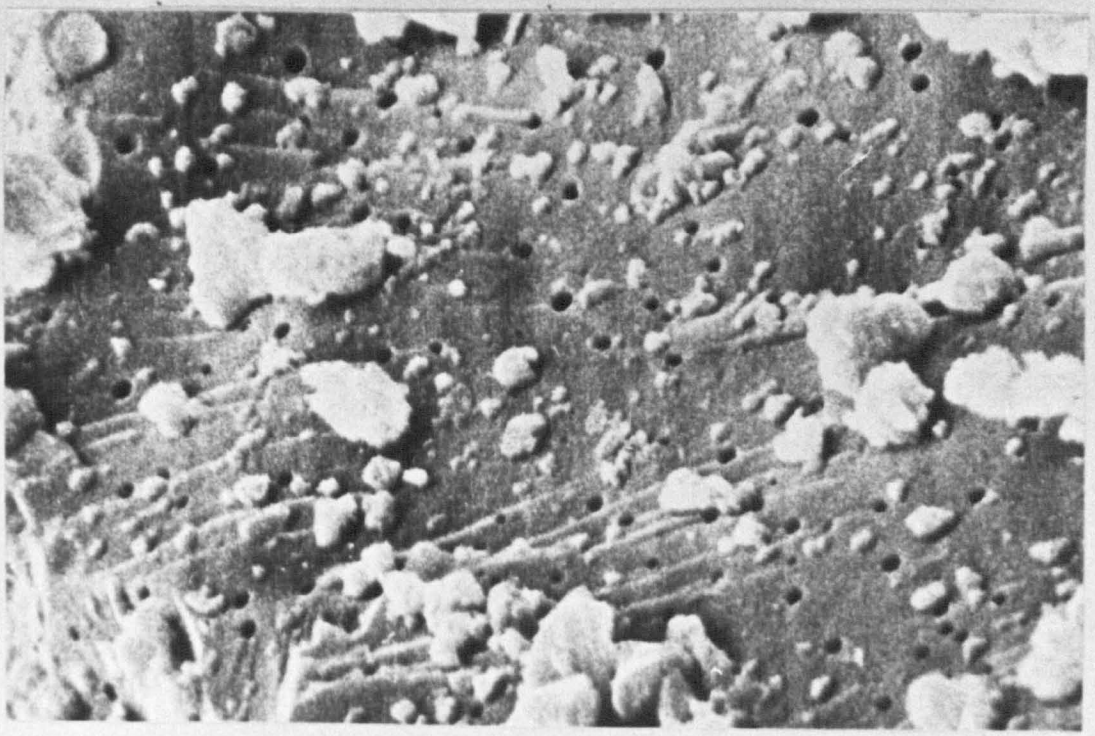

as given in Table 3.3; representative spectra are also given in Appendix 2. These results showed that treatment of the ASPA glass with an acid of pH 0.8 produced the following surface chemical changes:

1. Both the levels of Ca and F were reduced by a factor of about 0.5 from their initial values.
2. The Si peaks were increased by a factor of circa 2.2
3. The Al peaks were also increased by a factor of about 2.0.

Interpretation of the Electron Micrographs and of the ESCA Results

The changes in the physical surface structure and the reductions of the Ca and the F peaks of ASPA glasses treated with acids of pH circa 1.0, demonstrates that the dispersed phase of fluorite (CaF_2) was attacked and removed from the glass particle surface. The rapid change in pH with the commencement of treatment further suggests that this process is completed within one hour of treatment. However, the ESCA studies revealed that a proportion of both the calcium ions and the aluminium ions remained at the glass surface after treatment indicating these ions to be firmly embedded in the continuous phase of the glass structure and thus capable of forming primary (ionic) inter-facia bonds with polyacrylate matrix as discussed in detail in Section 3.9.

The increase in the Al and the Si content of the glass surface upon treatment was a direct consequence of exposing more of the bulk phase of the glass by removal of the dispersed phase of fluorite.

The effects of the acid treatment process are of interest as this treatment replicates the acid attack that occurs during the setting process of the ASPA cements. Electron micrographs of the fracture surfaces of ASPA cements as shown in Figure 3.8. have revealed

Table 3.3 Quantitative Data from E.S.C.A. Spectra of Acid Treated Glasses

Kinetic Energy (e.v.)	Designation	Ratios of Peak Heights	
		0.8/C	2.4/C
650	F Auger	0.53	1.13
795	F 1s	0.50	1.00
1045	Ca 2s	0.42	1.08
1134	Ca 2p 1/2	0.44	1.02
1138	Ca 2p 3/2	0.46	0.92
1333	Si 2s	2.11	1.19
1352	P 2p	1.24	1.20
1360	Al 2s	2.31	0.89
1375	Si 2p's	2.31	1.18
1405	Al 2p's	1.50	1.62
1420	Na 2s	0.81	0.81
1441	Ca 3s	0.60	1.40
1453	Na 2p	0.36	0.95
1459	Ca 3p's	0.73	1.00

0.8/C ratio of peak heights of the acid treated glass (pH 0.8) to that of the control.

2.4/C ratio of peak heights of the acid treated glass (pH 2.4) to that of the control.

NOTE: 650 - 1138 e.v. peaks at range of 10^4 cps

1333 - 1459 e.v. peaks at range of 3×10^3 cps.

Figure 3.8 Fracture Surfaces of ASPA Cements

A. Cement prepared by the Anhydrous Method. Magnification x 6K

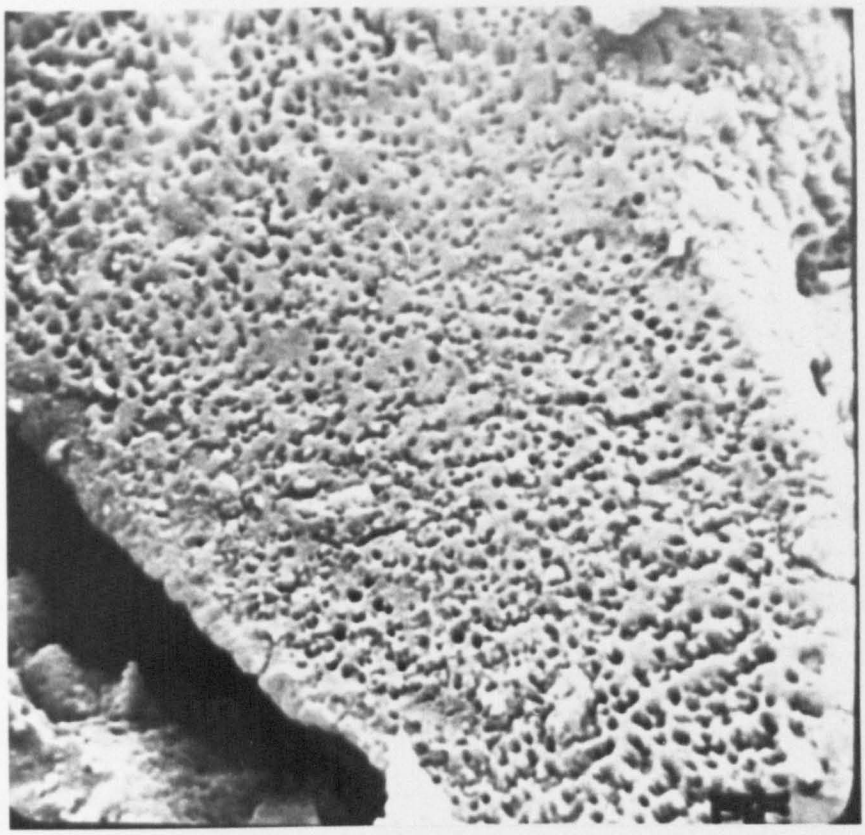

B. Cement prepared by the Aqueous Method. Magnification x 11K

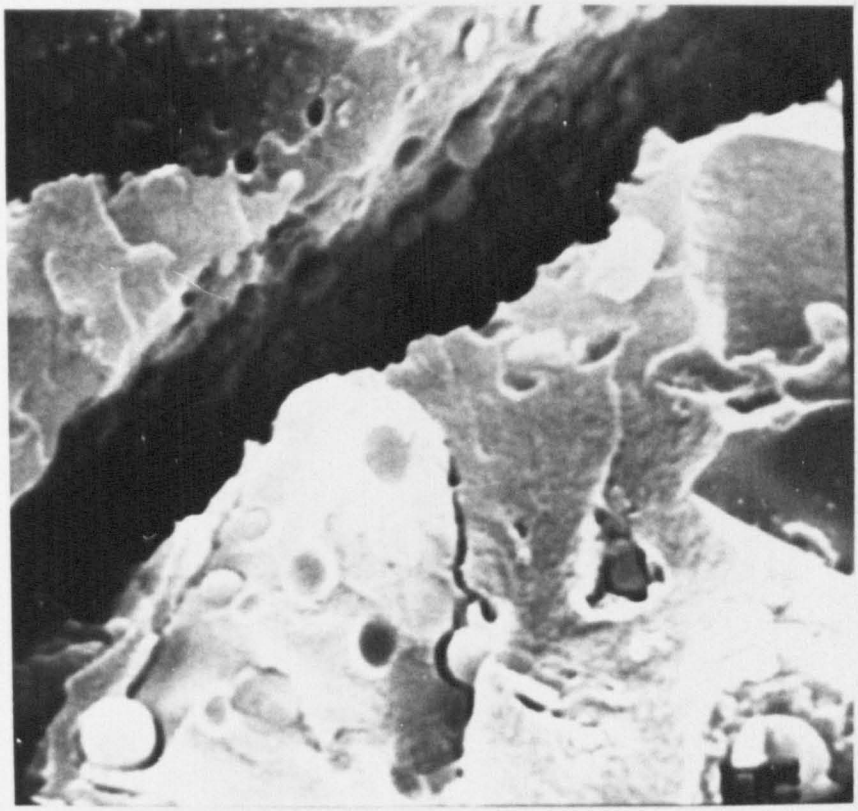

similarities to the acid treated (pH 1.0) glasses and shows that removal of the dispersed phase occurs during acid attack. However, closer examination (Figure 3.8(b)) has indicated that the calcium fluoride droplets are not fully dissolved by the polyacid but exist as small submicronic particles in the set cement. In such cases it is the phase boundary between the main bulk of the glass and the droplet which is attacked and is thus probably more amorphous than the droplet itself as the latter is known to contain crystals of fluorite (1,37,42).

3.2.3 Manipulative and Setting Properties of ATG Cements

The reduced calcium ion content of the ATG glass produced cement mixes of extended workability and with longer setting times than ASPA cement mixes as shown in Table 3.2 and in the rheometer trace of Figure 3.6. This enhanced workability of the ATG cements permitted larger mouldings to be fabricated and the decreased reactivity allowed cements of higher volume fractions of glass to be prepared as is discussed in Section 3.5.2.

The rheometer can be used to study the rate of cure of any cross-linking mechanism and has been used before for ionomer cements at ambient temperatures (1,39,49). The instrument comprises an oscillating paddle which passes through the sample and is connected to a pen recorder. As the material being tested crosslinks and its shear modulus increases, so the resistance to motion of the paddle is impeded which is recorded on the chart. The chart thus records the curing or hardening of the material as a function of time and allows qualitative comparison of the manipulative properties of viscous paste mixtures.

The workability and setting times of the ATG cements were progressively increased by treatment with stronger acids but these properties were optimised by treatment with an acid of pH 1.0, that is by acids which had removed significant proportions of the dispersed phase of fluorite. These findings also confirm earlier proposals that the rapid setting properties of ASPA cements were due to the rapid leaching of calcium ions from the glass and the subsequent formation of calcium polyacrylate (1,38).

3.2.4 Mechanical Properties of ATG Cements

The mechanical properties of the ATG cements were superior to the ASPA cements both in compression and in diametral tension as shown in Table 3.2. This improvement in properties occurred irrespective of the strength of the treatment acid although the use of strong acids, such as concentrated HCl, reduced the mechanical performance of the cements as such acids attacked the main phase of the glass as well as the dispersed phase as shown in Figure 3.7. Consequently an acid strength of pH 1.0 was selected for all other work as such glasses produced cements with both good mechanical and manipulative properties.

The superior mechanical properties of the ATG cements were attributed to the following factors:

1. Enhanced aluminium polyacrylate and primary interfacial bond formation.
2. Mechanical adhesion at the glass-matrix interface.
3. Improved interfacial wetting properties.
4. Reduced internal stress formation.

1. The reduced calcium content and enhanced aluminium content of the

Table 3.2 Properties of Cements Prepared from Acid Treated ASPA Glass (ATG)

Sample No.	pH of Treatment	Work Time (Min)	Setting Time (Min)	Comp. Strength (MPa)	Comp. Modulus (MPa)	Strain At fail (%)	Diametral Tensile Strength (1) (MPa)	Diametral Tensile Strength (2) (MPa)
1	Control	1.0	30	86.0±18.6	4122±498	2.09±0.35	21.9±3.4	-
2	2.8	2.0	45	113.3±25.6	4840±256	2.62±0.90	-	-
3	2.4	2.0	45	124.0±25.6	4886±287	2.62±0.10	-	-
4	1.8	12.0	120	116.4±25.0	4554±403	2.96±0.45	-	-
5	1.0	18.0	160	122.4±14.0	4408±479	3.38±0.31	27.6±6.2	21.3±3.2
6	0.8	12.0	190	104.7±7.3	3958±573	2.67±0.65	-	-
7	Conc.H Cl	20.0	240	56.3±14.5	4082 —	-	-	-

N.B. (1) Mould dimensions, diameter 6.25 mm, length 12 mm.

(2) Mould dimensions, diameter 20.0 mm, length 7.25 mm.

acid treated glass suggests that the ATG cements have greater potential for aluminium polyacrylate formation and less potential for calcium polyacrylate formation than the ASPA cements. It is proposed here that aluminium polyacrylate is mechanically stronger than calcium polyacrylate. Others have also suggested that the aluminium ions are responsible for the attainment of high strength in ASPA cements (1,37,38). Further, the ESCA studies revealed that the aluminium ions were firmly embedded in the main phase of the acid treated particle and were thus capable of providing a greater degree of primary interfacial bond formation with the polyacid than the ASPA system.

2. The physical surface of the acid treated glass (Figure 3.7) had numerous hemispherical holes and pits due to the removal of the dispersed phase. These features may have acted so as to improve the mechanical adhesion between the glass particle and the matrix, providing the viscous PAA matrix was capable of penetrating these holes. Such adhesive mechanisms are known to improve the strengths of epoxy-aluminium joints (183) and the mechanical performance of textile-rubber composites (112).

3. The retarded setting and improved manipulative properties of the ATG cements allowed greater time for intimate interfacial wetting to occur than with the ASPA cements. Also the removal of oxide surfaces and other contaminants by the acid treatment may have increased the surface free energy of the glass particle to present a surface more amenable to wetting by the polyacid. Both of these factors would enhance the degree of interfacial adhesion and thus produce stronger composites for the reasons discussed in

section 3.5.3. However, acid cleaned glass surfaces are known to oxidise rapidly and revert to their original wetting conditions within a few hours of treatment (149). The acid treatment process also removed some of the material which was loosely adhered to the glass particle, such as debris from the grinding process. This material would have produced a weak boundary layer at the interface reducing the strength of the ASPA cement. Further, the acid treatment could have removed other contaminants such as residual carbonate, as is found in some minerals (See section 3.7), which may react with the polyacid to form gaseous voids which would also reduce mechanical properties as described in section 1.5.6.

4. It has been suggested that any form of crosslinking mechanism reduces the free volume of a polymer molecule which leads to shrinkage and the subsequent development of internal or shrinkage stresses, in particular where such shrinkage is impeded,such as at an interface or by the network structure of the polymer itself (112). The rate and the extent of crosslinking or salt formation is reduced in the ATG system because less functional cations are available for reaction than in the ASPA system. Consequently, the level of internal stress formation is likely to be less in the ATG system. Stress relaxation studies of ionomer cements stored at low humidities (figure 3.23) showed that ATG cements had lower internal stresses and were less brittle than ASPA cements as is discussed in section 3.5.1. Also, the extended manipulative properties of the ATG cements provided more time for stress relaxation mechanisms to operate during setting than with the ASPA cements. These observations led to the suggestion that an optimum degree of crosslinking is required for mechanical performance and that excessive reaction, as with the ASPA cements, reduces mechanical properties.

3.2.5 Other Properties of A.T.G. Cements

ATG cements also displayed other properties of interest, they displayed less weight loss and greater mechanical strength than the ASPA cements as discussed in section 3.4.

The hydrolytic stability of ATG cements at ambient temperatures was similar to the ASPA cements, as shown later in Figure 3.18., but the ATG cements displayed greater retention of mechanical properties after immersion in boiling water as discussed in section 3.7.

3.3 Filled ASPA Cements

It was observed that the reactivity of the ASPA system could be controlled by partial replacement of the ASPA glass with either inert fillers, such as silica fillers and glass spheres, or with reactive fillers such as metal oxides and mineral fillers. These fillers were used to volumetrically replace ASPA glass so as to maintain a constant volume fraction of the dispersed phase (filler + ASPA glass) in the polyacrylate matrix. Although the fillers were found to decrease the reactivity of the system the manipulative, mechanical and hydrolytic properties of the filled cements were found to be dependent on the characteristics of the filler and the level of replacement of ASPA glass (ϕ_R) by the filler.

3.3.1. Manipulative and Setting Properties of Filled ASPA Cements

The workability and the setting time of the ASPA cement was progressively extended by increasing the volume fraction of filler in the cement, as shown in Figures 3.9 and 3.10 with typical rheometer traces of manipulative properties in Figure 3.11. For example the work time of the ASPA cement was increased from 1.0 minutes to 5.0 minutes by replacing 75% (ϕ_R = 0.75) of the ASPA glass with an inert filler. This reduced reactivity was due to the functional cation content of the cement mix being diluted by the filler. This effect was more pronounced with the use of inert fillers than with reactive fillers as the latter had surface leachable ions which contributed to the setting mechanism of the cement. The setting times of the highly filled (ϕ_R = 0.75) ASPA cements were similar to that of the ATG cements but the latter had longer workabilities and were thus more suitable for producing larger mouldings. The ATG cements had better moulding properties because the readily leachable calcium cations had been removed from the glass surface as discussed in the previous

Figure 3.9 General Trends of Filled ASPA Cements - Work Time

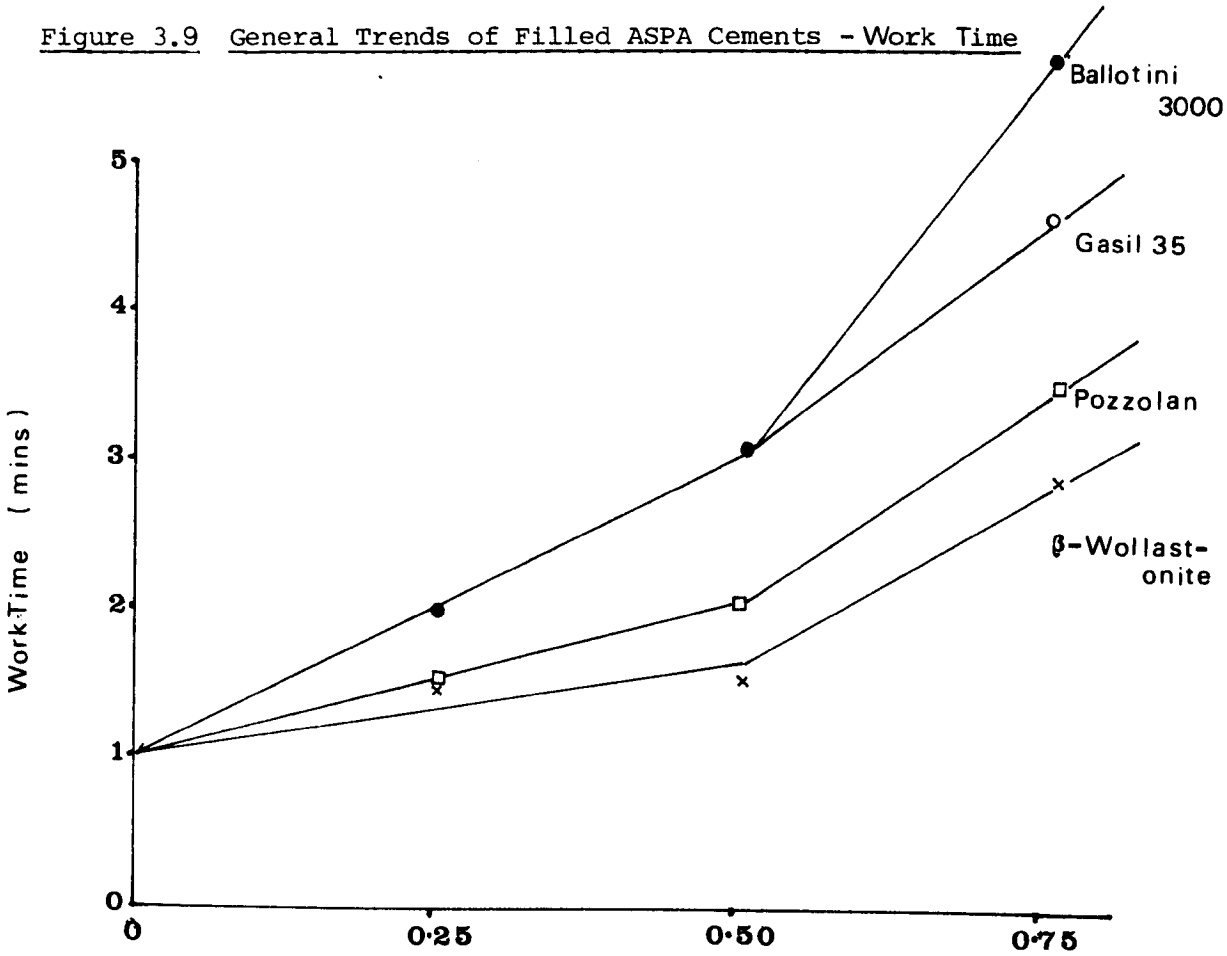

Figure 3.10 General Trends of Filled ASPA Cements - Setting Time

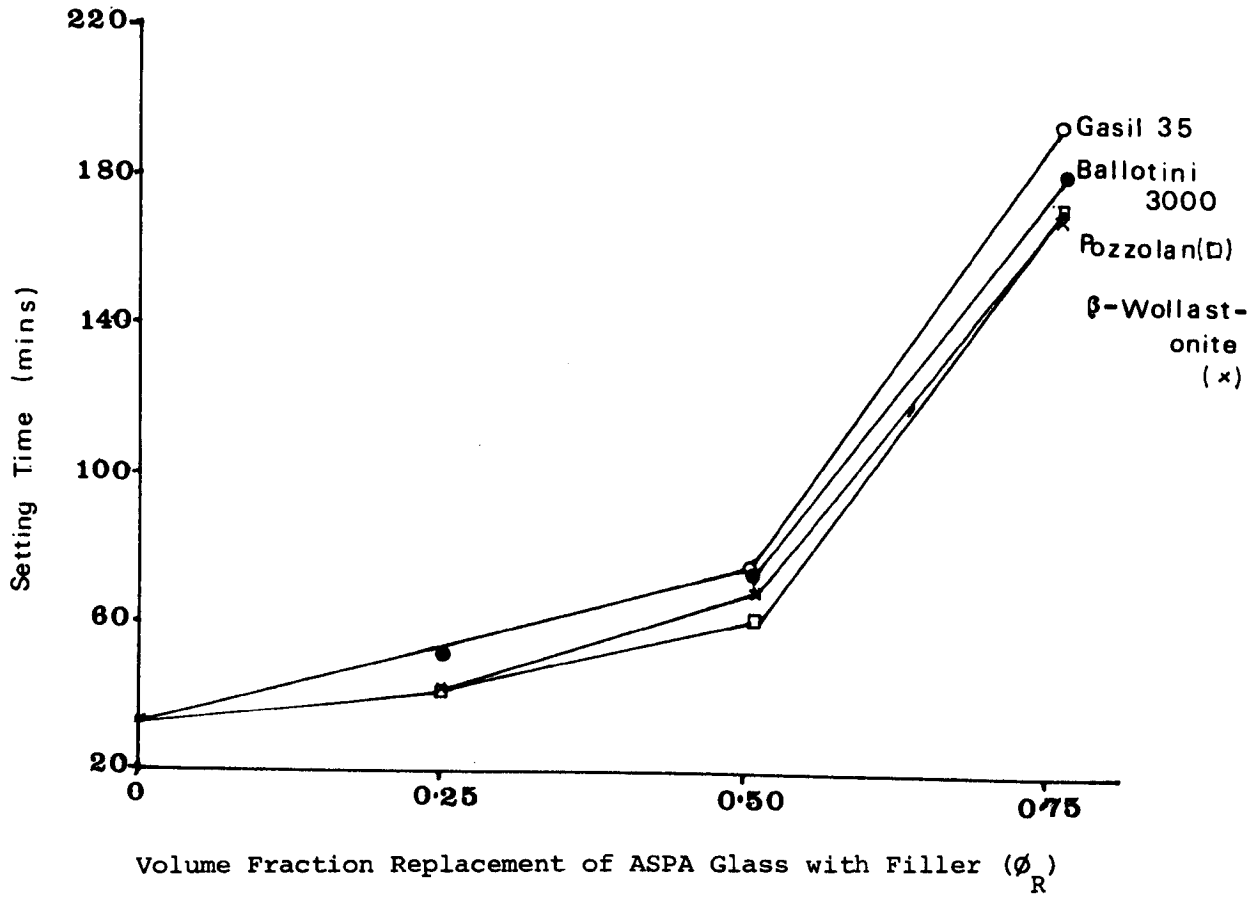

Figure 3.11 Manipulative Properties of Filled ASPA Cements (Rheometer trace)

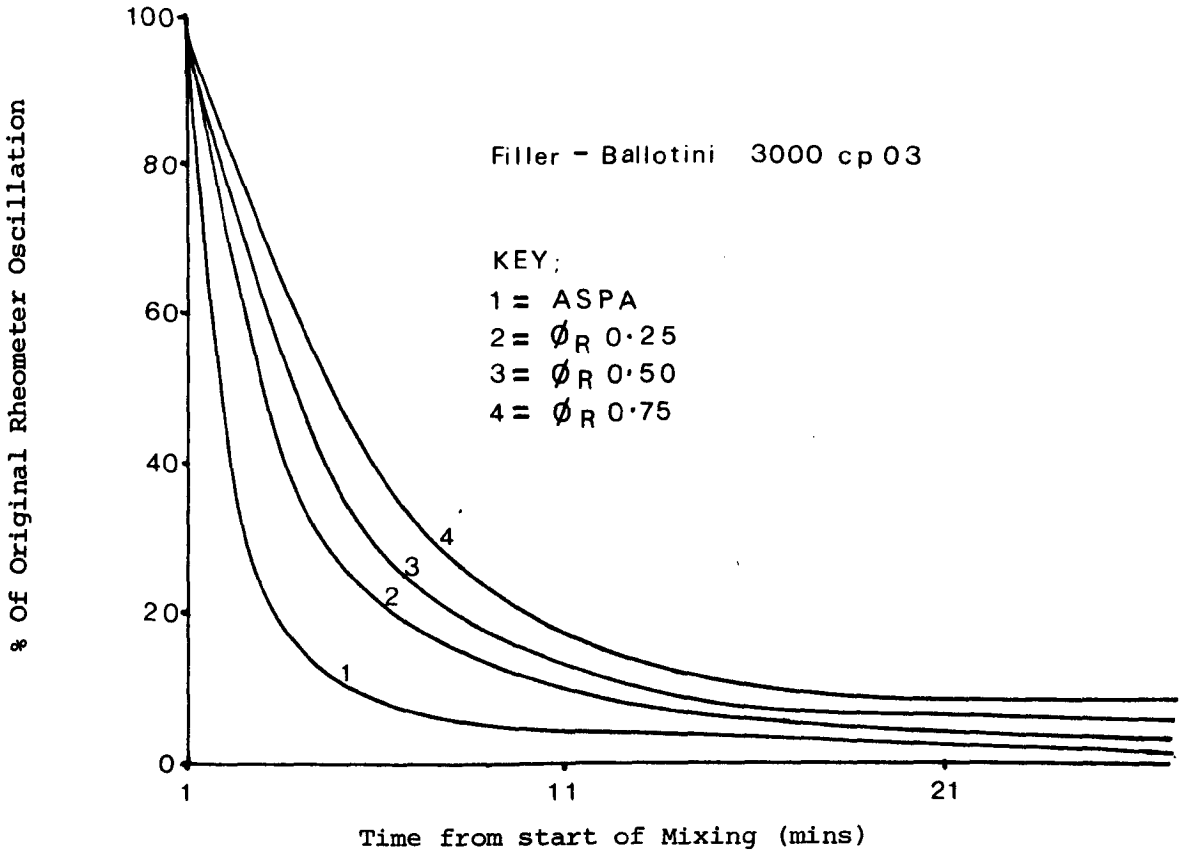

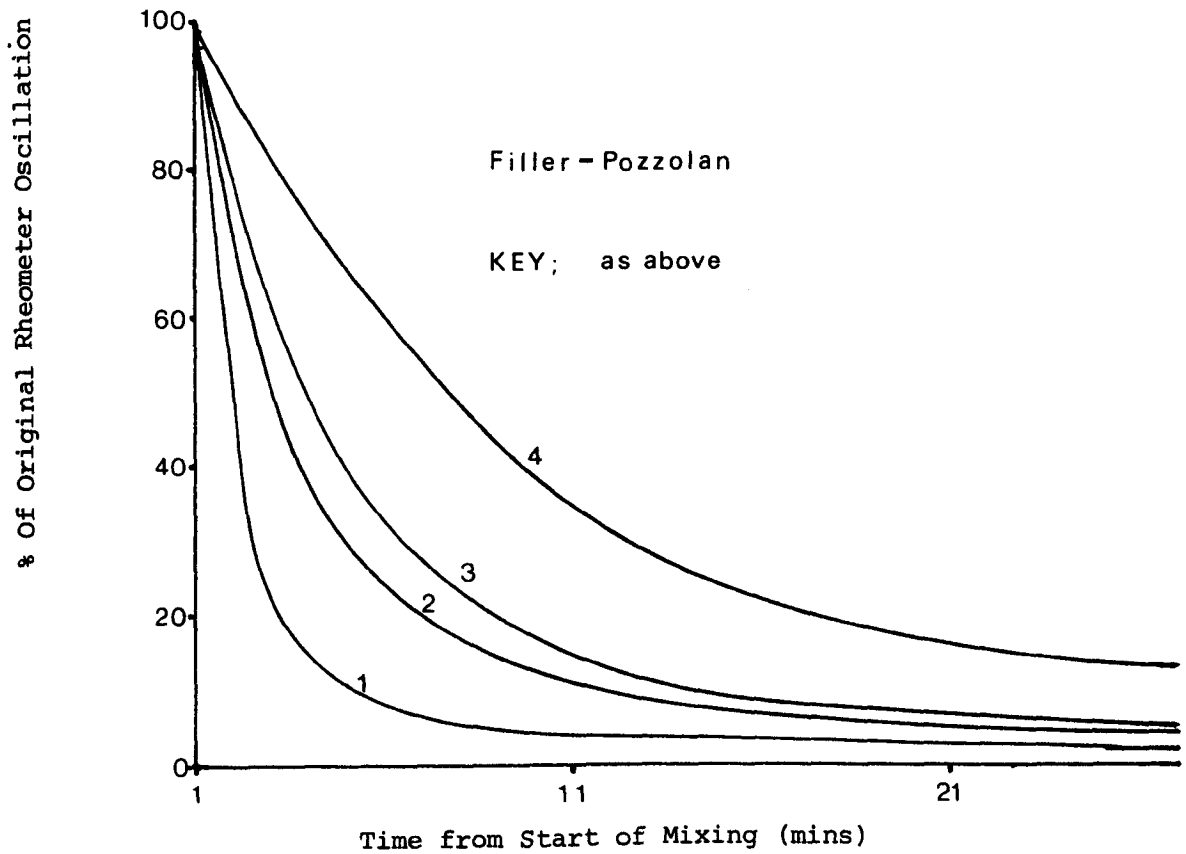

section. With the filled ASPA cements the readily leachable cations remained on the glass surface but were diluted in the cement mix.

Qualitatively, certain fillers were more readily wetted by the aqueous polyacid producing a more easily mixed and workable cement paste. These fillers (Ballotini spheres, silica G M 2 and aluminium hydrate) were found to have smooth surfaces, as shown in Figure 3.13, or had hydrated surfaces. Other fillers which had rough and porous surfaces produced cement pastes which were difficult to mix. For example, many of the reactive fillers were difficult to mix as their reaction with the polyacid increased the viscosity of the matrix and retarded wetting. Also, fillers with hydroscopic surfaces, such as talc and kaolin, competed for the free water of the polyacid and similarly increased the viscosity of the matrix making cement preparation difficult.

3.2. Mechanical Properties of Filled ASPA Cements

The mechanical properties of filled ASPA cements are given in Table 3.4 which demonstrates that the moduli of the cements were generally decreased with increasing volumetric replacement of ASPA glass. However, the strength of the cements displayed more complex behaviour showing a general increase at low volume fraction replacements of ASPA glass ($\emptyset_R$ = 0.25) with a general decrease in strength at higher volume fraction replacements. The strength of the highly filled ASPA cements ($\emptyset_R$ = 0.75) were found to be highly influenced by the characteristics of the filler, in particular its particle size distribution, its shape, its packing properties and the interfacial adhesion between the filler and the polymer matrix. Consequently the moduli and the strength of filled ASPA cements are discussed separately.

Table 3.4 The Mechanical Properties of Filled ASPA Cements

Filler	Volume Fraction Replacement ϕ_R	Comp. Strength (M Pa)	Comp. Modulus (M Pa)	Strain at Fail (%)
None	ASPA Cement (n = 18)	108.0-32.2	2625-382	3.78-1.63
SILICA FILLERS				
Gasil 35	0.25	133.2±8.5	2595±212	4.04±0.45
	0.50	103.4±19.9	2234±158	4.15±1.19
	0.75	117.8±9.3	2271±66	6.10±0.29
Gasil 644	0.25	101.6±5.6	2113±131	3.51±0.42
	0.50	116.6±18.3	2179±329	4.36±0.99
	0.75	100.5±20.4	2093±143	5.00±2.09
Gasil WP	0.25	126.0±23.4	2472±283	3.98±0.71
	0.50	126.9±16.9	2458±281	4.74±1.12
	0.75	66.1±13.5	1625±191	3.34±1.81
Gasil EBN	0.25	162.5±25.4	3307±822	5.12±0.94
	0.50	133.3±28.9	2271±252	5.50±1.57
	0.75	99.9±22.0	2091±221	4.45±1.05
Gasil AF	0.25	125.6±35.4	2537±335	3.98±1.33
	0.50	108.3±10.2	2143±256	4.53±1.05
	0.75	76.9±6.2	1567±252	4.74±0.65
GM2	0.25	107.2±10.6	2181±306	4.87±0.75
	0.50	98.7±29.1	2193±216	4.65±0.17
	0.75	96.0±10.6	2210±194	5.19±0.66
HP37	0.25	105.8±15.7	2325±147	4.29±1.27
	0.50	99.7±16.5	2305±264	4.74±1.47
	0.75	77.6±4.8	1680±198	6.77±0.63
EP20	0.25	83.1±10.0	2182±174	3.77±0.23
	0.50	58.2±4.6	1658±101	4.91±0.50
	0.75	39.2±1.7	915±13	6.86±0.84
Neosyl	0.25	107.2±18.6	2414±327	4.07±0.71
	0.50	77.5±3.8	2268±155	3.77±0.62
	0.75	72.9±9.7	1913±30	5.55±1.26
Microsil GP	0.25	98.8±25.4	2100±169	4.32±1.33
	0.50	111.9±30.0	1974±361	5.46±1.38
	0.75	78.3±15.1	1558±158	5.63±1.64
Garosil	0.25	124.3±23.8	2069±81	5.25±0.69
	0.50	113.2±11.2	2061±134	4.23±1.18
	0.75	98.2±15.8	2060±333	4.57±1.11

Table 3.4 Continued

Filler	Volume Fraction Replacement ϕ_R	Comp Strength (M Pa)	Comp. Modulus (M Pa)	Strain at Fail (%)
Garogel	0.25	115.7±7.0	2198±210	4.07±0.37
	0.50	98.1±23.7	1988±257	4.53±0.93
	0.75	71.6±14.5	1244±85	4.57±1.78
SPHERICAL FILLERS				
Ballotini 3,00CP00	0.25	120.5±15.2	3134±227	3.85±0.95
	0.50	105.1±6.3	3159±193	4.15±0.76
	0.75	84.2±2.3	2460±109	4.74±0.68
Ballotini 3,000CP03 (Silane coated)	0.25	111.4±14.7	2802±99	3.90±0.60
	0.50	116.0±15.1	3055±72	4.40±0.59
	0.75	104.2±6.8	2720±290	7.07±1.21
Ballotini 2429 CP00	0.25	119.1±13.3	2974±317	4.23±0.83
	0.50	94.8±6.0	2698±75	4.66±1.39
	0.75	73.8±2.7	2360±378	4.79±0.44
Ballotini 2024	0.25	114.9±9.6	2827±163	4.28±0.45
	0.50	82.2±4.1	2926±166	3.05±0.14
	0.75	42.9±3.4	2220±560	3.81±0.79
Pozzolan (P.F.A.)	0.25	92.9±27.3	2905±211	3.18±0.64
	0.50	92.4±25.7	2278±274	3.77±1.07
	0.75	112.9±25.7	2368±1.54	4.12±1.37
PLATE-LIKE FILLERS				
Talc	0.25	66.5±20.0	2118±182	2.19±1.09
	0.50	47.9±5.0	2124±87	3.33±0.42
	0.75	30.4±6.0	1708±67	2.46±0.56
Kaolin	0.25	82.6±10.2	2589±394	2.75±0.29
	0.50	39.3±4.0	2195±500	2.65±0.10
	0.75	36.8±12.8	1927±94	3.13±0.83
Porcelain Powder (1)	0.25	83.3±31.9	2458 -	3.72 -
	0.50	77.1±4.3	2685±119	3.10±0.59
	0.75	50.8±8.99	1987 -	2.20 -
OTHER FILLERS				
Nylon 66 Powder (Low Density)	0.25	98.5±21.5	2599±200	3.14±0.29
	0.50	99.0±18.3	2341±230	4.61±1.42
	0.75	84.0±4.8	2070±281	7.86±0.46
Aggregate Filler (Optimum Packing)	0.25	114.4±30.3	4357±730	3.44±1.02
	0.50	102.0±9.7	3107±298	3.89±0.50
	0.75	93.0±5.0	3246±519	4.49±0.63

Table 3.4 Continued

Filler	Volume Fraction Replacement ϕ_R	Comp Strength (M pa)	Comp Modulus (M pa)	Strain at Fail (%)
Polyethylene Powder (Low Adhesion)	0.25	51.6±13.5	2271±390	3.05±0.42
	0.50	33.5±4.0	1448±554	3.43±0.56
	0.75	43.9 n=2	1243	4.23
Synthetic Appetite (Calcium Poly-Phosphate)	0.25	141.8±25.8	2802±202	5.04±0.68
	0.50	106.6±18.1	2446±131	4.36±0.84
	0.75	76.2 n=2	1976 -	3.94 -
None	ASPA cement (2nd Series of Results) n = 8	118.2±35.3	4030±573	3.07±0.71
METAL OXIDE FILLERS				
Aluminium Oxide (acid grade)	0.25	92.9±17.2	3226±350	3.22±0.96
	0.50	94.9±5.8	3355±299	3.26±0.74
	0.75	85.4±14.7	2013±327	5.64±0.42
Aluminium Oxide (neutral grade)	0.25	118.1±15.0	3525±595	4.20±0.53
	0.50	135.0±8.0	3859±113	4.46±0.45
	0.75	125.6±15.2	2708±526	6.61±0.58
Aluminium Oxide (basic grade)(1)	0.25	44.3±3.5	1982±337	2.29±0.35
	0.50	109.0±18.1	3852±436	3.89±0.50
	0.75	124.8±12.9	2837±782	6.09±1.02
Aluminium Hydrate	0.25	110.7±18.8	3858±117	4.00±0.60
	0.50	109.9±9.0	3742±70	3.61±0.50
	0.75	85.2±8.3	2516±497	5.46±0.09
MINERAL FILLERS				
Willemite (2)	0.25	59.3 n=2	2667 -	2.46 -
	0.50	85.8±7.9	3806±503	2.48±0.53
	0.75	57.8 n=2	1487 -	5.76 -
Hardystonite (2)	0.25	51.1 n=2	1628 -	2.46 -
	0.50	51.0±20.3	1591±125	2.82±0.68
	0.75	31.4 n=2	1355 -	2.79
Flourspar	0.25	114.7±9.7	3884±507	3.18±0.40
	0.50	89.8±29.3	3718±392	2.65±0.45
	0.75	86.3±3.00	3021±528	3.76±0.42
Pseudo-Wollastonite	0.50	58.1±11.9	2259±2.60	2.88±0.17
ß-Wollastonite	0.25	111.7±15.4	3718±265	3.44±0.35
	0.50	87.3 n=2	2909 -	2.79
	0.75	Poor mould release		
ß-Wollastonite (treated)	0.75	89.7 n=2	3904	3.95±0.58

N.B: (1) Poorly mixed cements
(2) Highly voided cements

General Trends of Strength Properties

The general increase in strength of the filled cements at the ϕ_R = 0.25 level, which was an increase of 20%-30% in some cases, was attributed to the following two factors.

1. The extended workability and reduced reactivity of the filled cements permitted more time for thorough mixing and for processes of wetting to occur than with the ASPA cements. Thus composites were produced of improved interfacial adhesion and with well dispersed particles but without great reductions in the number of functional cations released during the setting process. This reinforces the proposals made with ATG cements that maximum strength occurs with a certain degree of cross-linking and that excessive reaction, as with the ASPA systems, may diminish the strength of the cement.

2. The use of low levels of fillers was found to promote greater packing efficiency of the total dispersed phase as shown in Table 3.7. However, increases in the packing fraction often leads to increased inter-particle contact and loss of strength unless some bi-modal packing exists as described in Section 1.5.5. Examination of the particle shape characteristics in Figure 3.13 suggests that finer particles of the spherical fillers may act in such a manner. These fine particles were not accurately detected in the particle size analysis as the techniques used were not suitable for particles smaller than one micron (178,179).

The compressive strengths of the cements at volume fraction replacements greater than ϕ_R = 0.25 were generally decreased but at ϕ_R = 0.75 certain fillers produced composites of similar strengths to the unfilled ASPA cements (circa 100 MPa). These fillers were Gasils 644 and 35, Silicas EBN and GM2, Ballotini 3,000 CP03 Glass Spheres and

the reactive fillers Pozzolan and Aluminium Oxide. This demonstrates that a high degree of cross-linking or salt formation is not a prerequisite for high mechanical performance and that strong cements can be made where the potential cation content is a quarter of the ASPA system. However, the mechanical properties of these highly filled cements were influenced by the characteristics of the filler and the following effects were observed.

Particle Size of The Fillers

The mean particle size of the filler, their proportion of material finer than one micron and the size of their largest particles are given in Table 3.5. along with manufacturers data for comparison. Complete particle size distributions of the fillers are given in Appendix 3. The Coulter technique was used for most of the silica fillers but was not suitable for use with more dense fillers and these tended to sink in the electrolyte and were not counted. In such cases the Optomax technique was employed. This technique, which uses an optical counting principle, necessitated good contrast between the filler and the dispersing medium and this was only achieved by coating the particles with fluorescent dyes.

The effects of filler particle size on the mechanical properties of filled ASPA cements was examined by comparing cements prepared with fillers of low aspect ratio (See Table 3.6) and excluded the use of reactive fillers and fillers with special adhesional properties such as the polyethylene powder. The results demonstrate that both compressive strength and compressive modulus are enhanced by the use of fillers with small mean particle sizes and with narrow particle size distributions. Relationships were found to exist between mean filler particle size and the compressive strength of

Table 3.5 Nominal Particle Size of Fillers and of ASPA Glass

Filler	Mean P.S. Manufacturers Data (μm)	Mean P.S. (μm)	Largest P.S. (μm)	% Smaller than 1.0 μm
ASPA Glass (batch 2)	10.0	3.75	25	15
SILICA FILLERS				
Gasil 35	2.8	3.25	25	10
Gasil 644	2.8	2.5	17	20
Gasil WP	15.0	14.5	42.5	0
Gasil EBN	8.0	7.0	25	8
Gasil AF	17.0	13.75	42.5	0
EP20	120.0	-	-	-
HP37	6.5	6.75	20	8
GM2	9.7	8.25	25	15
Neosyl	15.0	8.5	45	0
Microsil GP	13.0	6.25	25	10
Garosil	1.0	2.0	20	25
Girogel	<1.0	1.25	7.0	57
GLASS SPHERES				
Ballotini 3,000	4-44	5.75 (Optomax)	30	10
Ballotini 2429	53-105	52.0 (Optomax)	90	0
Ballotini 2024	105-210	-	-	-
MINERAL & METAL OXIDE FILLERS ETC.				
Pozzolan	-	8.3	60	7.5
Fluorspar	-	14.5 (Optomax)	60	7
Hardystonite	-	1.1 (Optomax)	16	46
Willemite		3.3 (Optomax)	18	24
Pseudo Wollastonite	-	2.1 (Optomax)	11	25
Aluminium Oxide (basic)	-	4.1 (Optomax)	60	20

Table 3.5 Cont'd Nominal Particle Size of Fillers and of ASPA Glass

Filler	Mean P.S Manufacturers Data (μm)	Mean P.S. (μm)	Largest P.S. (μm)	% Smaller than 1.0 μm
Aluminium Oxide (acid)	-	4.1 (Optomax)	60	20
Aluminium Oxide (neutral)	-	5.4 (Optomax)	35	7
PLATE-LIKE FILLERS				
Talc	-	19.0	45	0
Porcelain Powder	-	8.3	60	7.5
Kaolin	-	2.8	14	25
OTHER FILLERS				
Nylon 66 Powder	-	13.5	60	0

the composite. The effects of particle size on the strength of the cements was most pronounced at high filler levels (ϕ_R = 0.75) as the influence of the ASPA glass was less in these cements. Empirically, at this filler level a linear relationship was found to exist over a wide particle size range (1-150μm) as shown in Figure 3.12(a) and as given in Equation 3.1.

$$\sigma_{FIC} = \sigma_{ASPA} - M \log_{10} d \qquad 3.1$$

where: σ_{FIC} = Strength of filled ionomer (ASPA) cement

σ_{ASPA} = Strength of unfilled ASPA cement

M = Slope constant (28.7)

d = Particle diameter (μm)

This relationship was found to have a correlation coefficient (linear regression analysis) of 0.89.

The effects of volume fraction replacement of ASPA glass were also considered in conjunction with the particle size of the filler as shown in Figure 3.12(b). The following relationship (Equation 3.2) was found to exist but over a smaller particle size range than Equation 3.1.

$$\sigma_{FIC} = \sigma_{ASPA} - K (\phi_R d)$$

where: K = Slope constant (2.84)

This relationship was found to have correlation coefficient of 0.44 which was considerably lower than in Figure 3.11. This was attributed to the dominant influence of the ASPA glass on the strength of the cements at lower values of ϕ_R.

The intercept values of these two relationships, that is the

Figure 3.12(a) Relationship Between Particle Size of Filler and Compressive Strength of Filled Ionomer Cements; $\phi_R = 0.75$

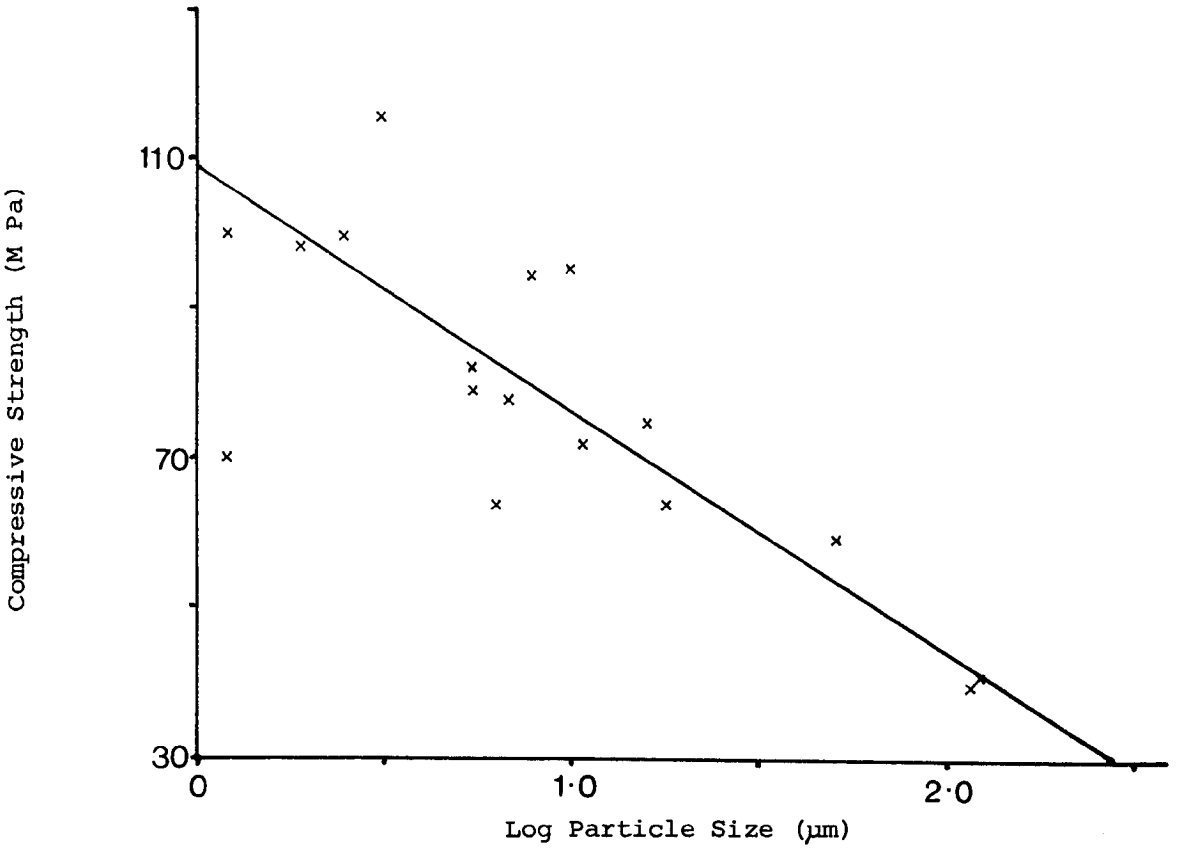

Figure 3.12(b) Relationship Between Particle Size of Filler and Compressive Strength of Filled Ionomer Cements: at all values of ϕ_R

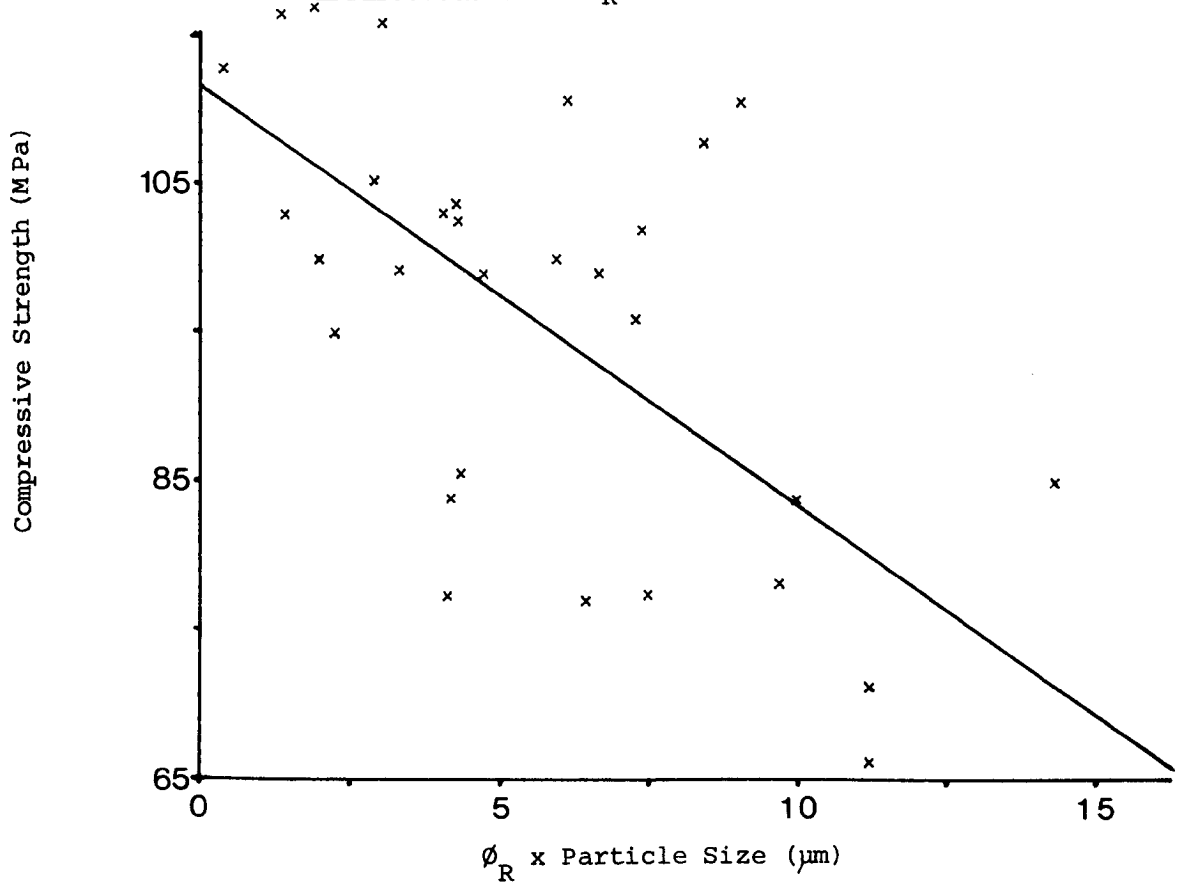

calculated strength of the unfilled ASPA cement, were found to be 111.2 MPa (Equation 3.1) and 112.3 MPa (Equation 3.2) which were both in good agreement with the value of 108.0 MPa found in practice.

It was evident that fillers with mean particle sizes close to one micron, such as the silica Garogel, did not perform as well as predicted by these equations. The strength and the modulus of these cements tended to deteriorate with increasing volume fraction of filler and at the ϕ_R = 0.75 level had a compressive strength and modulus values of 71.6 MPa and 1244 MPa respectively. This was considerably lower than silicas with mean particle sizes of 2-10 microns, such as Gasils 644 and GM2, which had strength and modulus values of circa 100 MPa and 2,000 MPa respectively at the ϕ_R = 0.75 level. This loss of mechanical performance with smaller fillers is similar to the loss of performance with small fractions (0 - 10 μm) of ASPA glass, as discussed in Section 3.5.1., and can be attributed to the larger surface area of these small particles not being adequately wetted by the polyacid.

Particle Shape of Fillers

The particle shapes of the fillers were determined from the electron micrographs as shown in Figure 3.13. Quantitative analysis of particle shape were not conducted due to difficulties in determining their aspect ratios. Photomicroscopy translates three dimensional structures into two dimensional pictures and only a few representative measurements could be made from each photograph and these aspect ratios are given in Table 3.6.

Qualitatively the effects of particle shape on the mechanical properties of filled ASPA cements were distinct with cements containing high aspect ratio fillers, such as talc, kaolin and

Figure 3.13 Particle Shape of Various Fillers

1. Spherical Filler Ballotini 3,000; Magnification 5 K

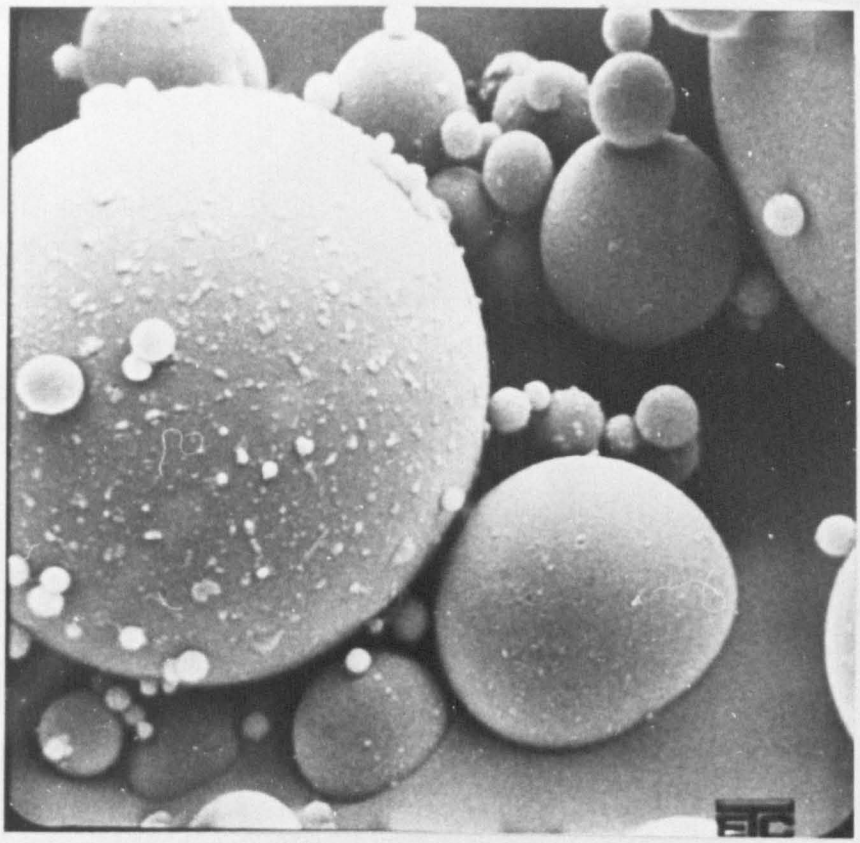

2. Spherical Filler Pozzolan (P.F.A.); Magnification 5 K

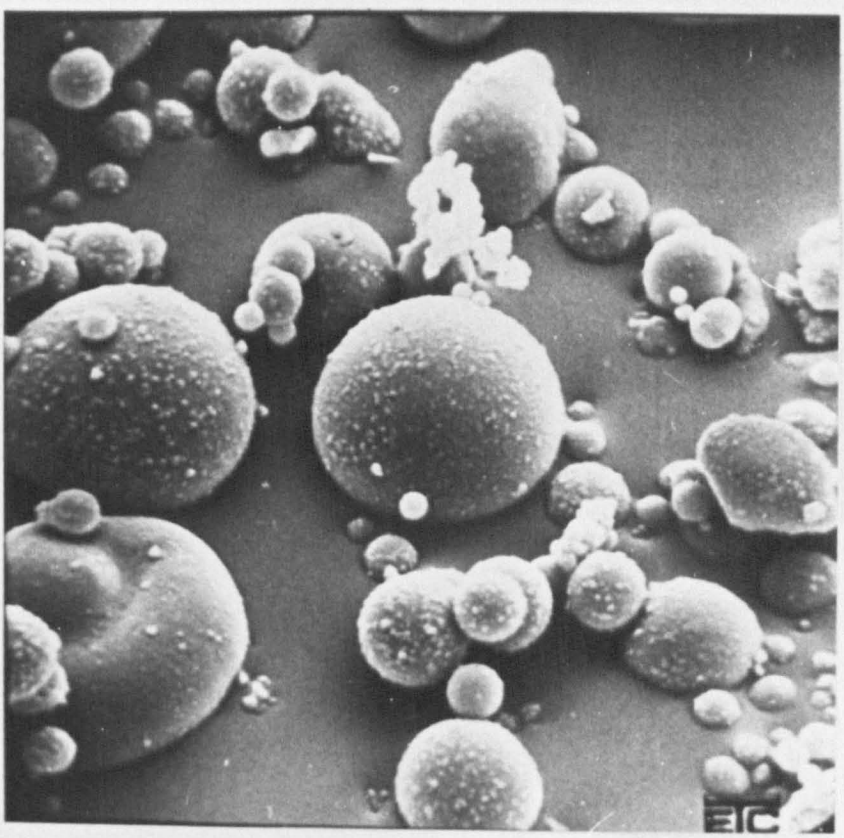

Figure 3.13 Continued

3. Silica Filler - GM2; Magnification 5 K

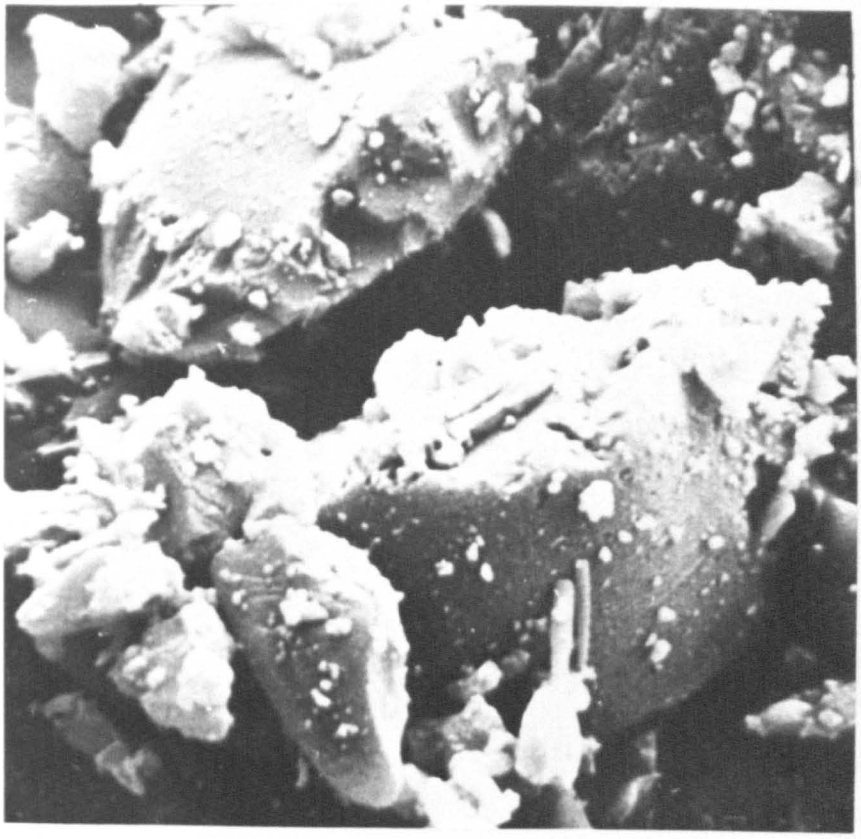

4. Silica Filler - EBN; Magnification 5K

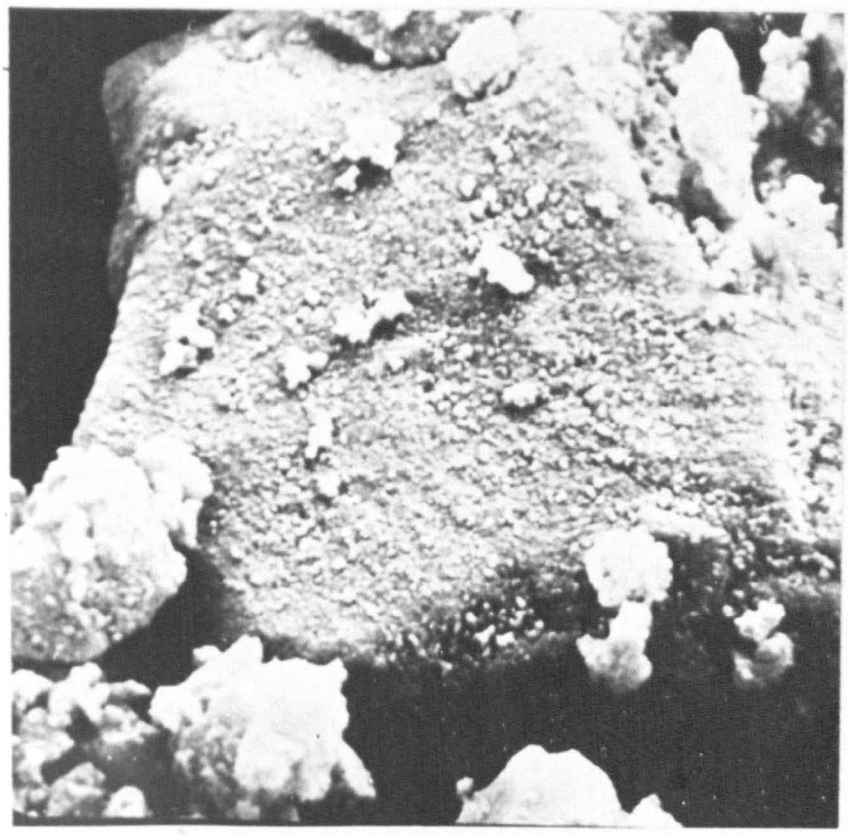

Figure 3.13 Continued

5. Silica Filler - Garosil; Magnification 5K

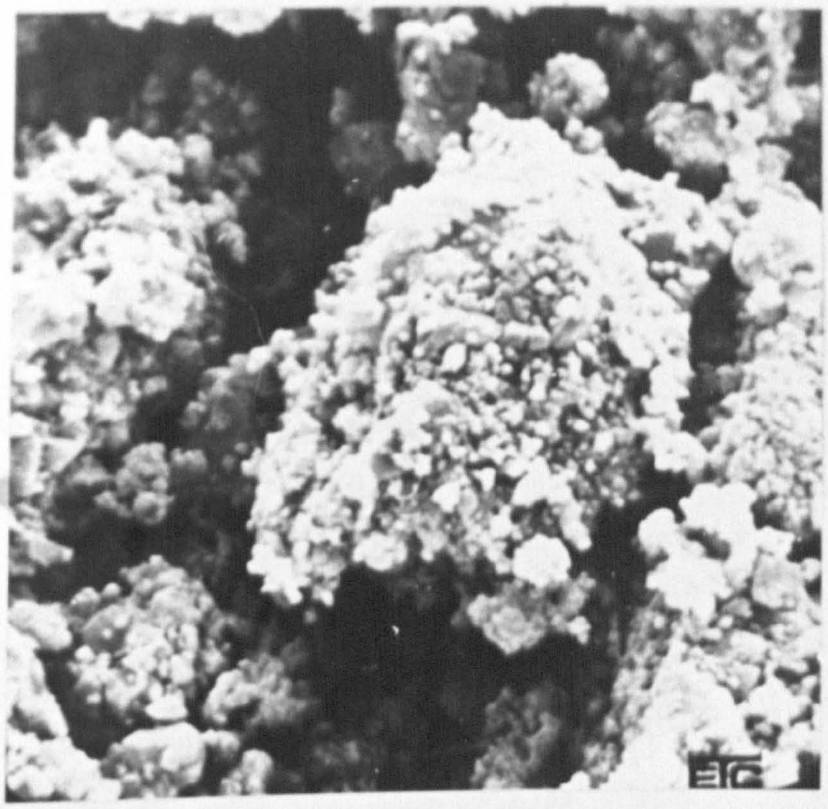

6. Filler - Nylon 66 Powder; Magnification 5K

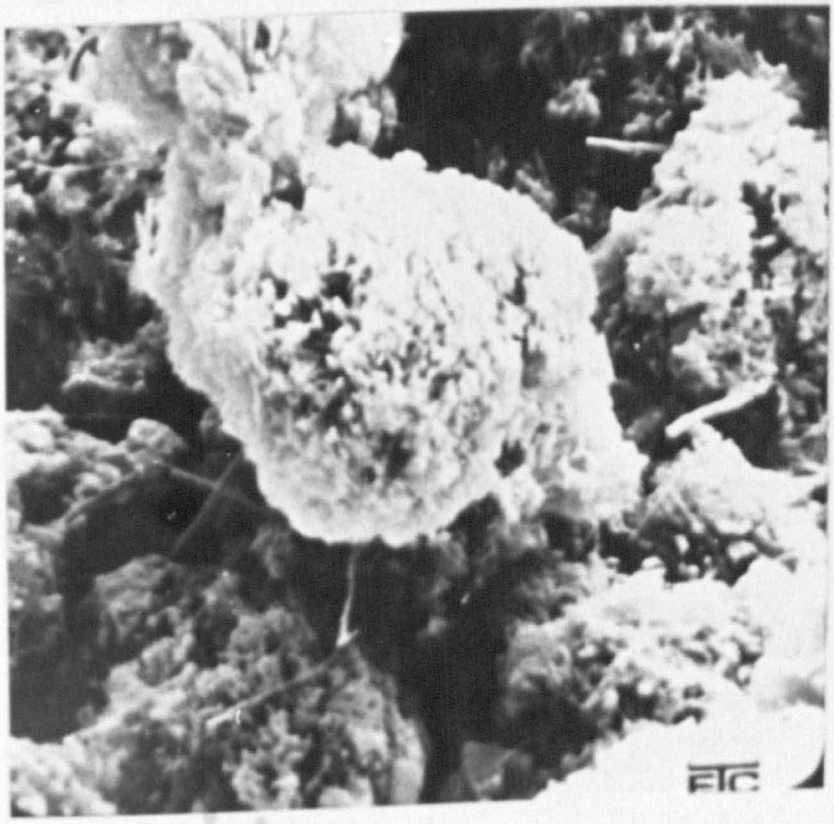

Figure 3.13 Continued

7. Plate Like Filler - Talc; Magnification 1 K

8. Plate Like Filler - Kaolin; Magnification 5 K

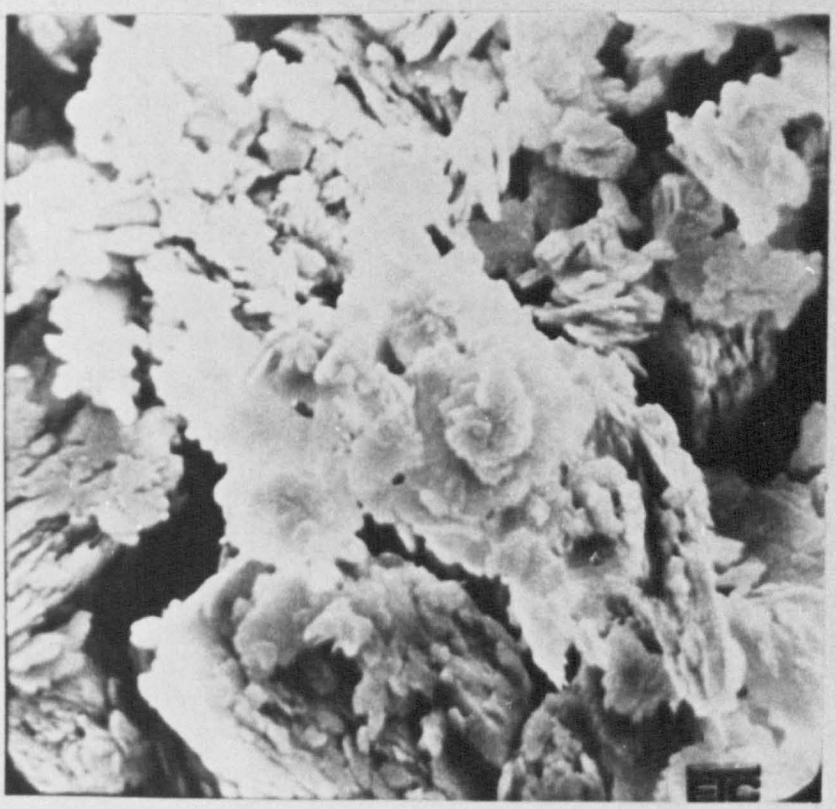

Figure 3.13Continued

9. Mineral Filler - Willemite; Magnification 5 K

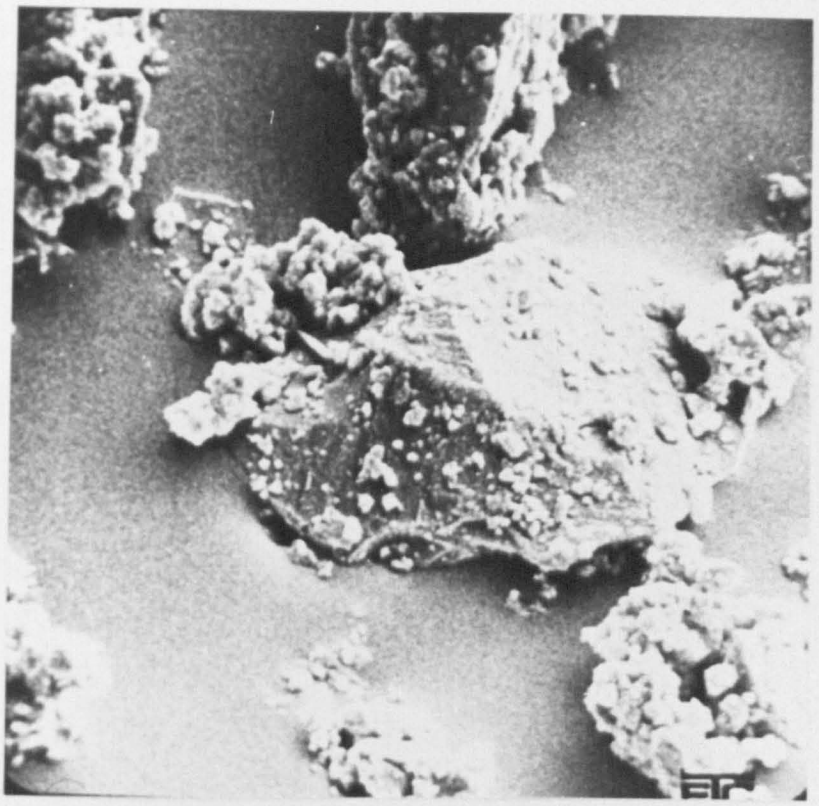

10. Mineral Filler - Fluorspar; Magnification 2 K

Figure 3.13 Continued

11. Mineral Filler - ß Wollastonite; Magnification 2 K

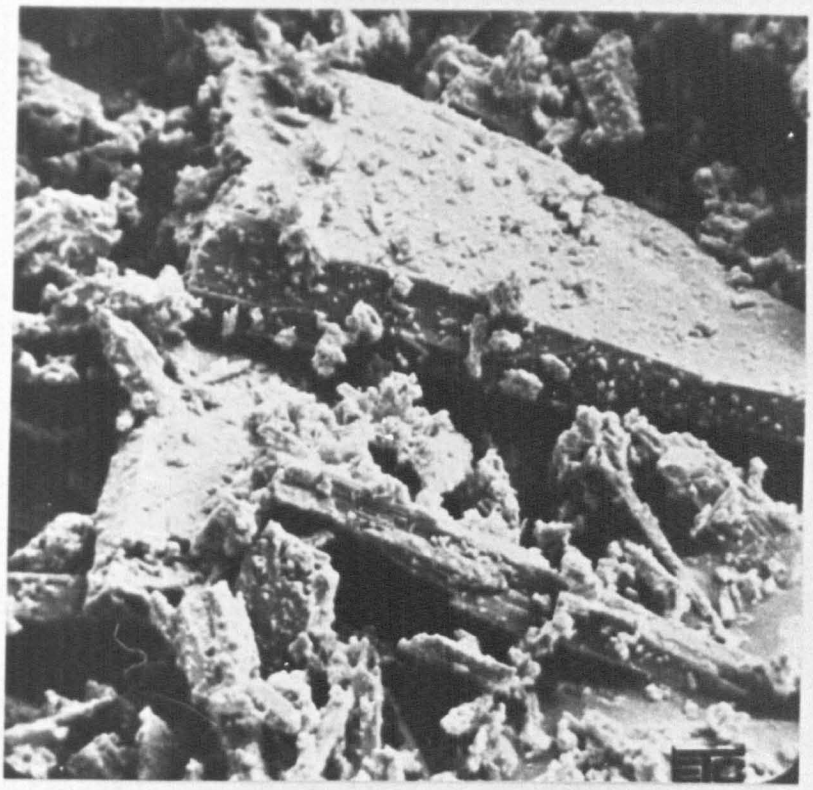

12. Metal Oxide Filler - Aluminium Hydrate; Magnification 1 K

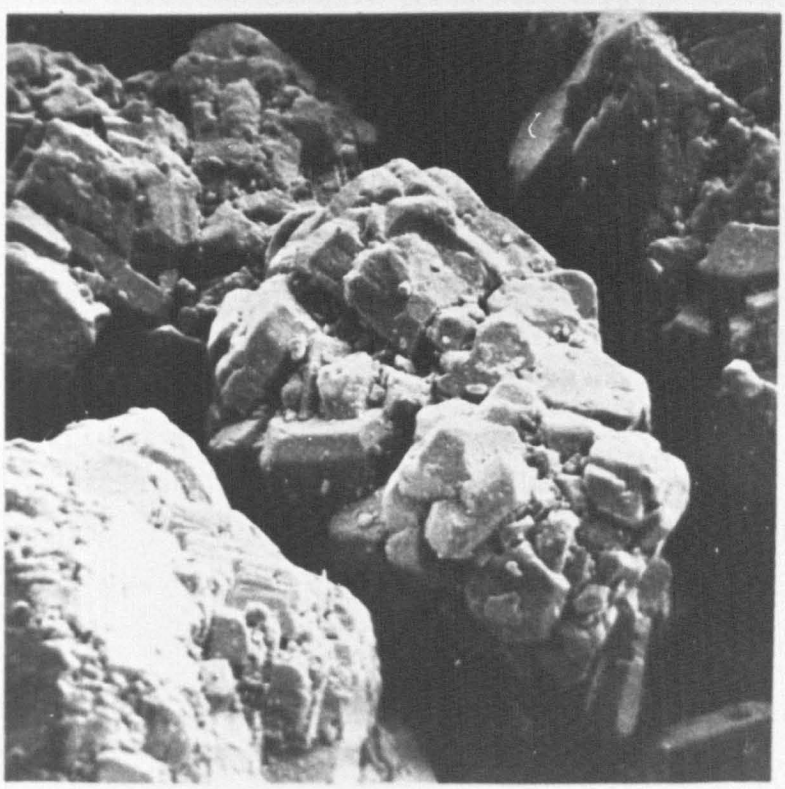

porcelain powder, being inferior to cements containing similar sized low aspect ratio fillers. However, others (97) have shown that composites filled with particles of high aspect ratios such as mica, were mechanically superior to composites filled with glass spheres but in this case the composites were injection moulded and the high aspect ratio particles were aligned with the composite displaying anisotropic behaviour. The low pressure moulding process used here probably led to a more random orientation of the plate-like particles and hence the reduced mechanical performance.

The spherical Ballotini and Pozzolan fillers were found to produce stronger composites than similarly sized silica fillers such as GM2 and HP37 whose shapes were polyhedral and contained corners and edges and thus only approximated to a spherical shape. It has been shown that fillers with such shapes produce weaker composites than smooth surfaced spherical fillers as these corners and edges can act as stress concentrators during loading and promote premature failure (93).

The surface topography of the filler was also found to influence the mechanical performance of the filled ASPA cements. In general, the smoother surfaced fillers such as the Ballotini spheres and the silicas GM2 and EBN produced stronger composites than similar sized silica fillers such as Microsil and Neosyl which had porous surfaces with fine material attached, as is shown in Figure 3.13. The latter structure is characteristic of amorphous silicas and the smoother surface characteristic of more crystaline silicas (184) although GM2 and EBN have been found to be amorphous to X-rays (185). Consequently, it is proposed that the smooth surfaced

fillers present surfaces which are more readily wetted by the polyacid than are the porous and irregular surfaced fillers and that this improved wetting leads to stronger composites. Also, some fillers, such as the porous silicas and the mineral fillers, had fine particles adhering to their surfaces which would act as a mechanically weak boundary layer at the filler-matrix interface and further reduce strength.

Packing Fractions of the Fillers

The packing fractions of the individual filler particles are shown in Table 3.6 and of certain filler-ASPA glass powder mixes in Table 3.7. The effects of particle packing efficiency upon the mechanical properties of the cements were difficult to assess due to the more dominant characteristics of particle size, particle shape and reactivity towards the polyacid. Further, most of the silica fillers displayed unusually low packing fractions which was attributed to their highly porous structures giving low values for the bulk density. However, a relationship was found to exist between packing fraction and compressive strength for other inert fillers of low aspect ratio. This linear relationship is shown in Figure 3.14 and demonstrates that increasing packing efficiency of the fillers (higher values of packing fraction) produced weaker composites,which was attributed to agglomeration of the particles in the matrix. Such behaviour is typical of particulate composites, as described in Section 1.5.5, and similar effects were observed with unfilled ASPA cements as discussed in Section 3.6.1. However, it is known (98) that the use of fillers with bi-modal particle size distributions increases both the packing fraction and the strength of the composite. The aggregate filler used here was believed to have efficient packing properties (45,49) and produced mechanically strong

Table 3.6 Physical Properties of Fillers and ASPA Glasses

Filler	Aspect Ratio	Bulk Density (Mg m-3)	True Density (Mg m-3)	Packing Fraction
ASPA Glass	1-2.0	1.32	2.47-3.00	0.44-0.53
ATG Glass	1-2.0	1.32	2.27-2.53	0.52-0.58
SILICA FILLERS				
Gasil 35	1-1.1	0.15	1.78	0.09
Gasil 644	1-1.5	0.14	2.01	0.07
Gasil WP	1-1.5	0.45	1.24	0.38
Gasil EBN	1-1.2	0.23	2.01	0.12
Gasil AF	1-1.7	0.35	1.34	0.26
EP 20	1-1.1	0.30	2.11	0.14
HP 37	1*	0.17	1.91	0.09
GM2	1-1.1	0.61	1.87	0.33
Neosyl	1-1.3	0.18	1.95	0.09
Microsil	1-1.3	0.20	1.90	0.10
Garosil	1-1.7	0.10	1.68	0.06
Garosil	1-1.6	0.80	2.46	0.34
GLASS SPHERES				
Ballotini 3,000	1	1.26	2.37-2.32	0.54
Ballotini 2429	1	1.50	2.47	0.61
Ballotini 2024	1	1.52	2.47	0.61
MINERAL & METAL OXIDES FILLERS Etc.				
Pozzolan	1	1.18	2.32	0.51
Fluorspar	1-3.4	-	-	-
Hirdystonite	1*	1.42	2.70	0.53
Willemite	1-1.7*	2.15	4.52	0.48
ß-Wollastonite	2.0-6.3	1.08	2.86	0.38
Pseudo Wollastonite	1.7-4.0	1.01	3.36	0.30

Filler	Aspect Ratio	Bulk Density (Mg m-3)	True Density (Mg m-3)	Packing Fraction
Aluminium Hydrate	1-1.1	1.37	2.46	0.56
Aluminium Oxide (a)	1-1.2	1.11-1.12	3.05-3.29	0.34-0.37
Synthetic Apatite	1*	1.58	3.04	0.52
PLATE-LIKE FILLERS (b)				
Talc	30	1.04	-	-
Porcelan Powder	12	1.14	2.35	0.14
Kaolin	10-20*	0.53	3.86	0.14
OTHER FILLERS				
Nylon 66	1-1.1*	0.23	1.12	0.21
Polyethylene Powder	-	0.78	0.95	0.82
Aggregate filler	-	1.95	2.80	0.70

NOTES:

* Resolution of micrographs insufficient for accurate determination.

(a) Aluminium oxides various grades ground to pass a 45 μm sieve.

(b) Aspect ratio-longest axis to particle thickness.

Table 3.7 Packing Fractions of ASPA/Filler Powder Mixtures

	Volumetric Replacement $\emptyset_R$	Bulk Density (Mg m^{-3})	True Density (Mg m^{-3})	Packing Fraction
ASPA	0	1.32	2.47	0.53
ASPA + Pozzolan Filler	0.25	1.45	2.44	0.59
	0.80	1.39	2.39	0.58
	0.75	1.29	2.35	0.54
ASPA + Ballotini Filler	0.25	1.65	2.34	0.70
	0.50	1.67	2.29	0.73
	0.15	1.71	2.24	0.76

Figure 3.14 Relationship Between the Filler Packing Fraction and the Compressive Strength of the Filled Ionomer Cements: ϕ_R = 0.75

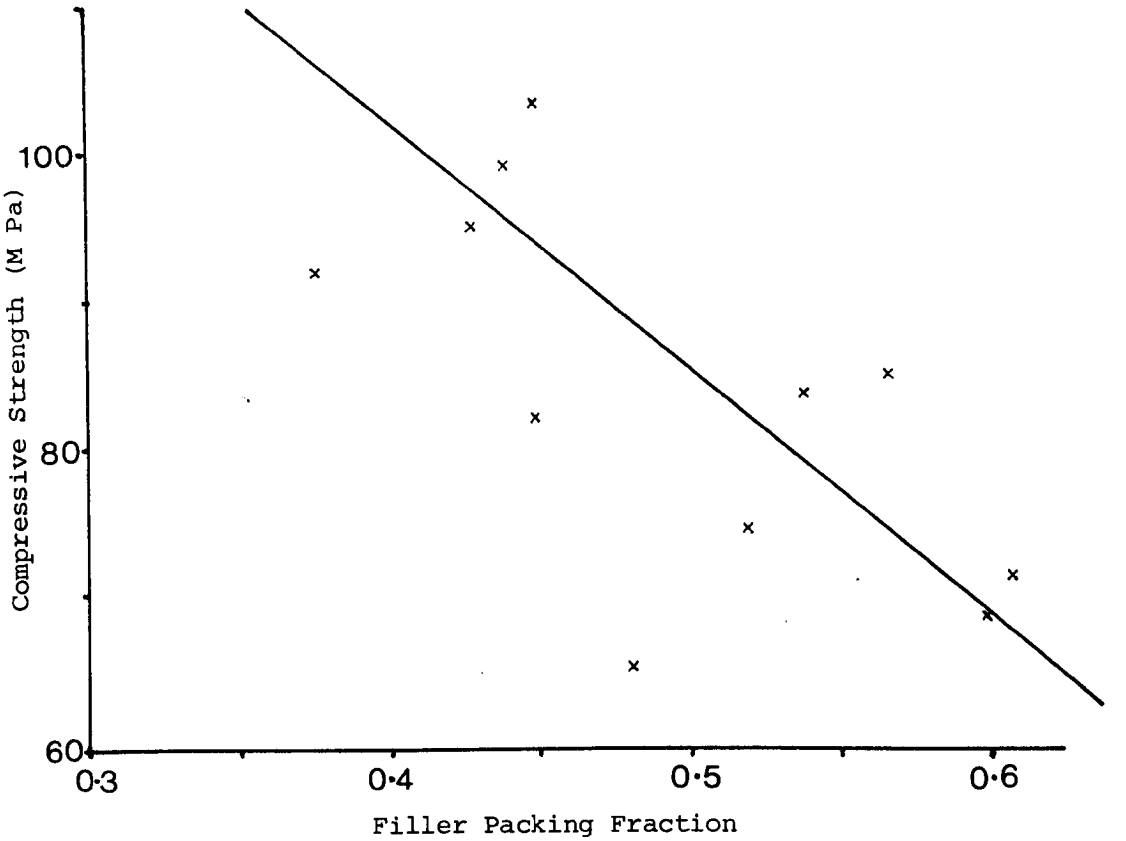

N.B. The above line was found to have a correlation coefficient (linear regression analysis) of 0.61 and a slope of 1.67

composites despite containing large ($\sim$ 50 μm) unreactive particles; the strength of the cements at ϕ_R = 0.75 was 93.0 MPa whereas Equation 3.1. would have predicted a strength of 52 MPa for such sized particles. Also, as discussed earlier the Pozzolan and Ballotini 3,000 glass sphere fillers appeared to contain fine particles which give bi-modal properties (See Figure 3.13) in particular when mixed with ASPA glass as shown by their high values of packing fraction in Table 3.7. This may be another factor to account for the relatively good performance of these filled ionomer cements.

Modulus of Filled-Ionomer Cements

The modulus properties of composite materials are known to be predominantly dependent upon the volume fraction of the filler and on other properties such as the particle shape, the extent of particle agglomeration in the composite and the interfacial adhesion between the filler and the matrix. These effects are described in Section 1.5.1. and a number of theoretical approaches have been developed to describe the relationship between modulus and volume fraction of filler as shown in Figure 1.7. Such theoretical analyses are difficult to apply to filled ionomer cements as they have complex structures with the filler providing a third phase in the ionomer cement. However, Carrillo (58) considered the ASPA system as analogous to an unfilled polymer and then considered the effects of filler addition although in practice the total volume fraction of the dispersed phase (ASPA glass + filler) in the PAA matrix remained constant. Such an approach has been adopted in this Section to demonstrate the effects of filler-additions to ASPA cements. The effects of varying the total volume fraction of the dispersed phase for ASPA, filled-ASPA and ATG cements is considered in more

detail from a theoretical point of view in Section 3.5.2.

Adopting Carrillo's approach, the relative modulus of the filled ionomer cements were found to generally decrease with increasing replacement of the ASPA glass as shown in Figure 3.15, and displayed similarity with the Sato-Furukawa relationship (Figure 1.7 and Appendix 1) for low adhesion between the filler and the matrix. Thus the loss of mechanical performance at higher volume fraction replacements can be attributed to this poor adhesion at the filler/PAA interface. It was also evident that mineral, metal oxide and silane coated fillers displayed greater modulus retention than other types of filler. Consequently, this behaviour strongly suggests that the interfacial adhesion between the ASPA glass and the PAA matrix is greater than the adhesion between the various fillers and the matrix. With the inert fillers only secondary bonding forces, such as Van de Waal's forces, could exist but with the ASPA glass there is potential for stronger interfacial bonding forces to operate, such as hydrogen bonds or primary (ionic) bonds. The formation of of interfacial ionic bonds is probable as ionic bonds are formed in the curing mechanism of ionomer cements and, as suggested in the study of ATG cements (Section 3.2), the glass particle may have surface metallic ions which are firmly embedded in the glass and are not liberated by acid attack.

The interfacial adhesion between the filler and the PAA matrix was improved, and hence the modulus improved, by using reactive fillers or fillers coated with a silane coupling agent. Two grades of Ballotini 3,000 glass spheres were used as shown in Table 3.4, the silane coated spheres (CPO3, coupling agent not disclosed but believed to be a silane methacrylate) produced mechanically superior filled

Figure 3.15 Modulus Behaviour of Filled ASPA Cements

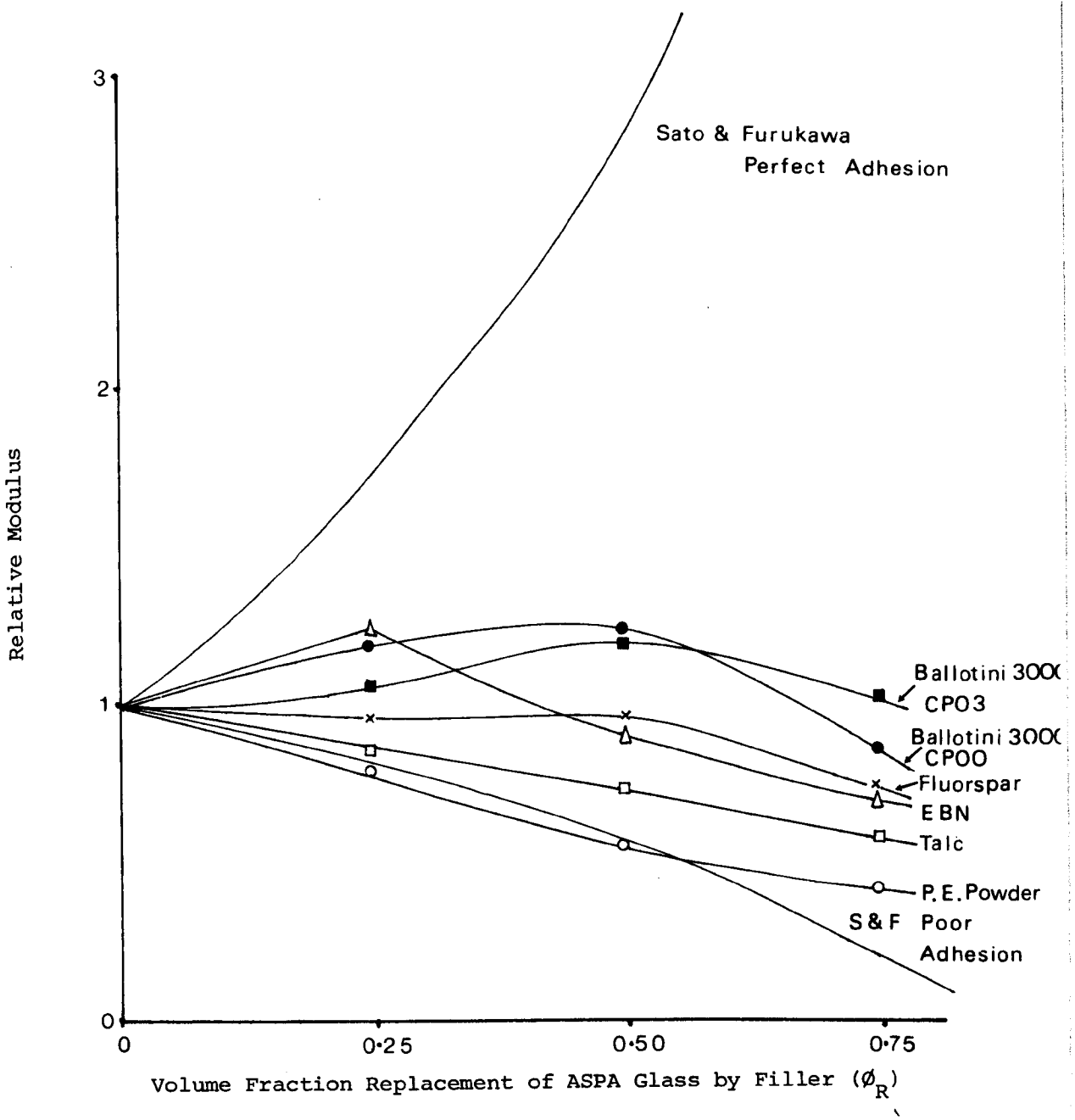

ionomer cements to the uncoated spheres (CPO3). It is well established that silane coupling agents promote interfacial adhesion in composites as described in Section 1.5.7, but the properties of the composite are dependent upon the compatibility of the coupling agent with the matrix. The choice of coupling agent is wide to allow selection for compatibility with the matrix (118-121) and the use of agents more compatible with aqueous PAA may produce stiffer and stronger filled ionomer cements as the coupling agent CPO3 was selected for compatibility with thermoplastic acrylic polymers which are normally hydrophobic. Others have shown coupling agents to have similar effects in ionomer cements (49,53) and in ionomers (18).

The ASPA cements filled with reactive fillers displayed good mechanical performance and in particular the Pozzolan filler which was found to have similar strength and stiffness to the unfilled ASPA cement at high values of ϕ_R. In such cases analysis by the ESCA technique revealed that these fillers had reactive metallic ions at their surfaces. For example the Pozzolan filler was found to have alumium ions and the Willemite filler zinc ions, their ESCA spectra are shown in Appendix 2. These Zn and Al cations would be capable ofsynergistically reacting with the PAA to give enhanced cross-linking in the matrix and to possibly give enhanced interfacial adhesion by promoting primary bond formation. However, the performance of the mineral and metal oxide filled cements was difficult to assess as they produced highly voided structures although this could be reduced by treating these fillers with an acid as is discussed in Section 3.7. For example the strength of ß-Wollastonite filled cements at ϕ_R = 0.5 was improved from 85.2 MPa to 116.2 MPa by this treatment.

Polyethylene powder was also used as a particulate filler as it is hydrophobic as is not wetted by the aqueous polyacid and thus gives poor interfacial adhesion. As expected this filler produced composites of inferior mechanical performance to other filled ASPA cements. For example at the $\emptyset_R$ = 0.75 filler level the polyethylene filled cements were found to have a compressive strength and modulus of 43.9 MPa and 1243 MPa respectively whilst other organic fillers, such as Nylon 66 powder, which would have provided a surface more suitable for wetting, was found to have a strength and stiffness of 84.0 MPa and 2625 MPa respectively at this filler level.

3.3. Hydrolitic Stability of Filled ASPA Cements

The hydrolytic stabilities of filled ASPA cements were measured by weight gain studies on water immersion as shown in Figures 3.16. These results demonstrate that the hydrolytic stabilities of filled ionomer cements were inferior to the stability of ASPA cements and the filled cements became progressively more unstable as the filler content increased. At high volume fraction replacements ($\emptyset_R$ = 0.75) the inert filled cements softened and started to disintegrate within 24 hours of water immersion but some of the reactive filled cements remained stable. This behaviour suggests that three factors determine the hydrolytic stability of these cements.

1. The degree of nerwork formation in the cement.
2. The nature of the metallic ions on the filler surface.
3. The nature of the interfacial bonding forces between the filler and the matrix.

A certain degree of nerwork formation is required for water stability, qualitatively a greater degree of reaction is required for water

Figure 3.16 Hydrolytic Stabilities of Filled ASPA Cements

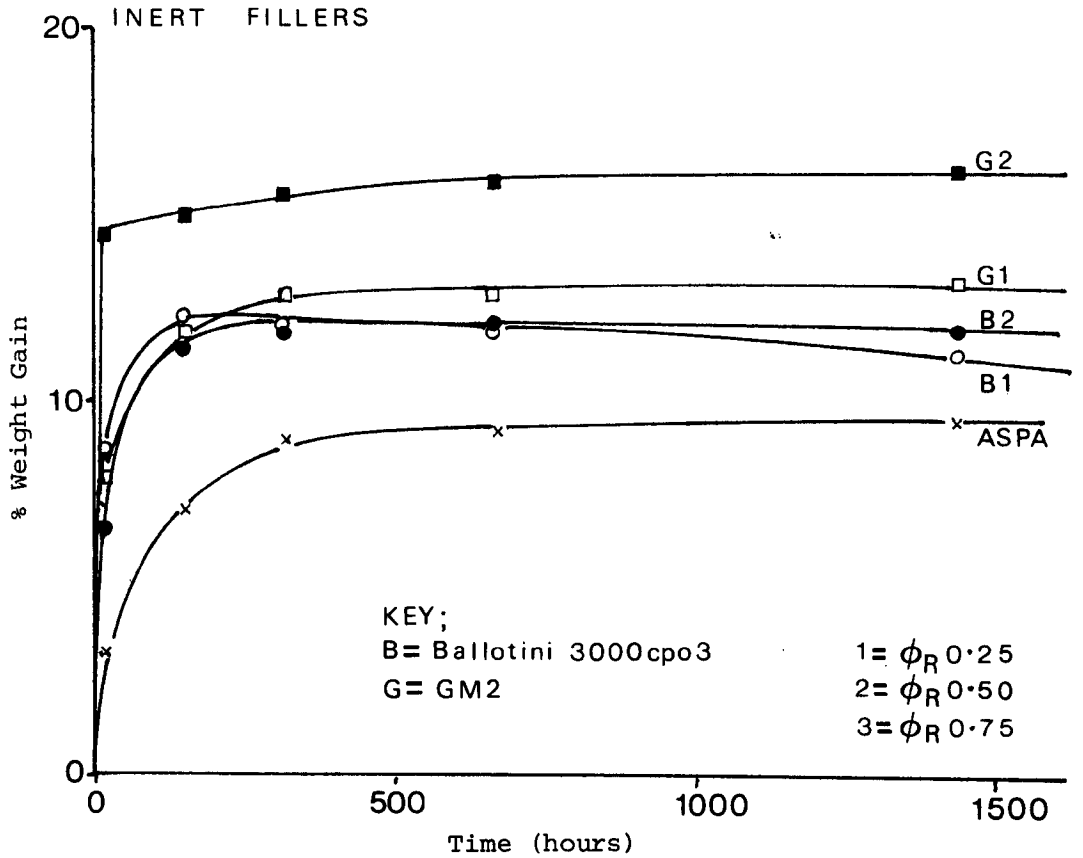

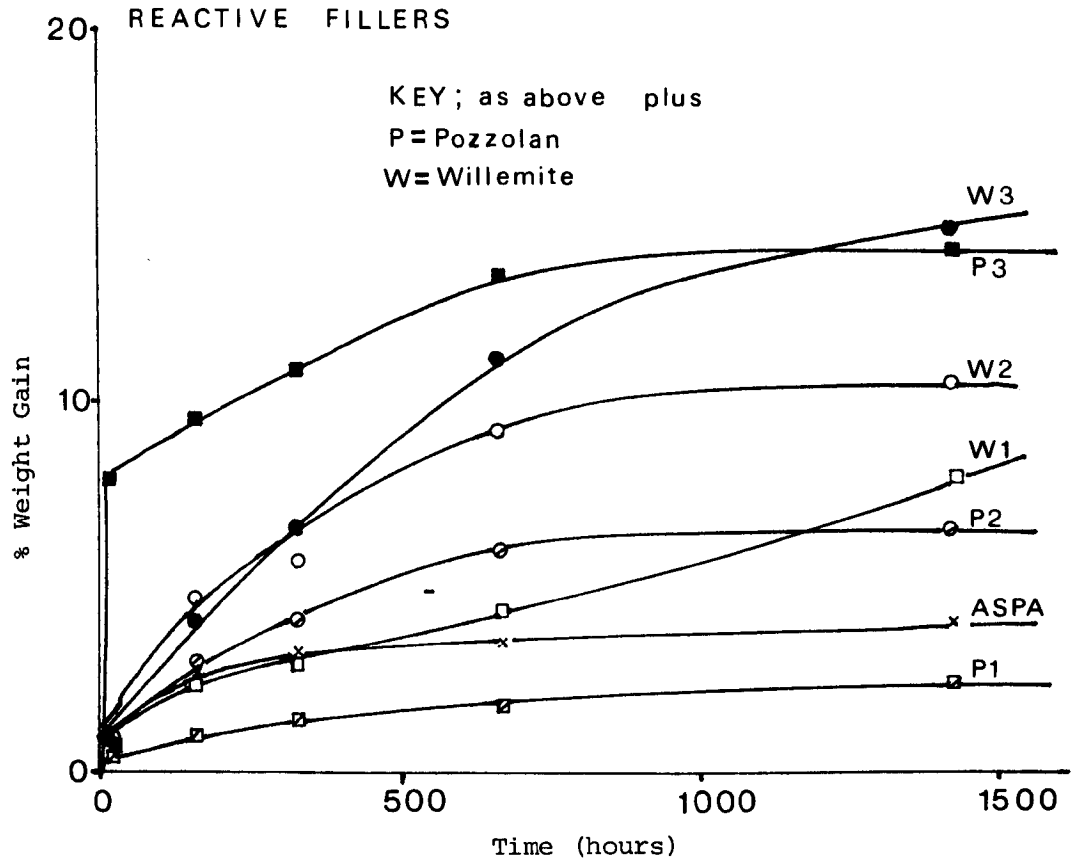

stability than to give good dry strength as discussed earlier in this section. The reactive fillers reacted with the polyacid in a synergistic manner to give a greater degree of network formation than when inert fillers were used.

The results show that the nature of the metallic cations on the filler surface has considerable influence on the hydrolytic properties. Reactive fillers such as Pozzolan and Willemite, whose surfaces were found by the ESCA technique to contain aluminium and zinc ions respectively, as shown in the spectra of Appendix 2, produced more stable cements than fillers which contained calcium ions such as ß -Wollastonite. Previous work with mineral and metal oxide-ionomer cements confirms this trend of hydrolytic stability as described in Section 1.3.2. and 1.3.3.

Hydrolytic stability is also affected by the nature of the interfacial bond. With the inert fillers, relatively weak secondary bonding forces would be operating at the interface with the polyacid and these are known to be displaced by water (112,133). However, with the reactive fillers there is potential for stronger primary bonding (ionic) forces to operate at the interface. Such forces are more resistant to hydrolysis (112,120,121) and thus form more stable cements.

.4 Filled ATG Cements

The decreased reactivity and extended workability of the ATG cements were further enhanced by partial replacement of the ATG glass with inert fillers but the use of reactive fillers

decreased the work time as shown in Figure 3.17. In this case metallic ions were leached from the filler more readily than from the ATG glass and contributed to the gellation of the cement. The extended setting times of the reactive filled cements in comparison with the ATG cements (Figure 3.17) suggest that the extent of cation liberation from the filler is limited and that these cations react in a manner which mainly contributes to the initial setting or workability of the cement. Consequently, the use of inert fillers in ATG cements would allow large mouldings to be fabricated and this would occur without serious loss of mechanical performance as shown in Table 3.8. The mechanical properties of the ATG filled cements were also dependent upon the physical properties of the filler in a similar manner to the filled ASPA cements. The hydrolytic stability of the filled ATG cements were generally inferior to their filled ASPA counterparts as shown in Figure 3.18. This was attributed to the degree of reaction in the filled ATG cements and their reduced network formation. This indicated that a certain degree of matrix crosslinking, or other forms of salt formation, are required before the matrix is rendered water soluble.

Figure 3.17 General Trends in Workability and Setting Times of Filled ATG Cements

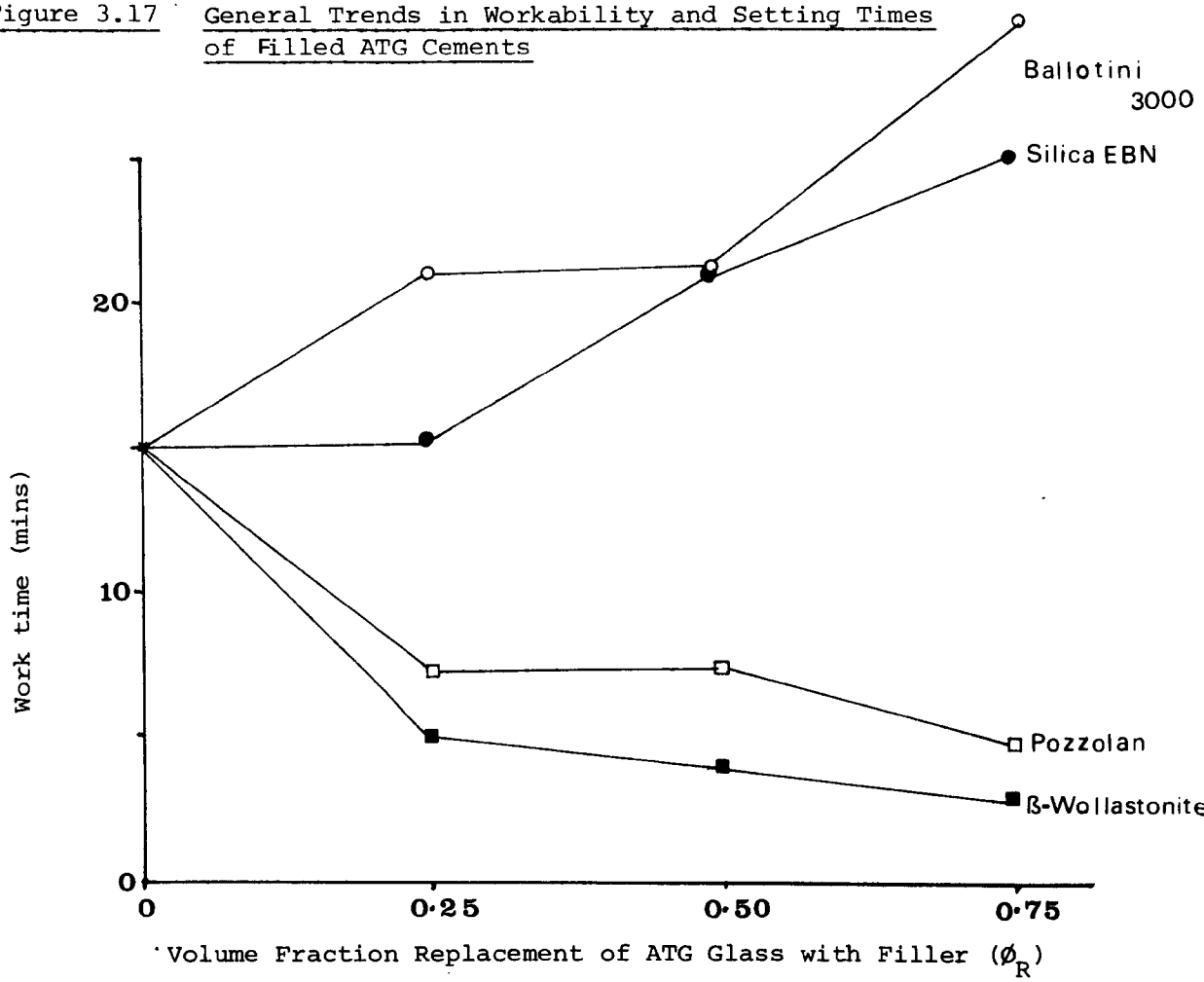

Table 3.8 The Mechanical Properties of Filled ATG Cements

Filler	Volume Fraction Replacement ϕ_R	Comp. Strength (M Pa)	Comp. Modulus (M Pa)	Strain at Fail (%)
None	ATG Cement (n = 12)	123.8±40.9	2702±189	3.27±0.56
Ballotini 3,000 CP03	0.25	104.9±15.4	2798±126	3.43±0.35
	0.50	108.3±7.8	2656±33	3.77±0.44
	0.75	77.2±0.5	2446±86	3.84±0.42
Gasil WP	0.25	85.4±10.0	2231±146	3.09±0.51
	0.50	111.2±13.2	2287±262	4.57±0.73
	0.75	92.1±10.1	1948±133	5.84±1.09
Gasil 644	0.25	82.8±13.6	2507±373	3.31±0.32
	0.50	109.0±16.4	2419±107	5.04±1.08
	0.75	84.9±11.8	1880±62	5.04±0.81
Gasil EBN	0.25	97.2±20.0	2447±247	3.31±0.58
	0.50	108.6±19.0	2269±374	4.07±0.83
	0.75	72.6±10.6	1705±85	4.57±0.68
Gasil GM2	0.25	157.7±19.58	2911±150	4.41±0.57
	0.50	146.7±26.66	2542±99	4.52±0.87
	0.75	117.5±12.04	2278±204	4.18±0.42
Garosil	0.25	152.8±2.85	2966±196	3.91±0.19
	0.50	91.8±11.10	2564±179	3.64±0.75
	0.75	106.5±14.21	2734±208	3.61±0.69
Pozzolan	0.25	146.9±11.13	2842±386	4.91±0.31
	0.50	127.0±33.3	2820±301	5.50±0.11
	0.75	102.5±15.1	2146±299	4.40±0.34
Aluminium Oxide (neutral grade)	0.25	124.9±9.15	2367±390	4.61±0.68
	0.50	166.8±23.1	3025±725	5.75±1.16
	0.75	152.0±15.3	3181±662	5.60±1.16

Figure 3.18 Hydrolytic Stability of Filled ATG Cements

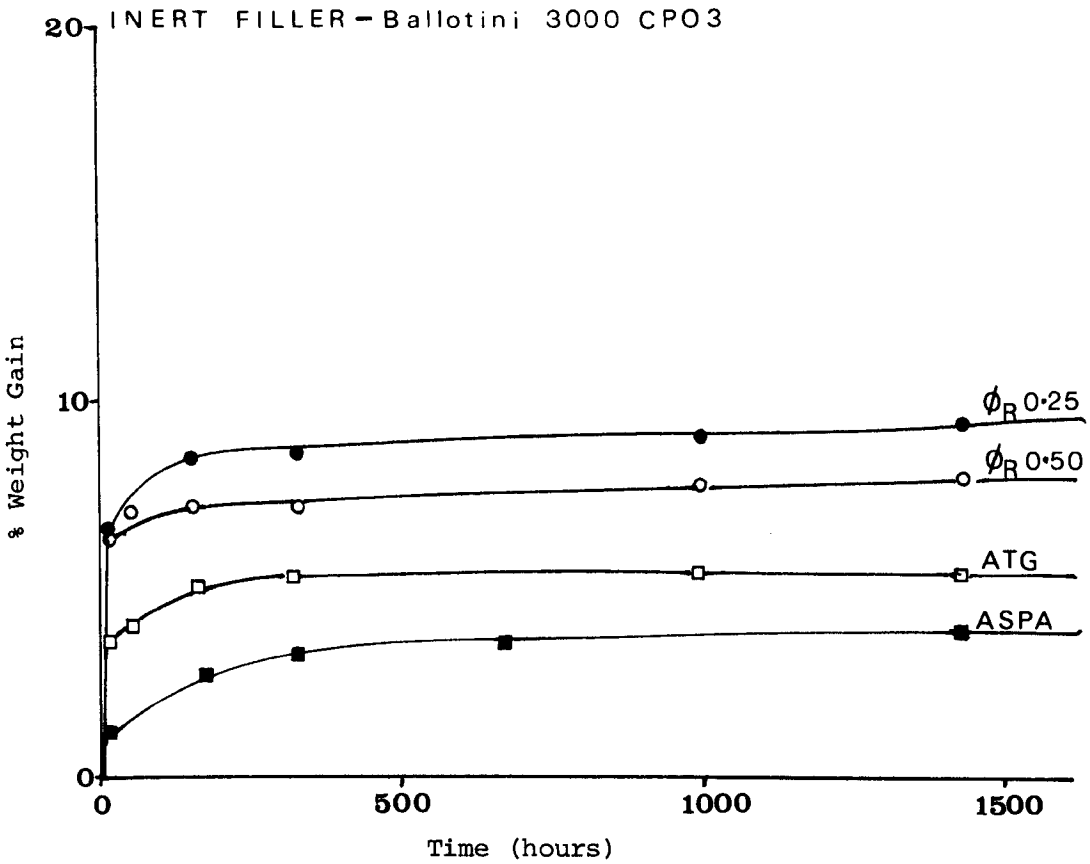

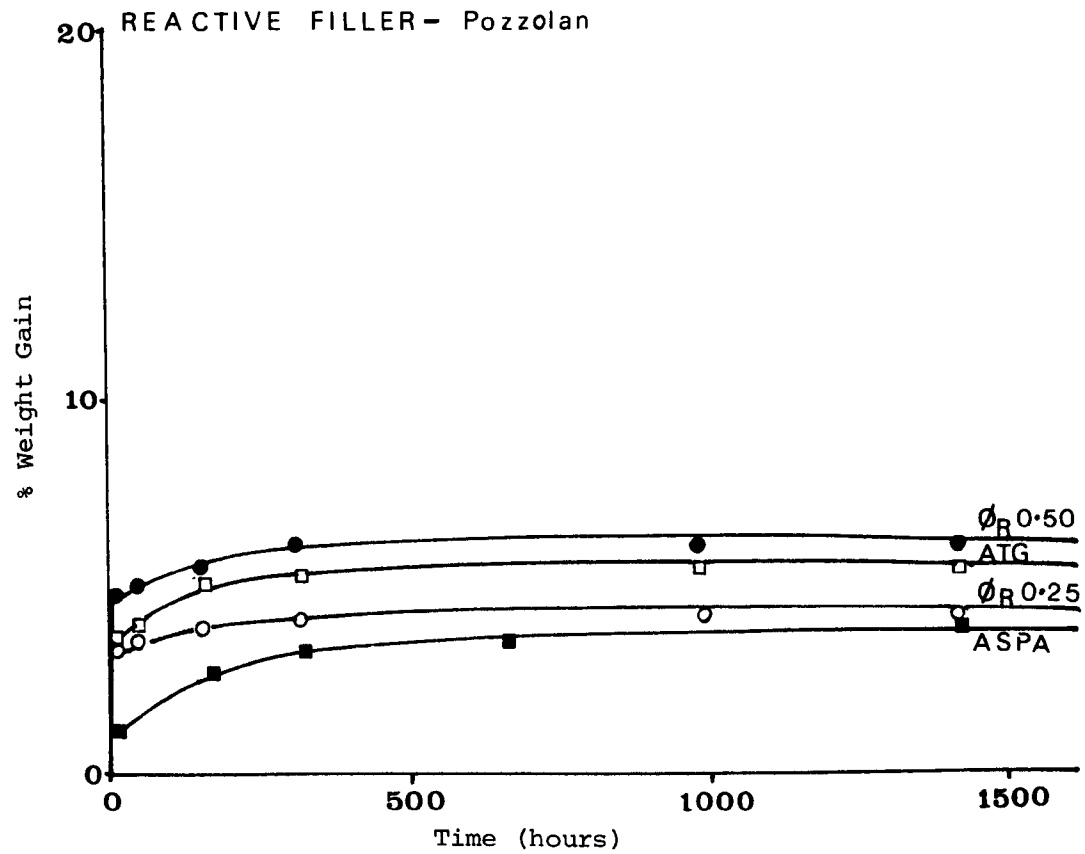

.4. The Effects of Humidity on the Mechanical Properties of Ionomer Cements

Variations in the humidity of the storage environment are known to affect the mechanical properties, shrinkage and weight retention of ASPA cements as described in Section 1.2.5. This cement has been found to have poor mechanical performance when stored in environments of 66% relative humidity or less. This behaviour has restricted the potential applications of the material and cements which retain strength in arid environments are desirable. Consequently, the effects of storage environment were investigated for ATG and for filled-ASPA cements. The mechanical properties of these cements systems were found to be influenced by the storage environment. The mechanical performance of the ATG cement at low humidity was superior to that of the ASPA cement which in turn was better than that of the filled-ASPA cements. Also, storage of ionomer cements in humid environments prior to exposure at low humidities was found to improve the mechanical properties of ASPA cements.

3.4.1. Comparison Between ASPA and ATG Cements

The storage humidity was found to affect the mechanical properties of ASPA and ATG cements as shown in Figure 3.19, with the effects on weight loss and shrinkage in Figures 3.20 and 3.21 respectively. These results show the ATG cements to have a better overall mechanical performance and to lose less weight than the ASPA cement at all the levels of storage humidity, yet both cements showed similar shrinkages. The difference in mechanical performance at low humidities was quite distinct with the ATG cement having a maximum compressive strength at 33% humidity of 187.0 MPa which was

Figure 3.19 Mechanical Properties of ASPA and ATG Cements stored at various Humidities

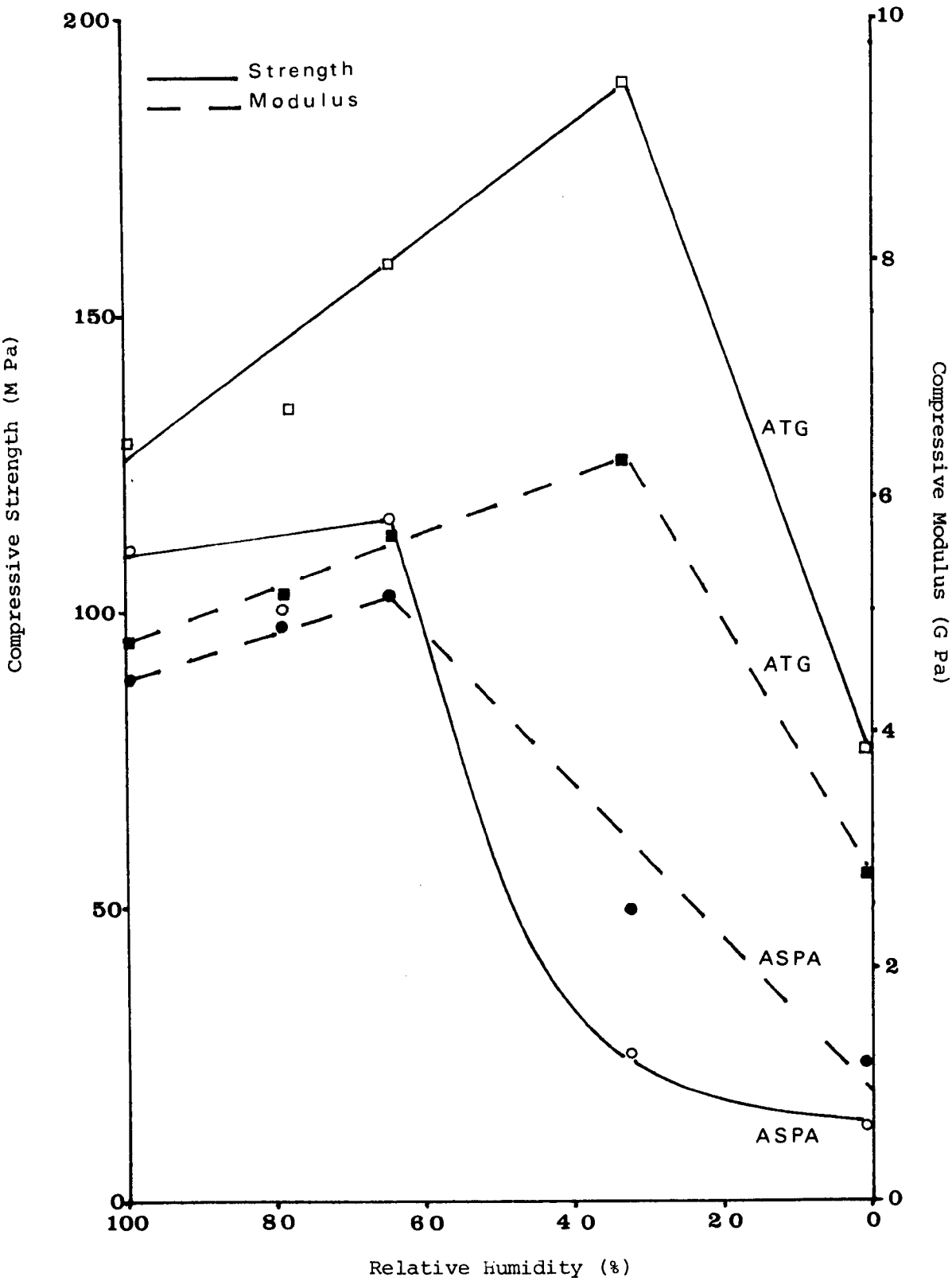

N.B. Cement Age 1 Month

Figure 3.20 Equilibrium Weight Loss of ASPA and ATG Cements stored in Different Humidity Environments

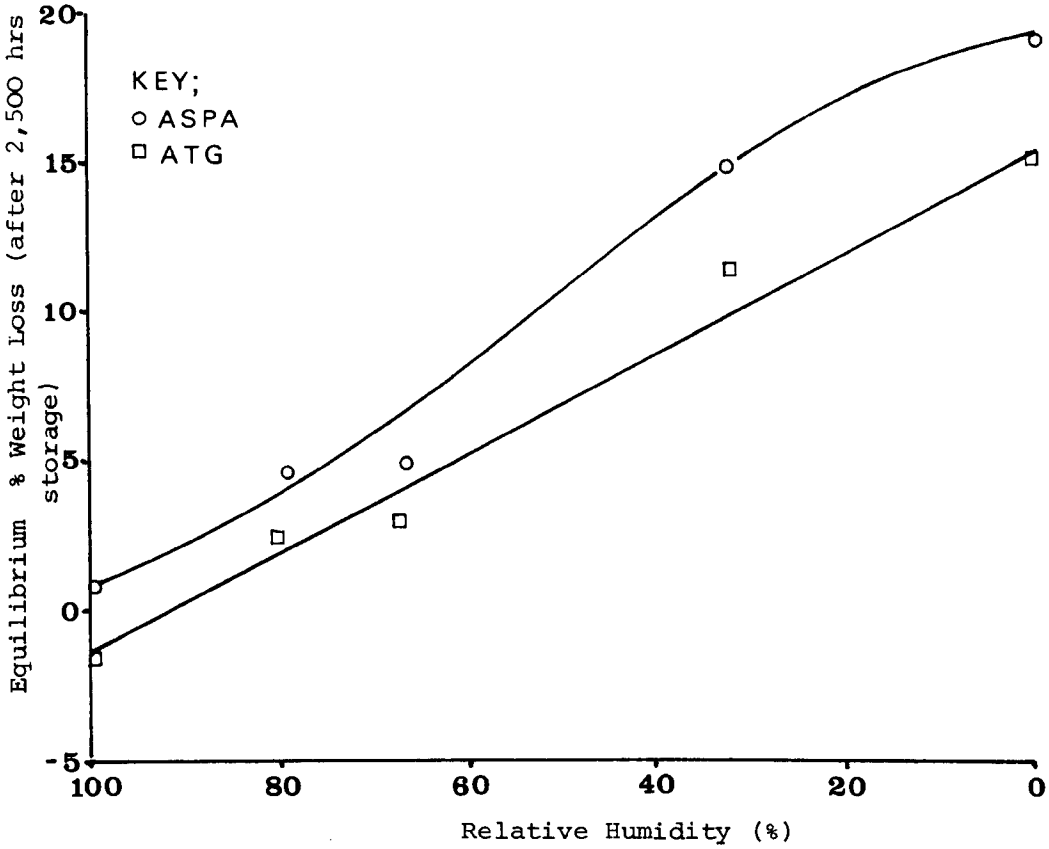

Figure 3.21 Equilibrium shrinkage of ASPA and ATG Cements stored in Different Humidity Environments

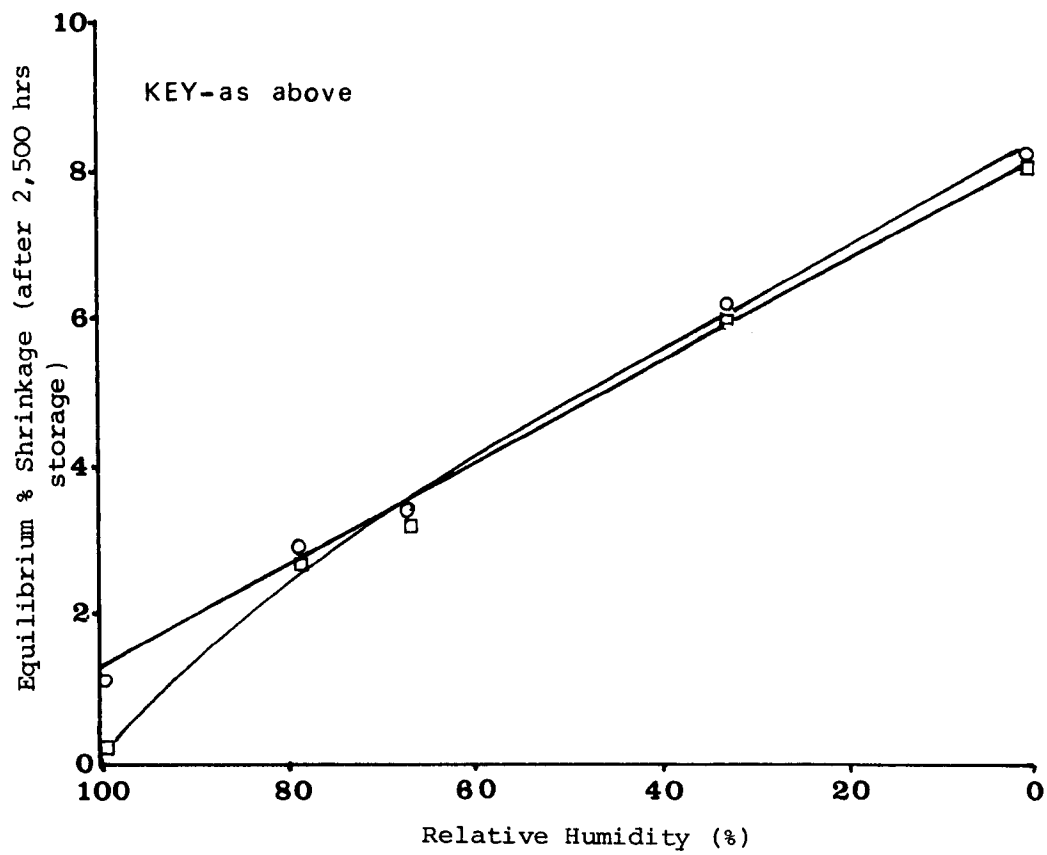

almost an order of magnitude stronger than the ASPA cement (23.2 MPa) at this humidity. At 0% humidity the strength of the ATG cement had declined to 63.0 MPa which was still considerably stronger than the ASPA cement which at this humidity had a strength of 11.9 MPa. The superior mechanical performance of the ATG cement at low humidities is attributed to the following factors:

1. The ability of the glass to retain water at low humidities.
2. The ability of the polyacid to retain water at low humidities.
3. The relationship between weight loss and shrinkage of the cements.

1. The acid treated glass contained proportionately more trivalent aluminium cations and less divalent calcium cations on its surface than the ASPA glass as discussed in Section 3.2. This suggests that the aluminium ions retained water more firmly than the calcium ions and that the aluminium polyacrylate formation in the set cement was more resistant to dehydration than the calcium polyacrylate. It is known that both Al^{3+} and Ca^{2+} co-ordinate six molecules of water each (186) but thermogravimetric studies of wetted glasses, as shown in Figure 3.22, demonstrate that the ATG glass holds more water at higher temperatures than the ASPA glass and particularly in the region of 60^{o} to $120^{o}C$. Thus, this water must be more firmly bound to the aluminium ion than the calcium ion. This is reflected by their electronegativity values on the Pauling scale of 1.5 and 1.0 respectively (186). Also the aluminium polyacrylate bond has been found to be partially covalent whereas the calcium polyacrylate bond is purely ionic (1,38,39,189,190). This is also discussed in Section 3.7. In set ionomer-cements aluminium polyacrylate has been found to be more hydrolytically stable than calcium polyacrylate (4,50) which reflects its stronger bonding ability, and consequently aluminium polyacrylate would also be more resistant to dehydration than calcium polyacrylate.

Figure 3.22 Thermogravimetric Studies of Wet ASPA Glass and Wet ATG glass

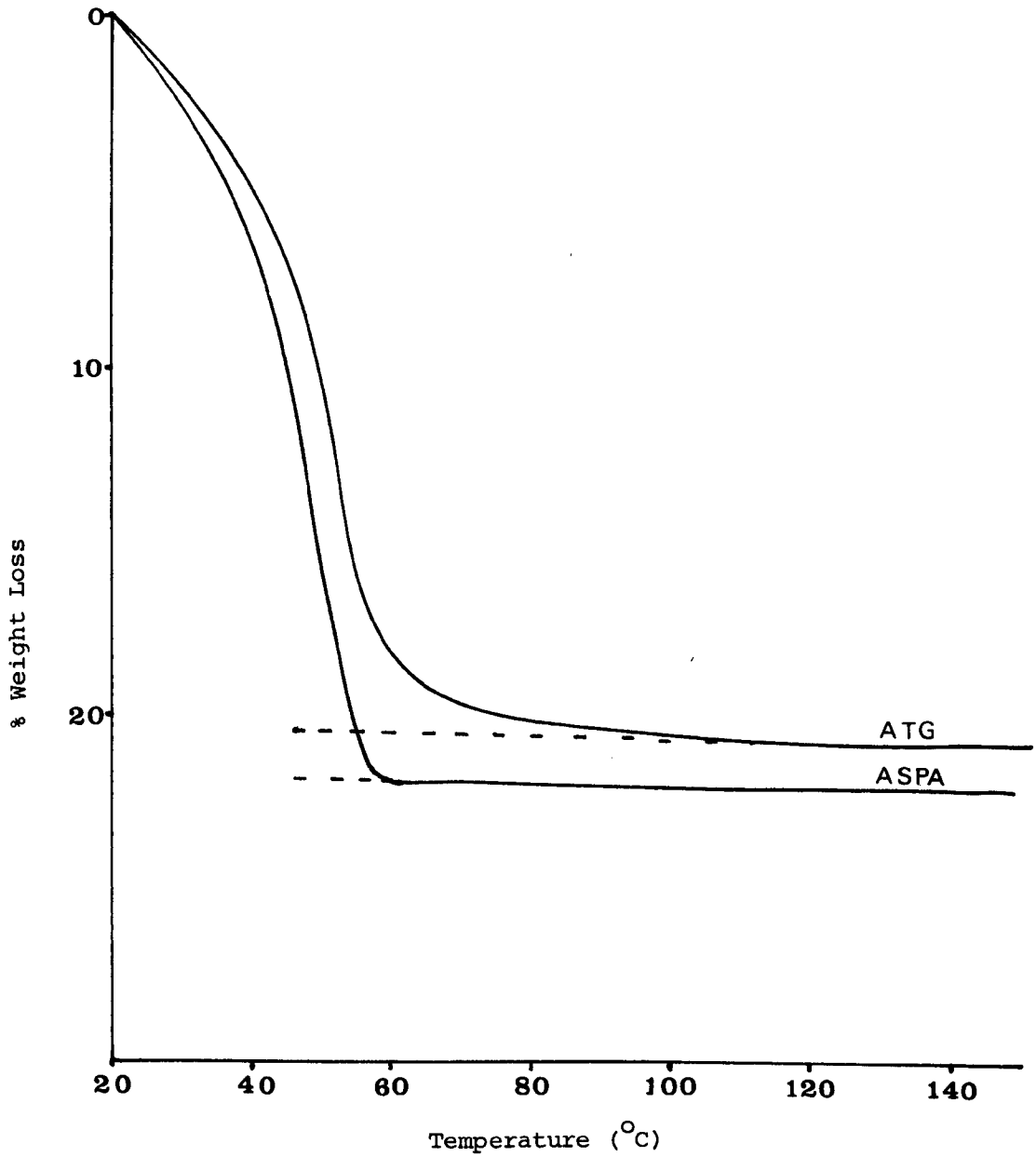

2. The ASPA system was found to leach a greater number of functional cations under acid attack than the ATG system as discussed in Section 3.2.2. Consequently, it is suggested that the polyacid was less reacted in the ATG system leaving more polyanionic sites ($-COO^-$) capable of retaining water as proposed by the Ikegami model of Figure 1.6, and this promotes greater weight retention in set cement. It is proposed that this water is firmly bound to the polyanion and is capable of withstanding dehydration by desiccation at 33% and 0% humidity. This effect would also leave a greater molecular weight of polymer between crosslinks making the ATG cement matrix more plasticised than the ASPA cement matrix at low humidities. Stress relaxation studies confirm this suggestion, as shown in Figure 3.23, with the ATG system displaying more plastic behaviour and greater stress relaxing properties than the ASPA system at low humidities.

3. Initial studies on the mechanical performance of ASPA cements had postulated that the poor performance in dry environments was due to excessive shrinkage causing interparticle contact with the composite (45,49). However, the ATG and ASPA systems displayed similar shrinkage at all levels of humidity and consequently the difference in mechanical performance at low humidities was attributed to the relationship between shrinkage and weight loss as postulated more recently by Hornsby (187). The ASPA system displayed greater weight loss per unit shrinkage than the ATG system, as shown in Figure 3.24, due to its poorer water retention properties. This removal of water with retarded shrinkage, which occurs with severe desiccation, is due to the inability of the matrix to contract and this leads to the development of internal stresses within the composite and to the

Figure 3.23 The Stress Relaxation of Ionomer Cements Stored at Various Humidities.

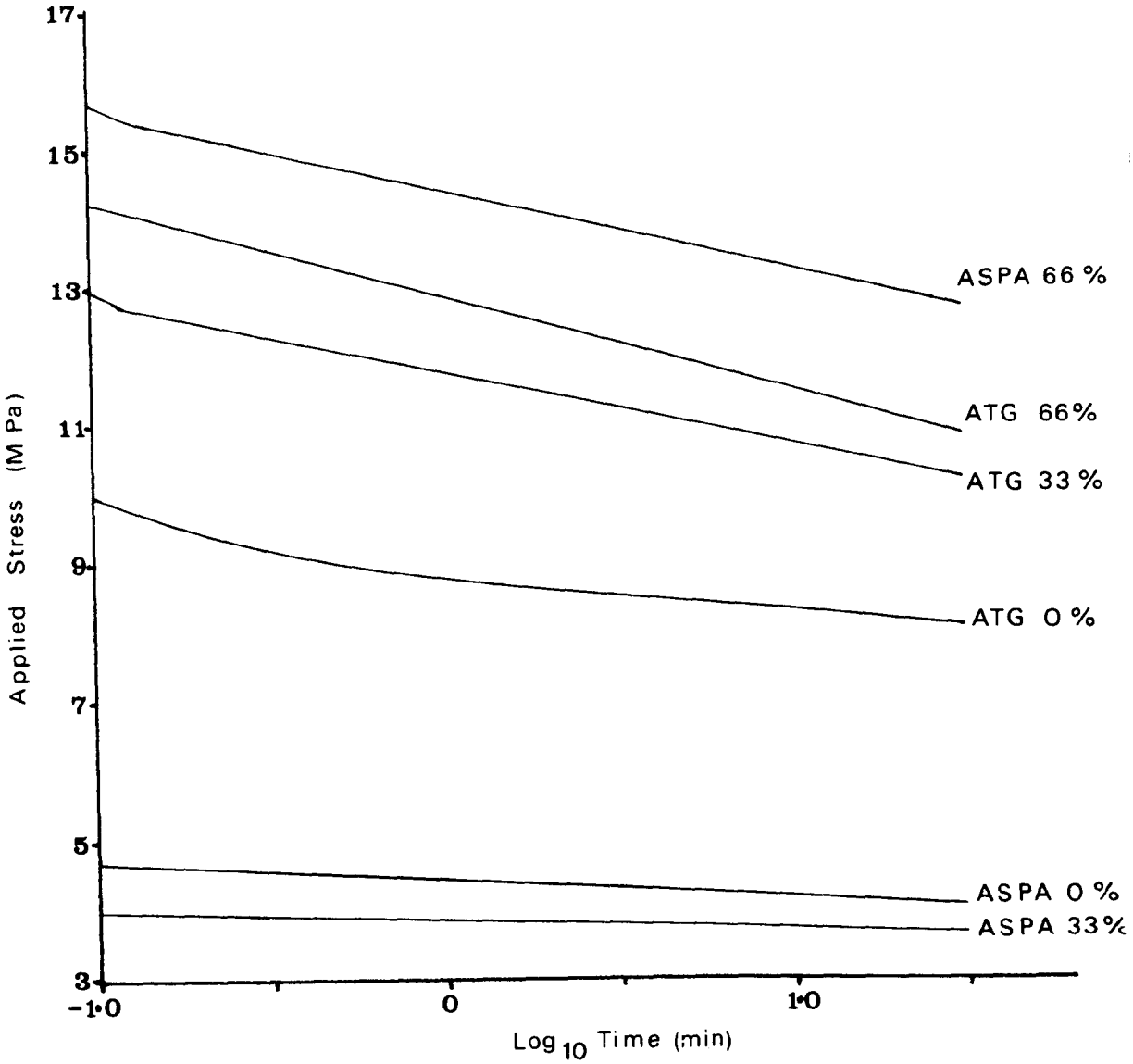

Cement	Humidity (%)	Stress Relaxation Function (σ^*) $\sigma^* = \frac{d\sigma}{d \log t}$
ASPA	66	1·33
ATG	66	1·16
ASPA	33	0·02
ATG	33	1·18
ASPA	0	0·015
ATG	0	0·84

Figure 3.24 Relationship Between Weight Loss and Shrinkage for ASPA and ATG cements

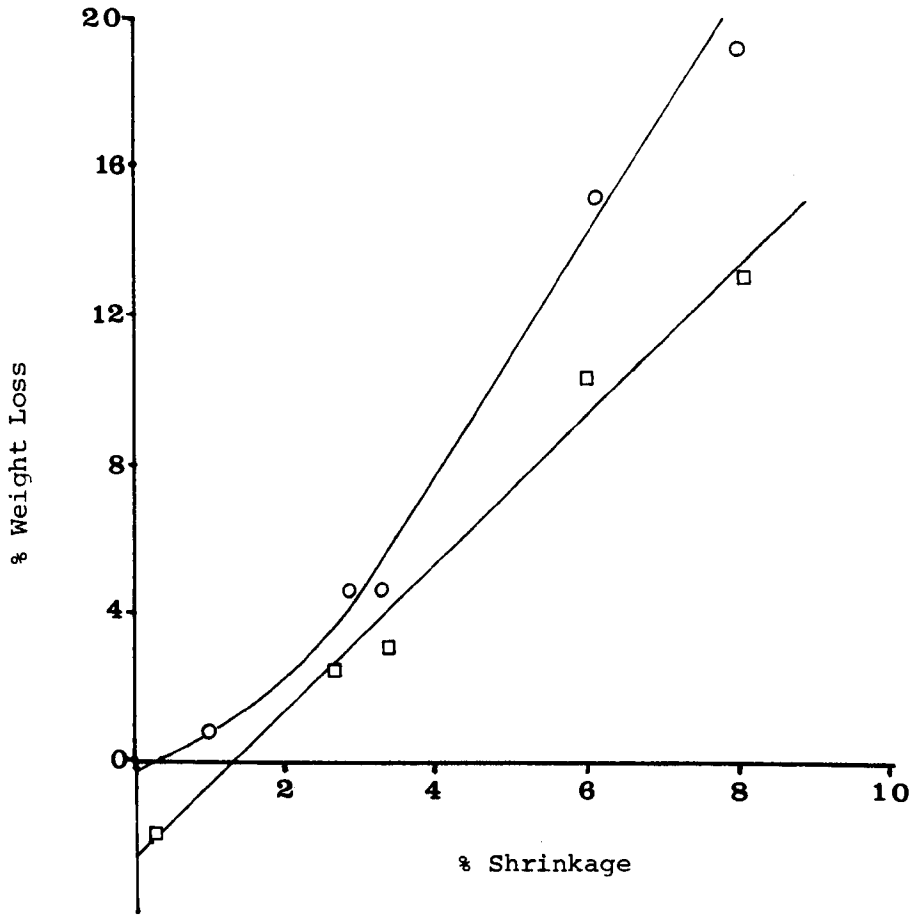

development of voids. The poor stress relaxation properties of ASPA cements stored at low humidities and the visible surface crazing of these cements both suggest a high internally stressed system. Additionally, voids were frequently observed on the fracture surface of dehydrated cements. The relationship between weight loss and shrinkage was more distinctive for the filled ASPA cement as is discussed in Section 3.4.3.

.2. The Effects of Curing Ionomer Cements in Humid Environments Prior to Exposure at Low Humidities

The mechanical properties and water retention of ionomer cements were improved by ageing the cement at 100% humidity prior to desiccation at lower humidities as shown in Figures 3.25 and 3.26 for ASPA and ATG cements respectively. These results demonstrate that both ASPA and ATG cements cured for seven days at 100% humidity had reduced weight loss when exposed to lower humidity environments but this was only accompanied by an improvement in mechanical performance in the ASPA cement from 59.9 MPa to 103.5 MPa at 33% humidity, the mechanical performance of the ATG cements at low humidities was virtually unaltered by this cure at high humidity. This improvement in mechanical performance has been observed before with ASPA cements (49,187) and has been attributed to more water being co-ordinated to metallic ions in the set cement, in particular to Al^{3+} ions which are believed to be continually liberated from the glass surface in the set ASPA cement. The lack of improvement in mechanical performance of the ATG cement at low humidities after storage for seven days at 100% humidity was probably because a large proportion of the Al^{3+} ions were more freely available to react with the polyacid and to co-ordinate water than in the ASPA cement. In the ASPA cement a high proportion of the Al^{3+} ions would be shielded and prevented from

Figure 3.25 The Effects of Cure at 100% R.H. on the Weight Loss and Mechanical Properties of ASPA Cements

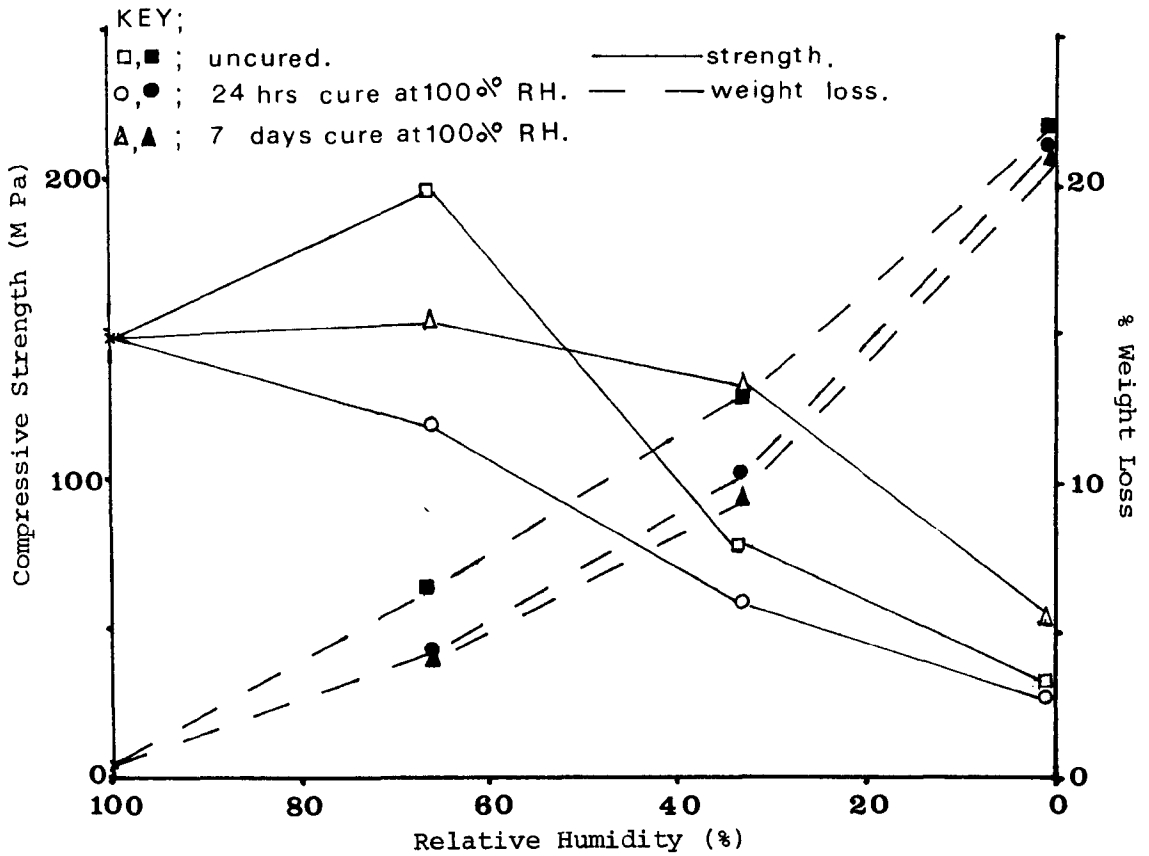

N.B. Cements aged 1 month after cure period

Figure 3.26 The Effects of Cure at 100% R.H. on the Weight Loss and Mechanical Properties of ATG Cements

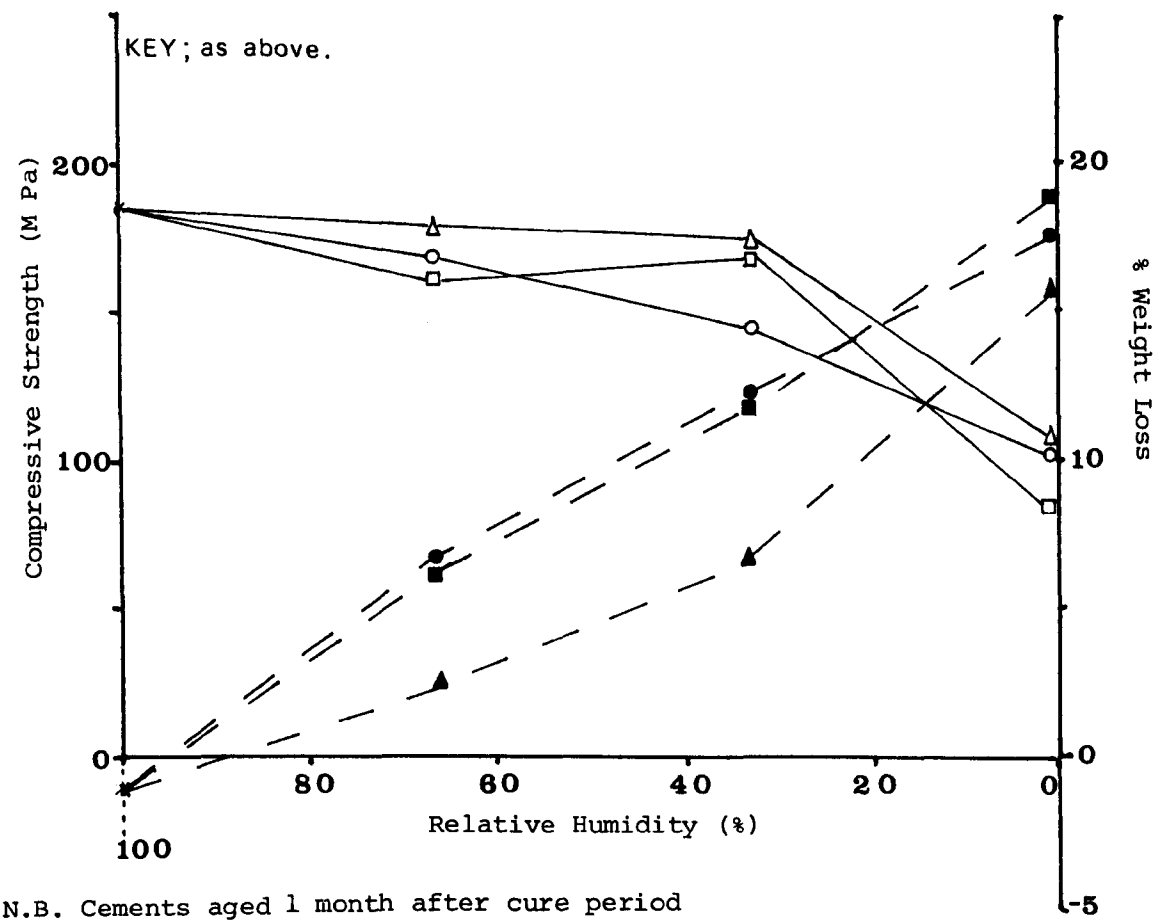

N.B. Cements aged 1 month after cure period

reacting by the dispersed phase of calcium fluoride at the glass particle surface. The Ca^{2+} ions would be preferentially attacked by the polyacid and would co-ordinate water themselves, thus depleting the free water available to co-ordinate with the Al^{3+} ions. Also the Ca^{2+} ions would rapidly produce a rigid calcium polyacrylate matrix which would restrict the mobility of Al^{3+} ions and retard their co-ordination with the free water.

4.3. Filled-ASPA Cements

The mechanical properties and weight losses of filled-ASPA cements stored at different humidities are shown in Figures 3.27 - 2.29 for systems containing Silica GM2, Ballotini 3,000 CPO3 glass spheres and Pozzolan fillers respectively. These fillers were selected for further evaluation as they were found to produce cements having good mechanical performance at 66% storage humidity as discussed in Section 3.3. The compressive strengths of the filled-ASPA cements displayed similar trends to the unfilled ASPA cements and likewise suffered a catastrophic loss of mechanical performance when stored at low humidities. These filled cements exhibited greater weight loss and shrinkage than the ASPA cements and these changes increased progressively with volumetric replacement (ϕ_R) of the ASPA glass. Correspondingly, the mechanical properties of the inert filled cements decreased but the reactive filler (Pozzolan) produced filled cements which were stronger than the ASPA cements at lower humidities. This effect was probably due to the synergistic curing effect of the polyacid with the reactive aluminium ions on this filler surface (See Section 3.3). Further, these ions were not removed from the filler surface by acid washing and thus may have reacted with the polyacid to form primary interfacial bonds giving rise to greater interfacial adhesion than with the inert fillers.

Figure 3.27 Mechanical and Weight Loss Properties of Filled ASPA Cements; Silica G.M.2 Filler

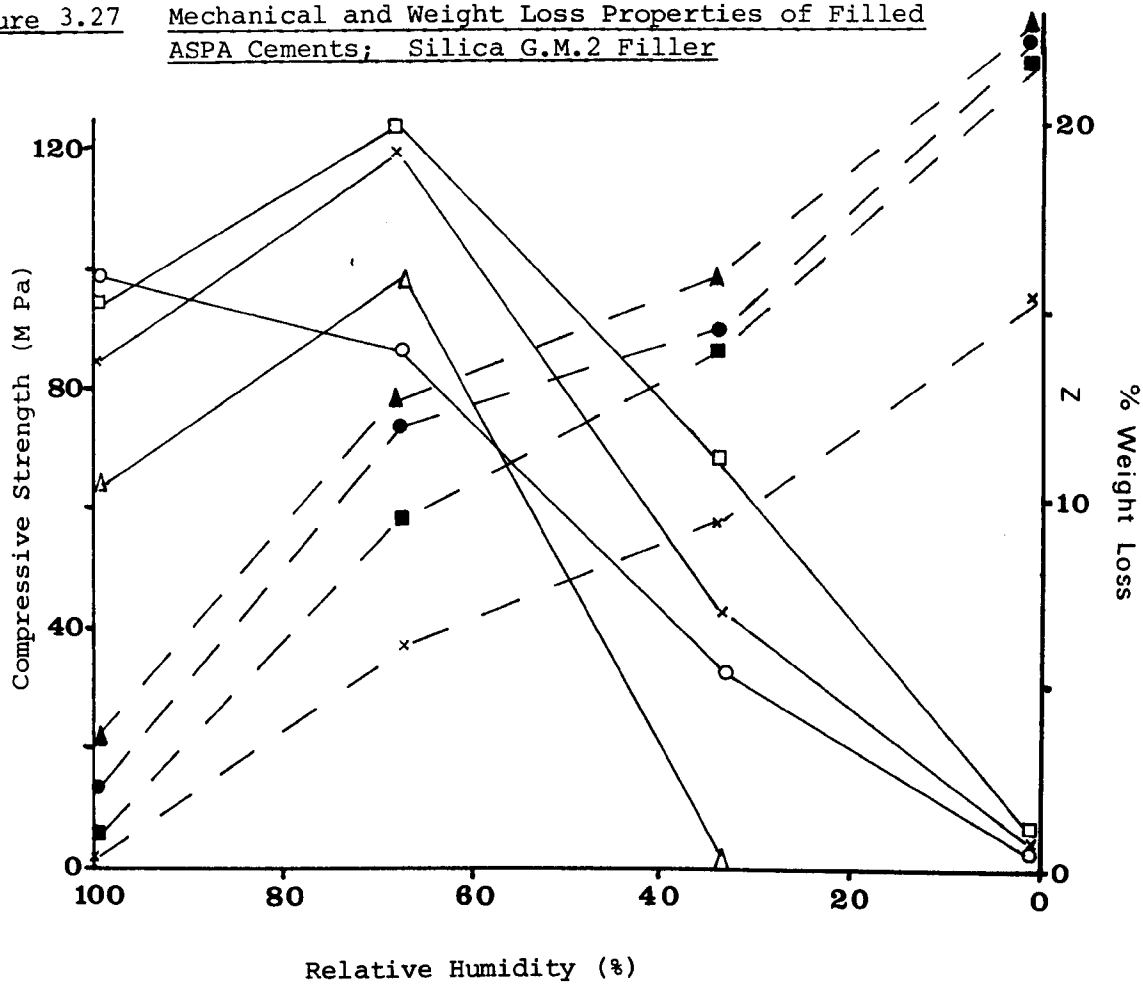

KEY;

——— Strength

— — Weight Loss

× = ASPA

□■ = ϕ_R 0·25

○● = ϕ_R 0·50

△▲ = ϕ_R 0·75

Figure 3.28 Mechanical and Weight Loss Properties of Filled ASPA Cements, Ballotini 3,000 CPO3 Filler

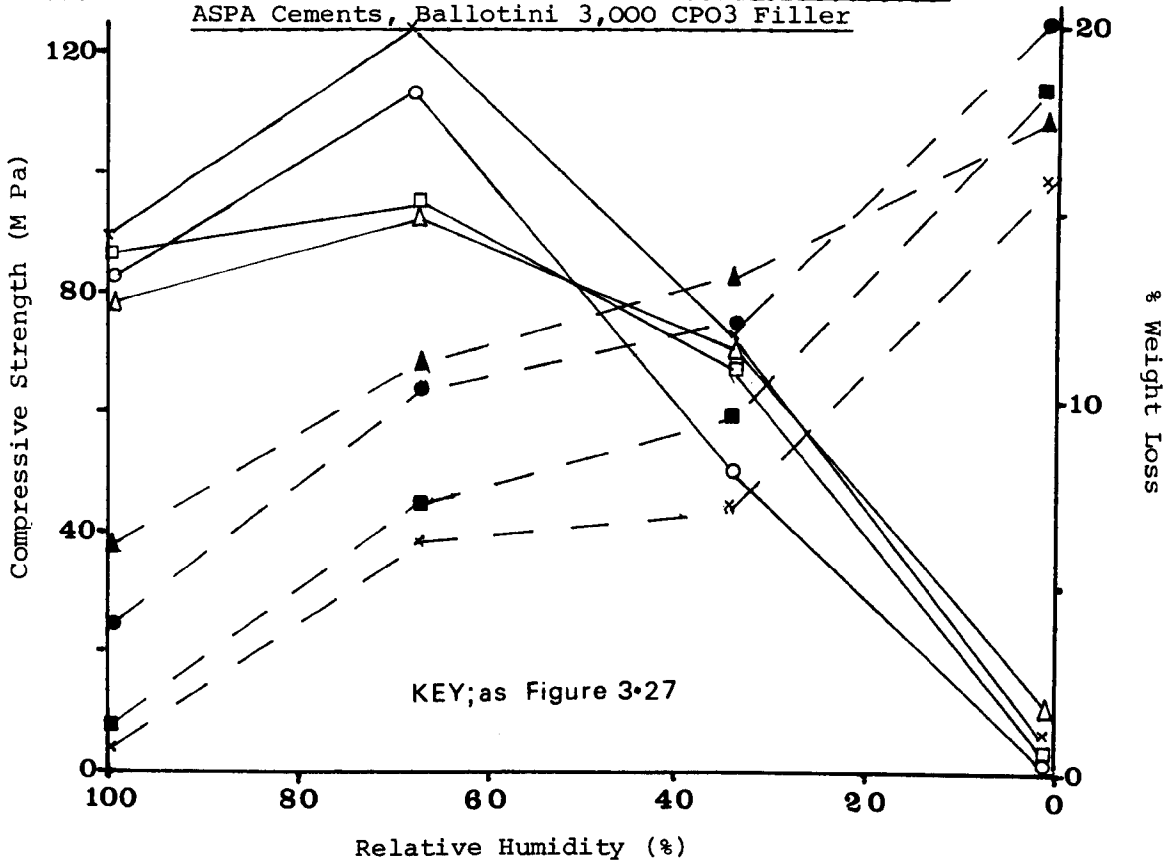

Figure 3.29 Mechanical and Weight Loss Properties of Filled ASPA Cements; Pozzolan P.F.A. Filler

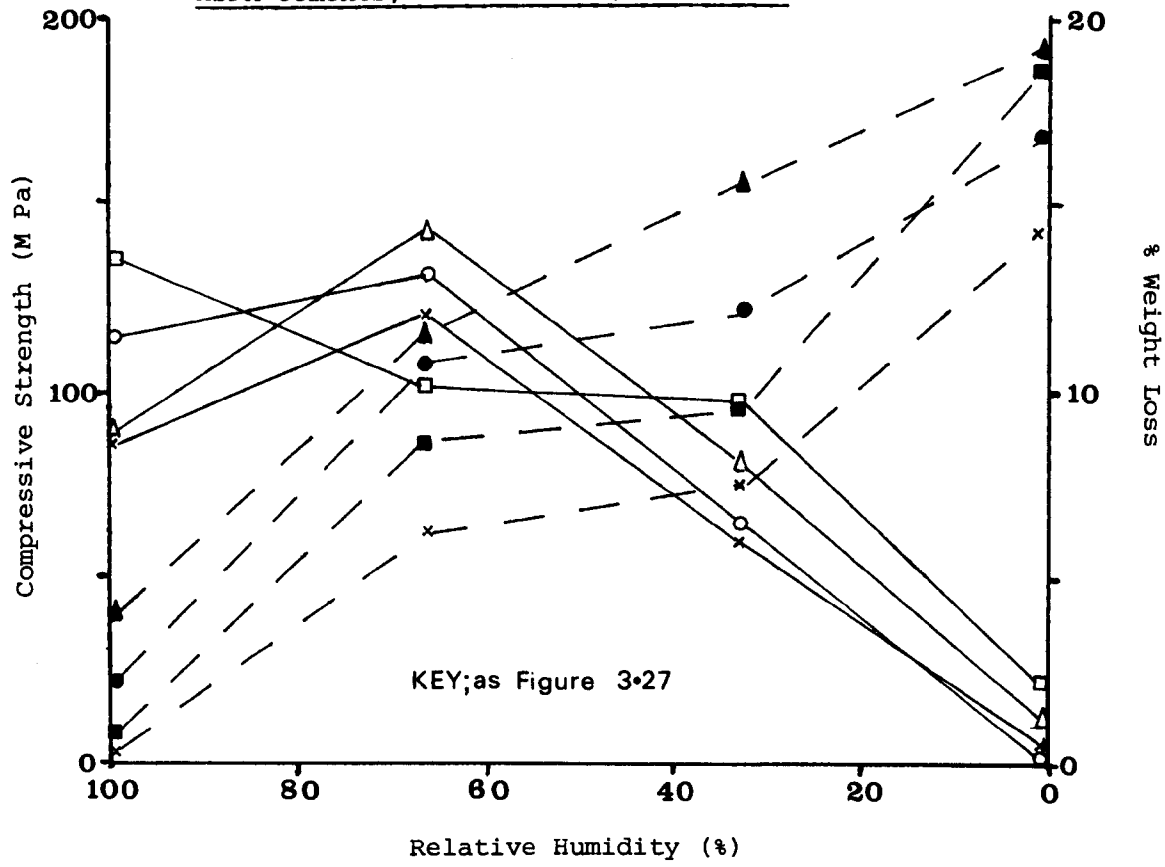

The relationship between shrinkage and weight loss was also found to be an important factor influencing the mechanical properties of the filled-ASPA cements. For example the inert filled (Silica GM2 and Ballotini spheres) cements and the unfilled ASPA cements displayed minimal weight loss on dehydration from 66% to 33% humidity without any shrinkage yet the mechanical performance of these cements fell dramatically. This was attributed to high weight loss per unit shrinkage increasing the internal stress and void content of the cements as discussed earlier in this section. The relationship between weight loss and shrinkage for these cements, as shown in Figure 3.30, indicates that a limiting value of 4% - 6% shrinkage occurs. Any further loss of water is not accompanied by further shrinkage and this behaviour coincides with the loss of strength. This limiting value of shrinkage has been observed before (49,187) and has been attributed to the physical constraints of inter-particle contact but it could also be due to the inability of the cross-linked network structure of the matrix to contract beyond a certain limit, particularly if strong interfacial bonding occurs.

4.4. The Role of Water in Ionomer Cements

Limitations of the Currently Held Theory

It has been proposed that there are two types of water in ionomer cements, and these are tightly bound and loosely bound water, but discrepancies have arisen in the ratios of tightly to loosely bound water in the cements as described in Section 1.2.5. These discrepancies can in part be attributed to the vagueness of these terms which need further explanation. The results of the weight loss studies in Figure 3.20 show that the loosely bound water, that is the water which can be removed by desiccation at 0% humidity, comprises

Figure 3.30. The Relationship between Weight Loss and Shrinkage for Filled ASPA Cements.

KEY; as Figure 3·27

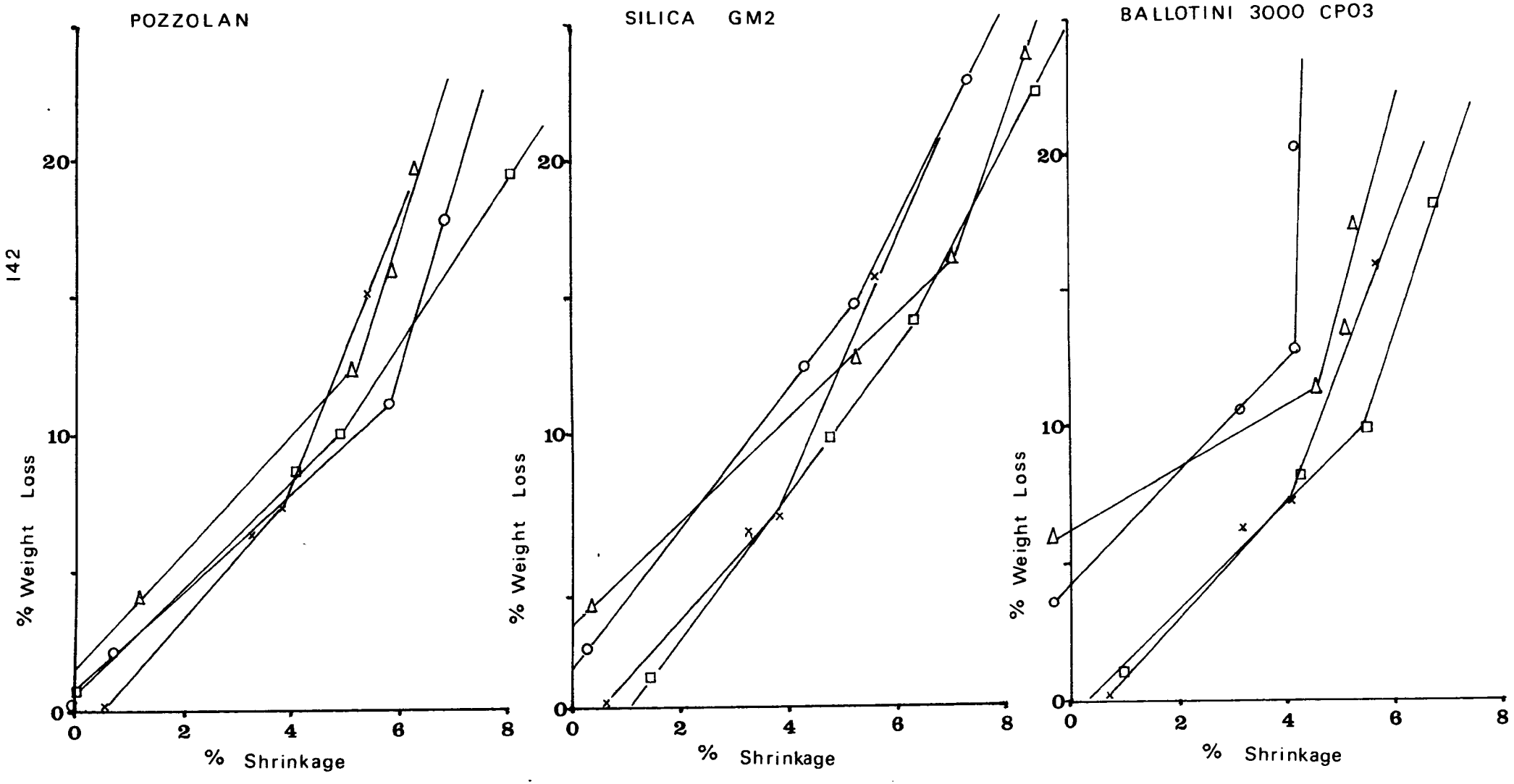

about 15% - 20% of the ionomer cement's weight (about 17% by volume) for cements prepared at a P:L ratio of 2:1 and with a 50% solution of PAA. This is consistent with the loose water defined by Hornsby et al (45,49,187). However, the results suggested that the water could be retained in several ways by the cement and further classifications are proposed, as follows:

Table 3.9 Proportions of Bound Water in Ionomer Cements

		ASPA	ATG
A.	Absorbed water	25%	15%
B.	Water weakly bonded to both the polyanion and to metallic cations	70%	65%
C.	Water firmly bonded to polyanion and to metallic ions	5%	20%

N.B. Wilson et al's (1) definition of loosely bound water corresponded to A.

Hornsby's (49,187) definition of loosely bound water corresponded to A +B.

About 25% of the water in ASPA cements and 15% in ATG cements can be removed by mild desiccation (e.g. at 66% humidity) and can thus be described as water absorbed in the structure of the cement. The loss of this water can be associated with the increase in strength that occurs with ASPA cements. With more severe desiccation (e.g. at 33% humidity) water weakly bound in the cement is removed, such as water from the oriented water sheath around the water bound to the polyanion chain in the Ikegami model (Figure 1.3) and water oriented around the water co-ordinated to the metallic ions. Also certain metallic ions, in particular the Ca^{2+} ions, may lose their co-ordinated water and this would give rise to the dramatic loss in mechanical performance of ASPA cements under such storage conditions. Such water could account for 70% of the loosely bound water in ASPA cements but the ATG cements lost less of this water due to their lower Ca^{2+} and

higher Al^{3+} content. The good mechanical performance of ATG cements at low humidity suggests that the tightly bound water, that is water not removed by desiccation at 0% humidity, is the water co-ordinated to the aluminium ions (See Figure 1.2). Also the stress relaxation properties of ATG cements suggest that water may also be firmly held by orientation around the polyanion to plasticise the polyacrylate matrix more effectively than in the ASPA cements. This accounts for about 20% of the water in ATG cements but only about 5% of the water in ASPA cements.

The currently held theory of water in ionomer cements also postulates that the slight shrinkage that occurs with mild desiccation tightens the structure of the cement to improve its mechanical performance (45,49,187). However, this approach fails to explain the mechanical behaviour of ionomer cements in general as this previous work showed a maximum mechanical performance for ASPA cements at 80% humidity with a corresponding shrinkage of 2.5% (Figure 1.3). The ASPA cements used here showed a maximum mechanical performance with dehydration to 66% humidity again with a corresponding shrinkage of 2.5% (Figures 3.19 and 3.21 respectively) but the ATG cements displayed a maximum mechanical performance with dehydration to 33% humidity with a corresponding shrinkage of 6%. At this level of shrinkage the ASPA cements were mechanically poor. Consequently, it is not the shrinkage of the cements which controls their mechanical performance but is more probably the states of hydration of the metallic ions in the cements as this was the major difference between the two systems studied here.

Low Water Content Cements

Although water loss from ionomer cements decreases mechanical performance, cements prepared without water or with low water contents are less sensitive to dehydration and, in certain cases, have improved mechanical properies (45,49). The work of Neilsen (16-18) and of Hopkins (47) suggests that ionomers prepared with low water contents or without water, would have superior mechanical properties, in particular stiffness, to the ASPA and ATG cements. For example, the ASPA and ATG cements had Youngs moduli of circa 3.5 G Pa whereas the anhydrous calcium and zinc polyacrylates of Neilsen (18) had moduli of 15 and 19 G Pa respectively (calculated from sheer modulus values given in Table 1.7 and assuming a Poisson's ratio of 0.35). Some of Neilsen's filled zinc ionomers had modulu of circa 40 G Pa, which is an order of magnitude greater than the ionomer cements used here. However, all these materials generally displayed strengths of similar order to the ASPA and ATG systems, with the exception of unfilled zinc polyacrylate which was considerably stronger. Consequently, reductions in the water content of ionomer cements during moulding would improve their stiffness, but this would be at the sacrifice of the ease of fabrication and the room temperature moulding properties of these materials which is one of their more attractive features. Low water content ASPA cements have been prepared by moulding under pressure (7-14 MPa) at ambient temperatures but were found to be of poor consistency and were mechanically inferior to ASPA cements prepared in the normal manner (49).

3.5 The Composite Properties of Ionomer Cements

It is well established, as described in Section 1.5, that the mechanical and physical properties of particulate composites are strongly influenced by parameters such as the glass particle size and shape, the packing properties of the particles, the volume fraction of the dispersed phase and the interfacial adhesion between the glass and the matrix. These factors were also found to affect the properties of ionomer cements as discussed below.

3.5.1 The Effectsof Glass Particle Size

Variations in the glass particle size of ASPA and ATG cements were found to affect both their manipulative and mechanical properties.

Manipulative Properties

Decreases in the glass particle size generally accelerated the work time and the setting rates of ASPA cements as shown in Table 3.10. This was attributed to the increased surface area of the smaller particles, as shown in Table 3.11, releasing more functional cations per unit volume of glass than with the reduced surface area of the larger sized particles. The effect of using smaller particles resulted in enhanced cross-linking and salt formation of the ionomer cement. This increased the viscosity of the cement paste and at a particle size range of 0-10 μm the ASPA cements were too viscous and too reactive to mix thoroughly. However, the use of the less reactive ATG glass at this size range conferred better workability to the cement.

Table 3.10 The Effects of Glass Particle Size on the Properties of Ionomer Cements

Particle Size range (μm)	Work Time (Min)	Setting Time (Min)	Comp. Strength (MPa)	Comp. Mod (MPa)	Strain at fail (%)
ASPA GLASS					
0-10	0.5	40	129.1±22.6	3937±272	3.69±0.67
10-20	1.5	100	132.2±19.2	4170±294	3.38±0.60
20-30	4.0	120	117.7± 9.2	3653±312	3.50±0.40
30-40	5.0	150	104.0± 7.6	3328±216	3.45±0.35
40-45	10.0	-	74.4± 7.2	2359±251	3.92±0.25
45-63	10.0	-	60.3± 1.9	2168±147	3.77±0.23
63-75	15.0	-	46.8± 4.3	1844±147	3.45±0.37
75-90	15.0	-	37.5± 2.9	1654±146	3.76±0.21
90-106	17.0	-	36.5± 3.7	1565±151	3.21±0.36
106	17.0	-	31.3± 4.7	1406± 66	2.93±0.62
(N.B. All results at a volume fraction of 0.42 and were the mean of 6 results)					
ATG					
0-10	2.0	-	92.3-50.3	5313(n=2)	2.62 (n=2)
10-20	3.0	-	135.6-14.5	4310-372	3.43-0.47
20-30	-	-	99.5-3.74	3251-319	3.55-0.69
30-40	-	-	95.0-5.75	3070-335	3.72-0.63
40-45	-	-	78.5-9.5	2287(n=2)	4.74 (n=2)
(N.B. Volume fraction 0.42 and were the mean of 4 results, unless otherwise stated)					

Mechanical Properties

Both the compressive strength and the modulus of the ASPA and ATG cements were found to generally increase with decreasing particle size as shown in Table 3.10. Between the particle sizes of 10-70 μm, linear relationships were found to exist for the strength and the modulus of ASPA cements as shown in Figures 3.31 and 3.32 respectively and as follows:-

For compressive strength;

$$\sigma_{ic} = K\,d + C \qquad 3.3$$

where; σ_{ic} = compressive strength of the ionomer cement.

d = particle diameter (μm).

K = slope constant, empirically found to be - 1.65.

C = Intercept constant, the compressive strength of zero particle size (i.e. unfilled matrix strength) empirically found to be 155.6 M Pa.

The relationship was found to hold with a linear regression correlation coefficient of 0.98.

For Compressive Modulus;

$$E_c = M\,d + C \qquad 3.4$$

where;

E_c = compressive modulus of the ionomer cement.

M = slope constant, empirically - 455.

C = Intercept constant, empirically 4755 M Pa.

This relationship had a correlation coefficient of 0.97.

Figure 3.31 The Effects of Glass Particle Size on the Compressive Strength of ASPA Cements

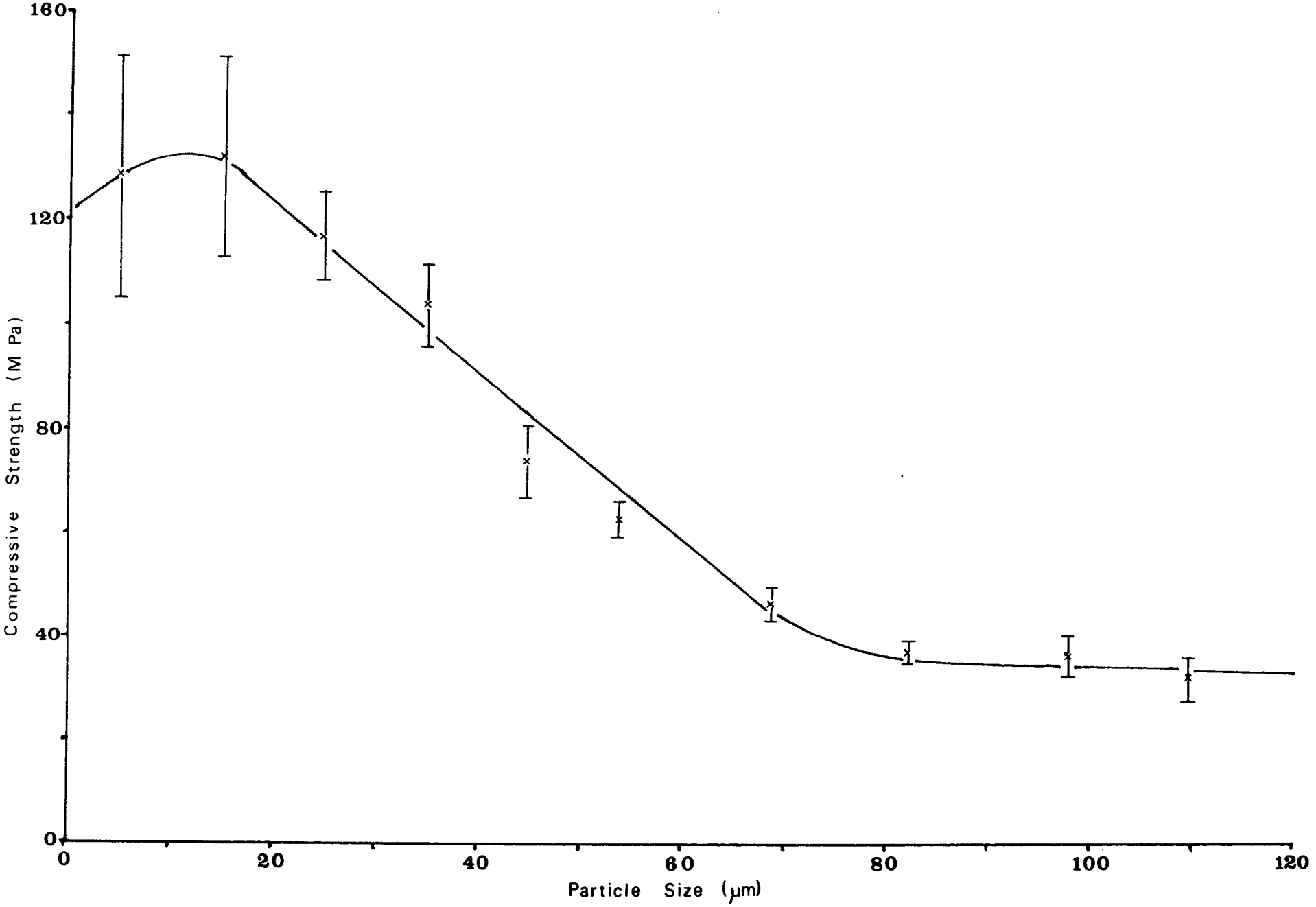

Figure 3.32 The Effects of Glass Particle Size on the Compressive Modulus of ASPA Cements

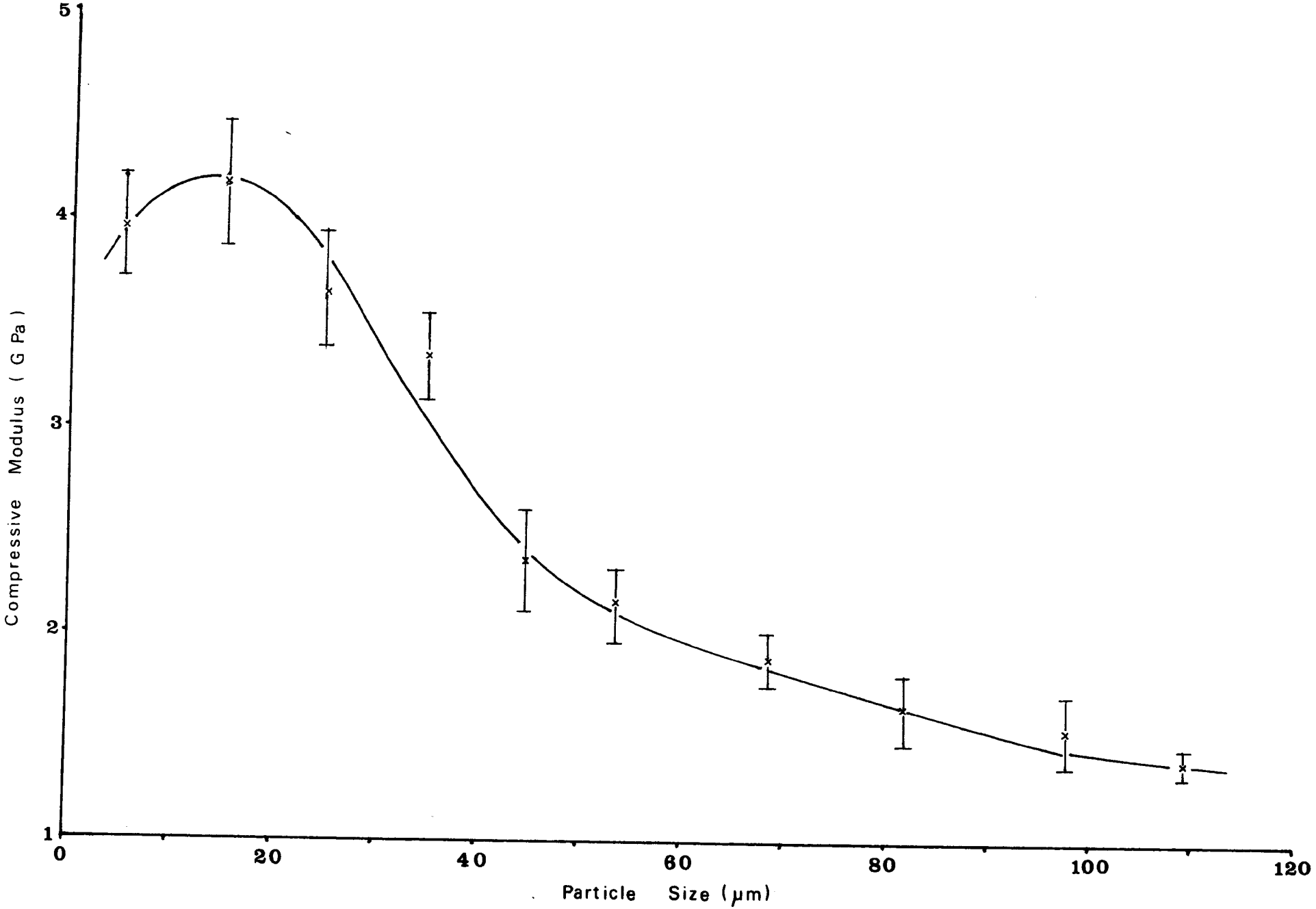

The strength relationship is typical of particulate composites and is similar to the relationship of Landon, Lewis and Boden (83), given as equation 1.8 in the introduction, except that the effects of volume fraction variations were not considered in conjunction with particle size here. The above equations demonstrate the dependence of strength on particle size but the dependence of modulus on particle size is unusual as most theoretical approaches consider stiffness to be independent of size (see Section 1.5.1). This suggests that these approaches are inadequate in describing the behaviour of ionomer cements and possibly composites in general as similar trends have been found in practice for conventional particulate composites (82). However, the results as shown in Figures 3.31 and 3.32, indicate that at larger particle sizes (greater than 70 μm) the mechanical properties of the ionomer cements tend to become independent of particle size and with such composites the above theoretical assumptions may well be valid.

The general increase in mechanical performance with decreasing particle size can be attributed to the following factors:

1. The increased surface area of the glass particles and the decreased interparticle distance
2. The packing properties of the glass particles.

The increase in surface area with decreasing particle size (Table 3.11) would increase the number of functional cations available for subsequent crosslinking or salt formation with the polyacid thus producing a stiffer and stronger matrix which would improve the mechanical performance of the composite. Further, it is well established (85-87, 91-93, 155) that the fracture energy of particulate composites is increased by using smaller particles. The fracture process involves deformation of the advancing crack

front between particles with dissipation of crack energy into the material as described in Section 1.5.3. The increased surface area and greater number of particles per unit volume with the smaller sized glasses would act to dissipate a crack path over a wider area than with larger particles and thus increase the fracture energy of the composite. Also, from geometric considerations, the interparticle distance would be decreased with the smaller particles and this would increase the energy required to deform an advancing crack front to enable it to pass between particles, again this would increase fracture energy. With ASPA and ATG cements, which both displayed Hookean behaviour with brittle fracture, this increase in fracture energy would increase both the strength and the stiffness of the composite. However, at smaller interparticle distances, the fracture process may change to that of a crack which cannot be deformed between particles and may pass directly through a particle or dewet at the interface and reduce composite strength (86,155), this may partially account for the decrease in mechanical performance with particles smaller than 10 μm. This may have also been due to the high surface area of these particles not being adequately wetted by the polyacid as such behaviour has been observed in other composites with mechanical response deteriorating once wetting was incomplete (188). The relatively poor mechanical performance of the cements at the 0-10 μm particle size was not due to the poor workability of the ASPA system or to over reaction of the matrix (as proposed in Section 3.2) as the more workable ATG cements of the same size displayed similar tendencies.

The packing fraction of the ASPA glasses were found to progressively increase with particle size as shown in Table 3.11. It is well established that efficient particle packing, as occurs with increasing

Table 3.11 Surface Area and Packing Fractions of ASPA Glasses of various Particle Sizes

Particle Size (μm)	Surface Area[1] (m^2g^{-1})	Bulk Density (Mgm^{-3})	Packing Fraction (2)
0-10	1.54	1.12	0.45
10-20	0.54	1.26	0.51
20-30	-	1.30	0.52
30-40	-	1.44	0.58
40-45	-	1.56	0.63
45-63	-	-	-
63-75	-	1.39	0.56
75-90	-	-	-
90-106	-	-	-
106	-	1.62	0.66

1. Particles greater than 20 μm were outside the resolution of the instrument.
2. True density ASPA glass = 2.47 Mg m^{-3}

Table 3.12 Mechanical Properties of Ionomer Cements with Bi-Modal Particle Size Distributions

Composition	Packing Fraction	Comp. Strength (MPa)	Comp. Modulus (MPa)	Strain at fail (%)
27% 0-10 μm ATG) 73% 63-75 μm ASPA))	0.66	72.0 ± 5.82	2880 ± 163	2.60 ± 0.10
27% 0-10 μm ATG) 73% 30-40 μm ASPA))	0.68	112.8 ± 13.9	4103 ± 543	3.8 ± 0.08

packing fraction, leads to increased interparticle contact and agglomoration which reduces the mechanical performance of composites (64,65,94) unless multimodal particle size distributions are employed (98). The increased interparticle contact of the ASPA cements containing larger glass particles would lead to enhanced agglomeration and to poorer particle dispersion in the matrix. Both of these effects would lead to reduced mechanical performance of the cement. With particles greater than 70 μm the mechanical performance, and in particular the strength of the cements, were found to be independent of particle size. This was probably due to the packing fractions of these larger glass particles approaching a constant value where a high degree of interparticle contact occurred. In such cases the mechanical performance of the composite was more influenced by the state of agglomeration than by the effects of particle size.

3.5.2 Optimum Particle Packing

Although increases in the packing fraction are known to decrease the mechanical performance of composites and of ionomer cements, as just discussed, the use of bimodal particle size distributions has been found to increase both the packing fraction and the mechanical properties of the composite (98). Consequently, various sized ASPA glasses were used to investigate the potential of bimodal particle sized ionomer cements.

The use of bimodal particle sized ASPA glasses produced ionomer cements which were mechanically superior to cements prepared from the dominant particle sized glass as can be seen by comparison of the results in Table 3.12 with those in Table 3.10. For example, cements prepared with 63-75 μm sized ASPA glass had a strength and

a modulus of 46.8 M Pa and 1844 M Pa respectively whilst bimodal particle sized cements, with 63-75 μm glass as the dominant size range, had strength and modulus values of 72.0 M Pa and 2880 M Pa respectively.

Two bimodal glass mixtures were used both having diameter ratios of circa 7:1 (coarse to fine particles) as this is known to give optimum bimodal packing of spheres (100,104). However, the first system had a coarse dispersion seven times larger than the largest particle size in the fine phase (10 μm) and the second seven times larger than the medium size of the fine phase (5 μm).

Although the packing fractions of these two glass mixtures were similar, as shown in Table 3.12, the smaller sized glass mixture produced stronger and stiffer composites due to the size effect of the dominant phase as discussed previously. Consequently, there may be advantage in using ASPA cements with a bimodal distribution with 10-20 μm particles as the coarse phase and 2-5 μm particles as the fine phase although it would be costly to classify particles of this size.

3.5.3 The Effects of the Volume Fraction of Glass in Ionomer Cements

The volume fraction of glass in ionomer cements and in particulate composites in general, is known to have considerable influence on their strength and stiffness as described in Sections 1.2.6. and 1.5 respectively. Consequently, this variable was investigated for ASPA and other ionomer cements such as the ATG system and certain filled ASPA cements. Increases in the volume fraction of the dispersed phase were found to influence both the manipulative and the mechanical properties of these cements as shown in Tables 3.13 and 3.14.

Manipulative Properties

The ionomer cements generally displayed a reduction in their workability as the volume fraction of the glass increased. This was attributed to more functional cations being released at the higher volume fractions of glass. These cations subsequently reacted with the polyacid matrix to further increase the viscosity of the cement paste making mixing more difficult. The ASPA system was more reactive at all volume fractions of glass than the filled ASPA cements as the latter had diminished functional cation contents. Similarly, the filled ASPA cements were more reactive than the ATG cements, as the latter had the readily leachable cations removed from its surface. For example, at volume fractions of 0.44 to 0.46 the ASPA cements and the highly filled ASPA cements (ϕ_R = 0.75) had work times of 1 and 2-3 minutes respectively whilst the ATG cement had a workability of 8 minutes.

Each ionomer cement system was found to have a maximum volume fraction of glass which was governed by the reactivity and manipulative properties of the system. The less reactive systems provided more time for thorough mixing to occur and also permitted higher volume fractions of the dispersed phase to be employed. For example, a maximum volume fraction of 0.50 was achieved with the ASPA cements whilst some of the highly filled ASPA cements and the ATG system permitted volume fractions of circa 0.60 to be achieved.

Mechanical Properties

The volume fraction of glass in the ionomer cements was found to influence their mechanical properties as shown in Tables 3.13 - 3.14. The unfilled ASPA and ATG cements and cements with low filler contents (ϕ_R = 0.25) all displayed improved strength and modulus enhancement with increasing volume fraction up to the point where

Table 3.13 The Effects of Volume Fraction on the Manipulative and Mechanical Properties of Ionomer Cements

P:L ratio (g:ml)	Volume fraction	Work Time (min)	Comp Strength (MPa)	Comp. Modulus (MPa)	Strain at fail (%)
ASPA Cements					
1.0:1	0.29	2.0	130.4±6.9	3700±404	4.23±0.24
1.5:1	0.38	1.5	96.4±25.4	4533 -	2.46 -
2.0:1	0.45	1.0	162.4±44.3	4638±320	3.72±0.94
2.5:1	0.50	0.75	85.9±21.6	4308 -	2.28 -
3.0:1	0.55	unwork-able	-	-	-
ATG Cements					
1.0:1	0.28	12.00	147.6±7.8	3565±225	5.41±0.30
1.5:1	0.37	10.00	132±13.1	3452±274	4.53±0.57
2.0:1	0.44	8.00	144.9±17.3	4073±3.63	3.64±0.32
2.5:1	0.50	5.00	133.3±27.6	4227±8.79	3.13±0.68
3.0:1	0.53	3.00	163.7(n=2)	4645 -	3.98 -
3.5:1	0.58	3.00	106.8±31.0	4729±972	2.43±0.20
4.0:1	0.64	unwork-able	-	-	

Table 3.14 The Effects of Volume Fraction on the Manipulative and Mechanical Properties of Filled-Ionomer Cements

BALLOTINI 3,000 CPO3

P:L ratio (g:ml)	Volume fraction	Work Time (mins)	Comp. Strength (MPa)	Comp. Modulus (MPa)	Strain at fail (%)
ϕ_R= 0.25					
1.0:1	0.30	2.0	75.8±16.6	2790±169	2.82±0.54
1.5:1	0.39	1.5	122.3±19.1	3603±216	3.84±0.54
2.0:1	0.46	1.0	141.0±24.6	4488±485	3.47±0.71
2.5:1	0.51	unwork-able			
ϕ_R= 0.50					
1.0:1	0.30	2.0	123.9±4.4	3079±359	4.44±0.51
1.5:1	0.40	1.5	116.9±18.8	3517±165	4.17±0.55
2.0:1	0.47	1.5	117.1±17.6	3852±580	3.55±0.44
2.5:1	0.52	1.0	140.2±26.7	3683±440	4.33±0.44
3.0:1	0.57	unwork-able	-	-	-
ϕ_R= 0.75					
1.0:1	0.31	2.5	98.2±8.6	2773±334	5.16±0.21
1.5:1	0.39	2.0	93.3±5.4	2903±229	4.18±0.35
2.0:1	0.47	2.0	95.8±3.2	2587 -	5.33±0.14
2.5:1	0.53	1.5	96.4±2.5	2754±303	4.29±0.69
3.0:1	0.57	1.0	100.4±7.4	2293±229	4.68±0.87
3.5:1	0.61	unwork-able			

Table 3.14 The Effects of Volume Fraction on the Manipulative and Mechanical Properties of Filled-Ionomer Cements

POZZOLAN FILLER

P:L ratio (g:ml)	Volume fraction	Work Time (min)	Comp. Strength (MPa)	Comp. Modulus (MPa)	Strain at fail (%)
ϕ_R= 0.25					
1.0:1	0.29	2.0	127.6±17.6	3631±366	4.32±0.5
1.5:1	0.38	2.0	144.3±26.9	4339±396	3.89±0.58
2.0:1	0.45	1.5	170.1±18.2	4840±174	4.01±0.26
2.5:1	0.51	unwork-able	-	-	-
ϕ_R= 0.50					
1.0:1	0.30	2.5	124.8±18.0	3518±235	4.96±0.64
1.5:1	0.39	2.0	136.0±11.5	3973±340	4.00±0.30
2.0:1	0.46	1.5	130.0±27.2	3990±653	3.55±0.85
2.5:1	0.51	1.0	151.9±23.7	4124±162	4.23±1.05
3.0:1	0.55	unwork-able	-	-	-
ϕ_R= 0.75					
1.0:1	0.30	3.5	83.9±3.0	2156 -	7.00±0.35
1.5:1	0.39	3.0	103.2±6.6	3177±474	5.33±0.51
2.0:1	0.46	3.0	109.4±12.7	3200±307	4.53±0.82
2.5:1	0.52	2.0	128.5±5.2	3080±300	5.08±0.02
3.0:1	0.56	1.0	103.2±26.8	3297 -	5.25 -
3.5:1	0.60	unwork-able	-	-	-

poor mixing occurred, where after mechanical properties deteriorated. The highly filled ASPA cements were less sensitive to volume fraction variations and displayed almost constant values of strength and stiffness with increasing volume fraction. This difference in behaviour between these cements and the unfilled cements was attributed to the poorer interfacial adhesion between the filler and the PAA matrix than with the ASPA and ATG glasses as was discussed earlier in Section 3.3.2. Interfacial adhesion is known to have significant effects on the mechanical properties of composites and is considered in more detail later in this section.

The ATG cements displayed similar trends in strength with increasing volume fraction to the ASPA cements but the ATG cements only achieved similar values of modulus to the ASPA cements at higher volume fractions of glass. This indicates that modulus is more sensitive than strength to the extent of reaction of the polyacid with metallic ions as the ATG glass was found to have less functional cations on its surface than the ASPA glass.

The strain at failure of the ionomer cements decreased linearly with increasing volume fraction for the unfilled cements. This behaviour, which is typical of particulate composites (see equation 1.8), also reflects a stiffening effect of the cement as it becomes more reacted with the metallic ions from the glass. However, the strain at fail of the filled ASPA cements decreased with increasing volume fraction and showed a minimum value of strain at a volume fraction of circa 0.5; at higher volume fractions the strain at fail of these cements tended to increase. This unusual behaviour was attributed to interfacial dewetting around the filler particle as such mechanisms are known to increase the strain at fail of composites (64,65).

It was also observed that the standard deviation of both the strength and the modulus results increased considerably as the volume fraction of the dispersed phase increased and this was discussed earlier in Section 3.1.

An analysis of the modulus and the strength of ionomer cements was conducted in a similar manner to the theoretical approaches described in Section 1.5.1 and 1.5.2. However, calculation of both the relative strength and the relative modulus were difficult due to a lack of data on the mechanical properties of the unfilled matrix. This situation is further complicated as progressive additions of ion-leachable glass to the polyacid matrix is bound to increase the extent of crosslinking or salt formation and alter the properties of the matrix itself.

Modulus values of 50% aqueous calcium polyacrylate (46,47) were too low (0.1 M Pa) and values of anhydrous polyacrylates (18) were too high (5.56 G Pa) for reasonable use in determining the relative modulus of the cements. Consequently, a matrix modulus value of 2,000 M Pa was obtained by extrapolation of the data in Tables 3.13-3.14 to zero volume fraction. The resulting relative modulus plots are shown in Figure 3.33, which shows that modulus is progressively increased with volume fraction of the dispersed phase. The relative modulus curves of the ASPA and the ATG cements were similar to the Sato-Fuorokawa relationship for perfect interfacial adhesion between the filler and the matrix (Figure 1.7 and Appendix 2) and to the Einstein hydrodynamic relationship (Equation 1.1 and Figure 1.7) which also assumes perfect adhesion. However, the highly filled ASPA cements displayed less modulus enhancement with increasing volume fraction and approached the Sato-Fourokawa relationship for poor interfacial adhesion, in particular at high volume fraction replacement

of ASPA glass ($\emptyset_R$ = 0.75). As discussed in Section 3.3.2, this behaviour demonstrates that the interfacial adhesion between the ion leachable glass and the PAA matrix is greater than the interfacial adhesion between the filler and the PAA. Again, this strongly suggests that the polyacid forms primary interfacial bonds with metallic ions on the ASPA and the ATG glass surfaces. Similarly, the cements containing the Pozzolan filler displayed greater modulus enhancement than cements filled with similar levels of Ballotini spheres. As discussed in Section 3.3.3, the Pozzolan filler had surface metallic ions which were capable of reacting with polyacid whilst the Ballotini spheres were inert towards the polyacid. Consequently, the Pozzolan filler was capable of providing a greater degree of interfacial adhesion with the PAA matrix than the Ballotini filler.

Strength values of the unfilled ASPA matrix could not be determined by extrapolation because of variable cement strengths at low volume fractions of glass. Consequently, convenient fitting curves were obtained by using the compressive strength value of anhydrous calcium polyacrylate of 106 M Pa (18), as shown in Figure 3.34. This value of strength was only used for convenience and was used with several reservations. For example, the unfilled but crosslinked ASPA matrix would contain appreciable amounts of the potentially stronger aluminium polyacrylate. Also, aqueous polyacrylates are considerably weaker than the anhydrous form and 50% aqueous solutions of calcium polyacrylate was found to have a low strength of only 0.6 M Pa (47) which was not suitable for use here. A matrix strength of 155.6 M Pa was obtained from the particle size studies (Equation 3.3) by linear extrapolation to a zero particle size. This value was too high to produce meaningful curves and was probably unrealistic due to deviations from the linear relationship at smaller particle sizes.

Table 3.33 The Relative Modulus of Ionomer Cements as a Function of Volume Fractions of the Dispersed Phase

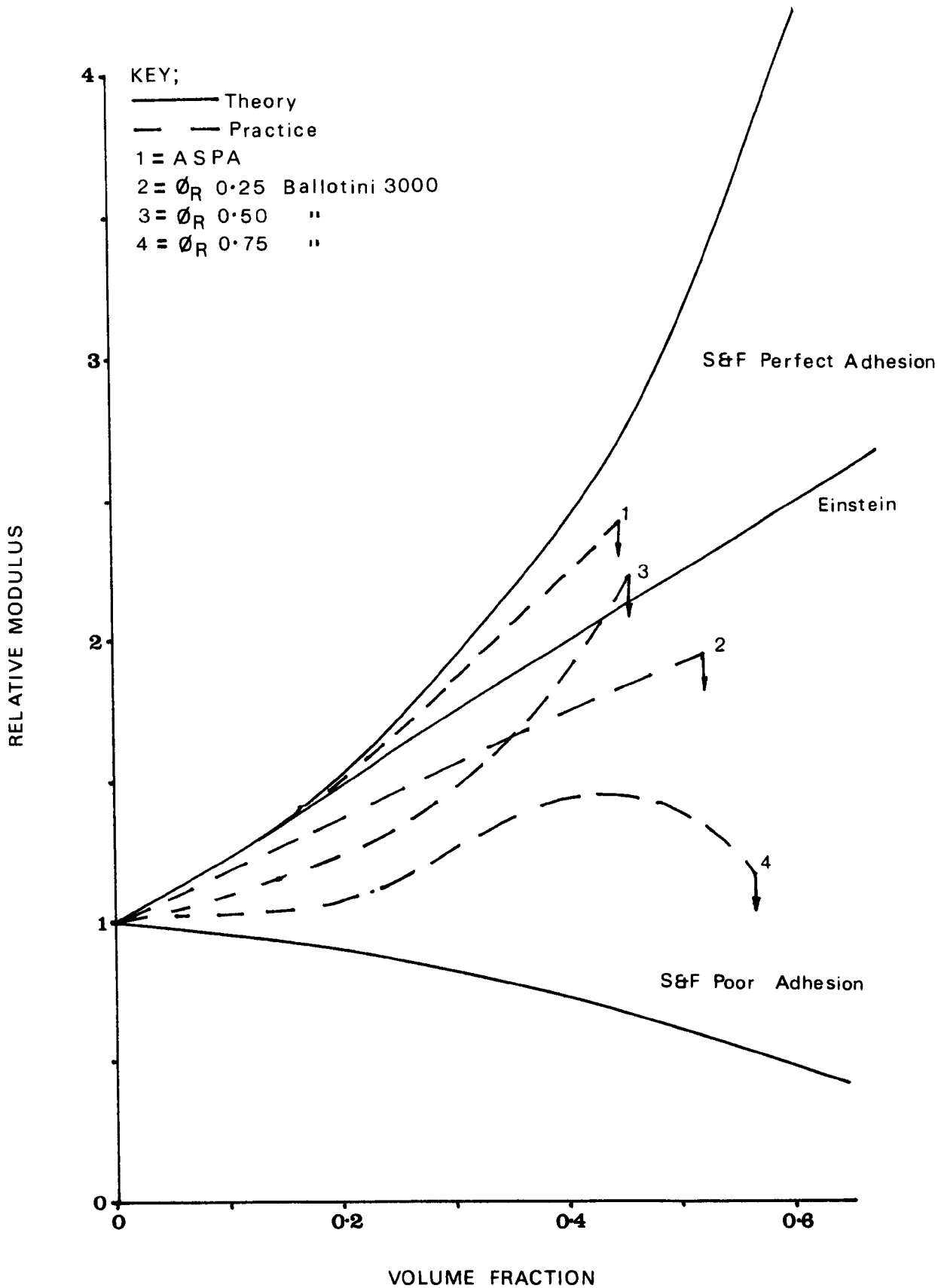

N.B. Data points omitted for clarity

Figure 3.33 Continued

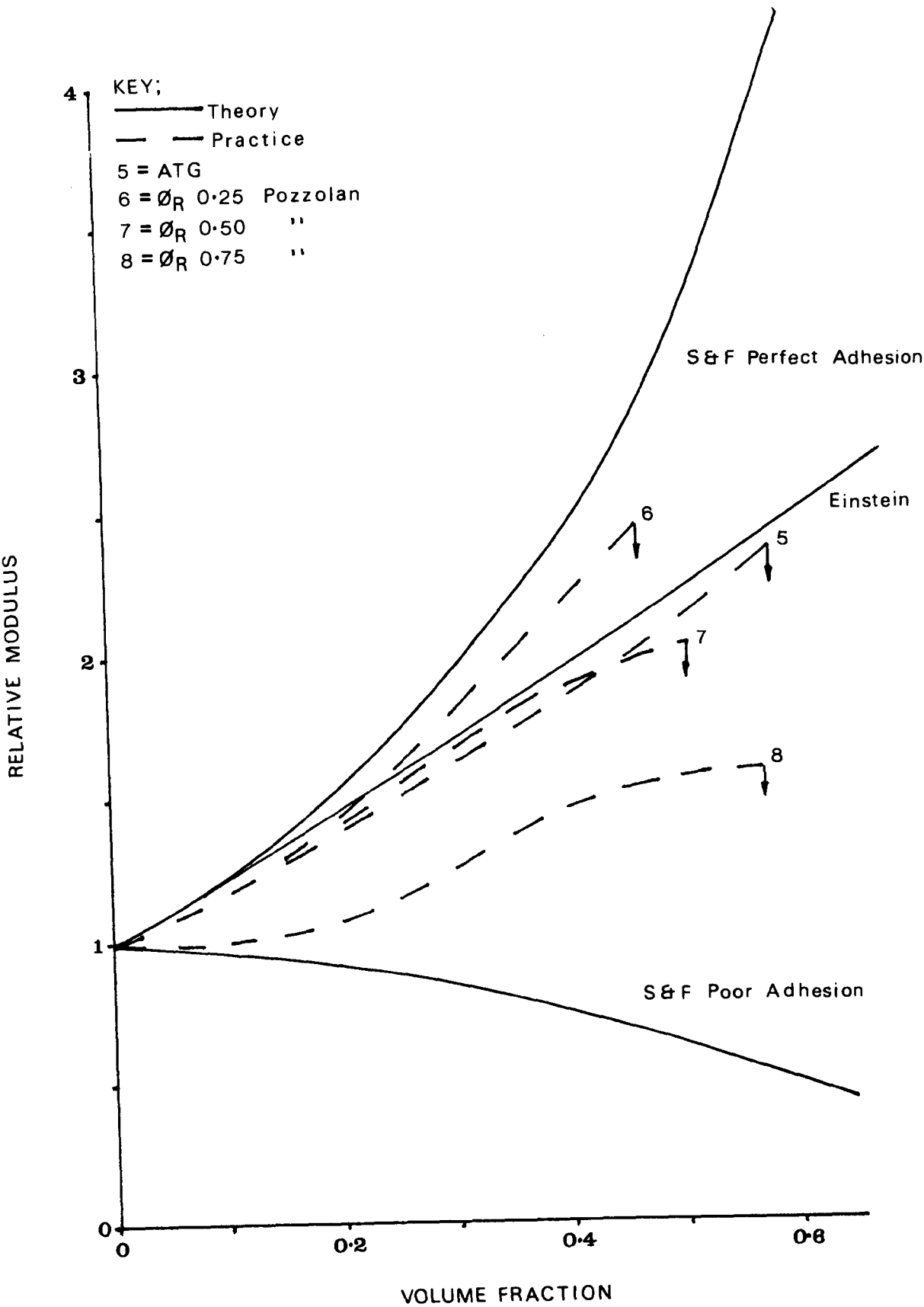

The results of Figure 3.34 demonstrate, with the exception of the highly filled ASPA cements, that the strength of the cements were enhanced as the volume fraction of glass increased. This behaviour is unusual for particulate composites which normally display a strength reduction with the addition of a filler as described in Section 1.5.2. The ionomer cements displayed greater relative strengths than those predicted by the Nicolais-Nicodemo relationship for perfect interfacial adhesion (88) as given in Equation 1.4 and in Figure 1.8. The relative strength curves also suggest that good interfacial adhesion exists between the ion leachable glasses and the polyacid matrix and that the general increase in performance with increasing volume fraction indicates that two processes are occurring simultaneously. Firstly, the matrix is being progressively reacted and crosslinked by the addition of the glass and thus becoming stronger and contributing to the strength of the composite. Secondly, the extent of interfacial adhesion is increased as the volume fraction of glass is increased and, if strong interfacial bonding occurs as discussed in more detail in Section 3.9, then this would contribute to the strength of the system. Again, the poorer performance of the highly filled ASPA cements reflects a lower interfacial adhesion between the filler and the matrix than between the ion-leachable glass and the matrix. Also the Pozzolan filled cements were stronger than the Ballotini filled cements, at similar filler levels, due to the greater extent of interfacial adhesion between the Pozzolan filler and the matrix as discussed earlier.

The strength relationships showed more clearly than the modulus curves the consequences of poor cement mixing. The strength of the cements declined at higher volume fractions because the cements became increasingly more difficult to mix. The decline in strength

Table 3.34 The Relative Strength of Ionomer Cements as a Function of Volume Fraction of the Dispersed Phase

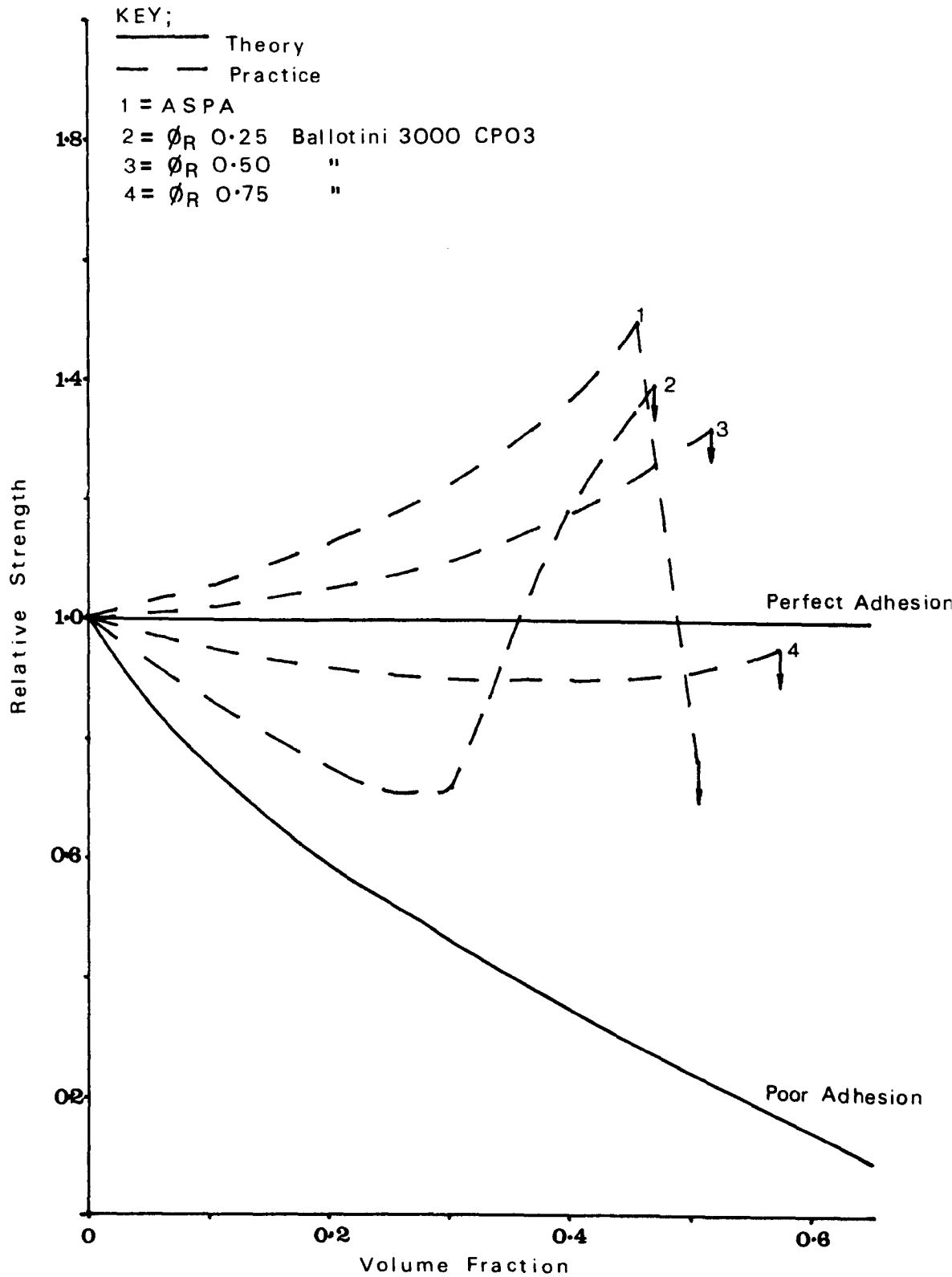

N.B. Data points omitted for clarity

Table 3.34 Continued

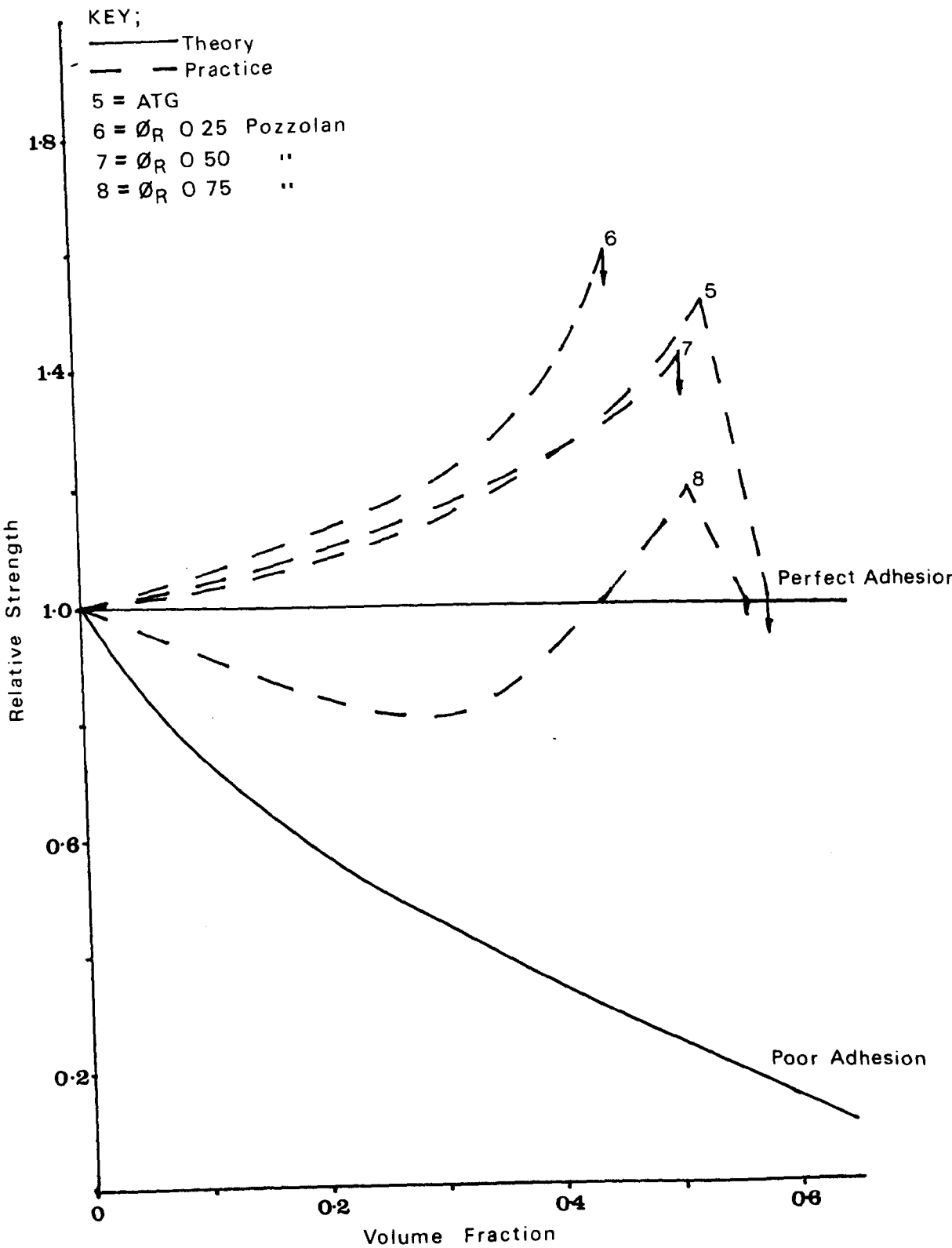

was thus attributed to poor dispersion of the glass in the matrix, poor wetting of the glass by the matrix and to the entrainment of air during the mixing of these viscous cement pastes. The modulus curves did not show this decrease before the maximum volume fraction because modulus was measured at lower strains than compressive strength where the consequences of the defects would be less evident.

3.5.4. The Effects of Interfacial Adhesion

The generally poor mixing properties of ionomer cements and the experimentally observed facts that aqueous solutions of PAA do not readily wet glass surfaces and that ASPA glass is not wetted by water have all led to the proposition that unfavourable wetting conditions exist at the glass polyacid interface. For example, a 30% aqueous solution of PAA was found to have an equilibrium contact angle of 58° on a clean smooth glass surface (microscope slide) at room temperature. Also, ASPA glass powder was found to float on distilled water, held up by interfacial forces despite its higher density. Consequently, the interfacial properties of ASPA cements were investigated by preparing cements by the anhydrous technique with additions of surfactants to the water of the cement mix to reduce its surface free energy. It was postulated that the use of surfactant solutions would improve interfacial wetting properties of the cement and thus improve its mechanical performance.

The effects of surfactant addition on the surface free energy of water is shown in Figures 3.35 and the strengths of ASPA cements prepared with these solutions is shown in Figures 3.36 and 3.37 for cements stored at 66% and 100% relative humidity respectively. The 66% humidity environment was employed to be consistent with the rest of the work in this thesis and the 100% humidity environment

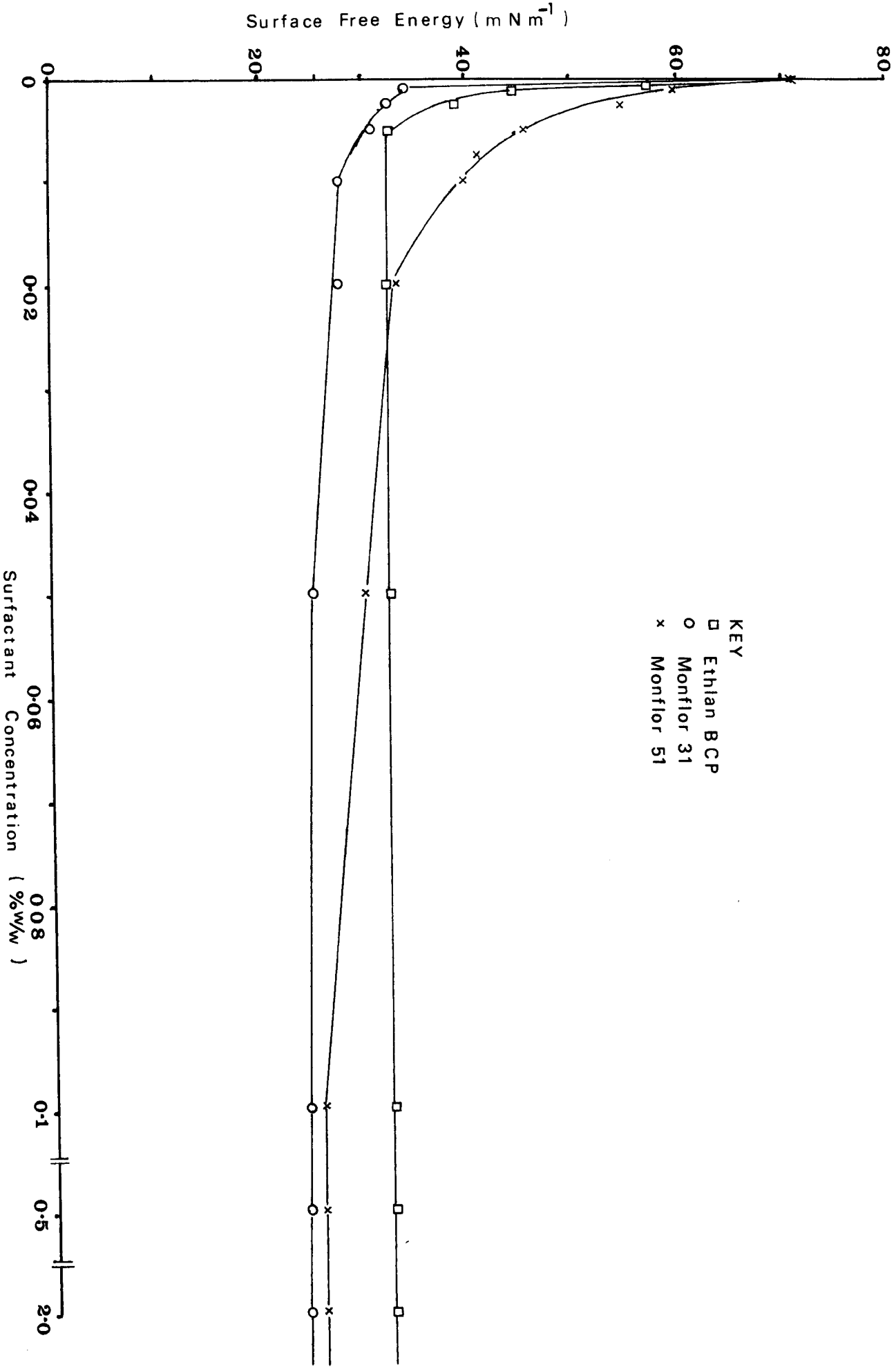

Figure 3.35 The Effects of Surfactant Concentration on the Surface Free Energy of Water

was selected to reduce the variability of the strength results as discussed in Section 3.1. The moduli of these cements were unaffected by surfactant addition.

The compressive strengths of the cements were improved by the use of surfactants at low concentrations confirming the proposal that ASPA glass is not readily wetted by water, which is the reaction solvent. For example, the strengths of the ASPA cements increased by over 40% from 83 M Pa to 117 M Pa on the addition of 0.005% w/w surfactant to the water of the cement mix. This behaviour, when considered in relation to classical wetting theory, suggests that the ASPA glass has a high value of the spreading pressure as given in the Young-Dupré equation (1.12). Thus the glass presents an oxidised surface for wetting which has a surface free energy less than 72.7 M m^{-1}, which is the surface free energy of water (182). Consequently, during the cementation reaction water and aqueous solutions of PAA do not spontaneously wet the ASPA glass but most probably form droplets with measurable contact angles on its surface. This leads to reduced interfacial contact with the possible entrapment of air at the interface which develops microvoids and cracks which can cause premature failure under conditions of stress (111,112). The use of surfactants reduced the surface free energy of the water and, as predicted by the Young equation (1.11), would have promoted better wetting of the glass and would have reduced the contact angle at the interface. If the surface free energy of the liquid became less than that of the solid surface then spontaneous wetting may occur. However, wetting is also retarded where rough surfaces are involved and is a dynamic process, the rate of which is governed by energetic considerations and the viscosity of the wetting liquid. The ASPA glass provided a rough

surface for wetting, as shown in the electron micrographs of Figure 3.7, and the rapid gellation of the polyacid matrix during setting would retard wetting and would prohibit the penetration of the polyacid or water into the microscopically rough surface of the glass. This highlights the importance of achieving good interfacial wetting at the onset of mixing. Also, the use of surfactants was found to aid the cement mixing process which may have led to better dispersion of the glass powder in the set cement.

The mechanical properties of the cements were found to be dependent on the concentration of the surfactant used. The ASPA cements obtained a maximum strength which corresponded to the concentration of surfactant required to reduce γ_w to its minimum value (i.e. 0.01-0.02% by weight). At higher surfactant concentrations the value of γ_w was unaltered but the strength of the cements tended to decline. It is known that at low concentrations surfactant molecules promote wetting by adopting positions in the surface of the wetting liquid (114,191), but at higher concentrations the available surface sites are occupied and the excess surfactant molecules act in other ways such as forming micelles or may be absorbed at other interfaces. The loss of mechanical performance at higher surfactant concentrations suggests that the excess surfactant was preferentially absorbed at the ASPA glass surface to give a mechanically weak boundary layer at the polyacid-glass interface, or that the surfactant molecules formed micelles which disrupted the network forming ability of the polyacid. The latter proposal is plausible as the addition of anionic surfactants at concentrations of 1-2% completely prevented gellation of 50% aqueous PAA solutions.

Figure 3.36 The Effects of Surfactant Addition on the Compressive Strength of ASPA Cements stored at 66% R.H.

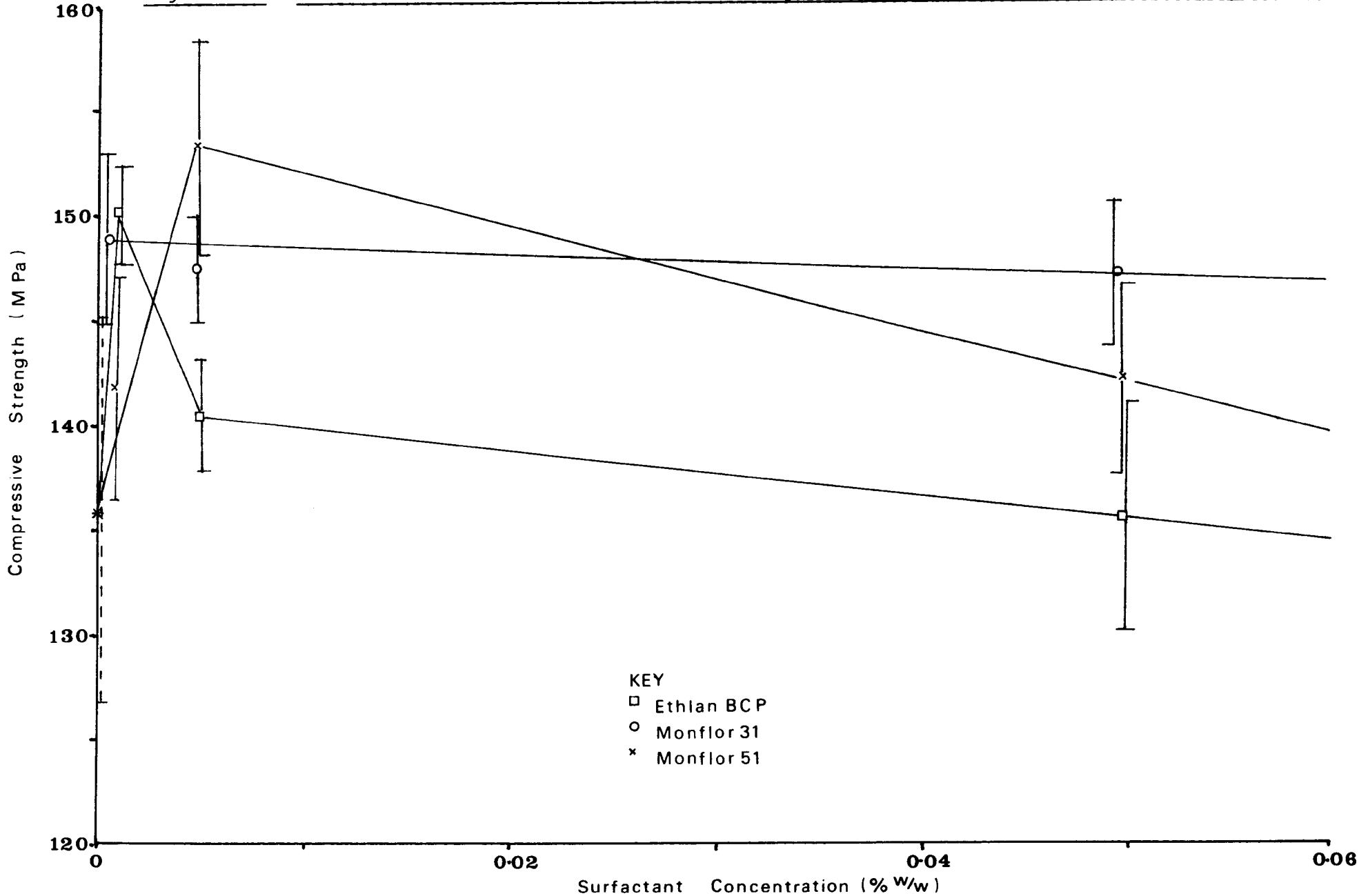

Figure 3.37 The Effects of Surfactant Addition at the Compressive Strength of ASPA Cements stored at 100% R.H.

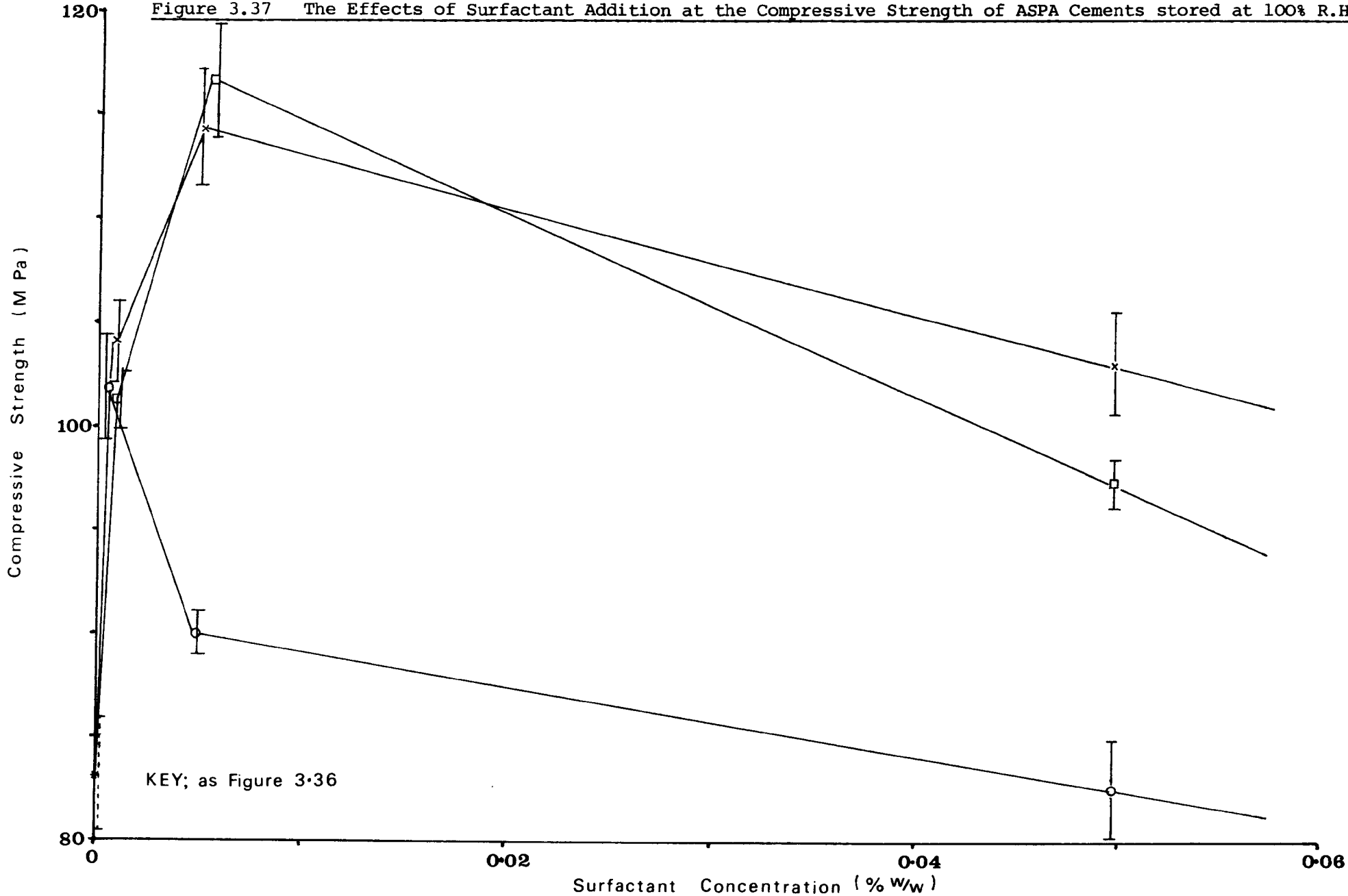

3.6 Alternative Ion Leachable Materials to ASPA Glass

The predominant use of ASPA glass in ionomer cement formulations has produced materials which have limited potential for applications outside of dentistry. For example, the ASPA system is rapid in set and only small moulding can be fabricated, these cements have poor mechanical performance in environments of low humidity and are expensive to use. The ATG system has a more controllable reactivity and produced cements which could be used at any humidity. However, any modification of the ASPA glass would only increase the cost of the cement, thus making the ATG system economically unattractive for applications outside of dentistry. Consequently, the use of alternative and less expensive ion leachable sources, such as glasses, minerals and metal oxides, may produce ionomer cements of controlled reactivity, with good mechanical properties and which are economically attractive for wider scale use.

3.6.1. Alternative Ion Leachable Glasses

As discussed in Section 3.2, the reactivity and the mechanical properties of ionomer cements are strongly influenced by the chemical composition of the glass particle surface. The ESCA studies suggested that glasses with low calcium contents are required to produce ionomer cements which are less reactive than the ASPA cement, whilst glasses with a high aluminium content would produce cements of greater strength and stiffness than the ASPA system, especially in low humidity environments as discussed in Section 3.4. Also, the replacement of fluorite in the ASPA glass with other fluxes, such as calcium oxide, may reduce the corrosive attack which occurs on furnace linings at fusion temperatures. Consequently, a number of calcium aluminosilicate glasses were

prepared with lower calcium and higher aluminium contents than the ASPA glass in order to produce glasses with similar cementing properties to the ATG system. Also, other glass formulations were evaluated to examine the potential of calcium oxide as an alternative flux to fluorite. The composition of these glasses is given in Table 2.1.

The use of other glass formulations which contained zinc ions were examined for ionomer cement formation and these are also given in Table 2.1. Zinc based glasses were chosen as zinc ions are known to react with polyacids to form strong and stable materials. For example, the work of Neilsen with zinc polyacrylate ionomers (16-18) and the zinc oxide based dental cements of Smith (28,29) suggest that strong and hydrolytically stable ionomer cements could be prepared by uxing zinc oxide as an alternative to ASPA glass. However, zinc oxide ionomer cements are rapid in set and are suited for use in dentistry. The reactivity of these zinc ions cements can be reduced by controlling the rate of metallic ion liberation under acid attack by incorporating the zinc ions into a glass structure.

These ion leachable glasses were ground and passed through a 45 micron sieve in a similar manner to the ASPA glass. The mechanical and manipulative properties of these novel glass ionomer cements are given in Table 3.15. These results demonstrate that ionomer cements of similar mechanical performance to the ASPA cement can be formed from low calcium content glasses such as BCI2 and BCI3. These glasses were either of similar reactivity to the ASPA system, as shown in the reometer traces of Figure 3.39, or were hydrolytically less stable than the ASPA cements, as shown in Figure 3.38, and thus offered no practical advantages as a replacement for ASPA glass.

Table 3.15 Properties of Novel Glass Ionomer Cements

Glass[1]	Volume fraction	P:L ratio	Work time (min)	Setting Time (min)	Comp Strength (MPa)	Comp. Mod. (MPa)	Strain Fail (% strain)
ASPA	0.42	2:1	1.5	70	69.6 ± 19.1	3628 ± 280	2.14 ± 0.39
BCI 1	-	2:1	30	-	Poor mould release		
BCI 2	0.42	2.4:1	2.5	60	107.9 ± 5.8	2830 ± 197	5.58 ± 0.34
BCI 3	0.42	2.3:1	10	160	77.7 ± 7.1	2259 ± 145	6.81 ± 0.89
Zn I	0.27	2:1	12	-	62.5 ± 6.9	2597 ± 100	3.47 ± 0.98
Zn I	0.42	3.5:1	10	150	71.3 ± 3.7	2453	3.55 ± 0.34
Zn 2	-	2:1	10	-	Poor mould release		
Zn 3	0.42	2.6:1	20	-	23.3 ± 0.9	1921	2.96
Zn 4	0.42	3.2:1	20	-	53.6 ± 8.6	-	> 15

(1) See Table 2.1 for composition of glass

Figure 3.38 Rheometer Trace of Novel Glass-Ionomer Cements

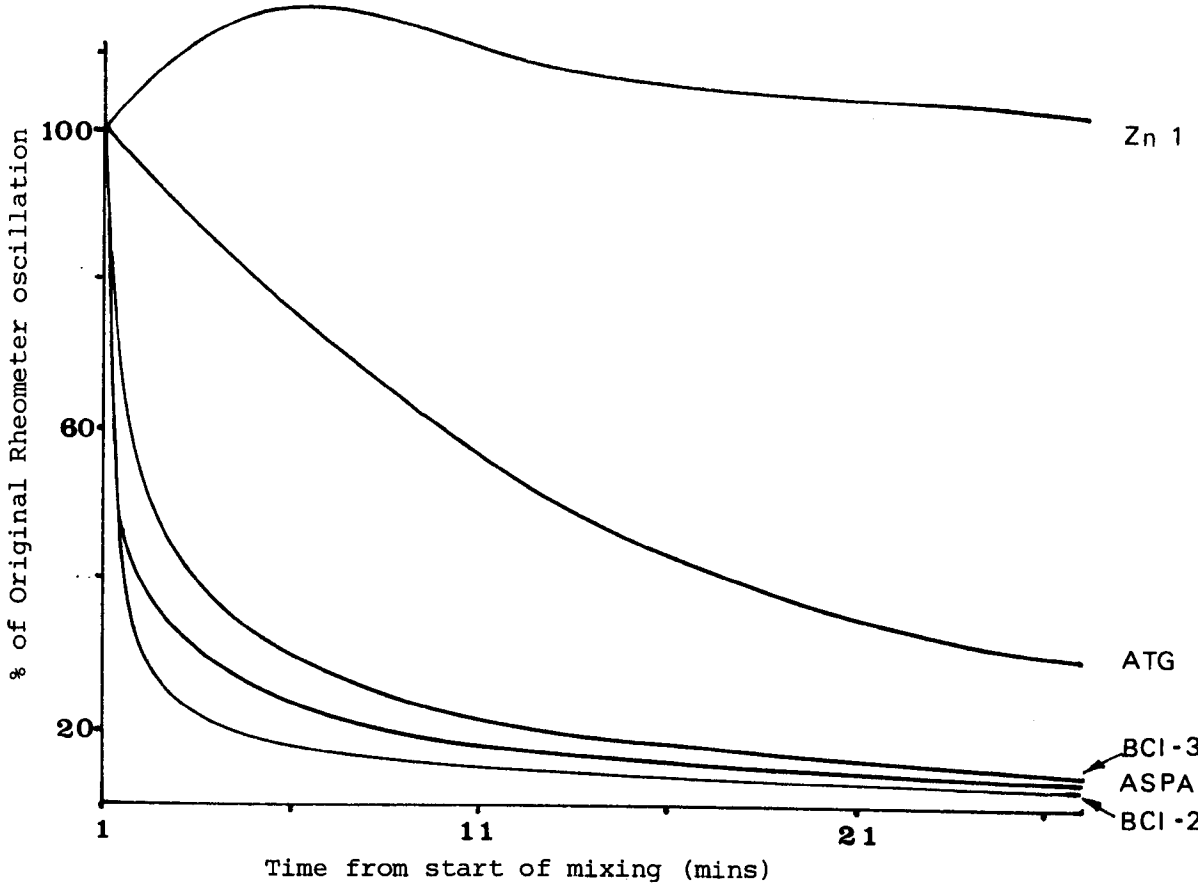

Figure 3.39 Hydrolytic Stability of Novel Glass-Ionomer Cements

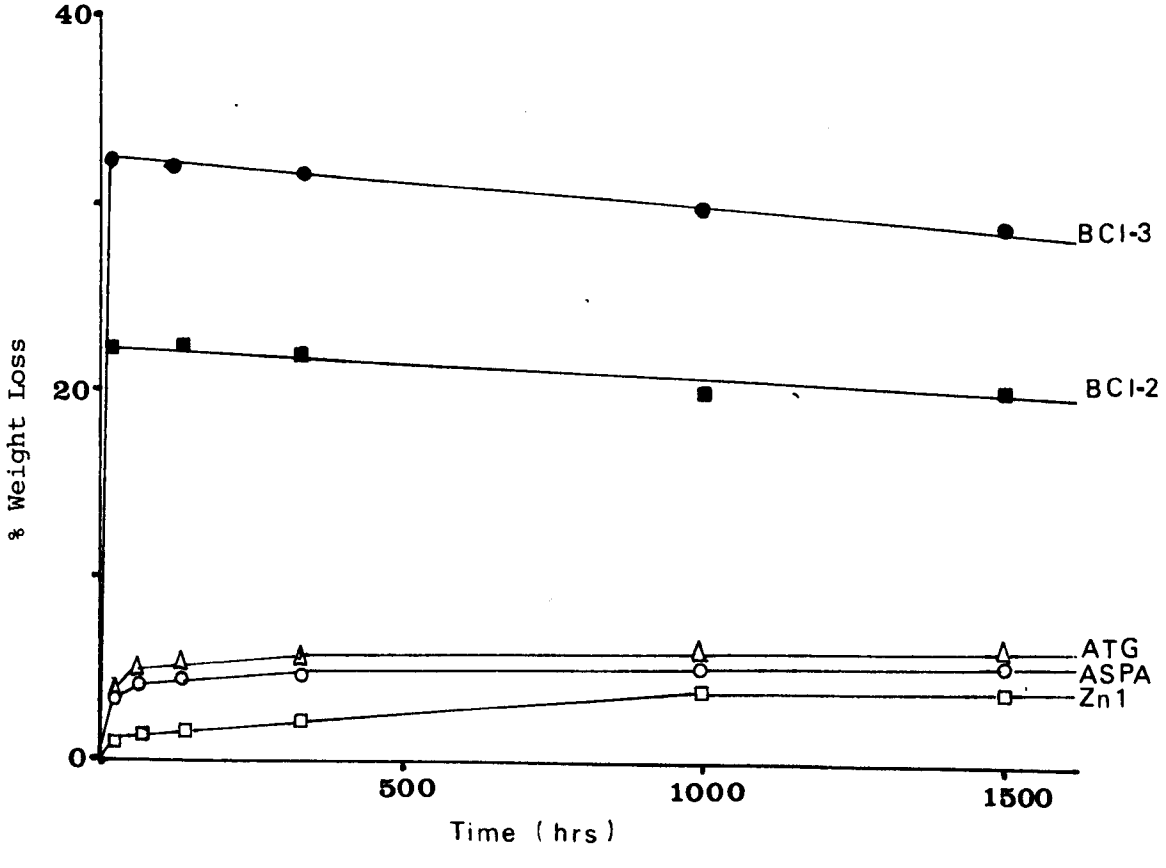

The zinc based glass ionomer cements, with the exception of Zn 1 glass cement, were weaker than the ASPA cements and were also hydrolytically unstable. The Zn 1 glass formed hydrolytically stable ionomer cements of similar mechanical performance to the ASPA cements and, in addition had good manipulative properties giving a work time of 10-12 minutes, much longer than the 1.5 minutes work time of the ASPA cement. Further the zinc glass formulations all melted at lower temperatures than the ASPA glass, their formulations were not as complex and they were not noticeably corrosive towards crucible and furnace linings. Consequently, the Zn 1 glass should have both economic and practical advantages as replacements to ASPA glass and other aluminosilicate glasses for non-dental ionomer cement applications.

The Zn I glass cement paste was also found to have unusual manipulative properties as shown in the rheometer trace of Figure 3.39. The viscosity of the cement paste mix decreased with time whilst subjected to conditions of shear. This behaviour suggests that during the initial setting period of these cements the zinc ions do not form permanent crosslinks with the polyacid molecules, but undergo some bond breakage or stress transfer mechanism and that the polyacid matrix exhibited some form of thixotropic behaviour.

3.6.2 Minerals and Metal Oxides

Previous work conducted with mineral ionomer cements (7,8,49) and with metal oxide ionomer cements (4,45,49) demonstrated that relatively inexpensive ion leachable materials could be used to form hydrolytically stable cements but the mechanical performance of these materials were generally inferior to ASPA cements. This was attributed to high void contents of these mineral and metal oxide cements as described in Sections 1.3.2 and Sections 1.3.3

respectively. Consequently, methods for reducing the void content of these cements were examined and other inexpensive ion leachable sources, such as the pulverised fly ash (PFA) Pozzolan, were evaluated.

The mechanical and manipulative properties of some metal oxide and some mineral ionomer cements are given in Table 3.16; only limited data is available due to difficulties in moulding these cements and to small quantities of the mineral samples. Generally, these mineral and metal oxide cements produced mouldable cement pastes with greater workabilities than the ASPA cement pastes. For example, workabilities of 10 minutes were achieved with ß-Wollastonite ionomer cements in comparison with 1.5 minutes for the ASPA system. However, these mineral and metal oxide ionomer cements were mechanically inferior to the ASPA system unless the minerals were treated to reduce the extent of void formation.

Voids may be generated in mineral and metal oxide ionomer cements by reaction of the polyacid with residual carbonate at the mineral or metal oxide particle surface. This reaction releases CO_2 gas which becomes entrapped in the cement structure and forms voids. Treatment of minerals such as ß-Wollastonite and Willemite with 1M HCl prior to cement formation removed the residual carbonate and produced cements of lower void content as shown in the photo-micrographs of Figure 3.40. This reduction in void content increased the mechanical properties of the cement. For example, untreated Willemite ionomer cements had a compressive strength of 50.8 M Pa and ionomer cements of the treated mineral had a compressive strength of 76.6 M Pa, comparable with the compressive strength of the control ASPA cement of 69.6 M Pa. Similarly, untreated ß-Wollastonite ionomer cements were so weakened by

voiding that they could not be released from the mould without breakage but the treated mineral cement had a compressive strength of 71.1 M Pa, again similar to that of the ASPA cement.

The incorporation of voids in a composite material, even at low volume fractions, is known to reduce the mechanical performance as described in Section 1.5.6. The photomicrographs of the mineral cement fracture surfaces (Figure 3.40) showed that these cements still contained considerable voiding after acid treatment. Also, ASPA cements are known to contain about 5% voids by volume (45,49). Consequently, further reduction in the void content of these cements would be desirable and would lead to cements of improved mechanical performance.

Table 3.16 Properties of Minerals and Metal Oxides-Ionomer Cement

Source	Volume fraction	P:L ratio	Work Time (min)	Setting Time (min)	Comp. Strength (MPa)	Comp. Mod. (MPa)	Strain fail (% strain)
ASPA	0.42	2.1	1.5	70	$69.6^{+}_{-}19.1$	$3628^{+}_{-}280$	$2.14^{+}_{-}0.39$
Al.Oxide (acid)	0.42 *	1.7:1	3.5	-	$50.9^{+}_{-}4.4$		
Al Oxide (neutral)	0.42 *	1.7:1	3.0	-	$43.2^{+}_{-}11.2$		
Al Oxide (basic)	0.42 *	1.7:1	2.5	-	$37.0^{+}_{-}3.4$		
ß-Wollastonite	0.42 *	1.6:1	10	-	Poor mould release - highly voided cement		
ß-Wollastonite (treated)	0.42 *	1.6:1	10	-	$71.7^{+}_{-}9.1$	3111 –	3·13
Willemite	0.42 *	3.3:1	3.5	-	50.8 (n=3)	2640 –	3·05
Willemite (treated)	0.42 *	3.3:1	3.5	-	76.6 (n=2)	2561 –	3·89
Pozzolan	0.46 *	2:1	7	24 hours	$24.4^{+}_{-}2.1$	$433^{+}_{-}36$	$8.22^{+}_{-}0.62$

* From bulk density calculations

Figure 3.40. Fracture Surface of Mineral Ionomer Cements.

A. Untreated Willemite Cement showing a highly voided structure.
Magnification x 50.

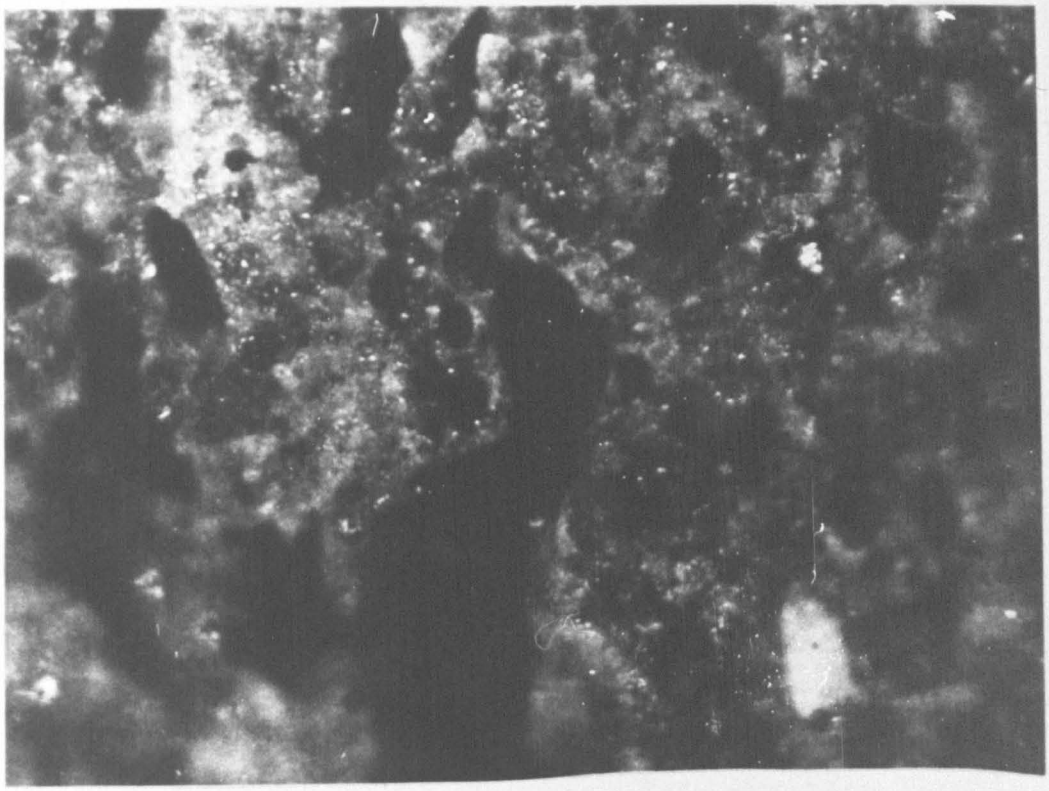

B. Treated Willemite Cement showing a lowly voided structure.
Magnification x 50.

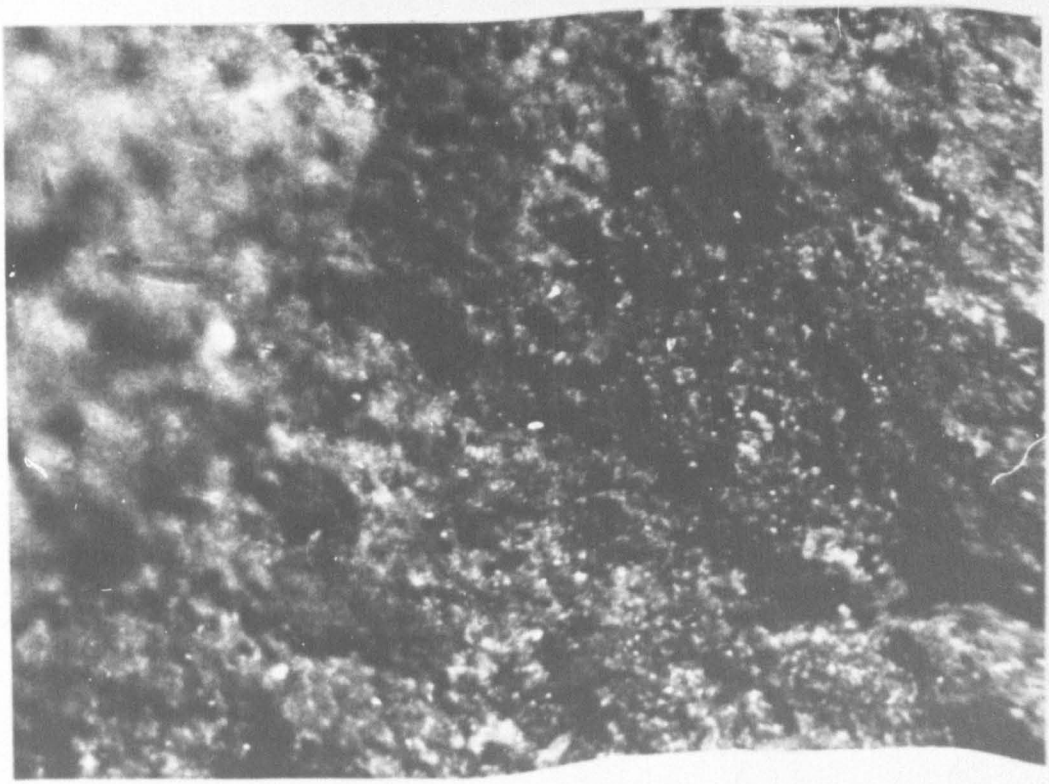

3.7 Novel Properties of Ionomer Cements: Mechanical Performance in Environments of High Humidity

The mechanical properties of conventional composite materials, such as glass/epoxy and glass/polyester composites, are known to be degraded by prolonged exposure in humid environments as described in Section 1.5.8. In contrast ionomer cements have been found to improve their mechanical performance on ageing in humid environments as shown in Figure 1.4. Consequently, ionomer cements offer potential advantage over convenitonal composites where retention of mechanical properties is required in humid conditions. To further examine this property of ionomer cements, composites were prepared of ASPA and ATG cements and of acid treated ASPA glass dispersed in matrix materials of polyester and epoxy resins. The acid treated glass was chosen in preference to the ASPA glass as the latter had a higher alkaline surface which is known to assist water absorption at the glass/polymer interface (148,149). These composites were stored for seven days at 66% R.H. and then hydrothermally aged by immersion in boiling water for 24 and 48 hours. This approach allowed direct comparison of the matrix properties and of the interfacial properties of the composites whilst excluding variables such as particle size, particle shape and volume fraction of the glass. This hydrothermal test has been used as an accelerated ageing test for composite materials with 24 hours immersion reckoned to be equivalent to 1 year's ageing in an aqueous environment. Although the nature of this test has been criticised (140), it correlates well to practical data collected for composites stored in humid environments at ambient temperatures (118).

The effects of hydrothermal ageing on the mechanical properties of the composites is shown in Figures 3.41 - 3.43. These results

Figure 3.41 Compressive Strengths of Composites with Hydrothermal Ageing

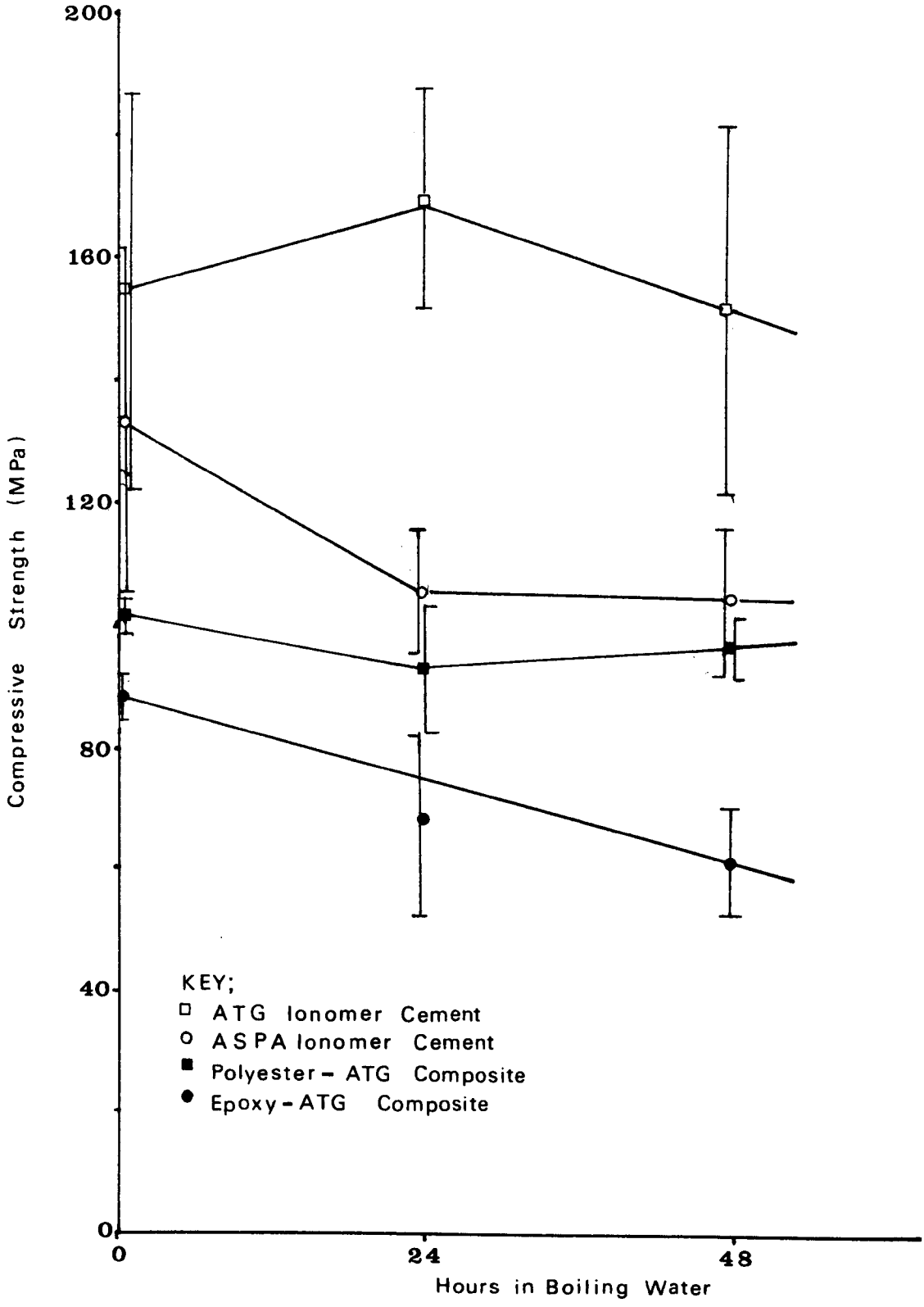

Figure 3.42 Compressive Moduli of Composites with Hydrothermal Ageing

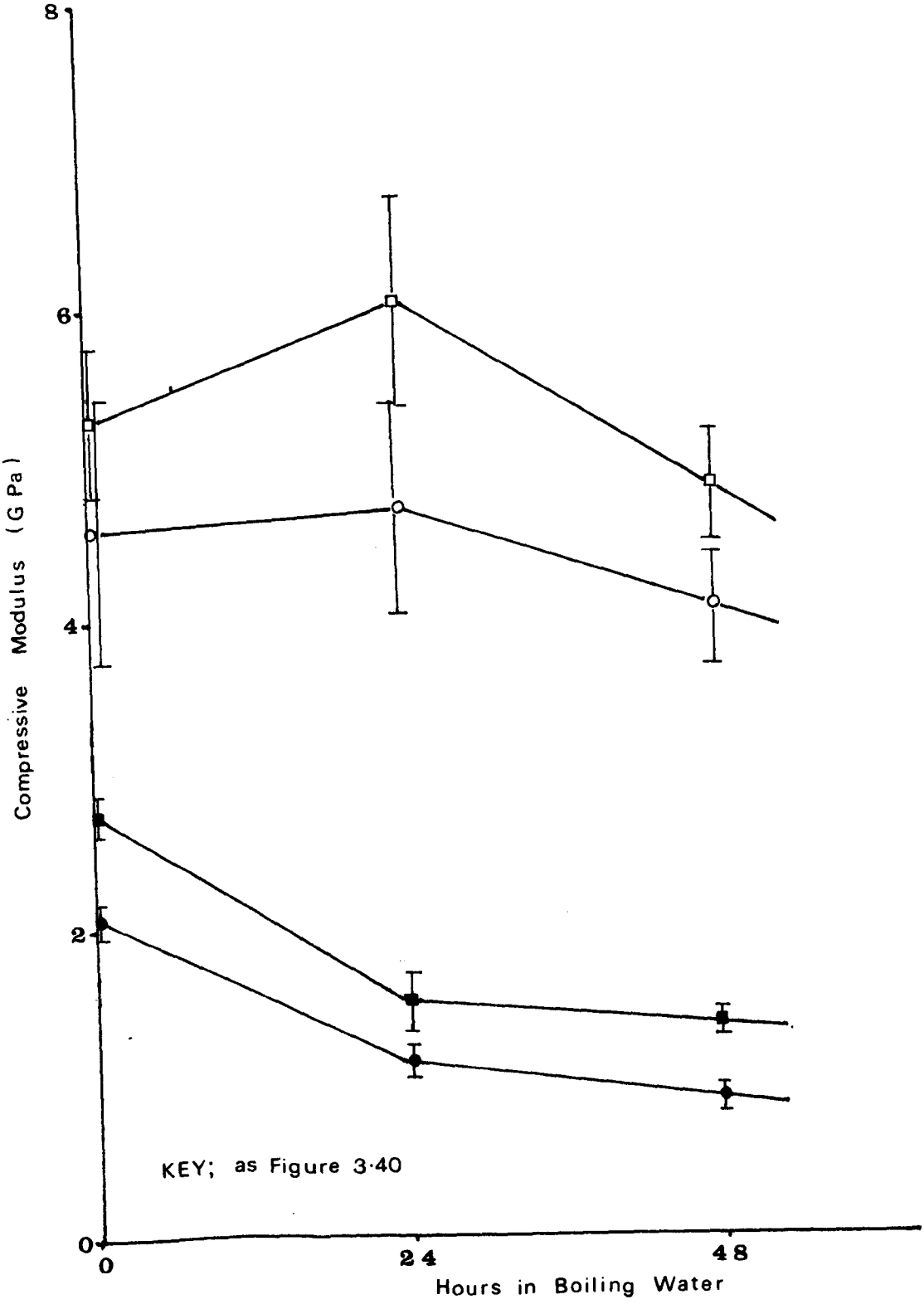

Figure 3.43 Strain at Fail Properties of Composites with Hydrothermal Ageing

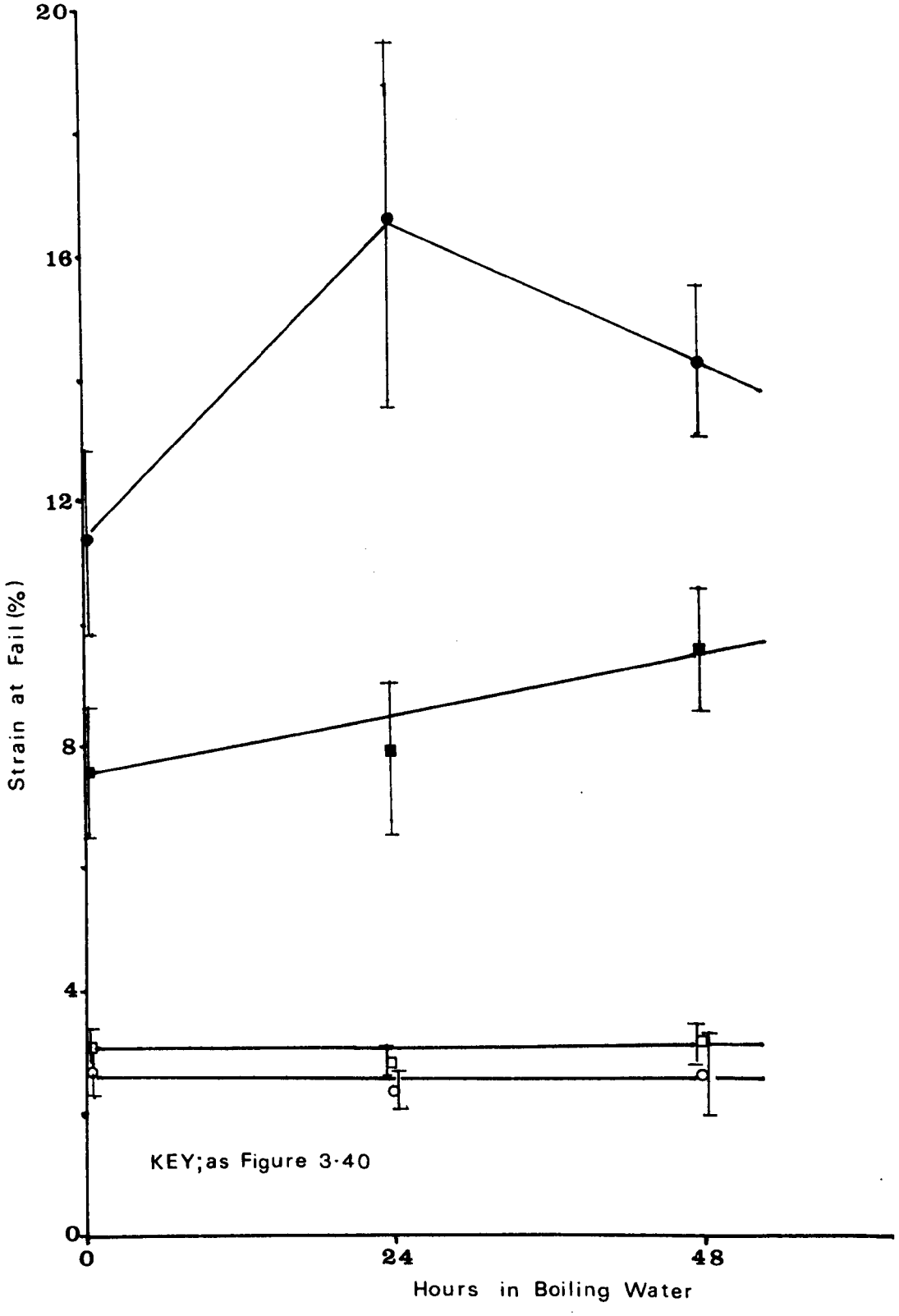

demonstrate that prior to hydrothermal ageing the ionomer cements were mechanically superior to the conventional epoxy and polyester composites. For example, the ATG cements had a compressive strength and modulus of 150 M Pa and 5.3 G Pa respectively, whilst the epoxy composite had a strength and modulus of 89 M Pa and 2.1 G Pa respectively. As both polyester and epoxy resins are known to have Young's Moduli of circa 4-5G Pa, which is higher than the modulus calculated for the unfilled metal polyacrylate matrix of the ionomer cements in Section 3.5.3. (circa 2.0 G Pa), then the superior mechanical performance of the ionomer cements can only be due to the differences in the interfacial adhesion between the glass particles and the matrix as will be discussed later.

The conventional composites were seriously degraded by hydrothermal ageing. Both the polyester and the epoxy composites lost over 50% of their initial stiffness within 48 hours of hydrothermal ageing (Figure 3.42). The polyester composite retained about 95% of its initial strength but the epoxy composite lost over 30% of its initial strength with hydrothermal ageing (Figure 3.41). It was also evident that the conventional matrix resins were plasticised by water as demonstrated by the progressive increase in strain at fail with hydrothermal ageing (Figure 3.43). In complete contrast the ionomer cements showed excellent retention of modulus and were not further plasticised by the water during ageing. The strength of the ASPA cements were degraded by about 10% with hydrothermal ageing but the strength of the ATG cements was found to increase on ageing. This difference between these two ionomer cements was attributed to the predominance of aluminium polyacrylate in the ATG cement. As discussed in Section 3.4, the aluminium ion has a higher electro-

negativity value on the Pauling scale (186) and thus forms stronger ionic bonds with the polyanions and co-ordinates water more firmly in its structure than the calcium polyacrylate which predominates in the ASPA cement. Also, spectroscopic studies by Wilson et al (1,38,39,189,190) indicated that the calcium polyacrylate bond is purely ionic whilst the aluminium polyacrylate bond may have some degree of covalency which would contribute to the bond's strength and its hydrolytic stability.

The loss of mechanical performance that occurs with conventional composites on hydrothermal ageing was attributed primarily to the absorption of water at the glass-matrix interface and to plasticisation of the matrix by water. This interfacial absorption of water is typical of conventional composites and is indicative of systems where only secondary bonding forces exist across the interface as such forces can readily be displaced by water (112,133). The use of silane coupling agents is known to improve the ageing properties of composites as shown in Figure 1.14 and this has been attributed to more polar bonding forces, such as hydrogen bonds, being formed at the coupling agent - glass interface. The loss of mechanical performance which occurs with hydrothermally aged silane treated composites suggests that these polar bonds are also displaceable by water. For example Nissan (192) has shown that hydrogen bonds can be dissociated by water which causes a loss of mechanical performance in hydrogen bond dominated solids such as cellulosic fibres. However, the formation of primary interfacial bonds would lead to more hydrolytically stable composites (112,120-122). It is proposed here that the superior mechanical properties of the ionomer cements prior to hydrothermal ageing and their good retention of mechanical properties upon ageing is due to primary interfacial bond formation as is discussed in detail in the next section.

The mechanical properties of the ionomer cements tended to increase with the first 24 hours immersion in boiling water and then decrease after 48 hours immersion. The increase in mechanical performance was attributed to increased crosslinking in the set cement, in particular crosslinking via aluminium ions at the glass particle surface. The decline in mechanical properties after 24 hours immersion was most probably due to hydrolysis of the metal polyacrylate bonds. However, with hydrothermal ageing of 48 hours the mechanical properties of the ionomer cements were similar to that of the unboiled cements. The hydrothermally aged ATG cement was found to be over 50% stronger and over 3 times stiffer than the hydrothermally aged polyester composite, which in turn was mechanically superior to the epoxy composite.

Conventional epoxy and polyester composites are known to be exothermic on cure which gives rise to residual stresses during cooling due to the differnces in thermal expansion between the filler and the resin as described in Section 1.5.8. Both residual and applied stresses are known to assist corrosion mechanisms such as hydrothermal ageing (112,143). In contrast, thermal analysis by differential scanning calorimetry under isothermal conditions at 50^{o}C, revealed that ionomer cements are thermally stable during cure and thus produce composites of low residual stress. This may be another factor which helps to account for the superior mechanical performance of the ionomer cements.

3.8 Interfacial Properties of Ionomer Cements

The work conducted in this thesis provides considerable evidence for the hypothesis that strong interfacial bonds are formed in certain ionomer cements. For example, the decline in mechanical performance and the introduction of hydrolytic instability upon the addition of fillers to ASPA cements, the modulus and strength enhancement with increasing volume fraction of glass in ionomer cements and the hydrothermal ageing properties of ionomer cements all provide indirect evidence of primary interfacial bond formation. The surface studies of acid treated ASPA glass (Section 3.2) provides more direct evidence for primary interfacial bond formation by demonstrating that some functional cations are not liberated from the glass under acid attack but remain embedded in the main structure of the glass and are thus capable of providing reactive sites for ionic interfacial bond formation. The surface studies also revealed that the acid attack of ASPA glass did not leave it completely sheathed by a siliceous gel as described in Section 1.2.4.

It is currently believed that the acid attack of ASPA glass that occurs during the setting of the cement depletes the glass surface of functional cations and leaves it completely sheathed in a siliceous hydrogel which also contains fluorite crystals. The idea of the hydrogel derives from dental technology by analogy with dental silicate cements (193,194) and is supported by evidence from X-ray microprobe analysis in conjunction with scanning electron microscopy, and from infra-red spectroscopy (1,37,38,42). However, results from the S.E.M. are difficult to interpret with ionomer cements due to the excessive loss of water from the polyacrylate matrix which occurs under the high vacuum conditions involved. This dehydration causes excessive

shrinkage of the matrix which in turn develops interfacial stresses leading to matrix-particle debonding, as is shown in the electron micrographs of Figure 3.8. This debonded region can give the appearance of an interfacial region depleted of functional cations at the surface during microprobe analysis. Infra-red spectroscopy is capable of detecting the formation of silica gel, which is bound to occur with such hydrated systems, but this technique can not be used to detect the location or the extent of coverage of the gel in the set cement. Also, the concept of the hydrogel completely sheathing the glass particle does not adequately explain the good mechanical properties of ionomer cements.

If the glass particles in a composite were completely sheathed by a hydrogel, then this hydrogel would act as a mechanically weak boundary layer between the glass particle and the crosslinked polyacrylate matrix to give poor interfacial adhesion. The strength of such a composite would be dependent upon the volume occupied by the matrix and its strength would decrease as the volume fraction of glass in the cement increased, as described by equation 1.5. Further, such systems would be prone to hydrolytic attack with water becoming absorbed by the hydrophilic siliceous gel causing a further weakening of the interfacial bond.

Clearly, revision of the interfacial bonding mechanisms of ionomer cements is required to more fully explain their mechanical behaviour. It is proposed here that primary ionic bonds or possibly hydrogen bonds are formed across the interface, as shown in Figure 3.44, and that these bonding mechanisms make a (very) significant contribution to the mechanical properties of the composite especially in humid or wet environments. The setting mechanism of ionomer cements where primary interfacial bonding occurs is shown schematically in Figure 3.45.

For clarity, it is assumed that the aluminium ions are an integral part of the glass surface and that the calcium ions exist in a dispersed phase at the glass surface and are readily leached by acid attack. In practice, as suggested by the surface studies (Section 3.2) and by previous work (1), a small proportion of the calcium ions would be retained in the glass and some of the aluminium ions would be liberated during acid attack. It is also assumed for clarity that the liberated calcium ions crosslink the matrix but other salt formations are possible as shown in Figure 1.2. This setting mechanism shows that the aluminium ions at the glass surface are capable of ionic interfacial bond formation with the polyacid. It is this bonding mechanism which gives ionomer cements their good mechanical properties in aqueous environments. The setting mechanism also shows that ATG cements have greater potential for ionic interfacial bond formation than ASPA cements as the ATG glass was found to have a greater proportion of aluminium ions on its surface than the ASPA glass (See Section 3.2). This greater extent of interfacial bonding with the ATG cement produced composites which were mechanically superior and more stable during hydrothermal ageing than the ASPA cements, which adds further support to this hypothesis.

Figure 3.44 Possible Interfacial Bonding Mechanisms in Ionomer Cements

PRIMARY INTERFACIAL BONDING MECHANISM

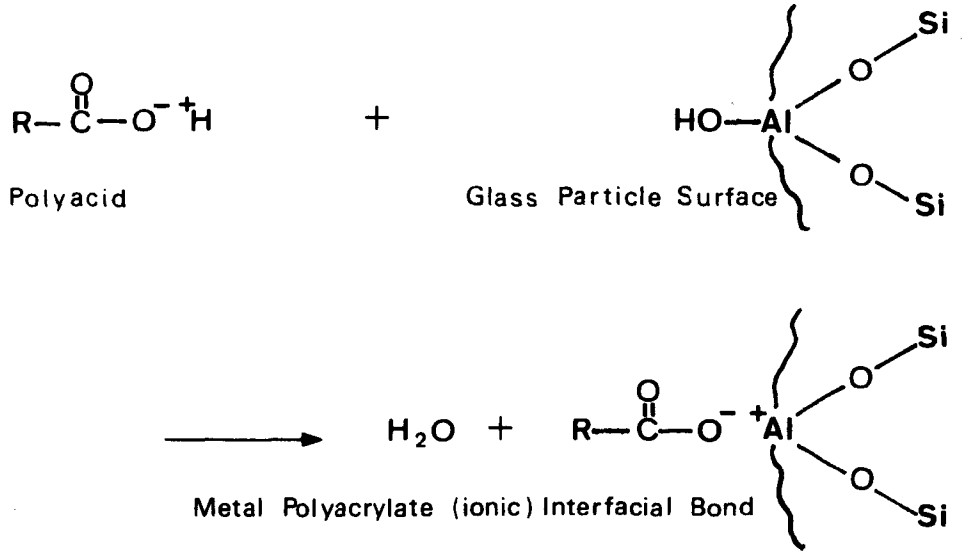

HYDROGEN BONDING MECHANISM

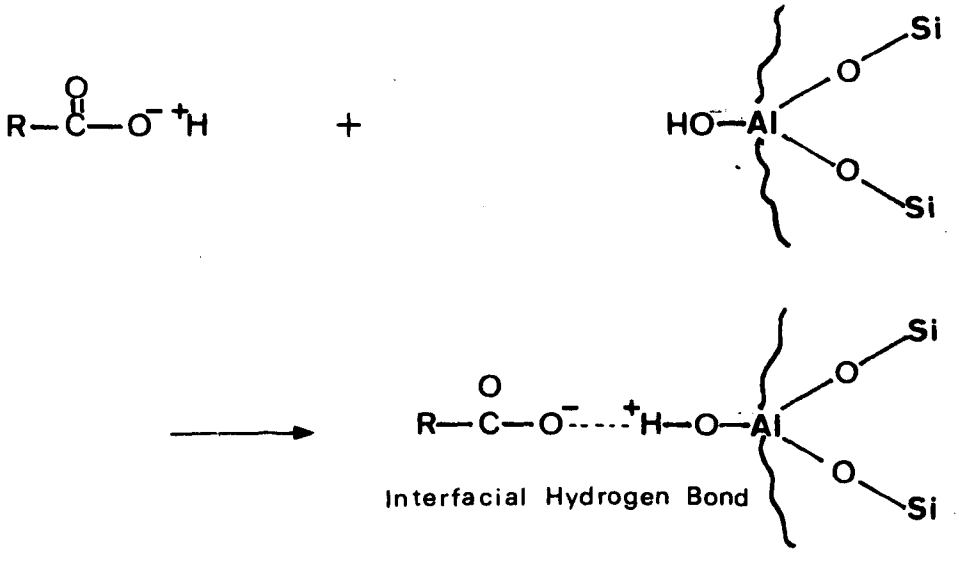

Figure 3.45 Proposed Mechanism for the Setting of Ionomer Cements.

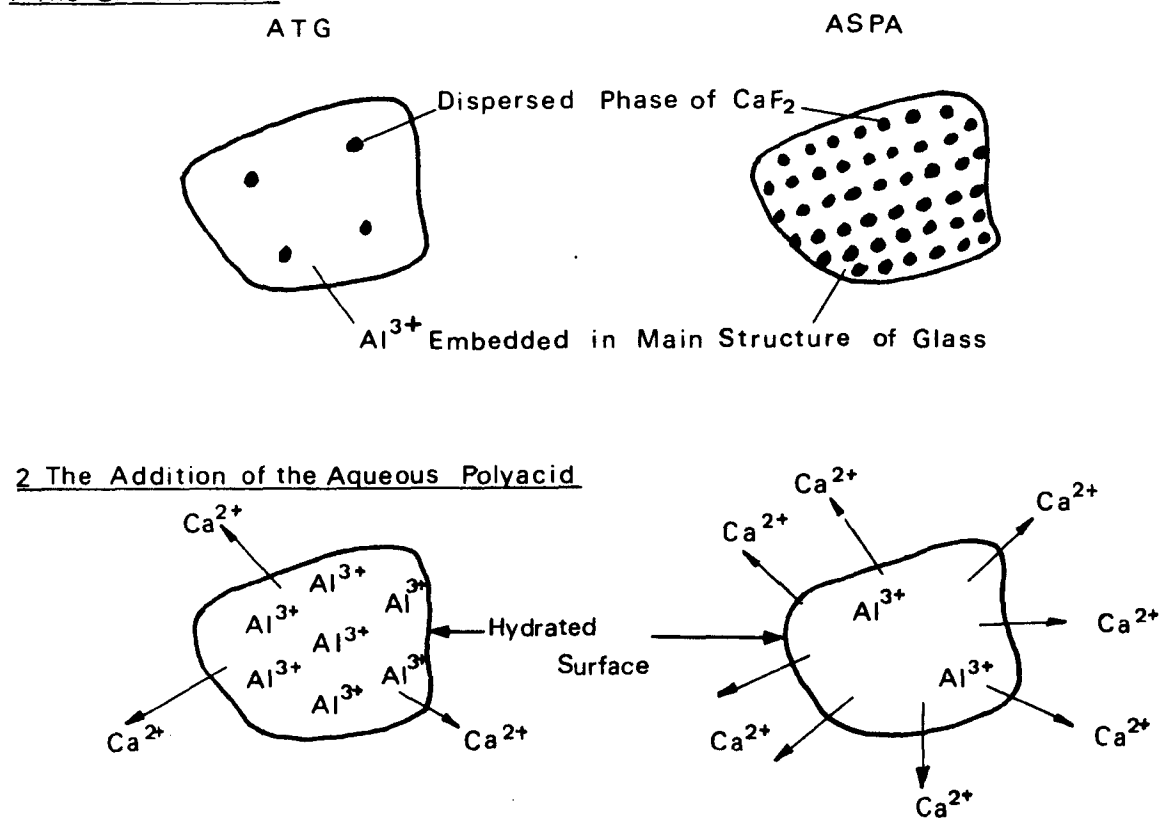

3.9 Suggestions For Further Work

1. The work presented in this thesis has demonstrated that the setting rates of ASPA cements can be controlled by modifying the glass and by the addition of fillers. However, these approaches are dependent upon the use of the expensive ASPA glass and alternative lower cost glasses would be advantageous. Although a number of glass formulations have been examined here, a more thorough investigation is required to develop aluminosilicate glasses and zinc based glasses suitable for large scale ionomer cement applications. The zinc based glasses are of particular interest as their melting temperature is lower than that of aluminosilicate glasses and their melt viscosity is suitable for fibre formation. The use of fibre reinforced ionomer cements could produce stiff composites which are more resistant to ageing in humid environments than conventionally used glass fibre composites.

2. Certain treated minerals and some metal oxides showed potential as particulate replacements to ASPA glass. However, ionomer cements prepared from these materials displayed greater porosity and inferior mechanical performance than the ASPA cements. Consequently a systematic study of void content and the development of methods for controlling voiding in these cements would be invaluable for increasing their potential as low cost particulate ionomer cement systems.

3. The superior performance of the ATG cements when stored in environments of low humidity has led to the proposal that aluminium ions co-ordinate water more strongly than calcium ions and that aluminium polyacrylate is more stable than calcium polyacrylate. This propsal needs investigation and a further understanding of the hydration of metallic ions is required.

4. The surface studies of ASPA and ATG glasses in conjunction with the mechanical and hydrothermal ageing properties of cements prepared from these glasses, strongly suggest that primary bonds are formed at the glass particle-polymer interface. However, more direct evidence is required to confirm this proposal.

5. The reduced reactivity of the filled ASPA systems and the ATG system has enabled larger mouldings to be fabricated than was hitherto possible with the unfilled ASPA cement. Consequently, there is need for further testing of these materials with, for example, measurement of their viscoelastic properties and their electrical properties which would be of interest as these topics have not been extensively studied.

6. The potential of other types of filler in filled ionomer cements should be considered and techniques devised for using oriented fibres as fillers as this would enhance the moduli of such composites. Also, the use of silane coupling agents which have compatibility with aqueous poly(acrylic acid) would be advantageous.

4. CONCLUSIONS

1. Ionomer cements have a variable mechanical performance which is influenced by the size and microstructure of the glass particle and by other factors such as the volume fraction of glass in the cement and the humidity of the storage environment.

2. The high reactivity of the ASPA system was reduced by acid treatment of the ASPA glass. This treatment was found to alter the microstructure and the surface chemical composition of the glass particle, in particular the number of calcium ions at the surface was reduced and the number of aluminium cations increased. Cements prepared from the acid treated glass were more workable and slower setting than ASPA cements due to reduced calcium polyacrylate formation but were mechanically superior to ASPA cements due to the enhanced formation of aluminium polyacrylate.

3. The high reactivity of the ASPA system was reduced by partial replacement of the ASPA glass with various fillers. The mechanical properties of filled ASPA cements were dependent upon the phsyical properties of the filler and in particular the size and the shape of the particle. In certain cases fillers could be used to replace 75% by volume of the ASPA glass without loss of mechanical performance in the set cement. The filled ASPA cements were hydrolytically less stable than the unfilled cements although stability was improved by the use of fillers which reacted with the polyacid matrix.

4. The reactivity of ATG cements was further reduced by partial replacement of the acid treated glass with fillers. The mechanical and

hydrolytic properties of filled ATG cements were also dependent upon the physical characteristics of the filler in a similar manner to the ASPA cements.

5. The mechanical properties of ASPA and filled ASPA cements were degraded in environments of low humidity but the ATG cements retained their mechanical properties in such environments. The mechanical properties of ionomer cements in arid environments was found to be dependent upon the cements' ability to retain water and on its relationship between weight loss and shrinkage. The superior mechanical performance of the ATG cements at low humidities was attributed to the enhanced aluminium polyacrylate formation in this cement and its ability to coordinate and retain water.

6. The mechanical properties of ionomer cements are dependent upon the size of the glass particle, the volume fraction of the dispersed phase and the extent of interfacial adhesion between the glass and the polyacrylate matrix.

7. Ionomer cements have a superior mechanical performance and are more resistent to hydrothermal ageing than similar composites prepared with polyester and epoxy resins. This superior mechanical performance was attributed to the formation of stronger and more permanent interfacial bonds in the ionomer cement.

8. The currently held theories regarding the interfacial properties of ionomer cements are inadquate in describing their hydrolytic and mechanical properties. A more plausible explanation was proposed by suggesting that ionomer cements, and in particular the ATG cement, form ionic bonds between the glass particle surface and the polyacid.

This proposal was supported by evidence from ESCA surface studies.

REFERENCES

1. A.D. Wilson; S. Crisp. Chpt.4 in Organolithic Macromolecular Materials, Applied Science, 1977

2. L. Holliday; Chapter 1, Composite Materials (Ed Holliday), Elsevier 1966

3. L. Holliday; Chapter 1. Ionic Polymers (Ed Holliday), Applied Science, 1975

4. A.L. Reader; PhD Thesis, Brunel University, 1974.

5. R.H. Kinsey; Ionomers, Chemistry and Development App. Polym. Symp. 11, 77, 1969.

6. J.M.C. Cowie; Polymers, Chemistry and Physics of Modern Materials, p.100 Intertext, 1973.

7. J.H. Elliot, P.R. Hornsby, A.D. Wilson, S. Crisp & S. Mason; J. Mat. Sci. 14, 2941, 1979.

8. J.H. Elliot, P.R. Hornsby, A.D. Wilson, P.S. Crisp; J.App. Chem. Biotechnol, 27, 369, 1977.

9. A. Eisenberg; Macromolecules, 6, 125, 1973.

10. A. Eisenberg, H. Matsuura, P.T. Yokoyama; J. Poly. Sci. A2, 9, 2131. 1971.

11. A. Eisenberg, M. King, M. Navratil; Macromolecules 6, 734, 1973..

12. A. Eisenberg, & M. Navratil; Macromolecules 6, 604, 1973.

13. A. Eisenberg, & H. Matsuura; J. Poly. Sci., Poly Phys.Ed. 14, 1201, 1976.

14. A. Eisenberg, & E.Shomamy; J. Poly. Sci. Poly Phys. Ed. 14, 1211, 1976.

15. A. Eisenberg, H. Matsuura & T. Tsutsui; J. Poly. Sci. Poly Phys. Ed. 18, 479, 1980.

16. L.E. Neilsen & W.E. Fitzgerald; Proc. Royal Soc. 282A, 137,1964.

17. L.E. Neilsen & J.E. Fields; J. App. Poly. Sci. 12, 1041, 1968.

18. L.E. Neilsen; Poly & Eng. Sci. 9, 356, 1969.

19. H. Place; Engineering Thermoplastics Supplement in Plast. & Rubber Week. p.24, May 31, 1980.

20. A.D. Wilson & B.E. Kent; J. App. Chem. Biotechnol 21, 313, 1971.

21. A.D. Wilson & B.E. Kent; Brit. Pat. 1316129, 1969.

22. A.D. Wilson & S. Crisp; Brit. Pat. 1422337, 1972.

23. K.A. Hodd & A.L. Reader; Brit. Pat. 1495255, 1973.

24. J.I. Hall; Brit. Pat. 1492038, 1977.

25. W.D. Potter, A. Conway, R. Dunning & R.J. Parry, U.S. Pat. 4,043,327, 1977,

26. A.D. Wilson & B.E. Kent; Brit. Dent. J. 132, 133, 1972.

27. A.D. Wilson & B.E. Kent; Brit. Dent. J. 135, 322, 1973.

28. D.C. Smith; J. Canad. Dent. Assoc. 37, 22, 1971.

29. D.C. Smith; Brit. Dent. J. 125, 381,1968.

30 A.D. Wilson; Brit. Poly. J. 6, 165, 1974.

31. A.D. Wilson; Aspects of Adhesion 8,p.285, Transcripta Books, 1974.

32. Anon; Chem. in Brit. 16, 11, 576. 1980.

33. B. Roos; Dentist - Private communications.

34. A. Grant; Brit. Poly. J. 10, 241, 1978.

35. S. Crisp, B.E. Kent, B.G. Lewis, A.J. Førner & A.D. Wilson; J. Dent. Res. 59, 1055, 1980.

36. S. Crisp, B.G. Lewis & A.D. Wilson; J. Dent. Res. 54, 1173, 1975.

37. T.I. Barry, P.R. Miller & A.D. Wilson; Conf. on the Silicate Industry p.881, 1973.

38. S. Crisp, H.J. Prosser & A.D. Wilson; J. Mat. Sci. 11, 36, 1976.

39. A.D. Wilson & S. Crisp; Br. Poly J. 7, 279, 1975.

40. G.M. Brauer; Poly-Plast. Technol. Eng. 9, 87, 1977.

41. J.M. Paddon & A.D. Wilson; J. Dent. 4, 183, 1976.

42. T.I. Barry, D.J. Clinton, A.D. Wilson; J. Dent. Res. 58,1072,1978.

43. B.E. Kent, B.G. Lewis & A.D. Wilson; J. Dent. Res. 58,1607, 1979.

44. S. Crisp, B.G. Lewis, S.A. Merson, H.J. Prosser & A.D. Wilson; Ind. Eng. Chem. Prod. Res. Dev; 19,(2),265, 1980.

45. J.H. Elliot, L. Holliday, P.R. Hornsby; Br. Poly. J. 7,297, 1975.

46. L. Holliday; The Mechanical Properties of the Metal Polyacrylate Internal Publication, Brunel University 1974.

47. R.P. Hopkins; Ind. Eng. Chem. 47, 2258, 1955.

48. A. Ikegami; Biopolymers 6, 431, 1968.

49. P.R. Hornsby; PhD Thesis, Brunel University, 1977.

50. K.A. Hodd & A.L. Reader; Brit. Poly. J. 8, 131, 1976.

51. H. Irving & R.J.P. Williams; J. Chem. Soc. 3192, 1953.

52. A.D. International, Private Communications 1981,

53. A. Eisenberg, M. Farb & L.G. Cool; J. Poly. Sci. A2, 4, 855, 1966.

54. A. Eisenberg; Pure & App. Chem. 46, 171, 1976.

55. D. Price; Project Report, B. Technol, Brunel University.1975.

56. S. Yamini; M. Phil. Thesis, Brunel University, 1976.

57. L.A. Killick; Project Report, B. Technol, Brunel University,1975.

58. J. Carrillo; M. Phil. Thesis, Brunel University, 1978.

59. K.H. Jackson; Project Report, B. Technol, Brunel University,1975.

60. De Trey Chemfil Product Data Sheet, A.D. International,1981.

61. H.A. Lancey, J. Mann & G. Pogany; Chapter 3 in Composite Materials (Ed Holliday) Elsevier 1966.

62. M. Pineri, R. Duplessix, S. Gauthier & A. Eisenberg; Chpt. 18 in Ions in Polymers (Ed. A. Eisenberg). Adv. in Chem. 187, Am. Chem. Soc., 1980.

63. W.D. Biggs, Chpt. 2 in Composite Materials (Ed. L Holliday), Elsevier 1966.

64. L.E. Neilsen; Mechanical Properties of Polymer & Composites, Dekker 1974.

65. L.E. Neilsen; J. Comp. Mat. 1, 100,1967.

66. L.E. Neilsen; J. App. Poly. Sci. 10, 97,1965.

67. S. Sahu & L.J. Broutman; Poly. Eng. Sci. 12,91, 1972.

68. R.B. Seymour; Poly. Plast. Technol. Eng. 7, 49,1976.

69. D.K. Hale; J. Mat. Sci. 11, 2105, 1976.

70. R.M. Christensen; Mechanics of Composite Materials, Wiley & Sons, 1979.

71. G.W. Brassell & K.B. Wischmann; J. Mat. Sci. 9, 307, 1976.

72. J.C. Halpin & J.L. Kardos; Poly. Eng. Sci. 16, 344,1976.

73. L. Nicolais; Poly. Eng. Sci. 16, 344, 1976.

74. T.S. Chow; J. Mat. Sci. 15, 1873, 1980.

75. T.G. Richard; J. Comp. Mat. 9, 108, 1975.

76. L.E. Neilsen; J. Comp. Mat. 2, 120, 1968.

77. L.E. Neilsen; J. App. Phys. 41, 4627,1970.

78. Y. Sato & J. Furukawa; Rubb. Chem. Technol. 36, 1081, 1963.

79. O. Ishai & L.J. Cohen; J. Comp. Mat. 1, 390, 1967.

80. O. Ishai & L.J. Cohen; J. Comp. Mat. 2, 302, 1968.

81. H.L. Price & J.B. Nelson; J. Comp. Mat. 10, 314, 1976.

82. H. Alter; J. App. Poly. Sci. 9, 1525, 1965.

83. G. Landon, G. Lewis, G.F. Boden; J. Mat. Sci. 12, 1605, 1977.

84. L. Nicolais & M. Narkis; Poly. Eng. Sci. 11, 194, 1971..

85. L. Nicolais, E. Drioli & R.F. Landel; Polymer. 14, 21, 1973.

86. L. Nicolais; Poly. Eng. Sci. 15, 137, 1975..

87. L. Nicolais, G. Guerra, C. Migliaresi, L. Nicodemo & A.T. Di Benedetto; Composites 12, 33, 1981..

88. L. Nicolais, & L. Nicodemo; Poly.Eng. Sci. 13, 469, 1973.

89. W.M. Speri & C.F. Jenkins; Poly. Eng. Sci. 13, 409, 1973.

90. O. Ishai & S.R. Bodner; Trans. Soc. Rheol. 14, 253, 1970.

91. F.F. Lange & K.C. Radford; J. Mat. Sci. 6, 1197, 1971.

92. J. Leidner & R.T. Woodhams; J. App. Poly. Sci. 18,1639,1974.

93. J. Leidner & M.R. Piggott; J. App. Poly. Sci. 18, 1619, 1974.

94. B.B. Boonstra & A.I. Medalia; Rub. Chem. Technol 36, 115, 1963.

95. P.I.A. Martin; Brit. Plast. 35, 95, 1965.

96. A.W. McKee; S.P.E. 18, 186, 1962.

97. F.W. Maine & P.D. Shepherd; Composites 5, 189, 1974.

98. J.D. Birchall, H.A. James & K. Kendall; Euro Pat. O 021 682A1,1980.

99. K.H. Sweeney & R.D. Geckler; J. App. Phys. 25, 1135, 1954.

100. R.J. Ferris; Trans. Soc. Rheol. 12, 281, 1968.

101 J.G. Brodnyan; Trans. Soc. Rheol. 12,357, 1968.

102. J.V. Sanders; Phil-Mag. A. 42, 705, 1980.

103. A.N. Patankar & G. Mandal; Trans. Jol. Brit. Ceram. Soc. 79, 59, 1980.

104. R.K. McGeary; J. Am. Ceram. Soc. 44, 513, 1961.

105. J.V. Milewski; Poly, Plast. Technol. Eng. 3, 101, 1974.

106. A.K. Malik & A. Ghosh; J. Comp. Mat. 8, 207, 1974.

107. G.W. Brassell, B.L. Butler & J.A. Hovak; J. Comp. Mat. 9, 288, 1975.

108. J.P. Gittrow; Composites. 2, 228, 1971.

109. M. Relis & I. Soroka; J. Am. Ceram. Soc. 63, 690, 1980.

110. C. Chamis; Chpt. 2 in Composite Materials 6, (Ed. E.P. Pluddemann), Academic Press, 1974.

111. W.C. Wake: Adhesion & the Formulation of Adhesives. Applied Science, 1976.

112. W.C. Wake; Chpt. 1 in Fillers for Plastics. The Plastics Institute, Iliffe Books, 1971.

113. G. Navascues & M.V. Berry; Chpt. 3 in Wetting Spreading & Adhesion (Ed. J.F. Padday), Academic Press, 1973.

114. N.K. Adam; The Physics & Chemistry of Surfaces. Clarendon Press, 1938.

115. W.A. Zissman; Constitutional Effects on Adhesion & Abhesion, in Adhesion & Cohesion (Ed. P. Weiss) Elsavier 1962.

116. F.M. Fowkes; Chpt. 9 in Treatise on Adhesion & Adhesives (Ed. R.L. Patric) E. Arnold, 1967.

117. O.K. Johannson, F.O. Stark, G.E. Vogel, R.M. Lacefield, R.M. Baney and D.L. Flaningham; Interfaces in Composites, p.168, ASTM STP452, 1969.

118. D.A. Scola; Chpt. 7 in Composite Materials 6, (as 110).

119. E.P. Plueddemann, M.A. Clark, L.E. Nelson & I.R. Hoffman; Mod. Plast. 39, 139, 1962.

120. E.P. Plueddemann; Chpt. 6 in Composite Materials 6, (as 110)

121. E.P. Plueddemann; Review paper given at Interfaces in Composites, P.R.I. Conference 1981.

122. O.K. Johannson, F.O. Stark, G.E. Vogel & R.M. Fleischmann; J. Comp. Mat 1 278, 1967.

123. M.W. Ranney, S.E. Berger & J.G. Marsden; Chpt. 5 in Composite Materials 6, (as 110).

124. M.O. Richardson; Chpt. 1 In Engineering Polymer Composites. (Ed. M.O. Richardson), Applied Science, 1977.

125. M.W. Pascoe; Chpt. 9, (as 124).

126. J.W. Williams; Chpt. 8, (as 124).

127. A.G.H. Dietz; p.49 in Mechanics of Composite Materials (Ed. F.W. Wendt et al), Permanon Press 1970.

128. S.R. Heller; p.69, (as 127).

129. H.S. Schwartz; p.113, (as 127).

130. L.N. Phillips; in Polymer Science 2 p. 1717, (Ed. A.D. Jenkins), North Holland, 1972.

131. K.A. Scott & K.T. Paul; Composites 5, 201, 1974.

132. H.T. Hahn; J. Comp. Mat. 10, 266, 1976.

133. W.D. Babscome; Chpt. 3 in Composite Materials 6, (as 110).

134. D.J. Vaughn & E.L. McPherson; Composites 4, 131, 1973.

135. G. Pritchard & N. Taneja; Composites 4, 199, 1973.

136. C.Y. Lundemo & S.E. Thor; J. Comp. Mat. 11, 276, 1977.

137. C.H. Shen & G.S. Springer; J. Comp. Mat. 11, 2, 1977.

138. W.C. Wake; Aspects of Adhesion, 7, 232, Transcripta Books, 1973.

139. S.W. Tsai; p.749, (as 127).

140. N. Fried; p.813, (as 127).

141. S. Belant and I. Petker; p.799, (as 127).

142. G. Gourdin; in Advances in Composite Materials, I.C.C.M. 3 1, 497, (Ed. A.R. Bunsell, et al), Pergamon Press, 1980.

143. J.E. Bailey, T.M.W. Fryer & F.R. Jones; p.514, (as 142).

144. J. Avestor, A. Kelly & J.M. Sillwood; p.556, (as 142).

145. B. Dewimille, J. Thoris, R. Mailfert & A.R. Bunsell, p.597, (as 142).

146. R.K. Jain & K.K. Asthana; p.613, (as 142).

147. R.H. Norman; Aspects of Adhesion 8, p.267, Transcription Books, 1974.

148. D.G. Metts; Chpt. 7 in Glass Fibre Handbook, S.P.E., Van Nostrand Reinhold, 1969.

149. W.J. Eakins; in Interfaces in Composites, ASTM 452, 137, 1969.

150. J.C. Goan & S.P. Prosen p.3, (as 149).

151. G.S. Springer; J. Comp. Mat. 11, 107, 1977.

152. C.H. Shen & G.S. Springer; J. Comp. Mat 11 250, 1977.

153. A.C. Loos & G.S. Springer; J. Comp. Mat 13 131, 1979.

154. J. Comyn, D.M. Brewis, R.J.A. Shalashi & J.L. Tegg; Adhesion 3, 13, Applied Science 1978.

155. D.C. Phillips; in Polymer Science 2, 1717, as 124.

156. M.J. Whitford; Private Communication, Brunel University 1980.

157. Versicol S. Technical & Processing Data. Allied Colloids.

158. Fine Silicas & Silicates; Crossfield Silicas, 1977.

159. Gasil Range and Applications; ibid. 1974.

160. Gasil Matting Agents for Surface Coatings; ibid, 1974.

161. Matting agents for Radiation Cured Systems; ibid. 1979.

162. Microsil Silicas in Rubber Formulations; ibid, 1978.

163. Powder Coatings with Silicas; ibid, 1978.

164. Ballotini Glass Microspheres; Plastichem Technical Bulletin 1978.

165. Garosil Range of Silicas-Data Sheets; Plastichem Limited. 1972.

166. The Agrément Board Certificate 75/283.

167. Dr. G. Bye; Private Communications; Blue Circle Technical Limited.

168. Ethylan N Range, Lankro Surfactants; Lankro Chemicals Limited.

169. Monflor 31. Product Data Sheet; I.C.I. Limited

170. Monflor 51. Product Data Sheet; I.C.I. Limited

171. Dr. R. Bidulph; Private Communications; R.T.Z. Borax Holdings Limited.

172. Araldite Resins, Product Data Sheets; Ciba Geigy Limited.

173. Strand Glass, Glass Fibre Materials Handbook; Strand Glass Co. Ltd.

174. R.C. West (Ed); Handbook of Chemistry and Physics. C.R.C. Press (56th Ed), 1975.

175. Wallace Shawbury Curometer Handbook; Wallace Shawbury Limited, 1979.

176. British Standard Specification for Dental Silicate Cements and Dental Silicophosphate Cements. Part 2. B.S. 3365 (1971).

177. A.D. Wilson; J. Dent. Res. 55, 1, 142, 1976.

178. Instruction Manual for Coulter Counter Model D (Industrial); Coulter Electronics Limited, 1975.

179. B.G. Fookes; Private Communications. Experimental Techniques Centre, Brunel University.

180. K. Siegbahn et al; Chapter 6 in X-Ray Photoelectron Spectroscopy (Ed. T.A. Carlson), Dowder, Hutchinson & Ross, 1978.

181. G.C. Ives, J.A. Mead & M.M. Riley; Handbook of Plastics Test Methods, Illife Book, 1971.

182. R.M. Tennent (Ed); Science Data Handbook, Oliver and Boyd 1976.

183. D.E. Packham; J. App. Poly. Sci. 18, 2237, 1974.

184. M. McEvoy; Surface Chemical Studies Silicas. Ph.D. Thesis, CNNA, 1980.

185. S.E. Maskery; Private Communications. Crossfield Silicas.

186. F.A. Cotton and G. Wilkinson. Advanced Inorganic Chemistry. Interscience 1972.

187. P.R. Hornsby; J.Chem.Tech. Biotechnol. 30, 595, 1980.

188. S.C. Shea; Polymer. 17, 836, 1976.

189. A.D. Wilson, S. Crisp, J. Dent, Res. 53, 1408, 1974.

190. A.D. Wilson, S. Crisp, J. Dent, Res. 53, 1420, 1974.

191. W. Black; Chapter 6 in Dispersion of Powders in Liquids (Ed. G.D. Parfitt), Elsevier, 1969.

192. A.H. Nissan; Macromolecules, 9, 840, 1976.

193. A.D. Wilson, B.E. Kent, R.F. Batchelor, B.G. Scott & B.G. Lewis; J. Dent. Res, 49, 307, 1970.

194. A.D. Wilson, B.E. Kent, D. Clinton & R.P. Miller; J. Mat. Sci. 7, 220, 1972.

APPENDIX 1

Equations Describing the Modulus of Particulate Composites

The nomenclature used in these equations are the same as that given in table 1.8 of the text, as follows:

Symbols

ϕ = Volume fraction

M = Generalised modulus term

Mr = Relative modulus = $\frac{M_c}{M_1}$

G = Shear modulus

E = Elastic modulus

K = Bulk modulus

ν = Poisson's ratio

η = Viscosity

σ = Tensile strength

σ_y = Tensile yield strength

ε = Strain

ε_f = Strain at fail

ϕ_{max} = Volumetric packing fraction = $\frac{\text{true volume}}{\text{apparent volume}}$

a = Aspect ratio = $^{l}/_{d}$

d = Particle diameter

l = Particle length

Other symbols are defined in the text.

Suffixes

c = Property of the composite

1 = Property of the matrix

2 = Property of the filler

v = Property of a void phase

The Hydrodynamic Einstein Equation (64,65)

$$\eta/\eta_1 = G/G_1 = (1 + K_E \phi_2)$$

Where K_E = the Einstein coefficient which has a value of 2.5 for spheres and is increased as the aspect ratio of the filler increases and as the extent of agglomeration increases.

This equation has several limitations, it is only valid for dilute solutions, is based on the assumption that the relative viscosity is equal to the relative shear modulus and is only applicable where the Poissons ratio of the composite is 0.5. This equation takes no account of the particle size, the extent of interfacial adhesion or the effects of voids.

The Hydrodynamic Mooney Equation (64,65)

$$\text{In } (G/G_1) = \frac{K_E \phi}{1 - \phi_2/\phi_{max}}$$

Comment:

Similar to the Einstein equation but considers the effects of particle agglomeration by considering the volumatic packing fraction (ϕ_{max}).

The Hydrodynamic Guth-Gold Equation (69,74,77)

$$G/G_1 = (1 + 0.67\, a\, \phi_2 + 1.62\, a^2\, \phi^2_2)$$

Comment:

Similar to Einstein equation but also considers the effects of particle aspect ratio (a).

The Kerner Equation (64,65,75,74)

$$K = \frac{\frac{K_1 \phi_1}{3K_1 + 4G_1} + \frac{K_2 \phi_2}{3K_2 + 4G_1}}{\frac{\phi_1}{3K_1 + 4G_1} + \frac{\phi_2}{3K_2 + 4G_1}}$$

Other modulus properties can be determined by applying the relationship between moduli;

$$E = 2G\ (1 + \nu) = 3K\ (1 - 2\nu)$$

This relationship simplifies where the modulus of the filler is much greater than that of the matrix to:

$$\frac{G}{G_1} = 1 + \frac{\phi_2}{\phi_1} \left\{ \frac{15\ (1-\nu_1)}{8 - 10\nu_1} \right\}$$

These equations are based on the relationships between the mechanical properties of the composites components. The Kerner equation predicts behaviour well for spherical inclusions in a polymer matrix but it takes no account of particle size, particle shape or the extent of interfacial adhesion.

The Halpin-Tsai Equation (72,74,77)

$$\frac{E}{E_1} = \frac{1 + 2\ Ca\ \phi_2}{1 - 2a\ \phi_2}$$

where $C = \left[\frac{E_2}{E_1} - 1\right] \left[\frac{E_2}{E_1} + 2a\right]$

Comments:

Similar to the Kerner equation in predictive value and takes account of particle shape.

The Sato-Furukawa Equation (65,78)

$$\frac{E}{E_1} = 1 + \frac{y^2}{2(1-y)}(1 - \tau\,\delta) + \frac{K_y^3\,(1 - 0.5_y)(1 - \tau\,\delta)}{(1-y)^2} + \frac{y^2}{(1-y)}\,\frac{\tau\,\delta}{y^3}$$

i.e.

$$\frac{E}{E_1} = \text{Volume Effect} + \text{Surface Effect} + \text{Cavitational Effect.}$$

Where:- $\tau = \dfrac{y^3\,(1 + y - y^2)}{3\,(1 - y + y^2)}$

$y^3 = \phi_2$

δ = An adhesion factor; 0 = perfect interfacial adhesion

1 = poor interfacial adhesion.

Comment:

This relationship is based on the concept of internal deformation for materials displaying rubber elasticity. It is a useful equation as it considers the effects of interfacial adhesion, where interfacial adhesion is poor the matrix dewetts from the filler which gives rise to an ellipsoidal shaped cavity in material. This equation is best applied to rubbers reinforced with spherical particles, it does not account for particle shape or for particle size.

The Neilsen Equation (64,77)

$$\frac{M}{M_1} = \frac{1 + A\,B\,\phi_2}{1 - B\,\Psi\,\phi_2}$$

Where:

A = A constant to account for factors such as particle geometry and the Poisson's ratio of the matrix.

$A = K_E - 1$

B = A constant which accounts for the relative moduli of the filler and the matrix

$$B = \frac{M_2/M_1 - 1}{M_2/M_1 + A}$$

Ψ = A factor dependent upon the agglomeration of the particles

$$\Psi = 1 + \left(\frac{1 - \phi_{max}}{\phi^2_{max}}\right)\phi_2$$

Comment:

A generalised equation of composite behaviour but does not directly account for the effects of particle shape and particle size or the effects of interfacial adhesion. (Indirectly the volumetric packing fraction is influenced by particle shape and particle size).

Hill's Equation (72,75)

$$G = \frac{1}{\beta}\left[\frac{G - G_1}{\phi_1}\right] + \left[\frac{G - G_2}{\phi_2}\right]$$

Where:

$$\beta = 0.6 - \frac{0.2K}{K + 1.33G}$$

Comment:

Similar to the Kerner equation is application and behaviour.

The Chow Equation (74)

$$\frac{E}{E_1} = 1 + \phi_2 \left[\frac{\left(\frac{K_2}{K_1} - 1\right) \mu_1 + 2 \left(\frac{G_2}{G_1} - 1\right) \lambda_1}{2 \lambda_1 \mu_3 + \mu_1 \lambda_3} \right]$$

Where:

μ = a function of the shear modulus

$$\mu = 1 + \left(\frac{G_2}{G_1} - 1\right)\left(1 - \phi_2\right) \alpha$$

α = a function of the aspect ratio (a)

λ = a function of the bulk modulus

$$\lambda = 1 + \left(\frac{K_2}{K_1} - 1\right)\left(1 - \phi_2\right) \beta$$

β = a function of the Poisson's ratio of the matrix (ν_1)

Comment:

Similar to the Kerner equation in application and limitation but does take account of the particle shape and is thus applicable to both particulate fibrous composites.

The Cohen-Ishai Equation (79,80)

$$E_c = E_1 (1 - \phi_v^{2/3}) \left[1 + \frac{\phi_2}{\frac{M}{M-1} - 3\sqrt{\phi_2}} \right]$$

Where $M = \frac{E_2}{E_{1v}}$

E_{1v} = Elastic modulus of unfilled but voided matrix.

Comment:

This equation has similar limitations to the Kerner equations but does consider the effects of voids.

Isostress Theory (75)

$$\frac{E_c}{E_1} = \frac{E_2}{\phi_2 (E_1 - E_2) + E_2}$$

Comment:

This equation is based on the relationship between the constituents of the composite and is applicable where $\nu_1 = \nu_2$ It takes no account of factors such as particle size, shape and the interfacial adhesion between filler and matrix.

Isotrain Theory (75)

$$\frac{E_c}{E_1} = \phi_1 + \frac{E_2}{E_1} \phi_2$$

Comment:

Similar limitations to Isostress theory and has little predictive validity for particulate fillers. It has more value for describing the behaviour of oriented long fibre filled composites tested along their longitudinal axis.

APPENDIX 2

Electron Spectroscopy for Chemical Analysis. Studies of ASPA Glass, Acid Treated Glasses and of Reactive Fillers

The ESCA Technique

ESCA is an analytical technique which can be used for elemental analysis for studying chemical structures and the nature of chemical bonding. The technique is essentially a surface technique capable of probing to depths of about 25 Å for metals and about 100 Å for organic materials (193). In principle the sample is irradiated by a monoenergetic x-ray source (e.g. Al K_α radiation) causing extensive ionisation of the sample. The ejected electrons are collected and analysed. Each element has its own discrete and characteristic set of binding energies (ionisation potentials) for both core and valence electrons. By measuring the kinetic energy of the emitted electrons information on their binding energies can be obtained by applying the following equation.

$$EK = h_\gamma - EB$$

Where

EK = Kinetic energy of emitted electrons

EB = Binding energy of care or valence electrons

h_γ = energy of x-ray source

Further, the nature of the radiation generates Auger electrons which can also be used for identification purposes. Thus the peaks on the spectra are a plot of the kinetic energy of the elements present against the number of electrons emitted. Such information can be used to identify the elements in a sample and to give quantitative measures of the proportions of each element present in the surface.

Operating Procedure

The specimen holder was covered with double sided adhesive to which the sample powders were adhered. The specimen holder was then placed in the sample chambre and spectra obtained under the following conditions:

Excitation Source	Aluminium (K_α 1487 e.v.)
Vacuum	Circa 10^{-6} Torr
Current	Circa 11 Ma 14 KV.

Kinetic Energy Scan range variable - between 300 and 1250 e.v.

step width	01. V
rate	0.05 volts sec^{-1}

Counter range either 10^4 c.p.s. or 3×10^3 to resolve small peaks.

The following are spectra of ASPA glass, acid treated ASPA glass and reactive fillers.

Sample 1. Untreated ASPA glass

Range 600-850 e.v.; 10^4 cps
Showing F Auger and F1s peaks.

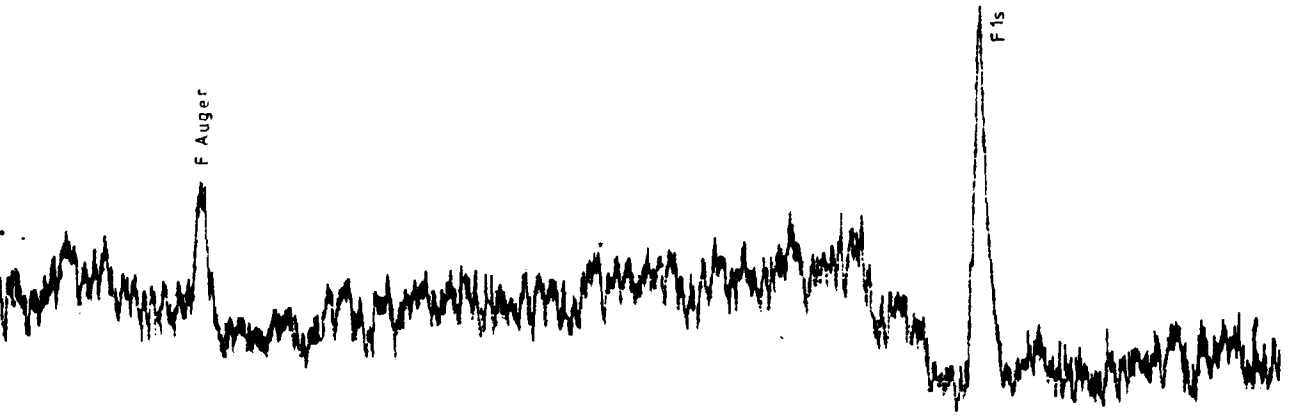

700 KINETIC ENERGY e.v. 800

Sample 2. Acid Treated Glass
pH 2.4

Range 600-850 e.v.; 10^4 cps
Showing F Auger and F1s peaks.

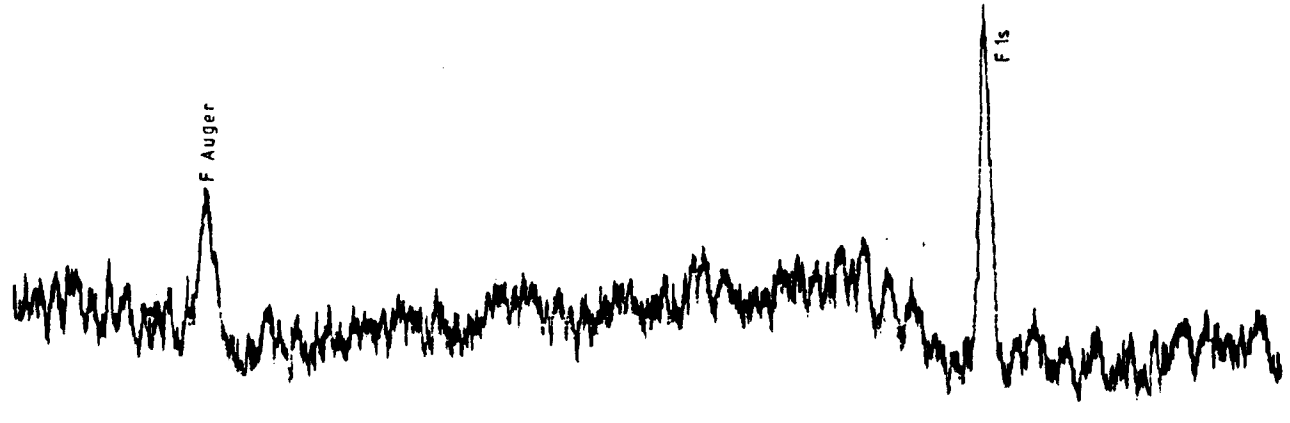

Sample 3. Acid Treated Glass
pH 0.8

Range 600-850 e.v.; 10^4 cps

Showing F Auger ad F 1s peaks

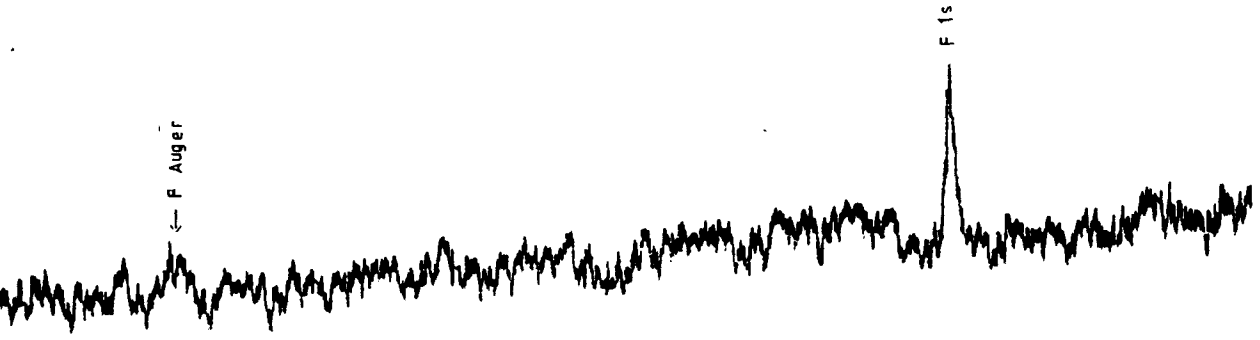

700 KINETIC ENERGY e.v. 800

Sample 1. Untreated ASPA glass

Range 1,000-1,250 e.v.; 10^4 cps.
Showing Ca 2s, $2p_{\frac{1}{2}}$, $2p_{3/2}$ and
Na Auger peaks.

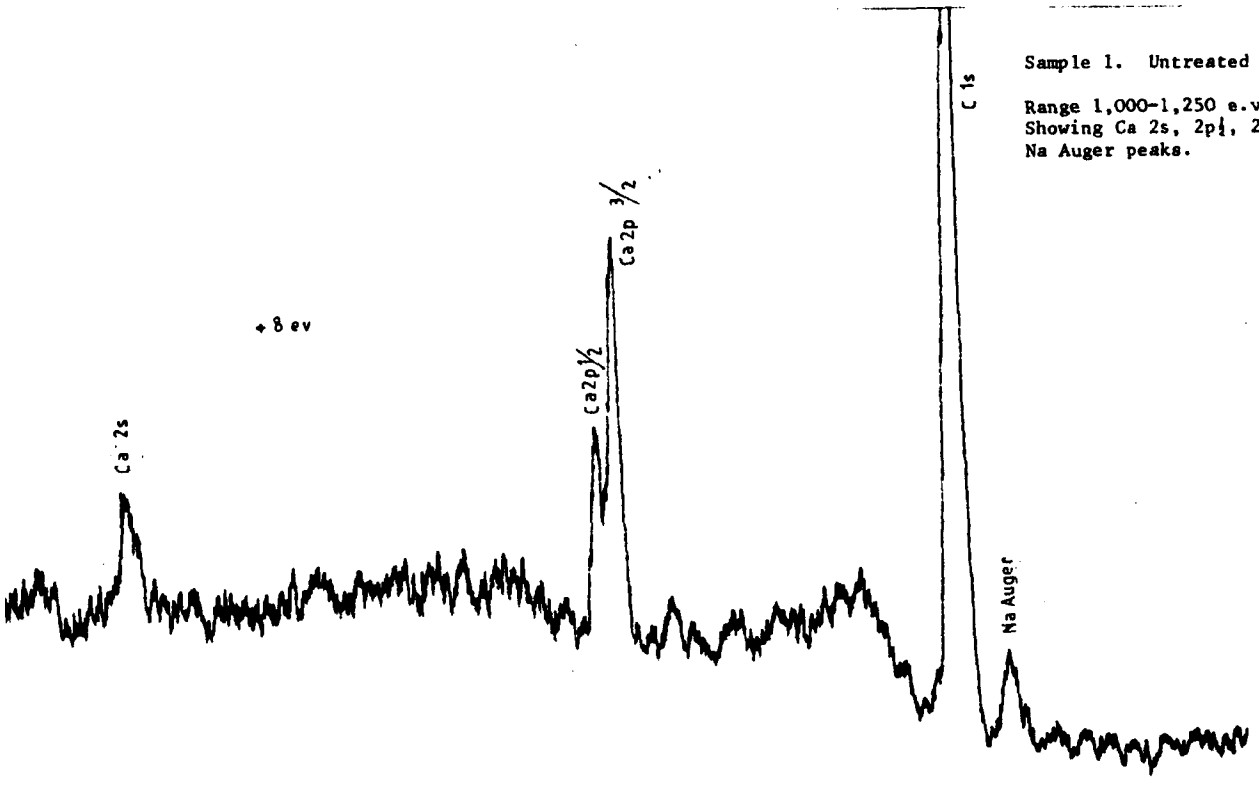

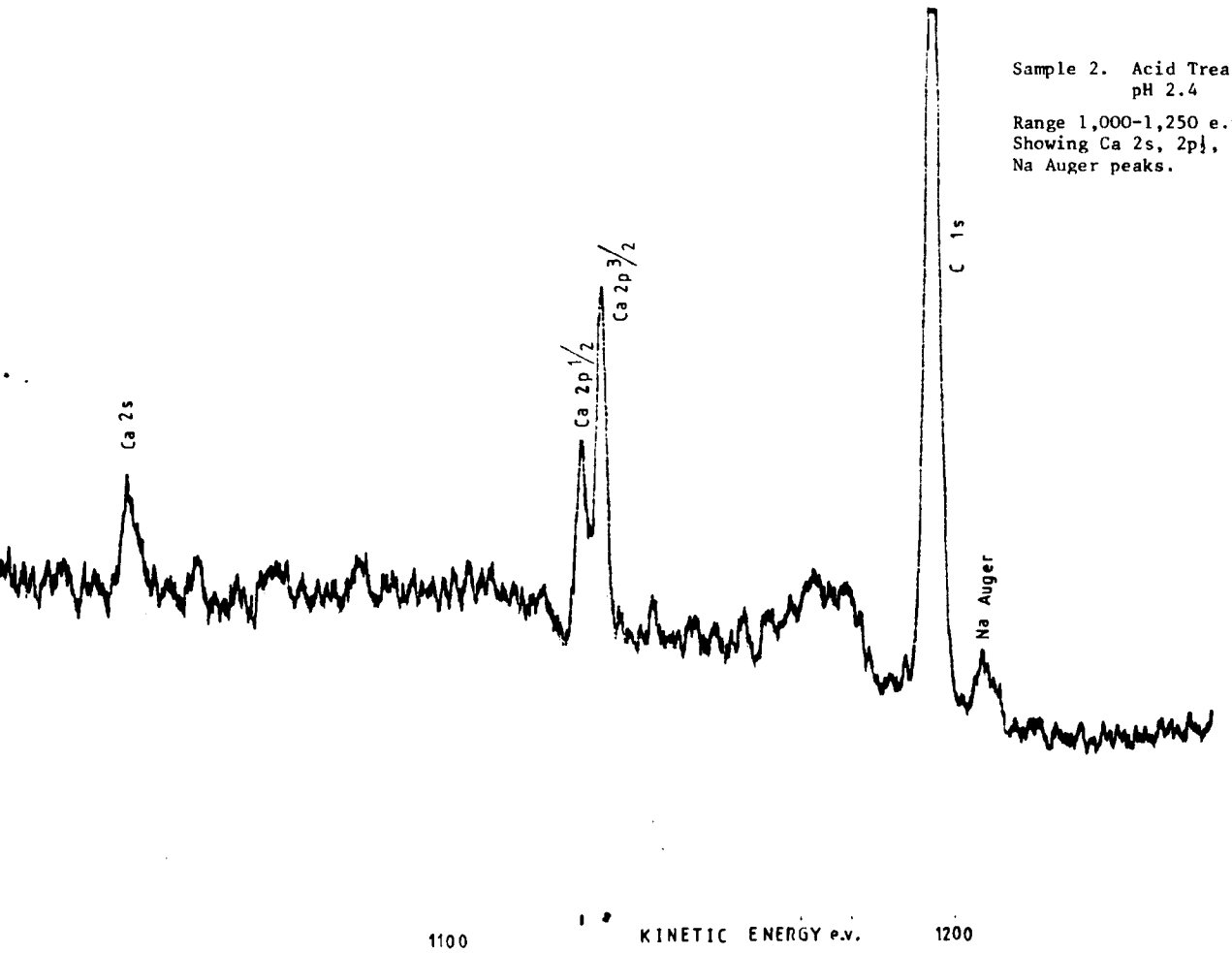

Sample 2. Acid Treated Glass
pH 2.4

Range 1,000-1,250 e.v.; 10^4 cps
Showing Ca 2s, $2p\frac{1}{2}$, $2p^3/2$ and
Na Auger peaks.

1100 KINETIC ENERGY e.v. 1200

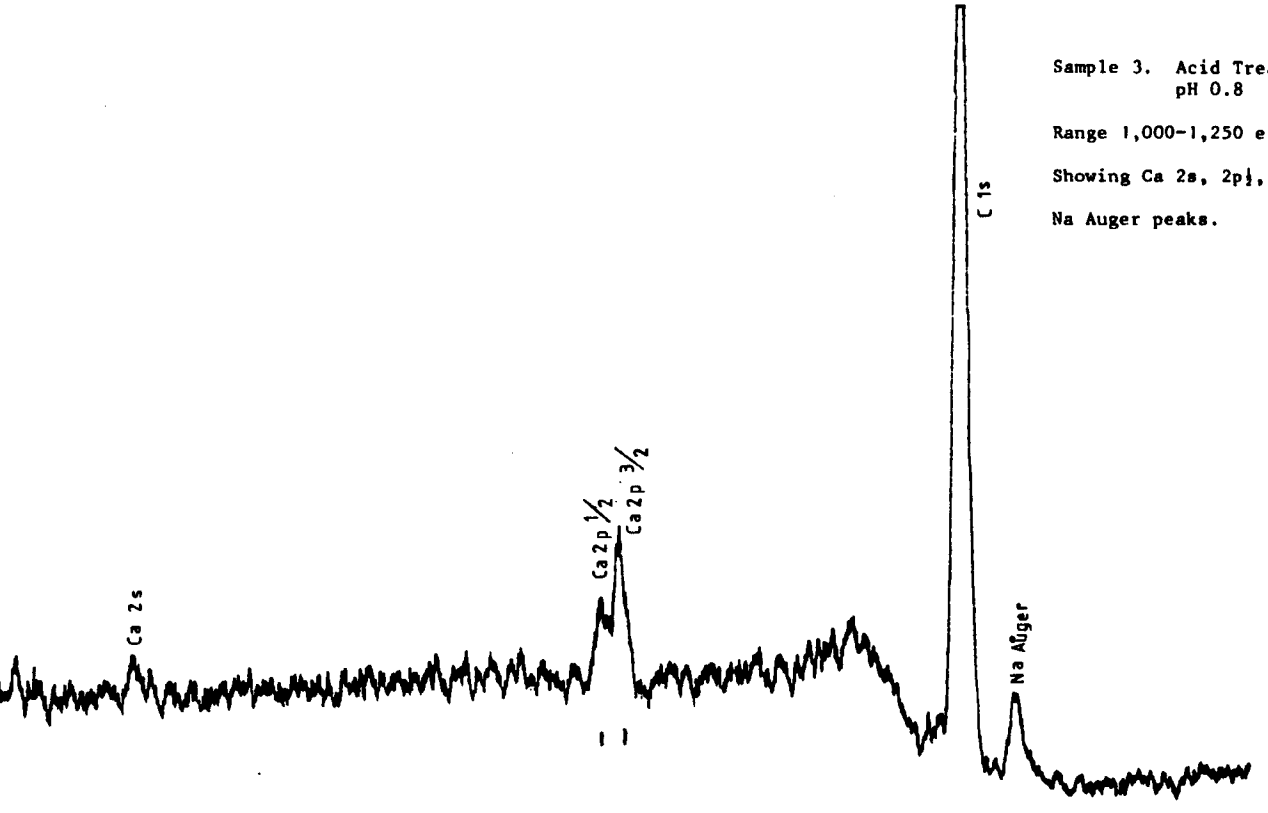

Sample 3. Acid Treated Glass
pH 0.8

Range 1,000-1,250 e.v.; 10^4cps

Showing Ca 2s, $2p\frac{1}{2}$, $2p^3/2$ ad

Na Auger peaks.

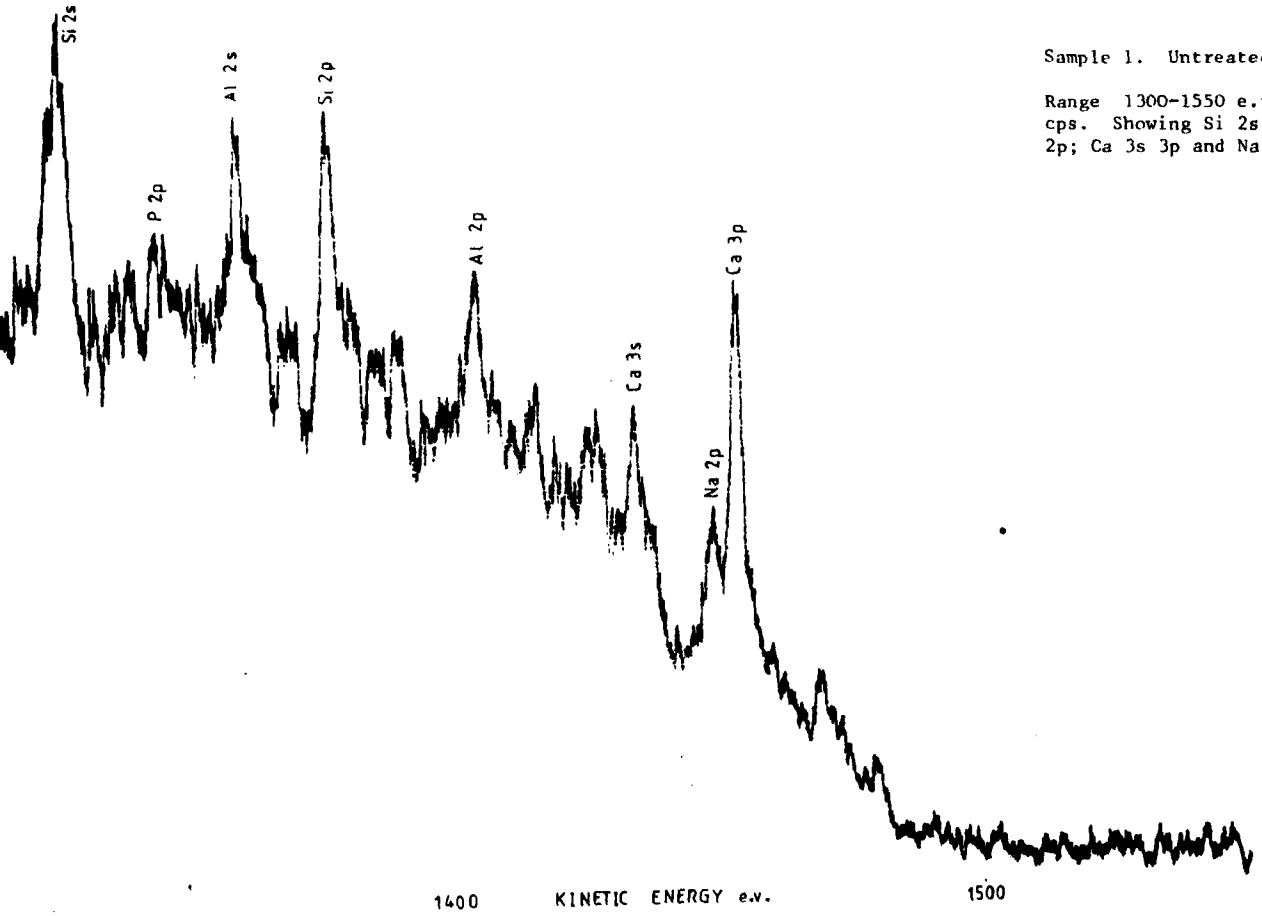

Sample 1. Untreated ASPA Glass

Range 1300-1550 e.v.; 3 x 10^3 cps. Showing Si 2s 2p; Al 2s, 2p; Ca 3s 3p and Na 2p peaks.

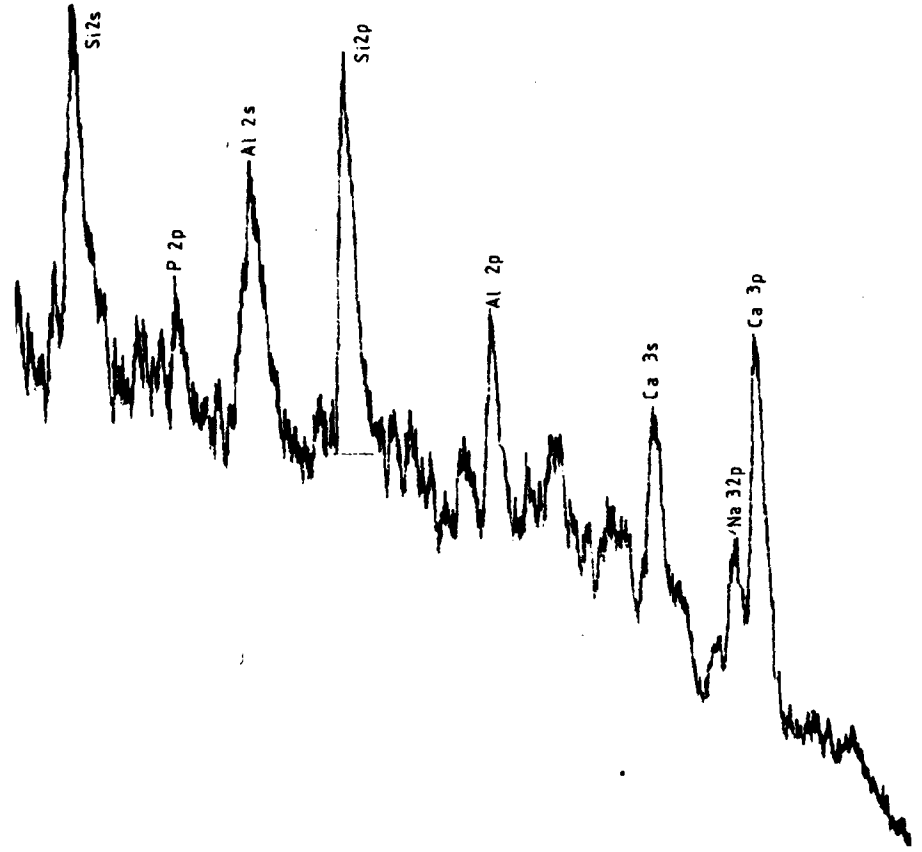

Sample 2. Acid Treated Glass pH 2.4.

Range 1300-1550 e.v. 3 x 10^3 cps Showing Si 2s 2p; Al 2s, 2p; Ca 3s 3p and Na 2p peaks.

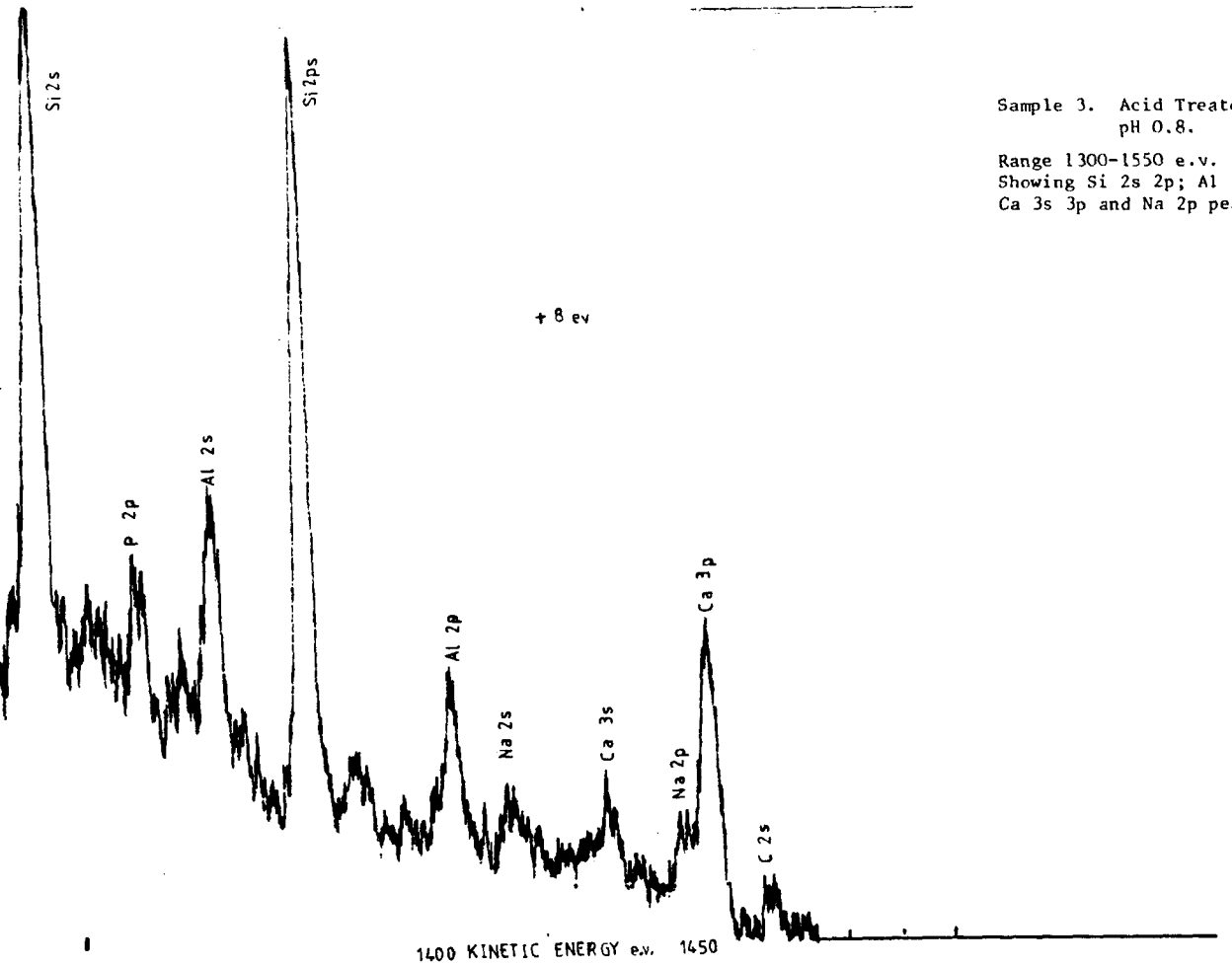

Sample 3. Acid Treated Glass
pH 0.8.

Range 1300-1550 e.v. 3×10^3 cps
Showing Si 2s 2p; Al 25, 2p;
Ca 3s 3p and Na 2p peaks.

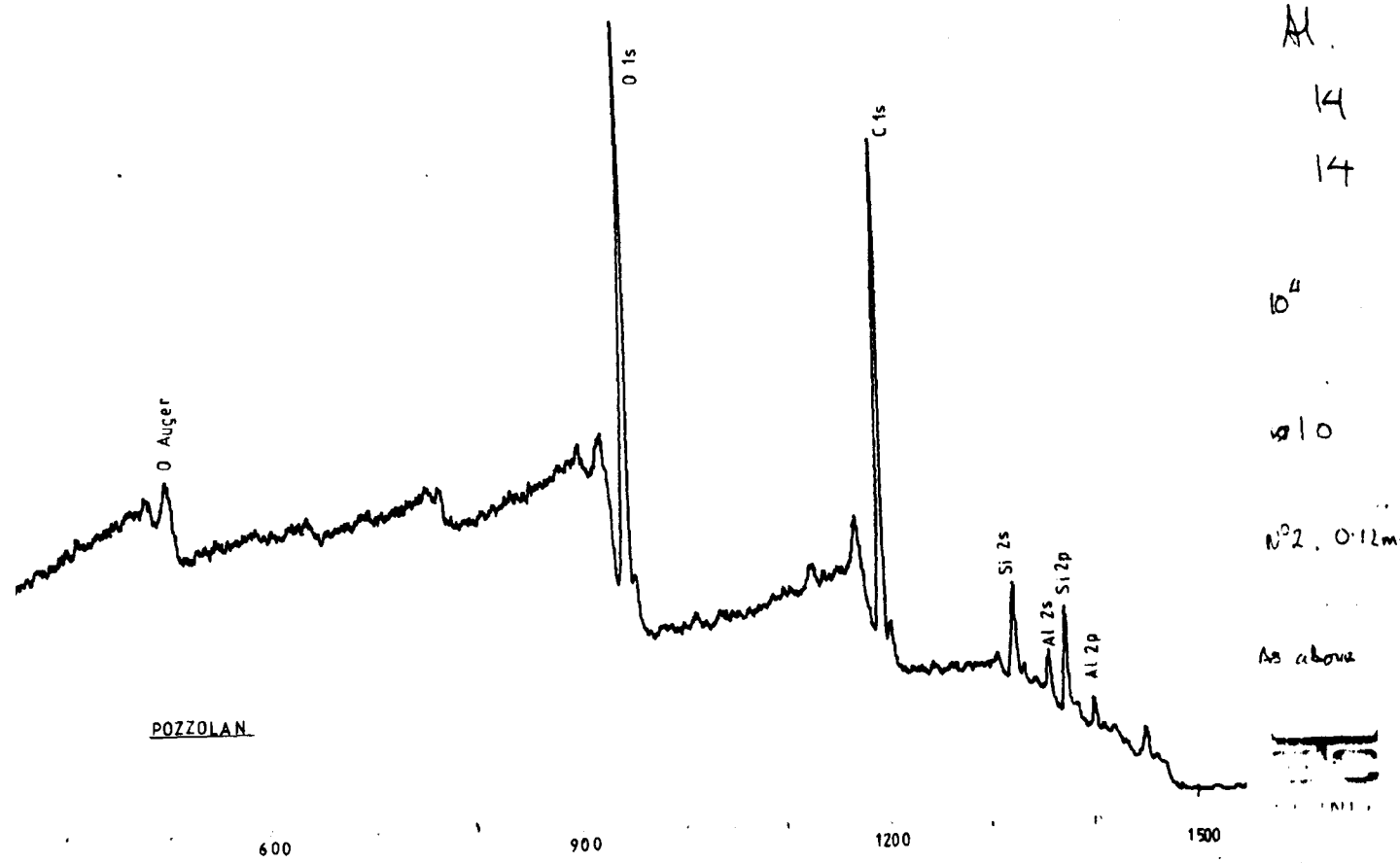

POZZOLAN

Al.
14
14
10^4
s 10
N°2. 0·12m
As above

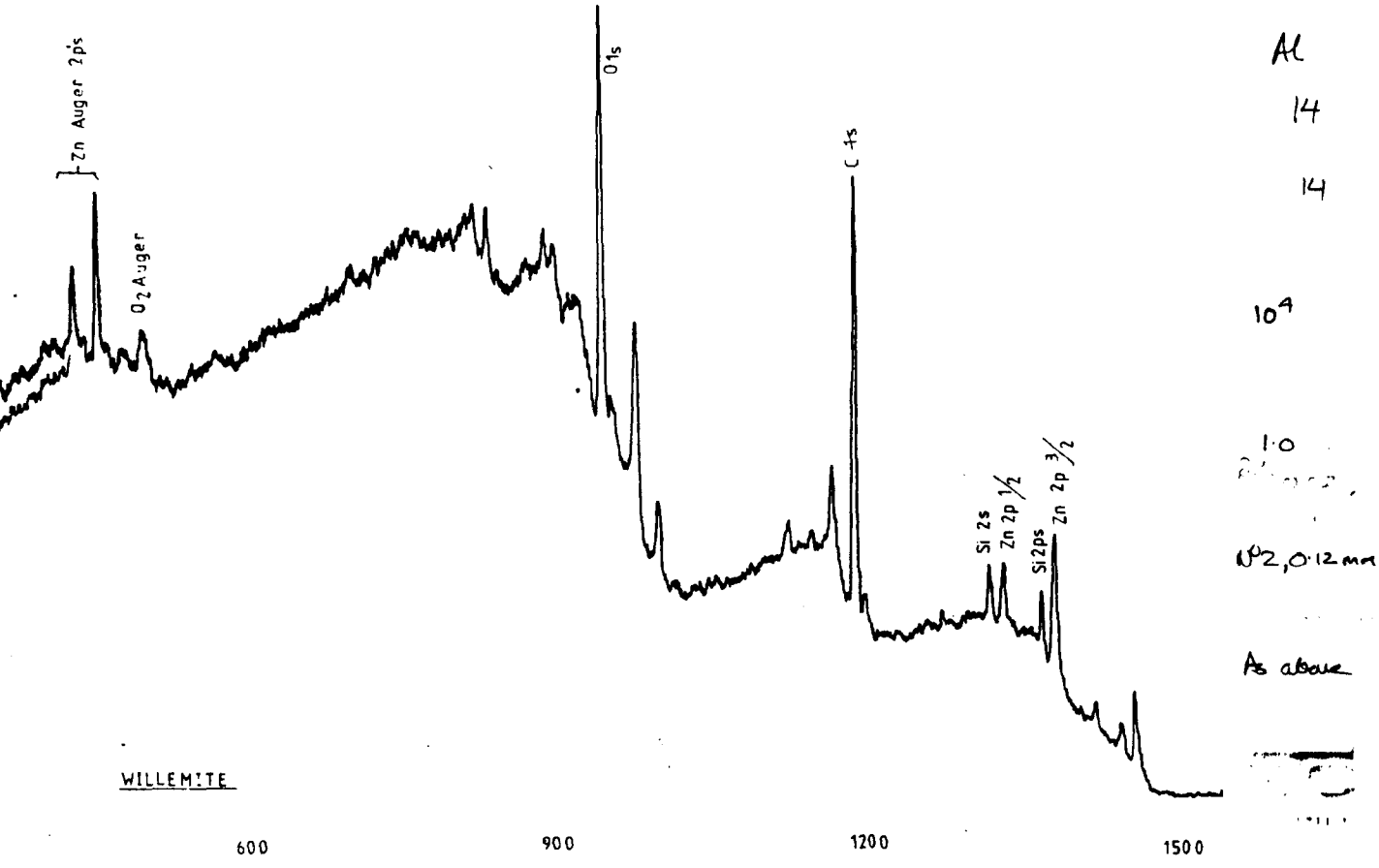
Zn Auger 2ps
O2 Auger
O1s
C 1s
Si 2s
Zn 2p 1/2
Si2ps
Zn 2p 3/2
Al
14
14
10⁴
1·0
N°2, 0·12mm
As above
WILLEMITE
600
900
1200
1500

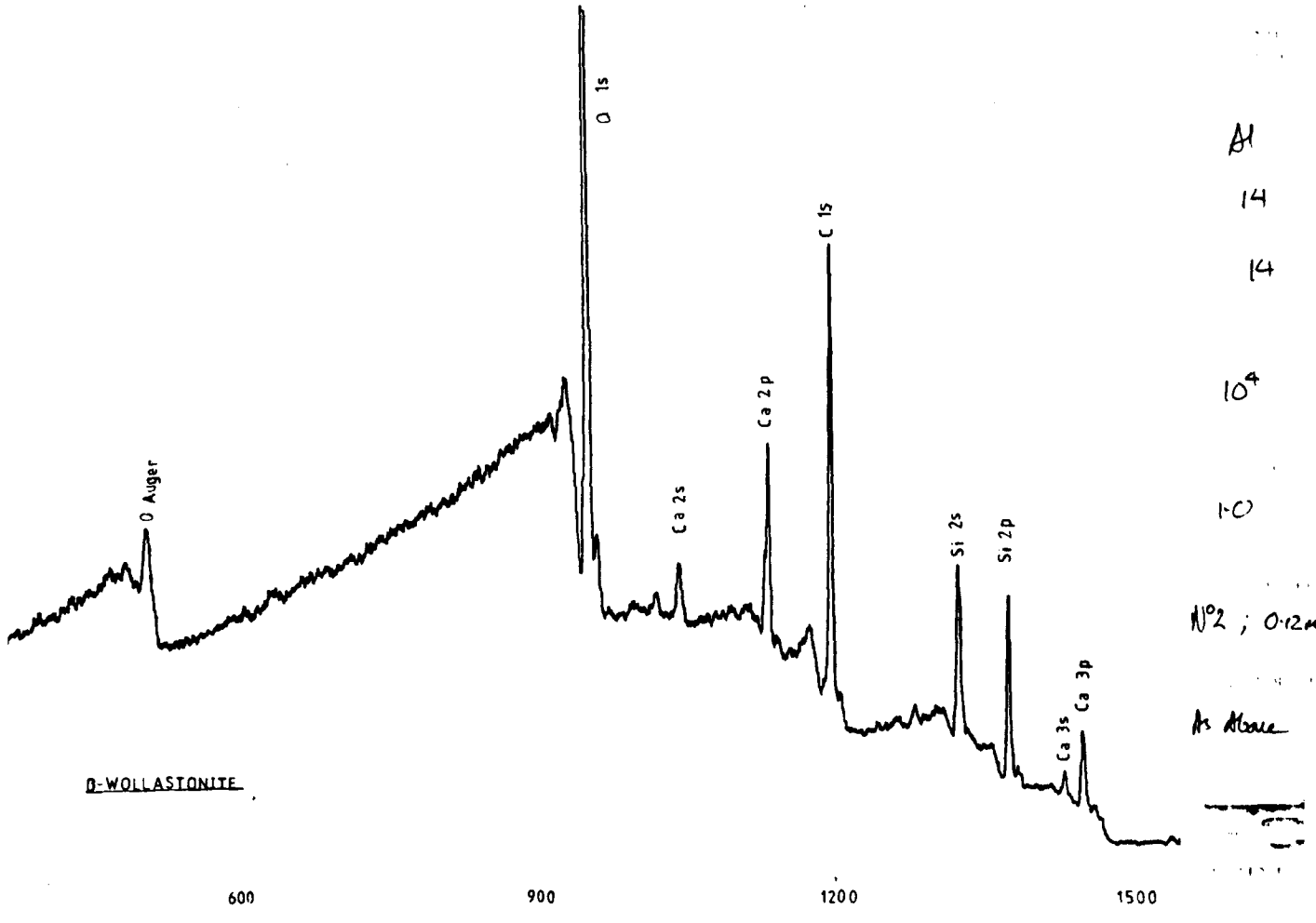
O 1s
O Auger
Ca 2s
Ca 2p
C 1s
Si 2s
Si 2p
Ca 3s
Ca 3p
Al
14
14
10⁴
1·0
N°2 ; 0·12mm
As Above
D-WOLLASTONITE
600
900
1200
1500

Appendix 3

Particle Size Analysis of Fillers and Glasses

The particle size distributions of various fillers and glasses were determined on either an Industrial Coulter Counter (178) or on an Optomax Automatic Particle Analyser (179).

The Coulter Technique

The coulter technique is based on an electrical principle as follows. A small amount of the sample is dispersed into an electrolyte and a fixed volume of the suspension (either 0.5 or 0.05 ml) is drawn through an orafice of known diameter (70μm or 140μm). The number of particles drawn through the orafice are counted as each particle generates an electrical signal. The magnitude of this signal is proportional to the size of the particle and, by altering the sensitivity threshold of the instrument, smaller particles can be progressively eliminated from the count. By conducting a number of counts and applying an arithmetic procedure to the raw data, a full particle size distribution can be obtained. Although the Coulter Counter is easy to use, it does have a number of practical limitations. For example, the full procedure is time consuming, dense particles sink in the electrolyte and are not counted, large particles may block the orafice and good dispersion is required to prevent aggregate formation. Where such problems occurred the Optomax technique was employed.

The Optomax Technique

The Optomax is a computer aided technique which is based on an optical principle and was used here in conjunction with a transmission light microscope. Small amounts of the sample were dispersed in a suitable medium which was applied to a microscope slide, covered, and then viewed through the microscope. The

microscope image was projected onto a display screen comprising of a number of picture points. The area occupied by the particle image (in terms of picture points) and the number of particles in the field of view were counted. By repeating this procedure for a number of fields of view and informing the computer of parameters such as the image magnification, limit sizes, increment size and total number of particles to be counted, a complete particle size analysis was readily obtained. However, good image contrast was required between the particles and the dispersing media. This was difficult to obtain and necessitated staining the particles with fluorescent dyes and finding dispersion media with markedly different refractive indicies to the particles.

The following particle size distributions were obtained by the coulter technique except those marked with an asterisk, which were obtained by the Optomax technique.

Particle Size Distributions of Various Fillers

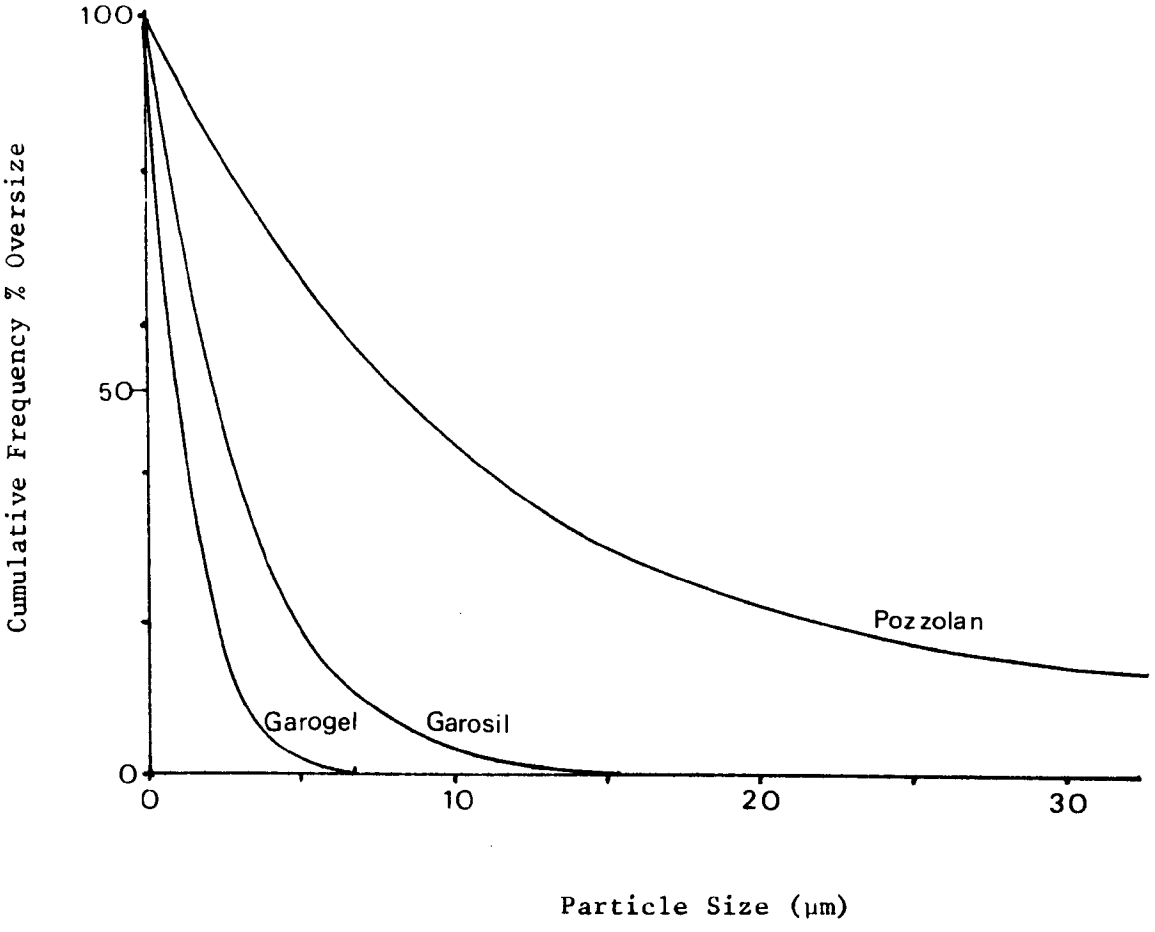

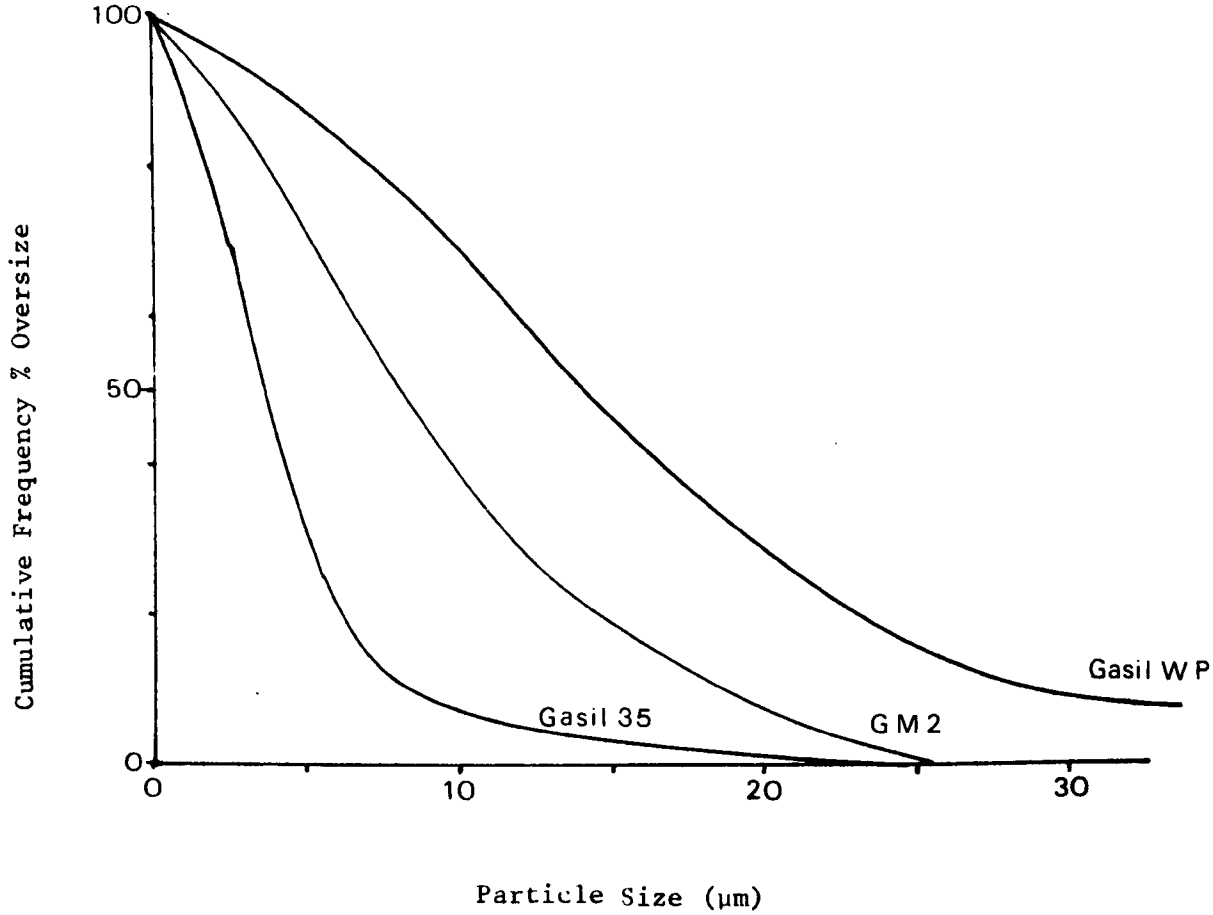

Particle Size Distributions of Various Fillers

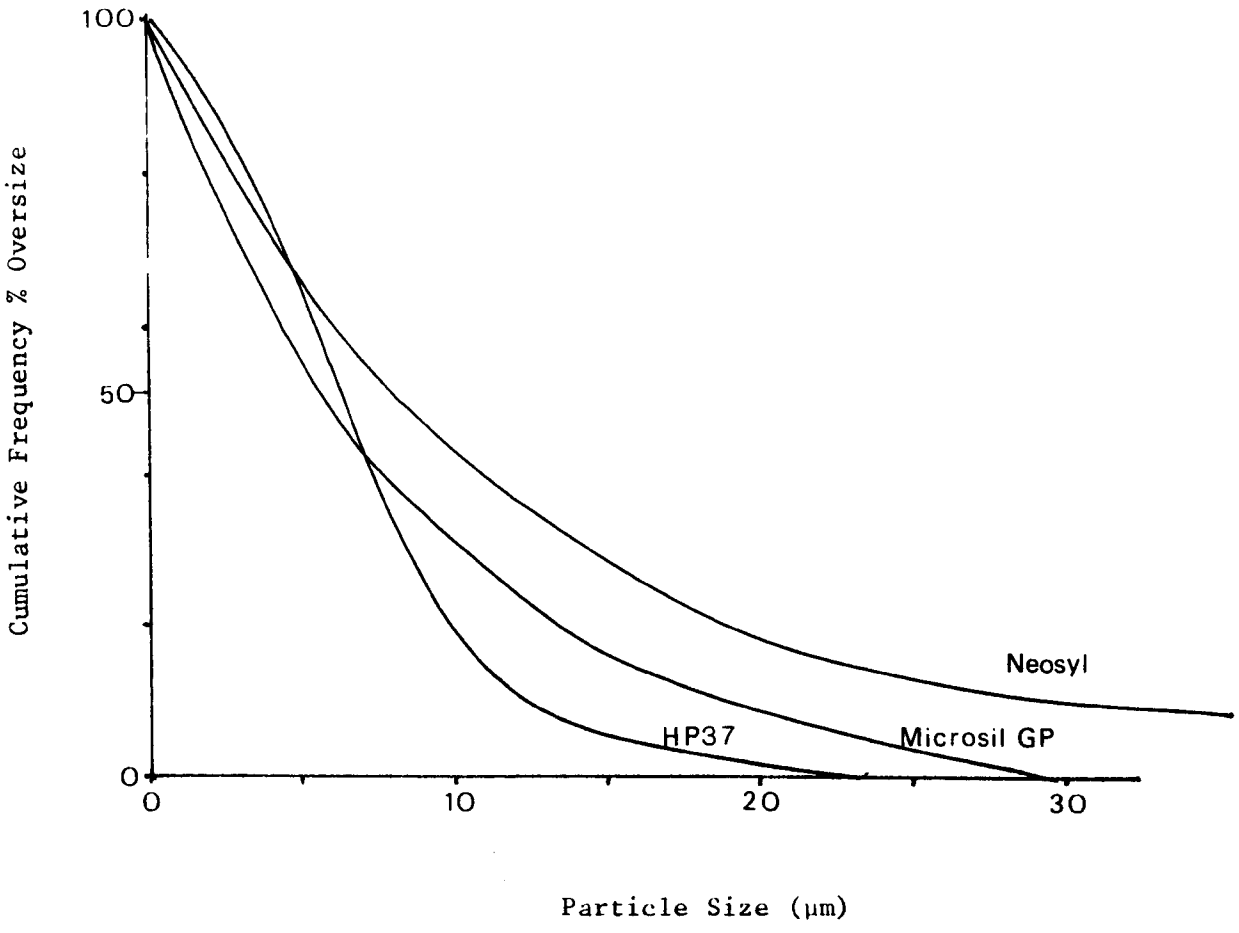

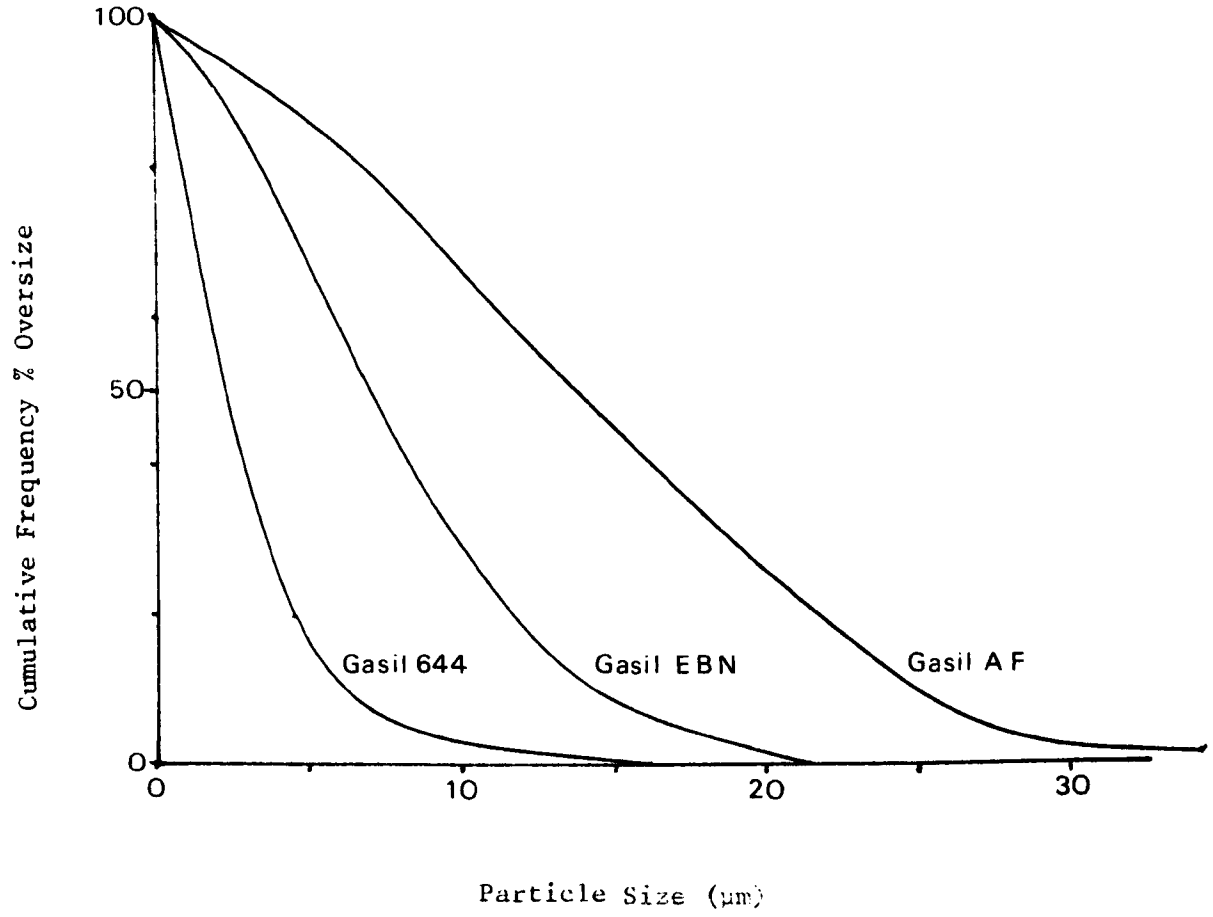

Particle Size Distributions of Various Fillers

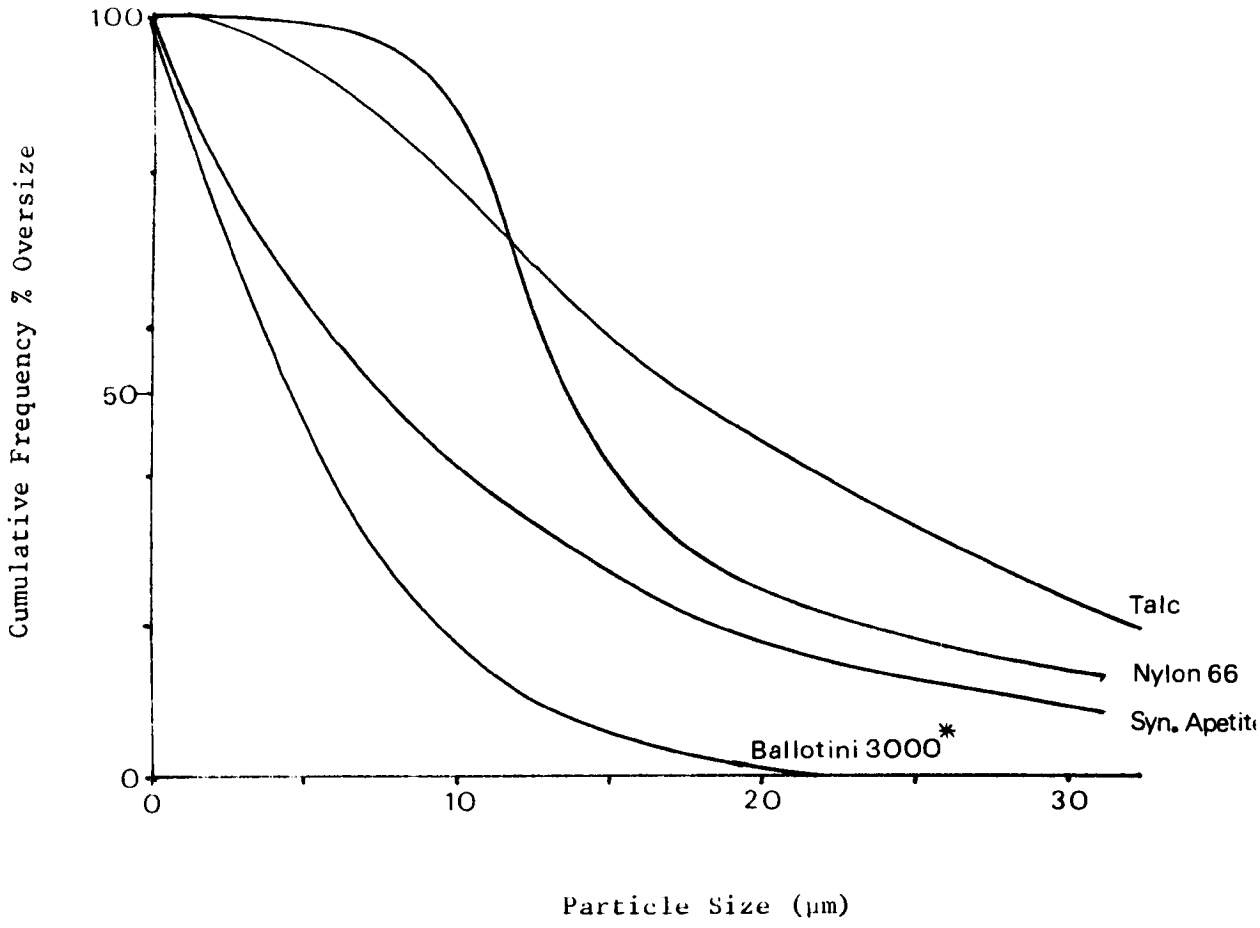

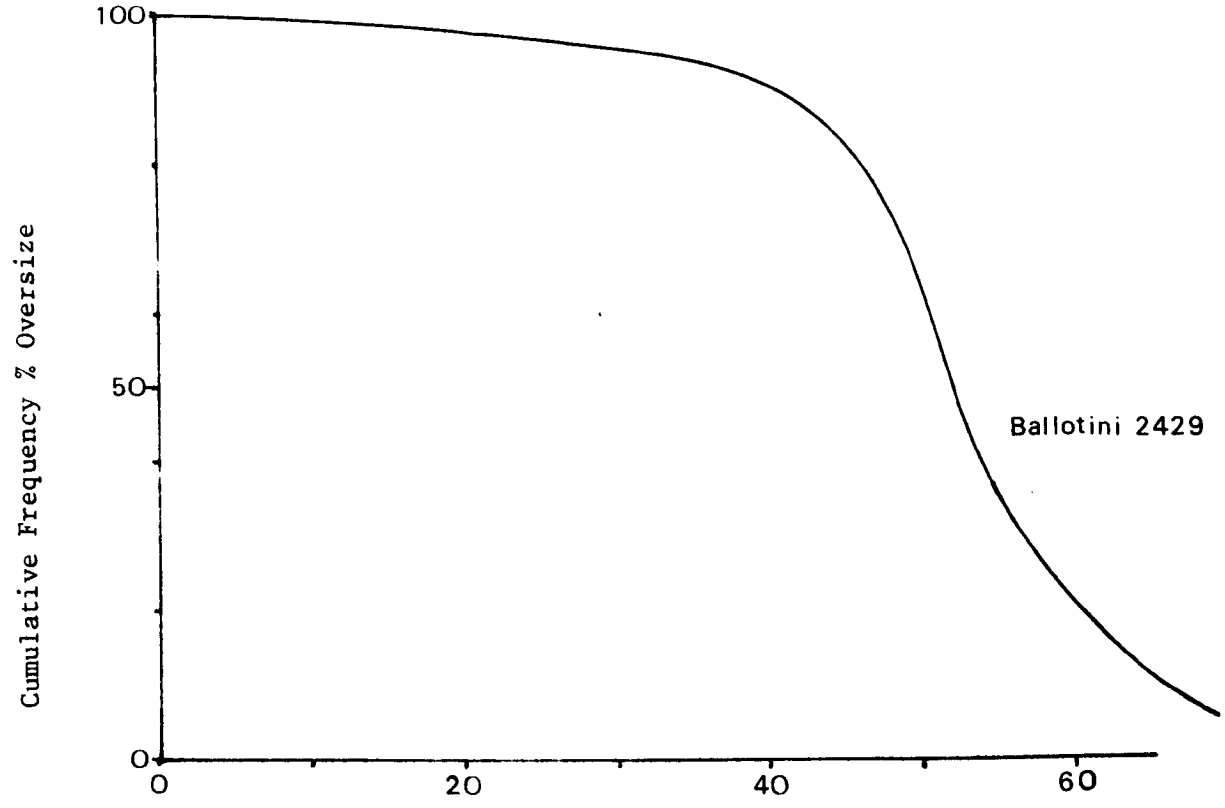

Particle Size Distributions of Various Fillers

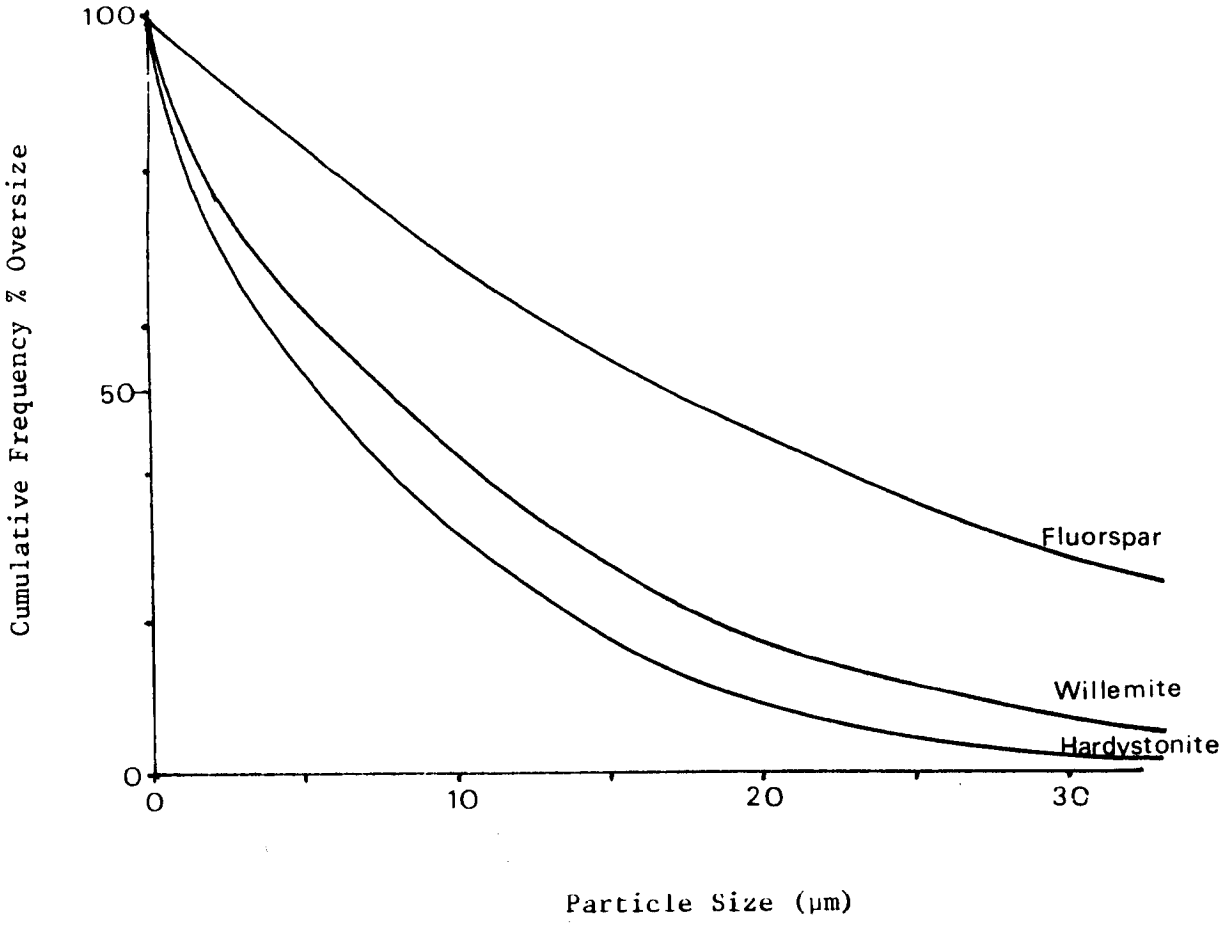

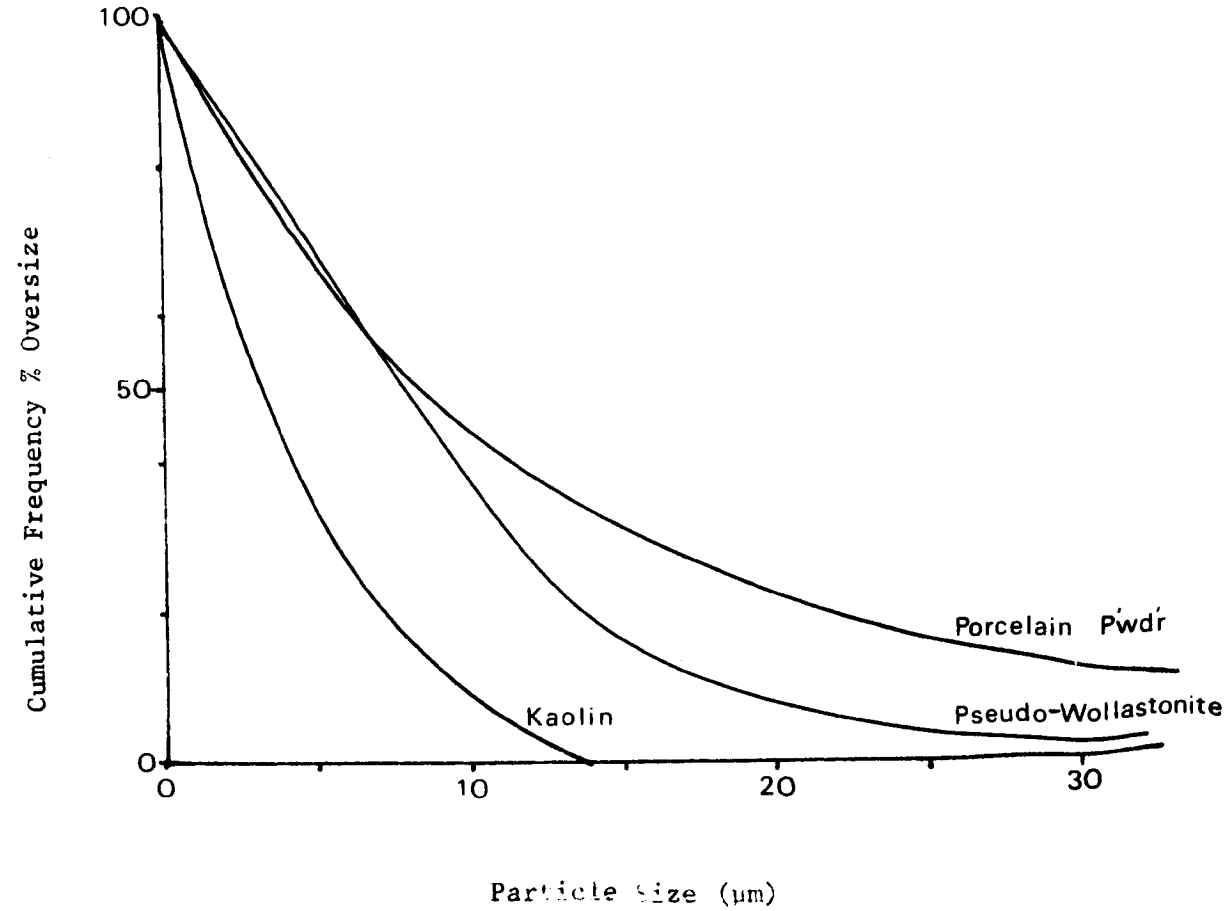

Particle Size Distributions of Various Fillers